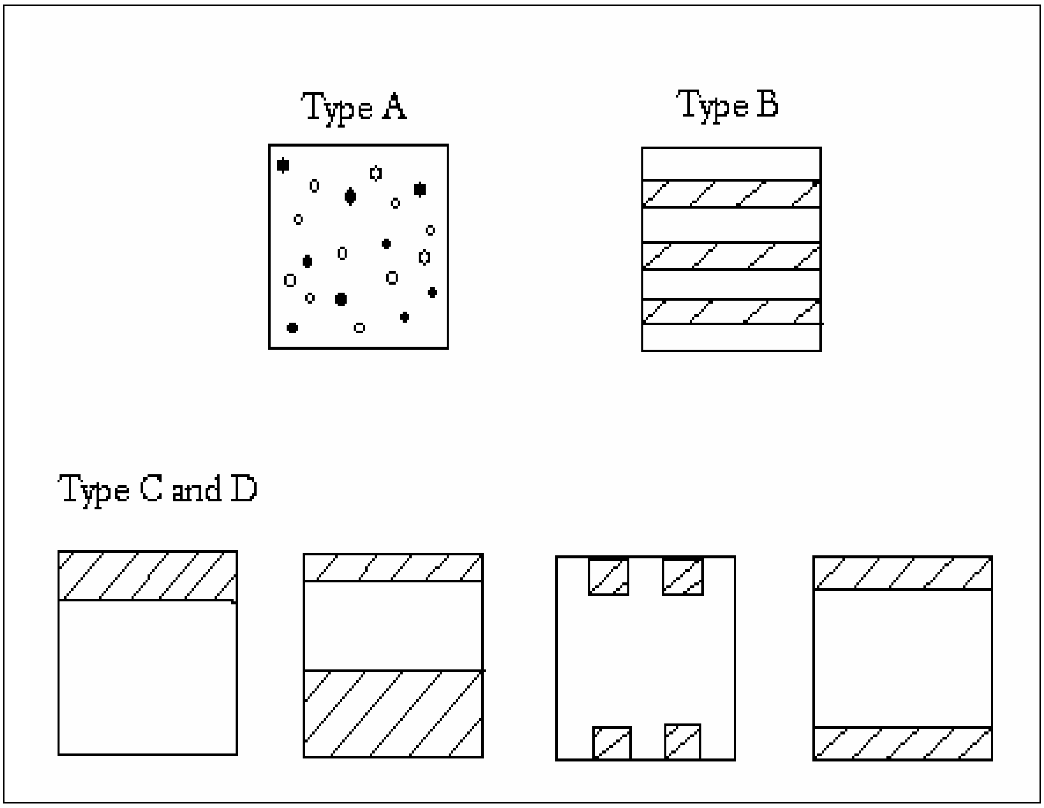

Figure 1.1: Schematic diagrams of hybrid types-all end view

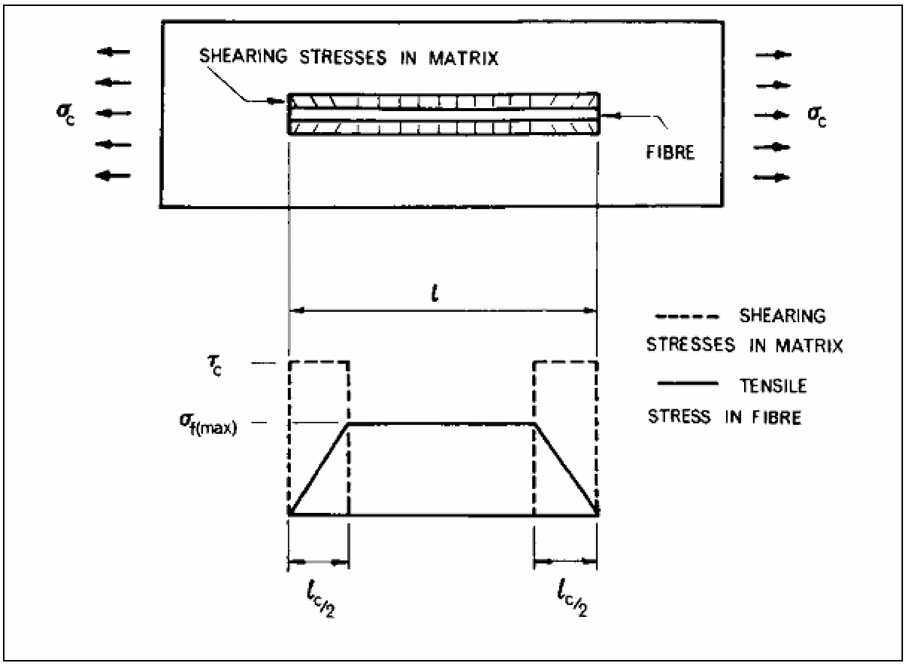

Figure 2.1: Stress distribution usually assumed for a given fibre in a discontinuous, aligned fibre composite subjected to a tensile stress, σ_c and at the point of failur

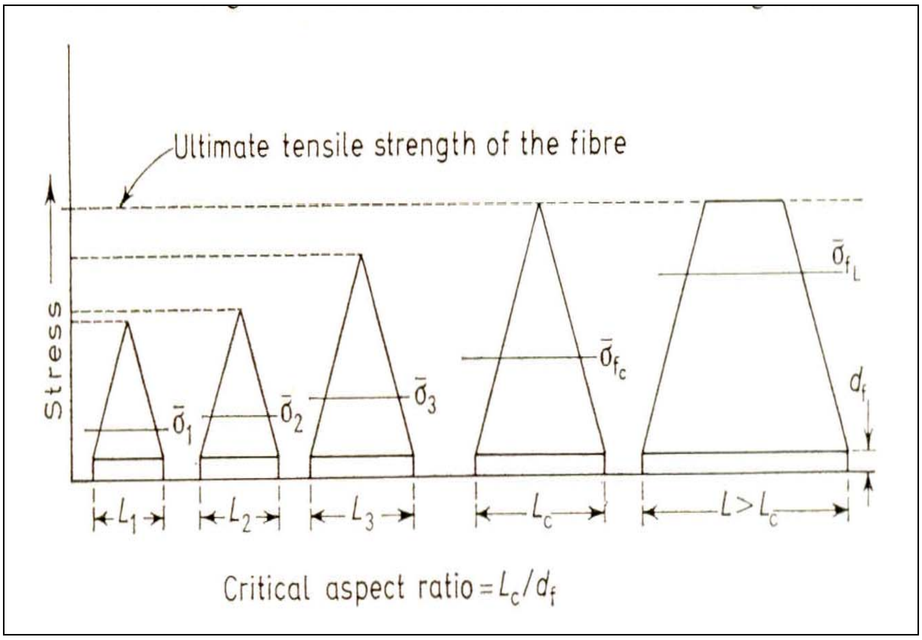

Figure 2.2: Variation of fibre stress with length

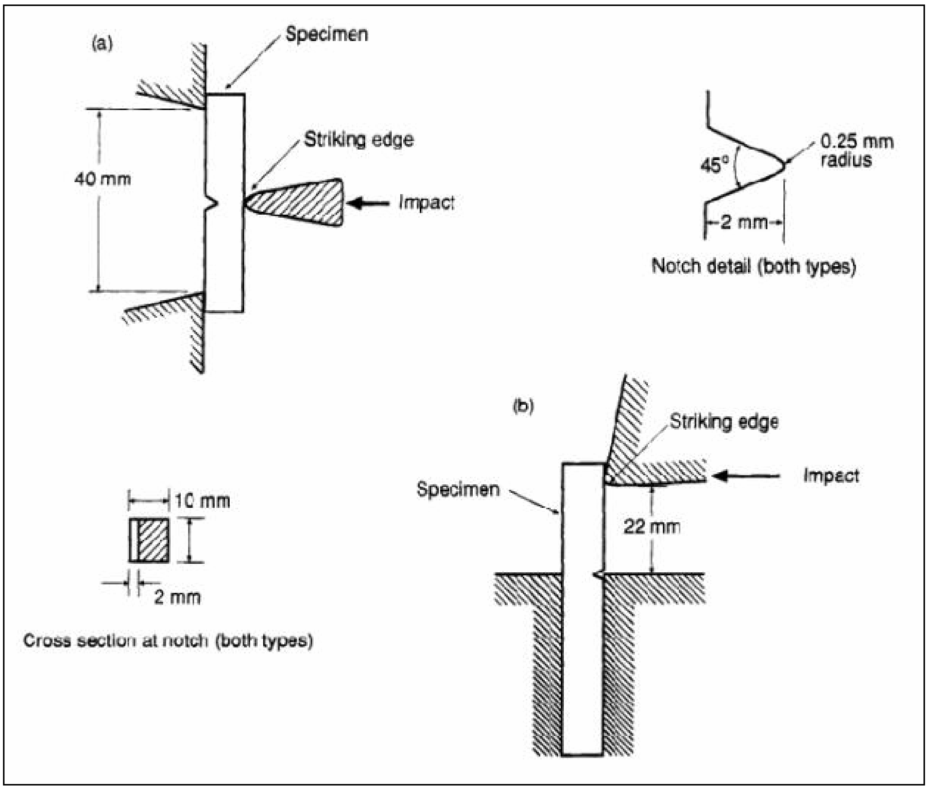

Figure 2.3: Specimens and loading configurations for (a) Charpy V-notch and (b)Izod tests

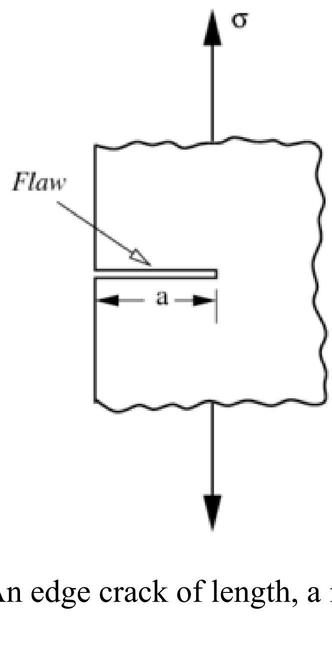

Figure 2.4: An edge crack of length, a in the material

Table 3.1
Specimens' abbreviation and formulation

Sample	V_f	Fibre	Description
SGD0	0.00	-	Technyl® A216 used as received in dry condition
SG50%RH0			Technyl® A216 used as received in 50%RH condition
SGW0			Technyl® A216 used as received in wet condition
SGD4	0.04	Short	Technyl® A216 V30, diluted with Technyl® A216 in dry condition
SG50%RH4			Technyl® A216 V30, diluted with Technyl® A216 in 50%RH condition
SGW4			Technyl® A216 V30, diluted with Technyl® A216 in wet condition
SGD8	0.08	Short	Technyl® A216 V30, diluted with Technyl® A216 in dry condition
SG50%RH8			Technyl® A216 V30, diluted with Technyl® A216 in 50%RH condition
SGW8			Technyl® A216 V30, diluted with Technyl® A216 in wet condition
SGD13	0.13	Short	Technyl® A216 V30, diluted with Technyl® A216 in dry condition
SG50%RH13			Technyl® A216 V30, diluted with Technyl® A216 in 50%RH condition
SGW13			Technyl® A216 V30, diluted with Technyl® A216 in wet condition
SGD16	0.16	Short	Technyl® A216 V30, used as received in dry condition
SG50%RH16			Technyl® A216 V30, used as received in 50% RH condition
SGW16			Technyl® A216 V30, used as received in wet condition

Table 3.1 (Continued)

SGD18	0.18	Short	Celanese® 1503-2, used as received in dry condition
SG50%RH18			Celanese® 1503-2, used as received in 50% RH condition
SGW18			Celanese® 1503-2, used as received in wet condition
SG75/C25D	0.22	Short	LNP® RC100-10, mixed with Celanese® 1503-2 in dry conditon
SG75/C25,50%RH			LNP® RC100-10, mixed with Celanese® 1503-2 in 50% RH condition
SG75/C25W			LNP® RC100-10, mixed with Celanese® 1503-2 in wet condition
SG50/C50D	0.26	Short	LNP® RC100-10, mixed with Celanese® 1503-2 in dry condition
SG50/C50,50%RH			LNP® RC100-10, mixed with Celanese® 1503-2 in 50% RH condition
SG50/C50W			LNP® RC100-10, mixed with Celanese® 1503-2 in wet condition
SG25/C75D	0.30	Short	LNP® RC100-10, mixed with Celanese® 1503-2 in dry condition
SG25/C75,50%RH			LNP® RC100-10, mixed with Celanese® 1503-2 in 50%RH condition
SG25/C75W			LNP® RC100-10, mixed with Celanese® 1503-2 in wet condition
SCD33	0.33	Short	LNP® RC100-10, used as received in dry condition
SC50%RH33			LNP® RC100-10, used as received in 50%RH condition
SCW33			LNP® RC100-10, used as received in wet condition

Table 3.2: Temperature settings on automatic injection moulding machine model Boy® 50M

Processing parameter	Unit	Glass fibre composite
Temperature setting Mould Rear Centre Front Nozzle	°C	80-100 270 275 280 285
Screw speed	RPM	50-60

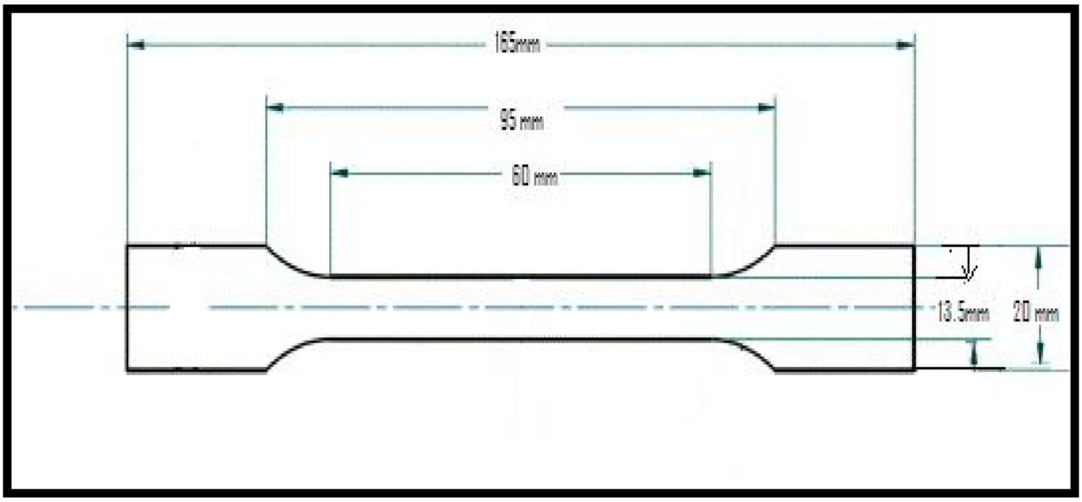

Figure 3.1: Dimensions of the tensile specimen

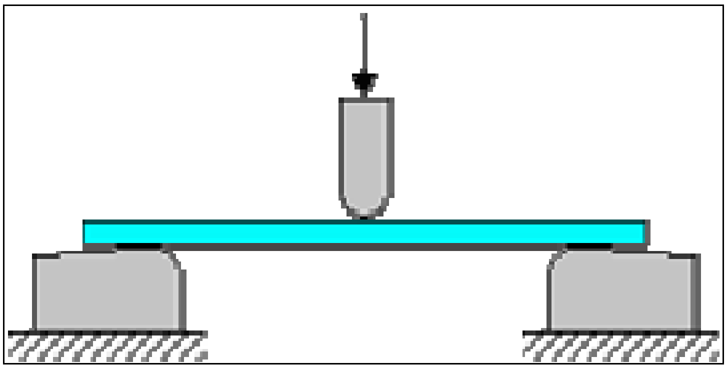

Figure 3.2: Specimen arrangement during the flexural test

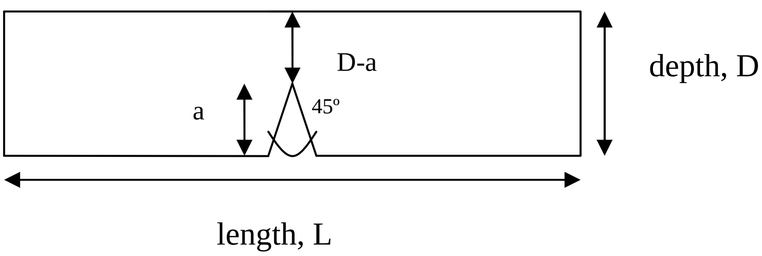

Figure 3.3: Single edge notch impact specimen

Table 4.1
Determination of fibre volume fraction

Sample	Fibre	Fibre weight fraction, W_f (%)	Weight of composite before heating (g)	Weight of fibre after heating (g)	Actual fibre weight fraction, W_f (%)	Average V_f
SC33	Carbon	44	0.46	0.20	44.10	0.33
			0.53	0.23	43.00	
			0.53	0.23	44.00	
SG4	Glass	8	0.51	0.04	7.99	0.04
			0.51	0.04	8.39	
			0.54	0.04	7.90	
SG8	Glass	17	0.47	0.08	16.93	0.08
			0.48	0.08	16.90	
			0.59	0.10	17.15	
SG13	Glass	25	0.51	0.13	24.42	0.13
			0.57	0.14	25.46	
			0.59	0.15	25.09	
SG16	Glass	30	0.74	0.22	29.97	0.16
			0.66	0.20	30.19	
			0.82	0.25	29.87	
SG18	Glass	33	0.52	0.17	31.87	0.18
			0.54	0.19	35.40	
			0.55	0.18	32.14	

Table 4.2
Thermal properties (from DSC measurements) of glass fibre composite at dry condition

Sample	**V_f (%)**	**T_m (ºC)**	**ΔH_m (J/g)**	**T_c (ºC)**	**$-\Delta H_m$ (J/g)**
SGD0	0	260.1	72.03	233.7	44.52
SGD4	4	260.3	66.51	234.1	41.14
SGD8	8	260.6	59.96	234.1	34.94
SGD13	13	260.9	53.65	234.1	32.38
SGD16	16	262.4	50.30	236.1	30.84

Table 4.3

Thermal properties (from DSC measurements) of glass fibre composite at 50% relative humidity condition

Sample	**V_f (%)**	**T_m (ºC)**	**ΔH_m (J/g)**	**T_c (ºC)**	**$-\Delta H_m$ (J/g)**
SG50%RH0	0	262.5	71.40	235.7	45.68
SG50%RH4	4	261.1	63.85	233.9	40.76
SG50%RH8	8	260.8	58.07	233.8	37.54
SG50%RH13	13	261.1	51.41	234.0	32.04
SG50%RH16	16	262.3	48.88	236.2	30.39

Table 4.4
Thermal properties (from DSC measurements) of glass fibre composite at wet condition

Sample	**V_f (%)**	**T_m (°C)**	**ΔH_m (J/g)**	**T_c (°C)**	**$-\Delta H_m$ (J/g)**
SGW0	0	262.9	66.14	236.0	43.11
SGW4	4	261.6	60.03	234.5	36.82
SGW8	8	260.9	55.88	234.3	34.83
SGW13	13	260.7	51.17	233.9	31.36
SGW16	16	262.5	47.05	236.2	30.49

Table 4.5
Thermal properties (from DSC measurements) of glass fibre composite at various conditions

Sample	V_f (%)	T_m (ºC)	ΔH_m (J/g)	T_c (ºC)	$-\Delta H_m$ (J/g)
SGD0	0	260.1	72.03	233.7	44.52
SG50%RH0		262.5	71.40	235.7	45.68
SGW0		262.9	66.14	236.0	43.11
SGD4	4	260.3	66.51	234.1	41.14
SG50%RH4		261.1	63.85	233.9	40.76
SGW4		261.6	60.03	254.5	36.82
SGD8	8	260.6	59.96	234.1	34.94
SG50%RH8		260.8	58.07	233.8	37.54
SGW8		260.9	55.88	234.3	34.83
SGD13	13	260.9	53.65	234.1	32.38
SG50%RH13		261.1	51.41	234.0	32.04
SGW13		260.7	51.17	233.9	31.36
SGD16	16	262.4	50.30	236.1	30.84
SG50%RH16		262.3	48.88	236.2	30.39
SGW16		262.5	47.05	236.2	30.49

Table 4.6
Thermal properties (from DSC measurements) of carbon fibre composite at various conditions

Sample	**V_f (%)**	**T_m (ºC)**	**ΔH_m (J/g)**	**T_c (ºC)**	**$-\Delta H_m$ (J/g)**
SCD33	33	257.1	34.58	231.4	21.95
SC50%RH33		257.5	35.20	231.5	21.85
SCW33		257.8	34.29	231.6	21.47

Table 4.7
Thermal properties of hybrid composite at dry condition

Sample	**Glass/Carbon**	**V_{fc} (%)**	**V_{fg} (%)**	**V_{ft} (%)**	**T_m (ºC)**	**ΔH_m (J/g)**	**Calculated* ΔH_m (J/g)**	**T_c (ºC)**	**$-\Delta H_m$ (J/g)**	**Calculated* $-\Delta H_m$ (J/g)**
SGD18	100/0	0	18	18	258.9	47.37	47.37	232.7	29.59	29.59
SG75/C25D	75/25	9	13	22	258.7	45.35	44.17	232.3	27.18	27.68
SG50/C50D	50/50	17	9	26	258.5	41.14	40.98	232.9	25.13	25.77
SG25/C75D	25/75	26	4	30	258.0	38.05	37.78	231.9	23.63	23.86
SCD33	0/100	33	0	33	257.1	34.58	34.58	231.4	21.95	21.95

Keynotes:

V_{fc} = volume fraction of carbon fibre in hybrid composites

V_{fg} = volume fraction of glass fibre in hybrid composites

V_{ft} = total volume fraction of fibre in hybrid composites

$V_{ft} = V_{fc} + V_{fg}$

$V_{ft} + V_m = 1$

* Calculated using simple ROM equation

Table 4.8
Thermal properties of hybrid composite at 50% relative humidity condition

Sample	Glass/Carbon	V_{fc} (%)	V_{fg} (%)	V_{ft} (%)	T_m (ºC)	ΔH_m (J/g)	Calculated* ΔH_m (J/g)	T_c (ºC)	$-\Delta H_m$ (J/g)	Calculated* $-\Delta H_m$ (J/g)
SGD18	100/0	0	18	18	259.4	48.97	48.97	232.6	29.25	29.25
SG75/C25D	75/25	9	13	22	259.2	42.89	45.53	232.9	27.24	27.40
SG50/C50D	50/50	17	9	26	258.9	40.49	40.73	232.4	25.63	25.55
SG25/C75D	25/75	26	4	30	258.5	37.47	38.64	232.4	24.59	23.70
SCD33	0/100	33	0	33	257.5	35.20	35.20	231.5	21.85	21.85

Table 4.9
Thermal properties of hybrid composite at wet condition

Sample	**Glass/Carbon**	**V_{fc} (%)**	**V_{fg} (%)**	**V_{ft} (%)**	**T_m (ºC)**	**ΔH_m (J/g)**	**Calculated* ΔH_m (J/g)**	**T_c (ºC)**	**$-\Delta H_m$ (J/g)**	**Calculated* $-\Delta H_m$ (J/g)**
SGD18	100/0	0	18	18	260.0	44.39	44.39	233.5	27.98	27.98
SG75/C25D	75/25	9	13	22	259.9	42.14	41.87	233.8	25.79	26.35
SG50/C50D	50/50	17	9	26	259.2	40.25	39.34	233.1	25.37	24.73
SG25/C75D	25/75	26	4	30	258.4	36.62	36.81	232.6	23.43	23.09
SCD33	0/100	33	0	33	257.8	34.29	34.29	231.6	21.47	21.47

Table 4.10
Thermal properties of hybrid composite at various conditions

Sample	Glass/Carbon	T_m (ºC)	ΔH_m (J/g)	T_c (ºC)	$-\Delta H_m$ (J/g)
SGD18	100/0	258.9	47.37	232.7	29.59
SG50%RH18		259.4	48.97	232.6	29.25
SGW18		260.0	44.39	233.5	27.98
SG75/C25D	75/25	258.7	45.35	232.3	27.18
SG75/C25,50%RH		259.2	42.89	232.9	27.24
SG75/C25W		259.9	42.14	233.8	25.79
SG50/C50D	50/50	258.5	41.14	232.9	25.13
SG50/C50, 50%RH		258.9	40.49	232.4	25.63
SG50/C50W		259.2	40.25	233.1	25.37
SG25/C75D	25/75	258.0	38.05	231.9	23.63
SG25/C75, 50%RH		258.5	37.47	232.4	24.59
SG25/C75W		258.4	36.62	232.6	23.43
SCD33	0/100	257.1	34.58	231.4	21.95
SC50%RH33		257.5	35.20	231.5	21.85
SCW33		257.8	34.29	231.6	21.47

Table 4.11
Thermomechanical data of glass fibre composite at dry condition

Sample	**V_f (%)**	**tan δ_{25}[A] (x 10^{-2})**	**α- transition**		**β-transition**	
			tan δ_{max}[B] (x 10^{-2})	**T_α[C] (˚C)**	**tan δ_{max}[B] (x 10^{-2})**	**T_β[D] (˚C)**
SGD0	0	5.12	8.21	55	3.83	-70
SGD4	4	1.24	7.40	68	3.37	-63
SGD8	8	0.87	5.87	68	2.67	-64
SGD13	13	0.93	5.22	71	2.40	-63
SGD16	16	3.45	4.32	52	2.41	-69

Keynotes:

A: loss tangent value at the temperature of 25ºC

B: maximum value of loss tangent

C: temperature at the maximum value of tan δ in α-transition

D: temperature at the maximum value of tan δ in β-transition

Table 4.12
Thermomechanical data of glass fibre composite at 50% relative humidity condition

Sample	V_f (%)	tan δ_{25}^{A} (x 10^{-2})	α- transition		β-transition	
			tan δ_{max}^{B} (x 10^{-2})	T_α^{C} (˚C)	tan δ_{max}^{B} (x 10^{-2})	T_β^{D} (˚C)
SG50%RH0	0	9.43	10.10	17	3.98	-74
SG50%RH4	4	7.24	7.72	18	3.74	-74
SG50%RH8	8	5.24	5.50	19	2.68	-75
SG50%RH13	13	4.65	4.85	19	2.43	-75
SG50%RH16	16	4.03	4.50	11	2.12	-76

Table 4.13
Thermomechanical data of glass fibre composite at wet condition

Sample	V_f (%)	tan δ_{25}^{A} (x 10^{-2})	α- transition		β-transition	
			tan δ_{max}^{B}(x 10^{-2})	T_α^{C} (˚C)	tan δ_{max}^{B} (x 10^{-2})	T_β^{D} (˚C)
SGW0	0	5.71	11.43	-13	-	-
SGW4	4	3.80	9.48	-17	-	-
SGW8	8	3.08	7.38	-19	-	-
SGW13	13	2.72	6.18	-18	-	-
SGW16	16	3.27	5.93	-16	-	-

Table 4.14
Thermomechanical data of glass fibre composite at various conditions

V_f (%)	Sample	Condition	tan δ_{25} [A] (x 10^{-2})	α- transition		β-transition	
				tan δ_{max} [B] (x 10^{-2})	T_α [C] (˚C)	tan δ_{max} [B] (x 10^{-2})	T_β [D] (˚C)
0	SGD0	Dry	5.12	8.21	55	3.83	-70
	SG50%RH0	50%RH	9.43	10.10	17	3.98	-74
	SGW0	Wet	5.71	11.43	-13	-	-
4	SGD4	Dry	1.24	7.40	68	3.37	-63
	SG50%RH4	50%RH	7.24	7.72	18	3.74	-74
	SGW4	Wet	3.80	9.48	-17	-	-
8	SGD8	Dry	0.87	5.87	68	2.67	-64
	SG50%RH8	50%RH	5.24	5.50	19	2.68	-74
	SGW8	Wet	3.08	7.38	-19	-	-
13	SGD13	Dry	0.93	5.22	71	2.40	-63
	SG50%RH13	50%RH	4.65	4.85	19	2.43	-75
	SGW13	Wet	2.72	6.18	-18	-	-
16	SGD16	Dry	0.35	4.32	52	2.41	-69
	SG50%RH16	50%RH	4.03	4.50	11	2.12	-76
	SGW16	Wet	3.27	5.93	-16	-	-

Table 4.15
Thermomechanical data of carbon fibre composite at various conditions

V_f (%)	Sample	Condition	tan δ_{25}[A] (x 10^{-2})	α- transition		β-transition	
				tan δ_{max}[B] (x 10^{-2})	T_α[C] (°C)	tan δ_{max}[B] (x 10^{-2})	T_β[D] (°C)
33	SCD33	Dry	1.10	4.83	69	1.66	-66
		50%RH	4.17	4.65	19	1.58	-76
		Wet	3.98	5.44	-11	-	-

Table 4.16

Thermomechanical data of hybrid composite at dry condition

Sample	Glass/Carbon	tan δ_{25} [A] (x 10^{-2})	α- transition		β-transition	
			tan δ_{max} [B] (x 10^{-2})	T_{α} [C] (˚C)	tan δ_{max} [B] (x 10^{-2})	T_{β} [D] (˚C)
SGD18	100/0	0.82	4.72	69	1.88	-64
SG75/C25D	75/25	1.05	5.09	66	1.89	-66
SG50/C50D	50/50	0.83	5.07	67	1.77	-66
SG25/C75D	25/75	1.15	5.07	66	1.72	-66
SCD33	0/100	1.10	4.83	69	1.66	-66

Table 4.17
Thermomechanical data of hybrid composite at 50% relative humidity condition

Sample	Glass/Carbon	tan δ_{25}^{A} (x 10^{-2})	α- transition		β-transition	
			tan δ_{max}^{B} (x 10^{-2})	T_{α}^{C} (°C)	tan δ_{max}^{B} (x 10^{-2})	T_{β}^{D}(°C)
SG50%RH18	100/0	4.86	5.10	18	2.05	-76
SG75/C25, 50%RH	75/25	4.42	4.79	16	1.86	-77
SG50/C50, 50%RH	50/50	4.35	4.57	18	1.77	-76
SG25/C75, 50%RH	25/75	4.36	4.60	17	1.59	-75
SC50%RH 33	0/100	4.17	4.65	19	1.58	-76

Table 4.18

Thermomechanical data of hybrid composite at wet condition

Sample	Glass/Carbon	tan δ_{25}[A] (x 10^{-2})	α- transition		β-transition	
			tan δ_{max}[B] (x 10^{-2})	T_α[C] (°C)	tan δ_{max}[B] (x 10^{-2})	T_β[D] (°C)
SGW18	100/0	2.80	5.37	-16	-	-
SG75/C25W	75/25	3.02	5.59	-14	-	-
SG50/C50W	50/50	3.30	5.52	-13	-	-
SG25/C75W	25/75	3.47	5.46	-12	-	-
SCW33	0/100	3.98	5.44	-11	-	-

Table 4.19
Thermomechanical data of hybrid composite at various conditions

Glass/Carbon	Sample	Condition	tan δ_{25} [A] (x 10^{-2})	α- transition		β-transition	
				tan δ_{max} [B] (x 10^{-2})	T_α [C] (˚C)	tan δ_{max} [B] (x 10^{-2})	T_β [D] (˚C)
100/0	SGD18	Dry	0.82	4.72	69	1.88	-64
	SG50%RH18	50%RH	4.86	5.10	18	2.05	-76
	SGW18	Wet	2.80	5.37	-16	-	-
75/25	SG75/C25D	Dry	1.05	5.09	66	1.89	-66
	SG75/C25, 50%RH	50%RH	4.42	4.79	16	1.86	-77
	SG75/C25W	Wet	3.02	5.59	-14	-	-
50/50	SG50/C50D	Dry	0.83	5.07	67	1.77	-66
	SG50/C50, 50%RH	50%RH	4.35	4.57	18	1.77	-76
	SG50/C50W	Wet	3.30	5.52	-13	-	-
25/75	SG25/C75D	Dry	1.15	5.07	67	1.72	-66
	SG25/C75, 50%RH	50%RH	4.36	4.60	17	1.59	-74
	SG25/C75W	Wet	3.47	5.44	-12	-	-
0/100	SCD33	Dry	1.10	4.83	69	1.66	-66
	SC50%RH33	50%RH	4.17	4.65	19	1.58	-76
	SCW33	Wet	3.98	5.44	-11	-	-

Table 4.20
The fibre characteristics of glass fibre composites

Sample	V_f (%)	Percentage of fibre with length, L			L_n (mm)	L_w (mm)
		L< 0.2 mm	L< 0.4 mm	L< 0.6 mm		
SG4	4	20.5	74.9	93.4	0.33	0.41
SG8	8	22.0	78.2	96.6	0.31	0.38
SG13	13	22.2	75.0	93.3	0.33	0.42
SG16	16	33.0	83.4	98.3	0.27	0.34
SG18	18	45.4	94.3	99.7	0.23	0.27

Table 4.21
Tensile properties of glass fibre composites at different condition

Sample	V_f (%)	Tensile strength (MPa)			Tensile modulus (GPa)			Fracture strain (%)		
		Dry	50%RH	Wet	Dry	50%RH	Wet	Dry	50%RH	Wet
SG0	0	53.11	49.80	35.30	0.71	0.62	0.38	231.20	348.99	148.69
SG4	4	88.72	59.91	43.26	1.64	0.62	0.38	6.94	33.15	29.54
SG8	8	121.37	74.52	58.65	2.42	1.25	0.73	8.03	15.98	14.62
SG13	13	151.62	118.18	72.42	3.06	1.79	1.29	8.96	9.38	10.29
SG16	16	159.17	104.37	84.85	3.81	2.81	2.31	8.18	9.92	9.64

Table 4.22
Tensile properties of carbon fibre composites at different condition

V_f (%)	Sample	Condition	Tensile strength (MPa)	Tensile modulus (GPa)	Fracture strain (%)
33	SCD33	DRY	227.55	7.04	5.55
	SC50%RH33	50%RH	188.36	5.04	6.07
	SCW33	Wet	117.76	4.45	7.19

Table 4.23
Tensile properties of glass/carbon hybrid fibre composites at different condition

Sample	Composition of carbon fibre composites (%)	Tensile strength (MPa)					
		Dry		50%RH		Wet	
		Experimental	Calculated*	Experimental	Calculated*	Experimental	Calculated*
SG18	0	168.81	168.81	130.31	130.31	90.55	90.55
SG75/C25	25	173.51	185.00	129.44	144.50	90.75	98.25
SG50/C50	50	184.64	200.00	144.76	159.00	101.71	105.50
SG25/C75	75	201.94	215.00	155.92	174.50	113.06	112.75
SC33	100	227.55	227.55	188.36	188.36	117.76	117.76

* Calculated using simple ROM equation

Table 4.24
Tensile properties of glass/carbon hybrid fibre composites at different condition

Sample	Composition of carbon fibre composites (%)	Tensile modulus (GPa)					
		Dry		50%RH		Wet	
		Experimental	Calculated*	Experimental	Calculated*	Experimental	Calculated*
SG18	0	3.65	3.65	2.63	2.63	2.01	2.01
SG75/C25	25	4.64	4.51	3.70	3.23	2.45	2.61
SG50/C50	50	5.84	5.32	4.66	3.77	3.45	3.24
SG25/C75	75	6.39	6.24	4.47	4.40	3.97	3.79
SC33	100	7.04	7.04	5.04	5.04	4.45	4.45

Table 4.25
Tensile properties of glass/carbon hybrid fibre composites at different condition

Sample	Composition of carbon fibre composites (%)	Fracture strain (%)					
		Dry		50%RH		Wet	
		Experimental	Calculated*	Experimental	Calculated*	Experimental	Calculated*
SG18	0	9.00	9.00	10.46	10.46	11.74	11.74
SG75/C25	25	6.93	8.12	7.69	9.43	8.47	10.79
SG50/C50	50	6.65	7.32	6.70	8.33	8.54	9.51
SG25/C75	75	6.05	6.40	6.41	7.01	7.59	8.33
SC33	100	5.55	5.55	6.07	6.07	7.19	7.19

Table 4.26
Flexural properties of glass fibre composites at different condition

Sample	V_f (%)	Flexural strength (MPa)			Flexural modulus (GPa)			Flexural displacement (mm/mm)		
		Dry	50%RH	Wet	Dry	50%RH	Wet	Dry	50%RH	Wet
SG0	0	140.08	110.38	81.98	2.23	1.14	0.52	0.09	0.13	0.20
SG4	4	115.52	147.30	46.08	2.59	1.23	0.79	0.07	0.12	0.09
SG8	8	168.07	191.15	81.06	3.81	2.67	1.49	0.07	0.10	0.08
SG13	13	219.59	231.51	105.72	5.55	3.72	2.39	0.05	0.09	0.06
SG16	16	272.32	251.04	189.65	6.40	4.70	3.20	0.05	0.07	0.08

Table 4.27
Flexural properties of carbon fibre composites at different condition

V_f (%)	Sample	Condition	Flexural strength (MPa)	Flexural modulus (GPa)	Flexural displacement (mm/mm)
33	SCD33	DRY	432.22	27.14	0.02
	SC50%RH33	50%RH	363.32	14.01	0.04
	SCW33	Wet	255.43	9.29	0.04

Table 4.28
The experimental and calculated flexural strength of hybrid fibre composites

Sample	Composition of carbon fibre composites (%)	Flexural strength (MPa)					
		Dry		50%RH		Wet	
		Experimental	Calculated*	Experimental	Calculated*	Experimental	Calculated*
SG18	0	323.92	323.92	240.10	240.10	199.78	199.78
SG75/C25	25	349.94	356.25	280.16	271.25	212.83	215.05
SG50/C50	50	375.04	387.50	313.93	302.50	227.40	230.94
SG25/C75	75	407.32	418.75	331.32	333.75	243.25	245.44
SC33	100	432.22	432.22	363.32	363.32	255.43	255.43

* Calculated using simple ROM equation

Table 4.29
The experimental and calculated flexural modulus of hybrid fibre composites

Sample	Composition of carbon fibre composites (%)	Flexural modulus (GPa)					
		Dry		50%RH		Wet	
		Experimental	Calculated*	Experimental	Calculated*	Experimental	Calculated*
SG18	0	7.61	7.61	4.22	4.22	3.36	3.36
SG75/C25	25	10.67	13.53	6.23	7.25	4.54	5.53
SG50/C50	50	14.37	19.09	8.36	9.50	5.86	7.04
SG25/C75	75	18.38	24.51	10.37	11.75	7.14	8.55
SC33	100	27.14	27.14	14.01	14.01	9.29	9.29

Table 4.30
The experimental and calculated flexural displacement of hybrid fibre composites

Sample	Composition of carbon fibre composites (%)	Flexural displacement (mm/mm)					
		Dry		50%RH		Wet	
		Experimental	Calculated*	Experimental	Calculated*	Experimental	Calculated*
SG18	0	0.05	0.05	0.09	0.09	0.08	0.08
SG75/C25	25	0.04	0.05	0.06	0.08	0.06	0.07
SG50/C50	50	0.03	0.04	0.05	0.07	0.05	0.06
SG25/C75	75	0.03	0.03	0.04	0.05	0.04	0.05
SC33	100	0.02	0.02	0.04	0.04	0.04	0.04

Table 4.31
The average values of fracture energy, peak load and notch to depth ratio of glass fibre composites at dry condition

Sample	V_f (%)	a/D	Fracture energy (mJ)	Peak load (N)
SGD0	0	0.1	536.13	836.50
		0.2	313.24	658.92
		0.3	227.18	523.03
		0.4	198.40	464.52
SGD4	4	0.1	127.38	506.12
		0.2	120.77	452.10
		0.3	90.58	421.42
		0.4	74.46	296.35
SGD8	8	0.1	308.86	817.76
		0.2	212.57	613.76
		0.3	150.47	503.70
		0.4	123.07	406.47
SGD13	13	0.1	642.90	1144.63
		0.2	332.32	816.66
		0.3	210.26	553.80
		0.4	188.96	522.33
SGD16	16	0.1	613.13	1743.74
		0.2	360.52	1289.25
		0.3	281.33	957.69
		0.4	226.42	822.66

Table 4.32

The average values of fracture energy, peak load and notch to depth ratio of glass fibre composites at 50% relative humidity condition

Sample	V_f (%)	a/D	Fracture energy (mJ)	Peak load (N)
SG50%RH0	0	0.1	2281.00	1257.53
		0.2	1228.85	934.44
		0.3	803.81	696.57
		0.4	721.04	580.49
SG50%RH4	4	0.1	309.44	771.80
		0.2	203.56	603.42
		0.3	152.63	523.72
		0.4	107.56	389.33
SG50%RH 8	8	0.1	680.98	1172.12
		0.2	320.54	794.26
		0.3	231.60	719.86
		0.4	169.68	416.53
SG50%RH13	13	0.1	1116.53	1660.90
		0.2	560.54	1213.95
		0.3	358.28	906.64
		0.4	253.90	610.44
SG50%RH16	16	0.1	1220.93	1723.15
		0.2	787.17	1343.51
		0.3	525.15	955.51
		0.4	295.40	624.21

Table 4.33
The average values of fracture energy, peak load and notch to depth ratio of glass fibre composites at wet condition

Sample	V_f (%)	a/D	Fracture energy (mJ)	Peak load (N)
SGW0	0	0.1	5726.40	965.18
		0.2	3033.95	765.99
		0.3	1883.62	587.60
		0.4	1347.55	483.10
SGW4	4	0.1	1875.55	960.16
		0.2	1221.80	742.03
		0.3	837.97	566.38
		0.4	622.87	447.38
SGW8	8	0.1	1774.80	1147.61
		0.2	1137.85	870.02
		0.3	739.88	669.88
		0.4	547.80	509.01
SGW13	13	0.1	1814.05	1334.71
		0.2	1232.81	1043.46
		0.3	974.34	759.63
		0.4	907.90	567.18
SGW16	16	0.1	1647.62	1520.13
		0.2	1265.93	1212.35
		0.3	728.15	805.90
		0.4	709.25	647.12

Table 4.34

The critical strain energy release rate, G_c and the critical stress intensity factor, K_c values of glass fibre composites at dry condition

Sample	**V_f (%)**	**a/D**	**G_c (kJm^{-2})**	**K_c($MPa\sqrt{m}$)**
SGD0	0	0.1 0.2 0.3 0.4	9.12	4.55
SGD4	4	0.1 0.2 0.3 0.4	2.82	3.14
SGD8	8	0.1 0.2 0.3 0.4	5.75	4.48
SGD13	13	0.1 0.2 0.3 0.4	10.52	5.91
SGD16	16	0.1 0.2 0.3 0.4	10.83	9.40

Table 4.35
The critical strain energy release rate, G_c and the critical stress intensity factor, K_c values of glass fibre composites at 50% relative humidity condition

Sample	**V_f (%)**	**a/D**	**G_c (kJm^{-2})**	**K_c($MPa\sqrt{m}$)**
SG50%RH0	0	0.1 0.2 0.3 0.4	42.07	6.53
SG50%RH4	4	0.1 0.2 0.3 0.4	6.41	4.34
SG50%RH 8	8	0.1 0.2 0.3 0.4	12.27	5.99
SG50%RH13	13	0.1 0.2 0.3 0.4	20.04	8.47
SG50%RH16	16	0.1 0.2 0.3 0.4	24.92	8.04

Table 4.36
The critical strain energy release rate, G_c and the critical stress intensity factor, K_c values of glass fibre composites at wet condition

Sample	V_f (%)	a/D	G_c (kJm^{-2})	K_c ($MPa\sqrt{m}$)
SGW0	0	0.1 0.2 0.3 0.4	102.10	5.19
SGW4	4	0.1 0.2 0.3 0.4	38.64	5.24
SGW8	8	0.1 0.2 0.3 0.4	35.77	6.16
SGW13	13	0.1 0.2 0.3 0.4	40.72	7.16
SGW16	16	0.1 0.2 0.3 0.4	36.57	8.07

Table 4.37
The average values of fracture energy, peak load and notch to depth ratio of carbon fibre composites at various conditions

Sample	V_f (%)	a/D	Fracture energy (mJ)	Peak load (N)
SCD33	33	0.1	686.02	2371.78
		0.2	320.15	1708.68
		0.3	258.54	1007.60
		0.4	225.58	865.60
SC50%RH33		0.1	683.91	2178.80
		0.2	420.53	1514.80
		0.3	341.99	1223.20
		0.4	253.03	892.50
SCW33		0.1	1077.00	1642.30
		0.2	803.90	1244.14
		0.3	631.83	1075.14
		0.4	507.46	890.54

Table 4.38
The critical strain energy release rate, G_c and the critical stress intensity factor, K_c values of carbon fibre composites at various condition

Sample	**V_f (%)**	**G_c (kJm^{-2})**	**K_c($MPa\sqrt{m}$)**
SCD33	33	11.27	11.50
SC50%RH33		14.57	11.17
SCW33		24.55	8.99

Table 4.39
The average values of fracture energy, peak load and notch to depth ratio of hybrid composites at dry condition

Sample	Composition of carbon composites (%)	a/D	Fracture energy (mJ)	Peak load (N)
SGD18	0	0.1 0.2 0.3 0.4	711.83 456.41 270.45 219.03	1779.08 1146.27 746.13 534.54
SG75/C25D	25	0.1 0.2 0.3 0.4	781.10 368.05 334.50 194.10	1850.04 1365.60 966.87 685.57
SG50/C50D	50	0.1 0.2 0.3 0.4	1014.73 643.46 271.55 215.90	2391.03 1764.14 1046.55 1001.05
SG25/C75D	75	0.1 0.2 0.3 0.4	720.67 336.22 268.07 222.80	2086.76 1659.18 1286.28 738.38
SCD33	100	0.1 0.2 0.3 0.4	686.02 320.15 258.54 225.58	2371.78 1708.68 1007.60 865.60

Table 4.40
The average values of fracture energy, peak load and notch to depth ratio of hybrid composites at 50% relative humidity condition

Sample	Composition of carbon composites (%)	a/D	Fracture energy (mJ)	Peak load (N)
SG50%RH18	0	0.1 0.2 0.3 0.4	1487.20 902.63 443.43 359.37	2069.80 1267.40 915.70 784.33
SG75/C25,50%RH	25	0.1 0.2 0.3 0.4	1490.67 829.73 397.95 375.40	2338.70 1707.23 1047.15 925.33
SG50/C50,50%RH	50	0.1 0.2 0.3 0.4	1385.12 606.53 532.30 299.73	2350.40 1611.37 1356.36 912.72
SG25/C75,50%RH	75	0.1 0.2 0.3 0.4	950.82 550.40 337.92 268.70	2336.10 1730.55 1191.87 962.13
SC50%RH33	100	0.1 0.2 0.3 0.4	683.91 420.53 341.99 253.03	2178.80 1514.80 1223.23 892.57

Table 4.41
The average values of fracture energy, peak load and notch to depth ratio of hybrid composites at wet condition

Sample	Composition of carbon composites (%)	a/D	Fracture energy (mJ)	Peak load (N)
SGW18	0	0.1	1796.80	1365.30
		0.2	1207.68	1119.84
		0.3	1052.08	802.74
		0.4	991.56	675.14
SG75/C25W	25	0.1	1526.30	1577.57
		0.2	1177.68	1275.65
		0.3	949.16	918.33
		0.4	716.97	691.58
SG50/C50W	50	0.1	1859.90	1818.36
		0.2	970.94	1299.48
		0.3	599.92	911.60
		0.4	728.30	657.98
SG25/C75W	75	0.1	1335.66	1737.43
		0.2	882.91	1333.22
		0.3	645.14	963.82
		0.4	636.46	667.82
SCW33	100	0.1	1077.00	1642.30
		0.2	803.90	1244.14
		0.3	631.83	1075.14
		0.4	507.46	890.54

Table 4.42

The critical strain energy release rate, G_c and the critical stress intensity factor, K_c values of hybrid composites at dry condition

Sample	**Composition of carbon composites (%)**	**G_c (kJm^{-2})**	**K_c($MPa\sqrt{m}$)**
SGD18	0	12.41	8.34
SG75/C25D	25	12.45	9.30
SG50/C50D	50	16.27	11.86
SG25/C75D	75	11.53	10.85
SCD33	100	11.27	11.50

Table 4.43
The critical strain energy release rate, G_c and the critical stress intensity factor, K_c values of hybrid composites at 50% relative humidity condition

Sample	**Composition of carbon composites (%)**	**G_c (kJm^{-2})**	**K_c($MPa\sqrt{m}$)**
SG50%RH18	0	27.72	9.85
SG75/C25,50%RH	25	26.68	11.55
SG50/C50,50%RH	50	24.16	11.71
SG25/C75,50%RH	75	17.86	11.73
SC50%RH33	100	14.57	11.17

Table 4.44
The critical strain energy release rate, G_c and the critical stress intensity factor, K_c values of hybrid composites at wet condition

Sample	Composition of carbon composites (%)	G_c (kJm^{-2})	K_c($MPa\sqrt{m}$)
SGW18	0	41.43	7.60
SG75/C25W	25	34.31	8.34
SG50/C50W	50	35.22	8.97
SG25/C75W	75	28.68	8.90
SCW33	100	24.55	8.99

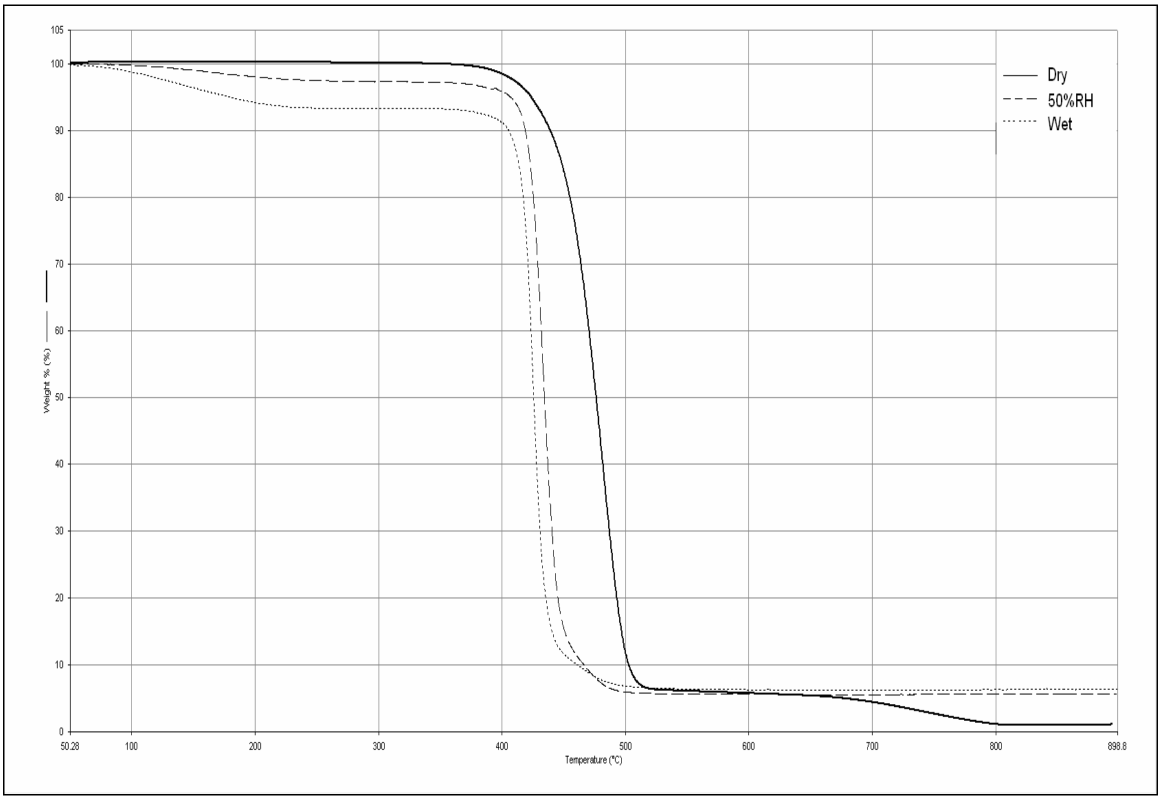

Figure 4.1 TGA thermographs of unreinforced polyamide 6,6 at different conditions

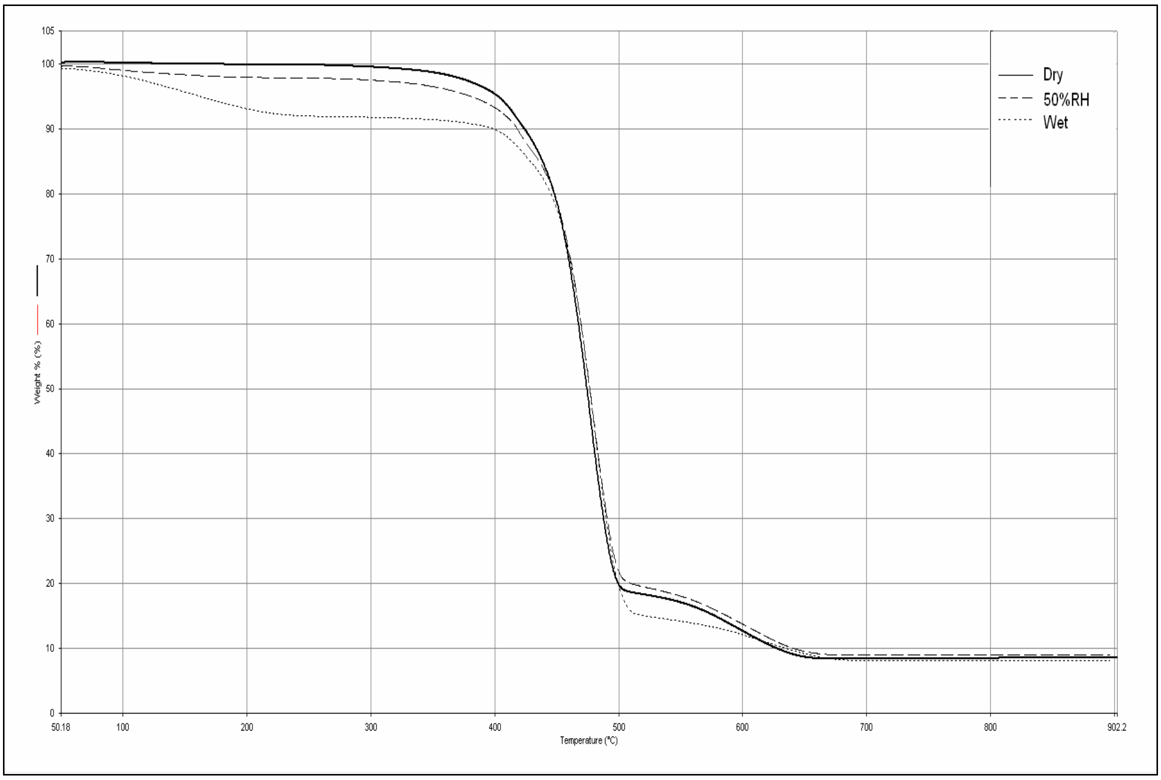

Figure 4.2: TGA thermographs of glass fibre composite (4% V_f) at different conditions

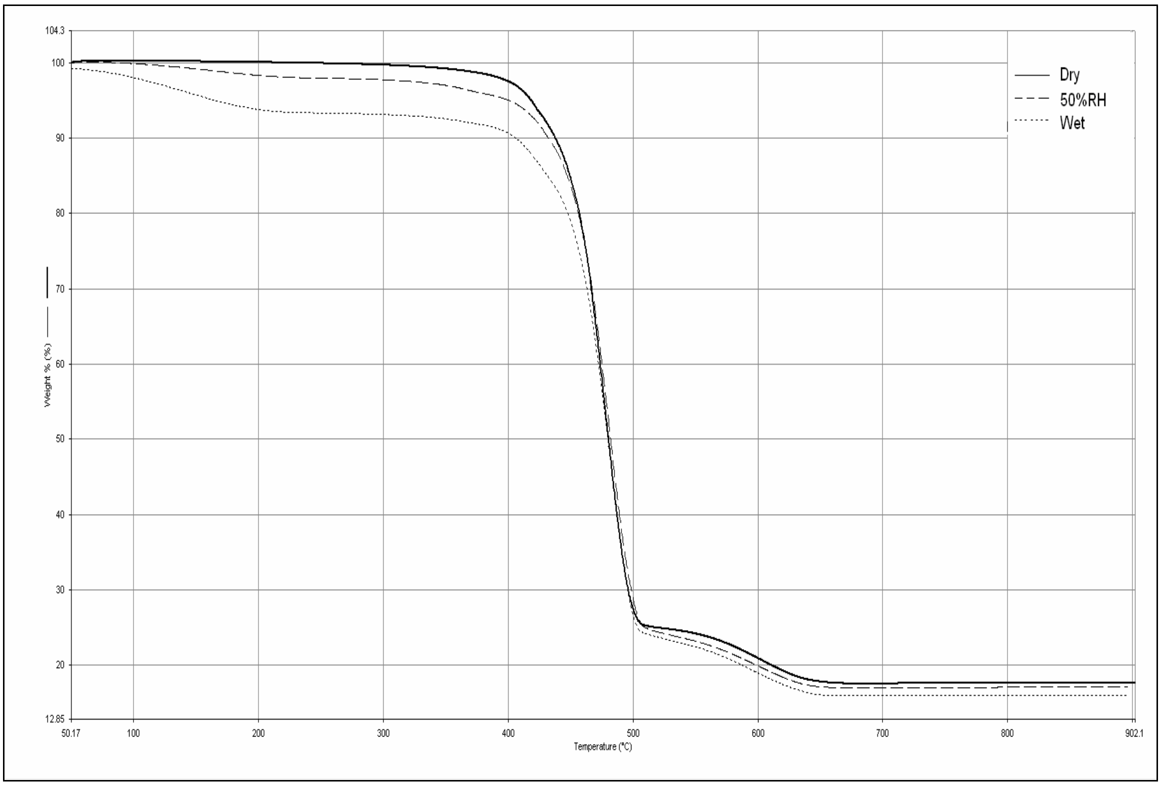

Figure 4.3: TGA thermographs of glass fibre composite (8% V_f) at different conditions

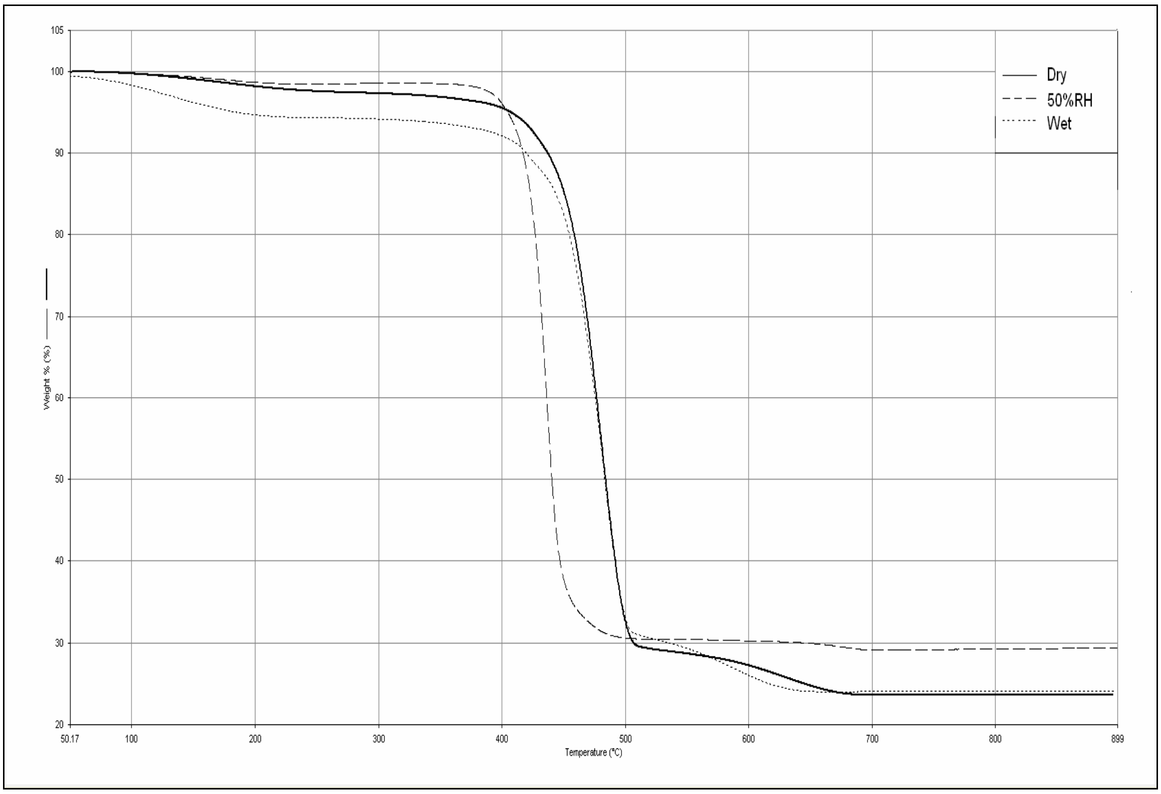

Figure 4.4: TGA thermographs of glass fibre composite (13% V_f) at different conditions

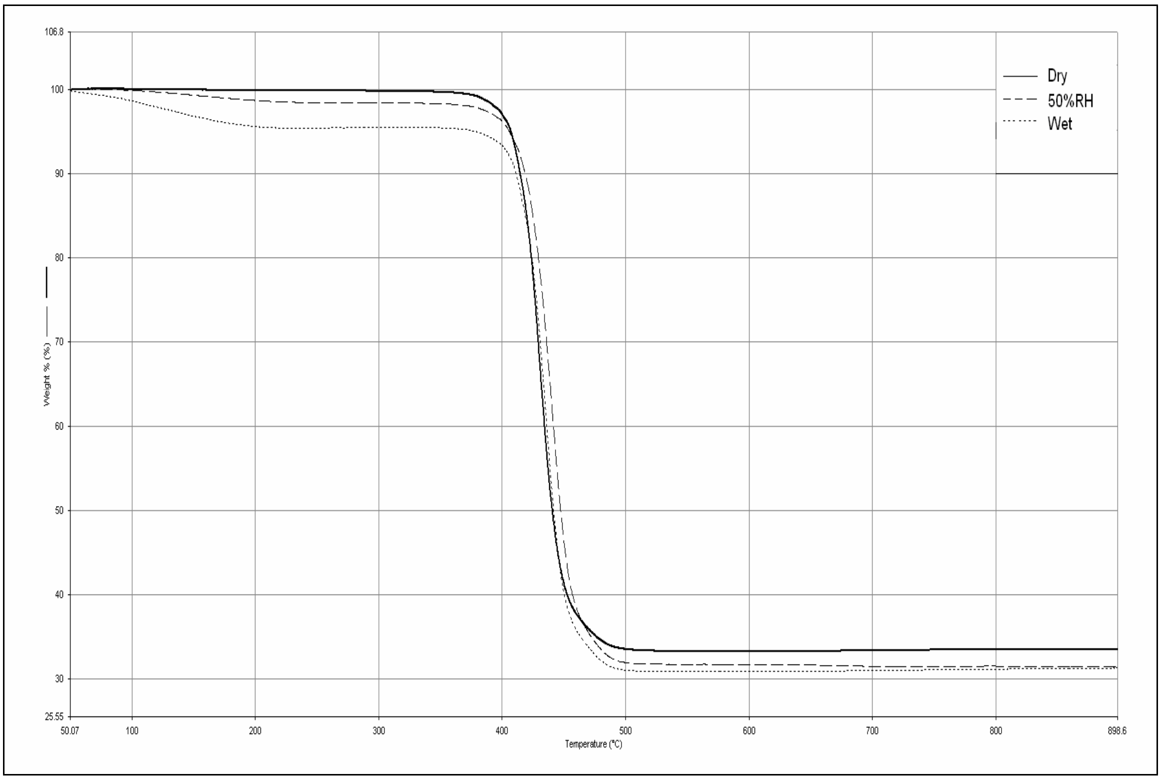

Figure 4.5: TGA thermographs of glass fibre composite (16% V_f) at different conditions

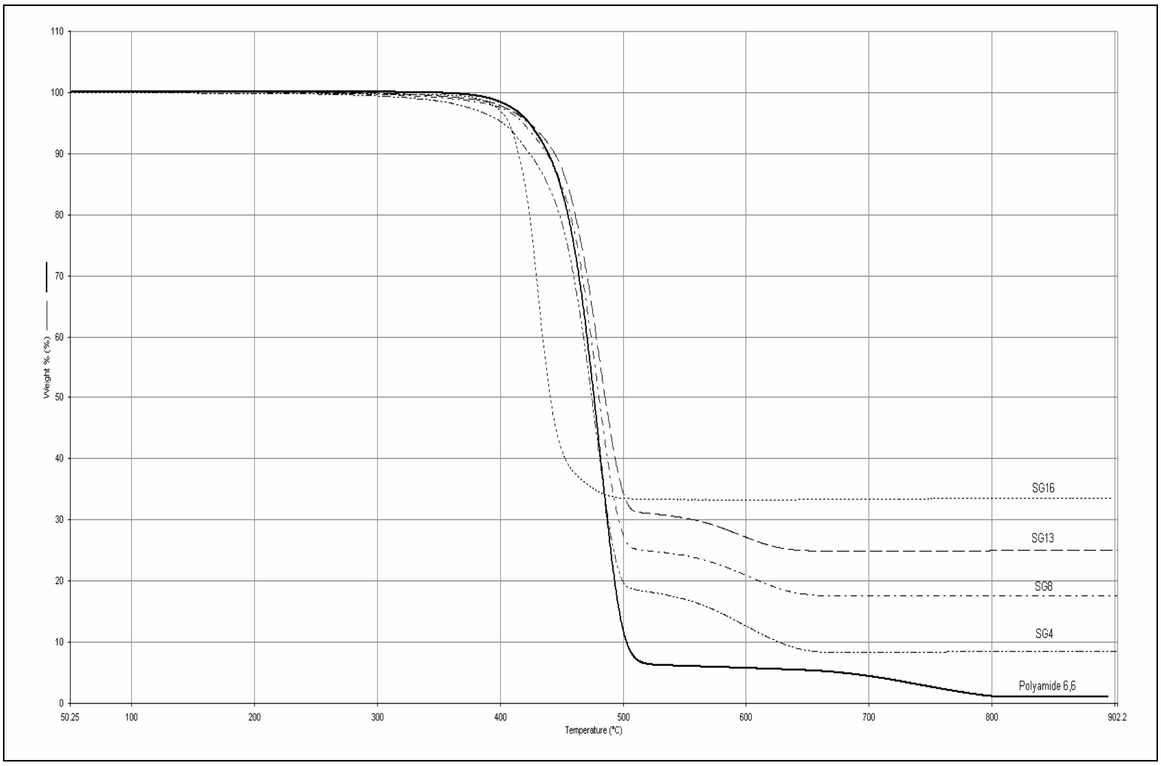

Figure 4.6: TGA thermographs of glass fibre composite at various fibre volume fractions under dry condition

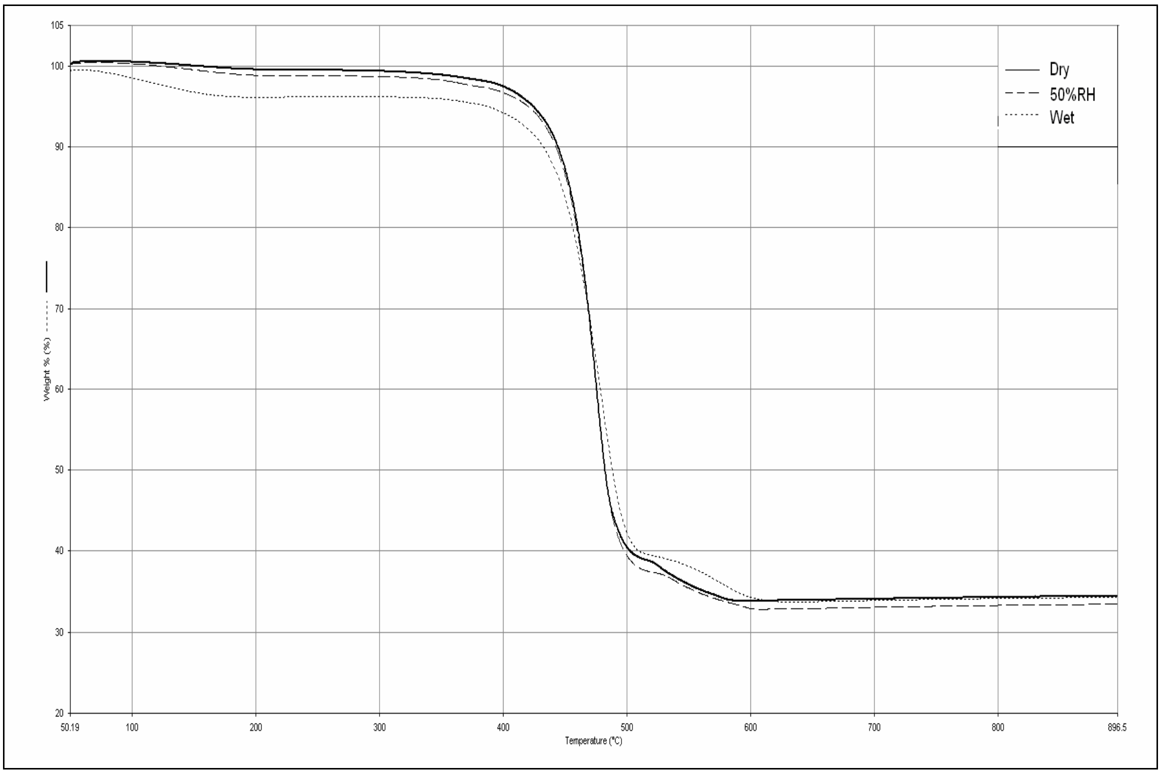

Figure 4.7: TGA thermographs of glass fibre composite (18%V_f) at different conditions

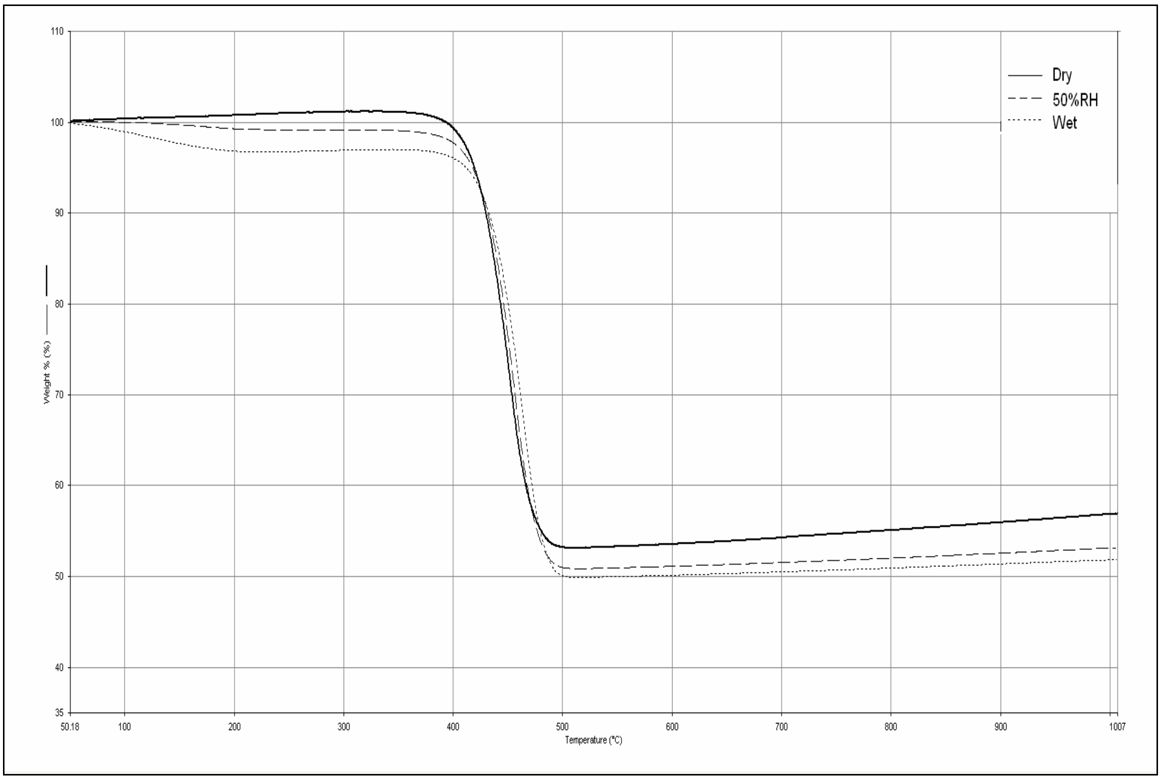

Figure 4.8: TGA thermographs of carbon fibre composite (33%V_f) at different conditions

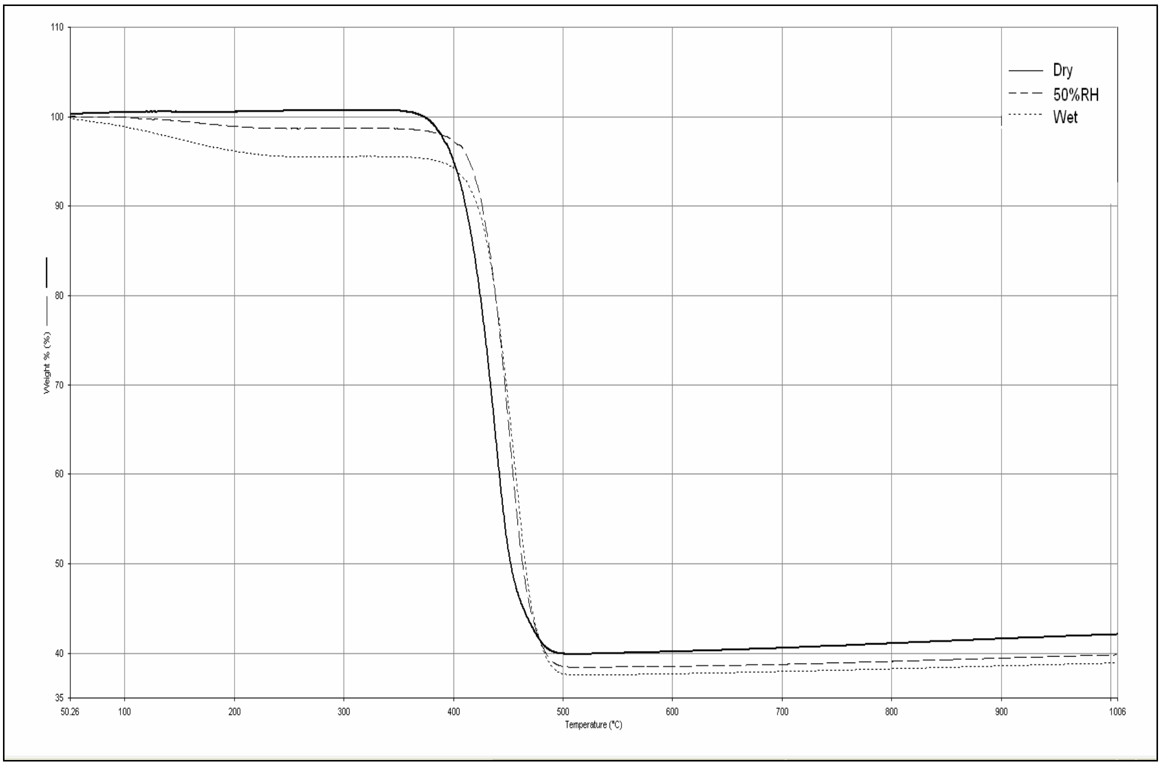

Figure 4.9: TGA thermographs of glass/carbon hybrid fibre composite (SG75/C25) at different conditions

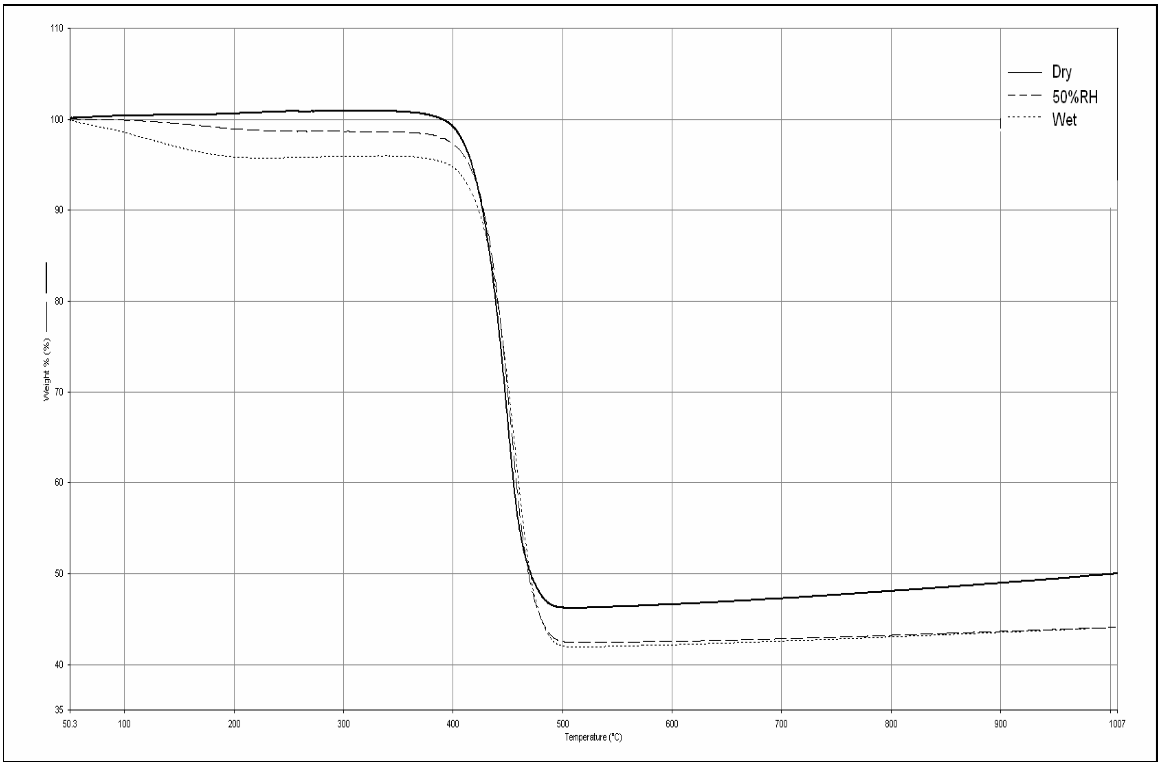

Figure 4.10: TGA thermographs of glass/carbon hybrid fibre composite (SG50/C50) at different conditions

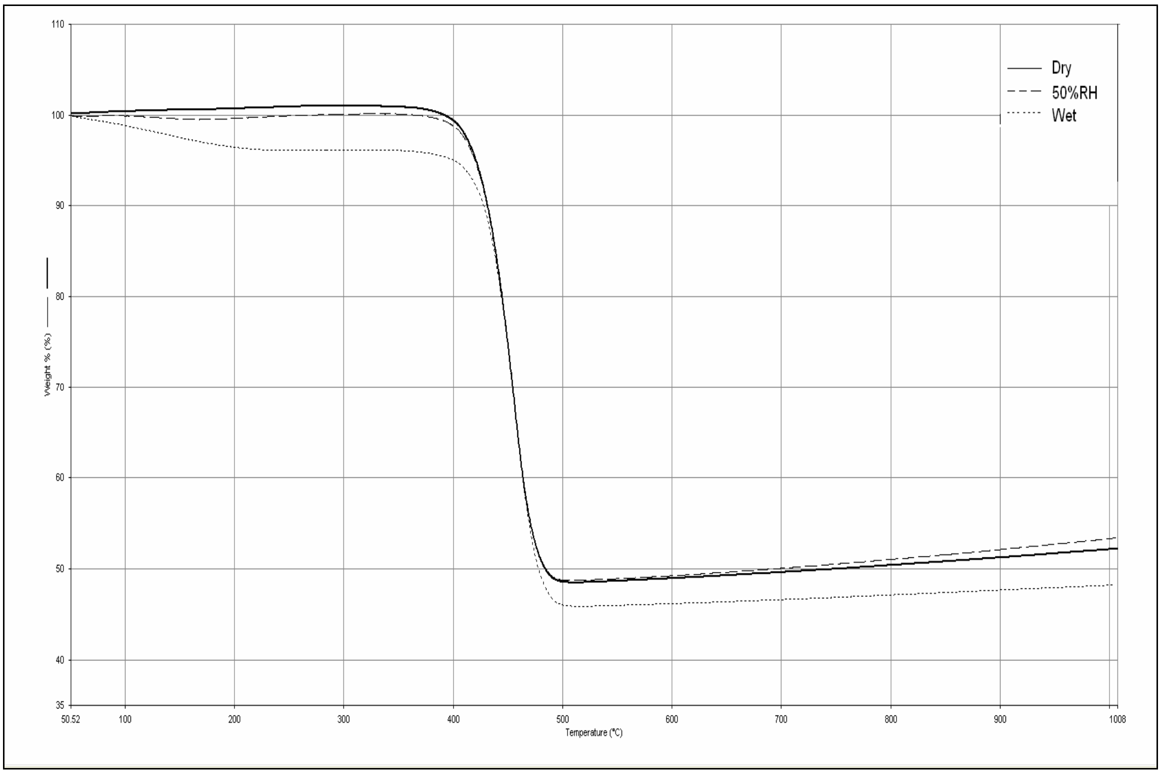

Figure 4.11: TGA thermographs of glass/carbon hybrid fibre composite (SG25/C75) at different conditions

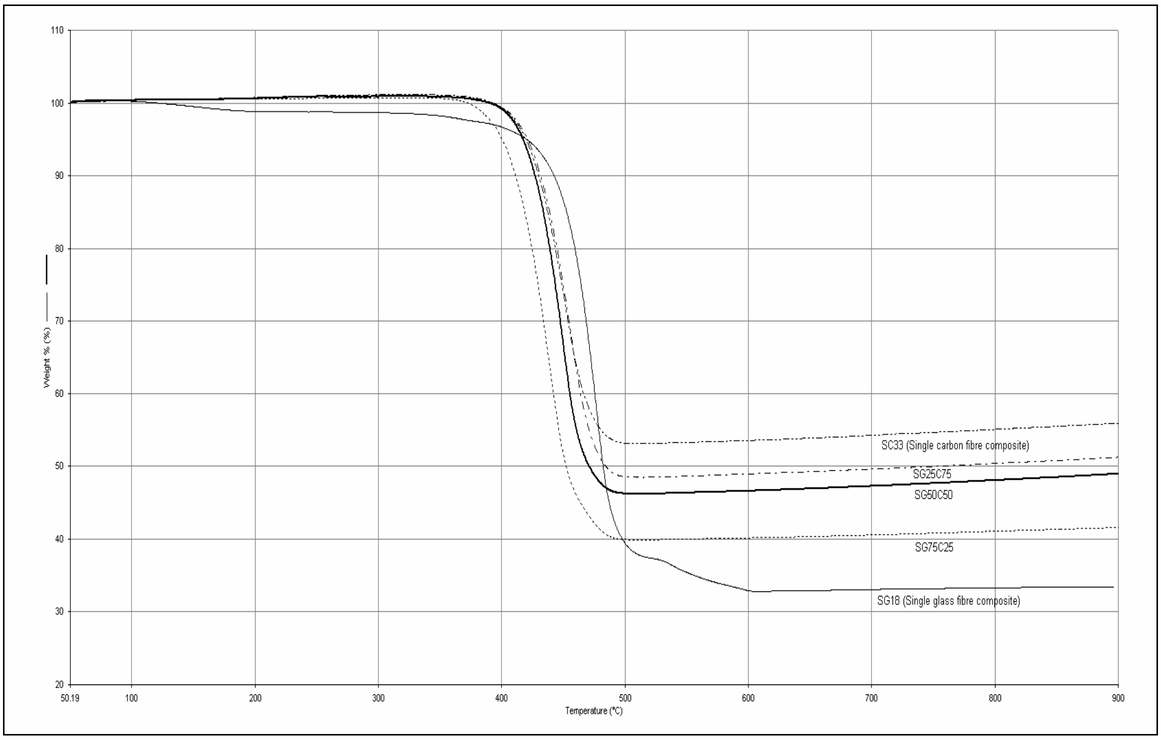

Figure 4.12: TGA thermographs of hybrid composites at different carbon fibre content

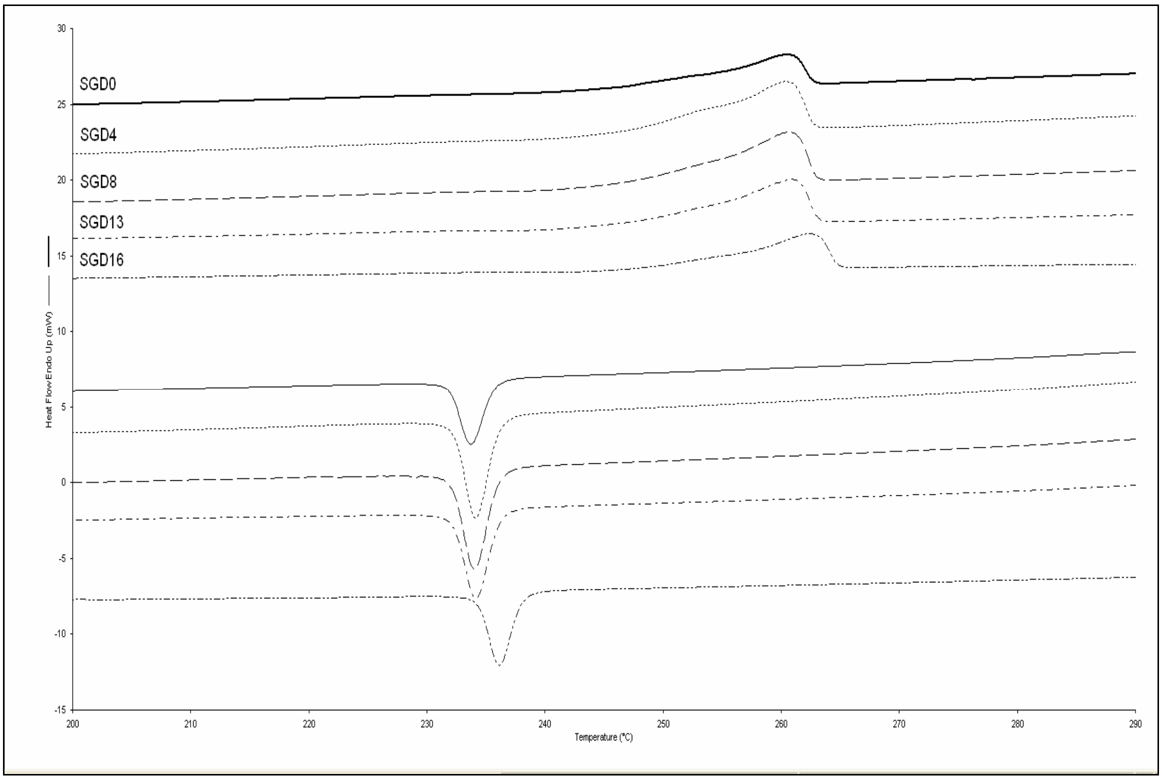

Figure 4.13: DSC results of glass fibre composites with various volume fractions at dry condition

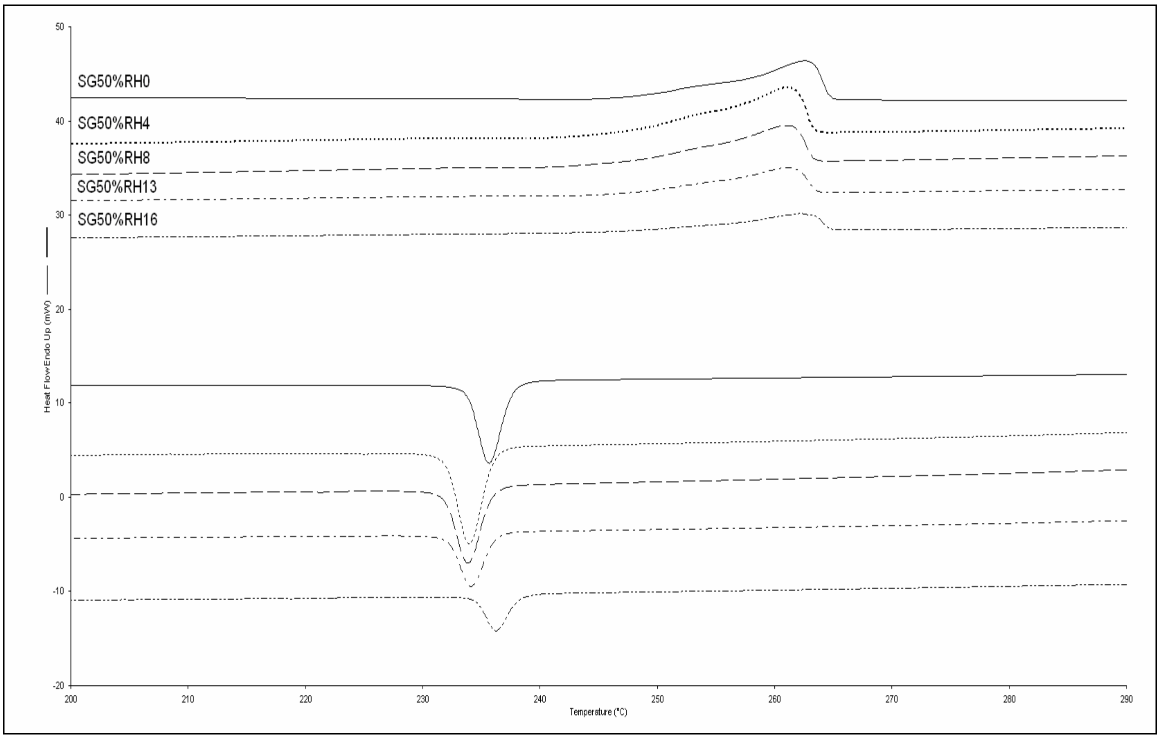

Figure 4.14: DSC results of glass fibre composites with various volume fractions at 50% RH condition

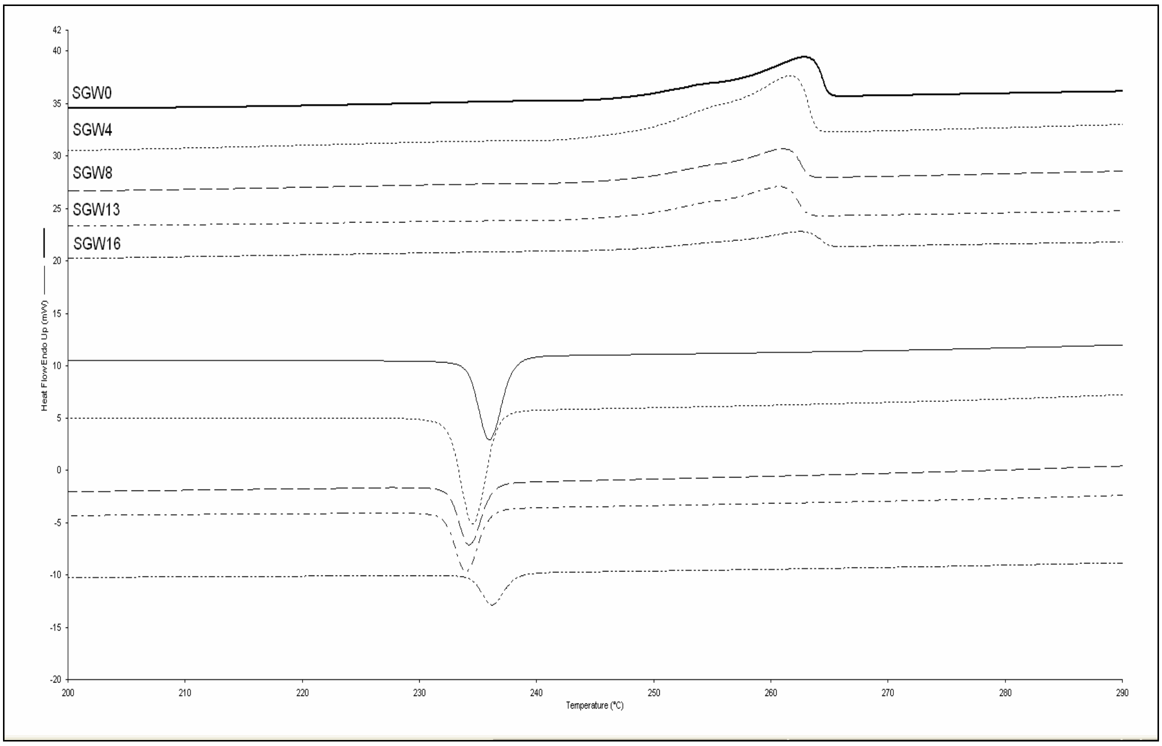

Figure 4.15: DSC results of glass fibre composites with various volume fractions at wet condition

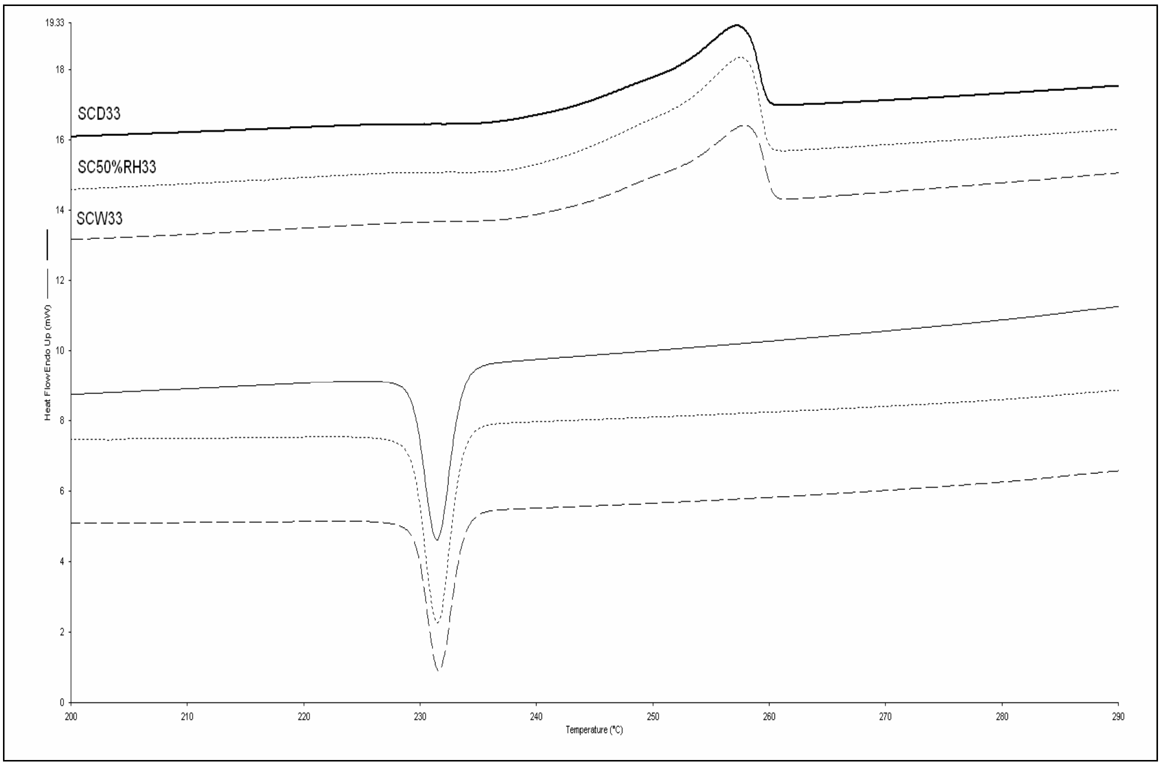

Figure 4.16: DSC results of single carbon fibre composites at various conditions

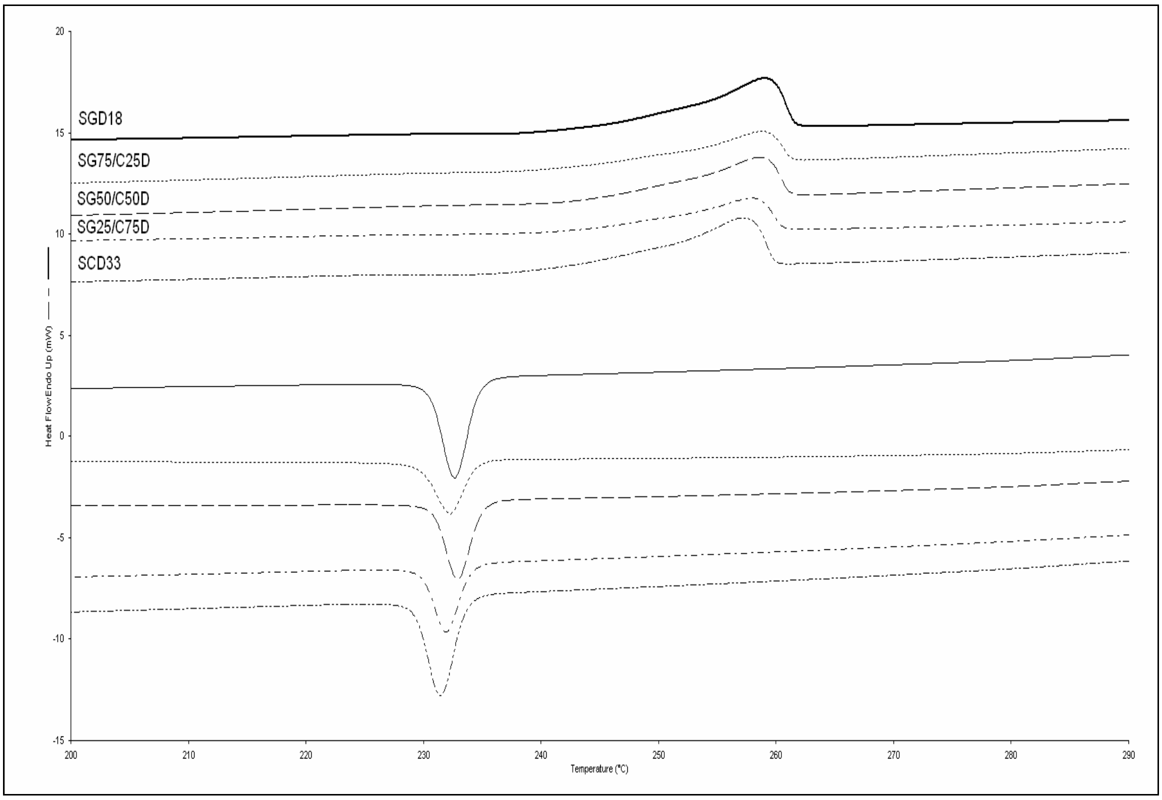

Figure 4.17: DSC results of hybrid fibre composites with different carbon fibre content at dry condition

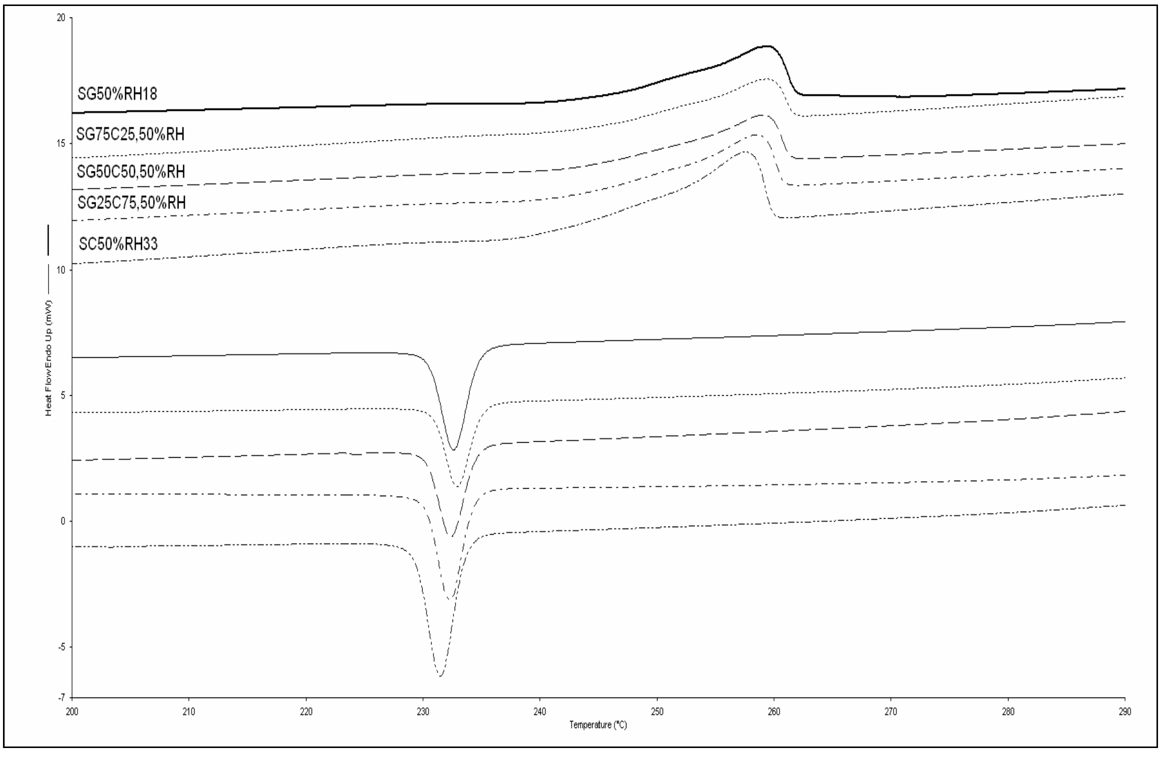

Figure 4.18: DSC results of hybrid fibre composites with different carbon fibre content at 50% RH condition

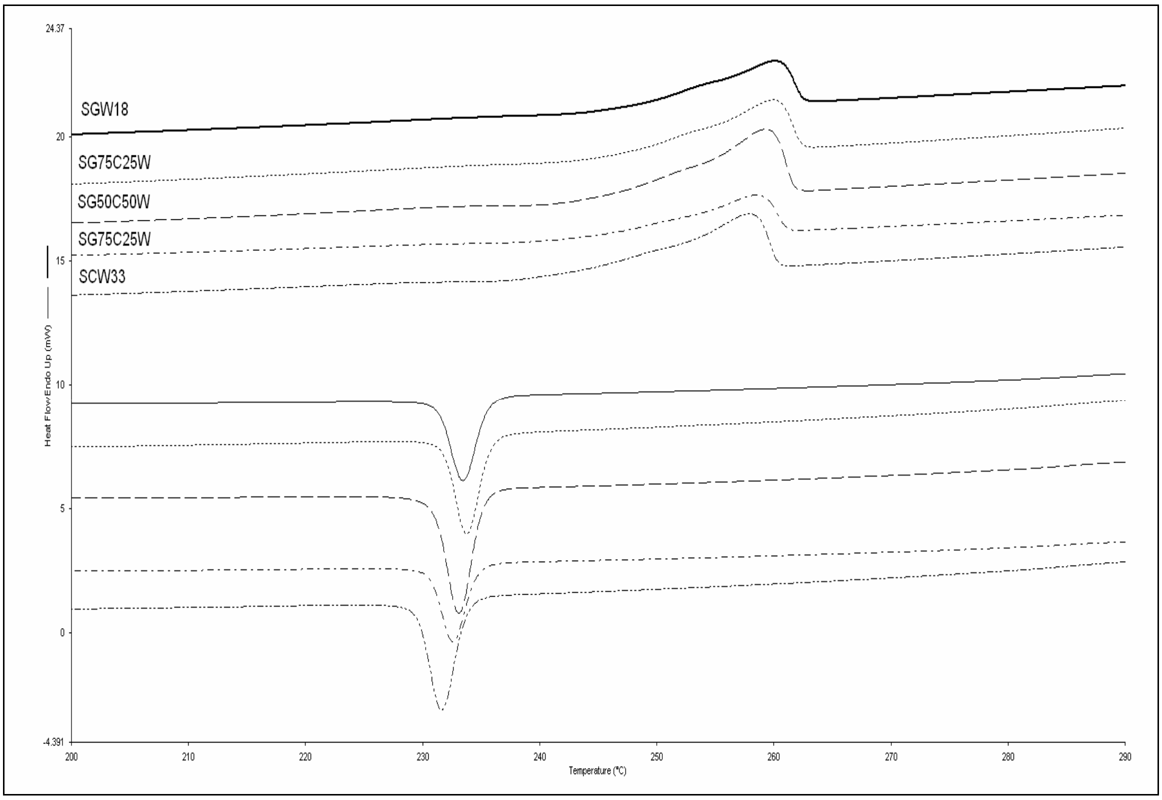

Figure 4.19: DSC results of hybrid fibre composites with different carbon fibre content at wet condition

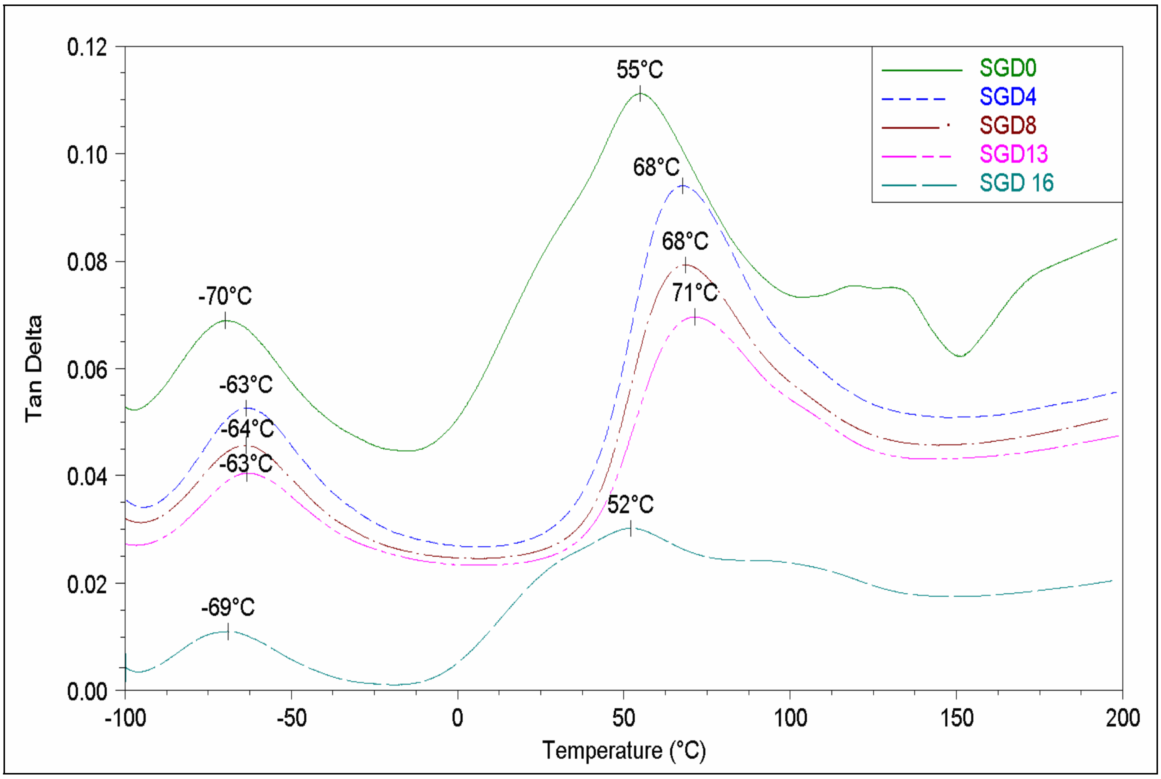

Figure 4.20: The tan delta–temperature behaviour of injection-moulded short glass fibre composites at dry condition

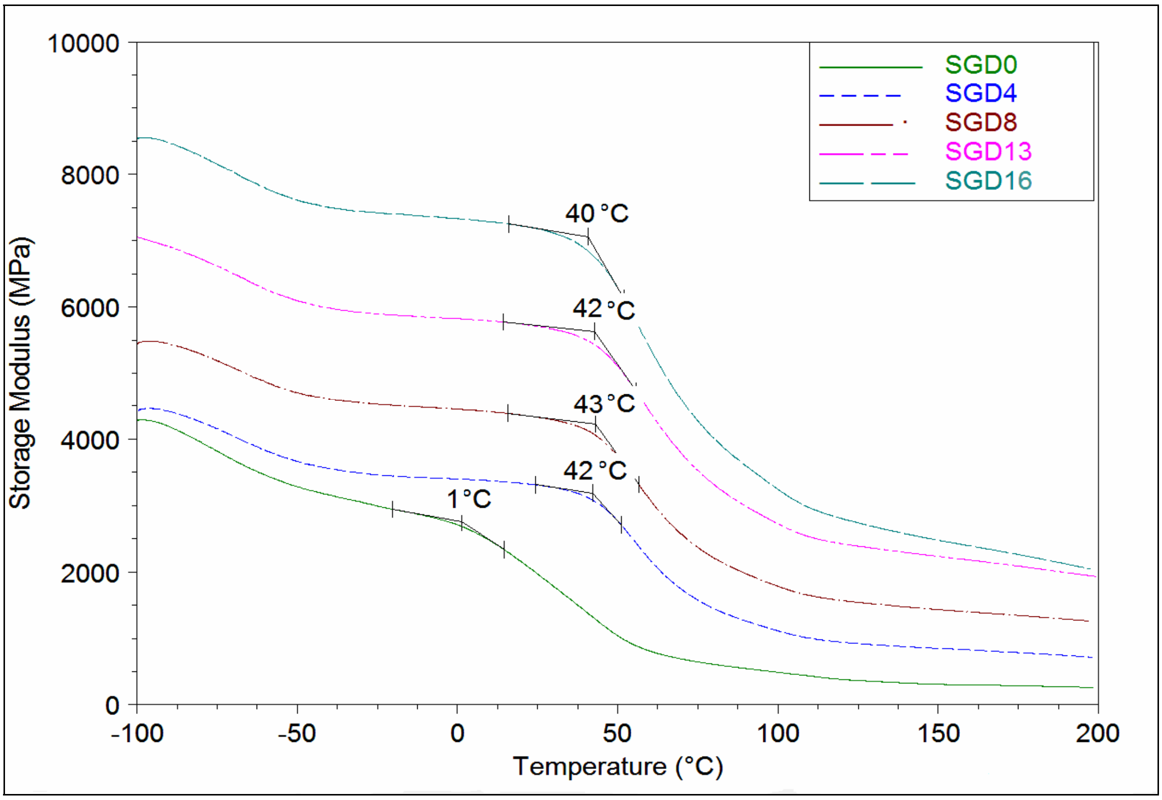

Figure 4.21: The storage modulus–temperature behaviour of injection- moulded short glass fibre composites at dry condition

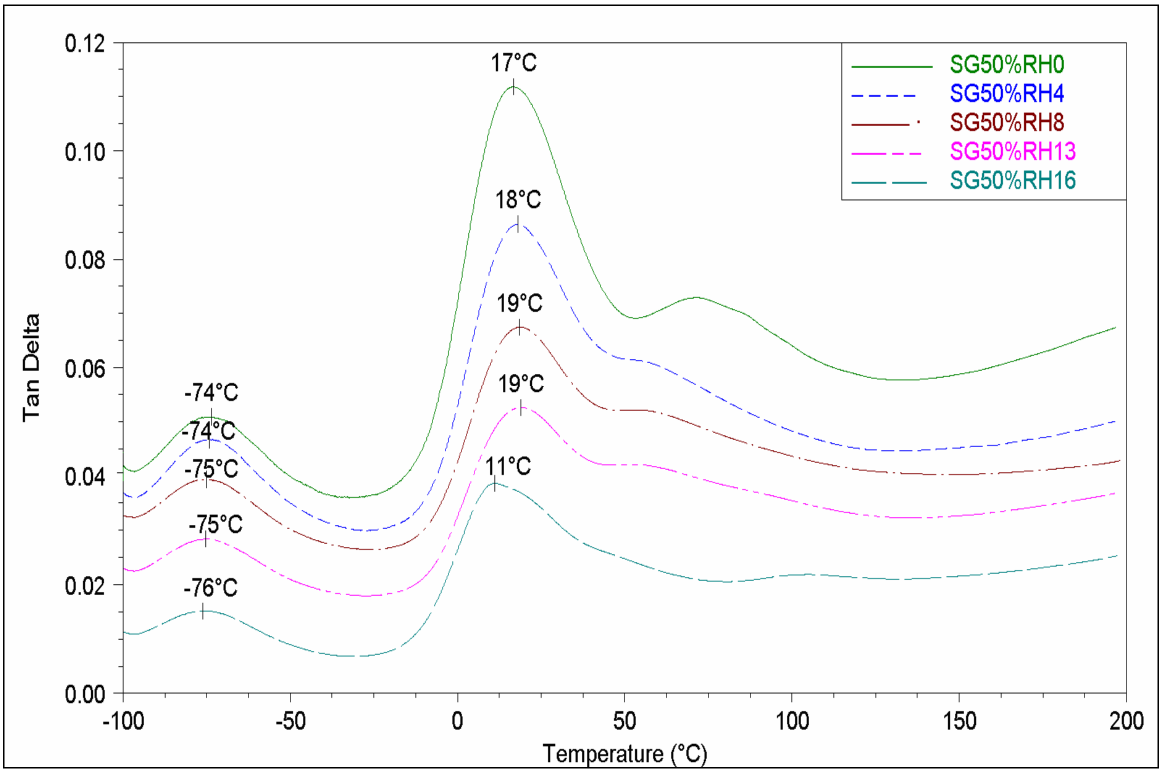

Figure 4.22: The tan delta–temperature behaviour of injection-moulded short glass fibre composites at 50% RH condition

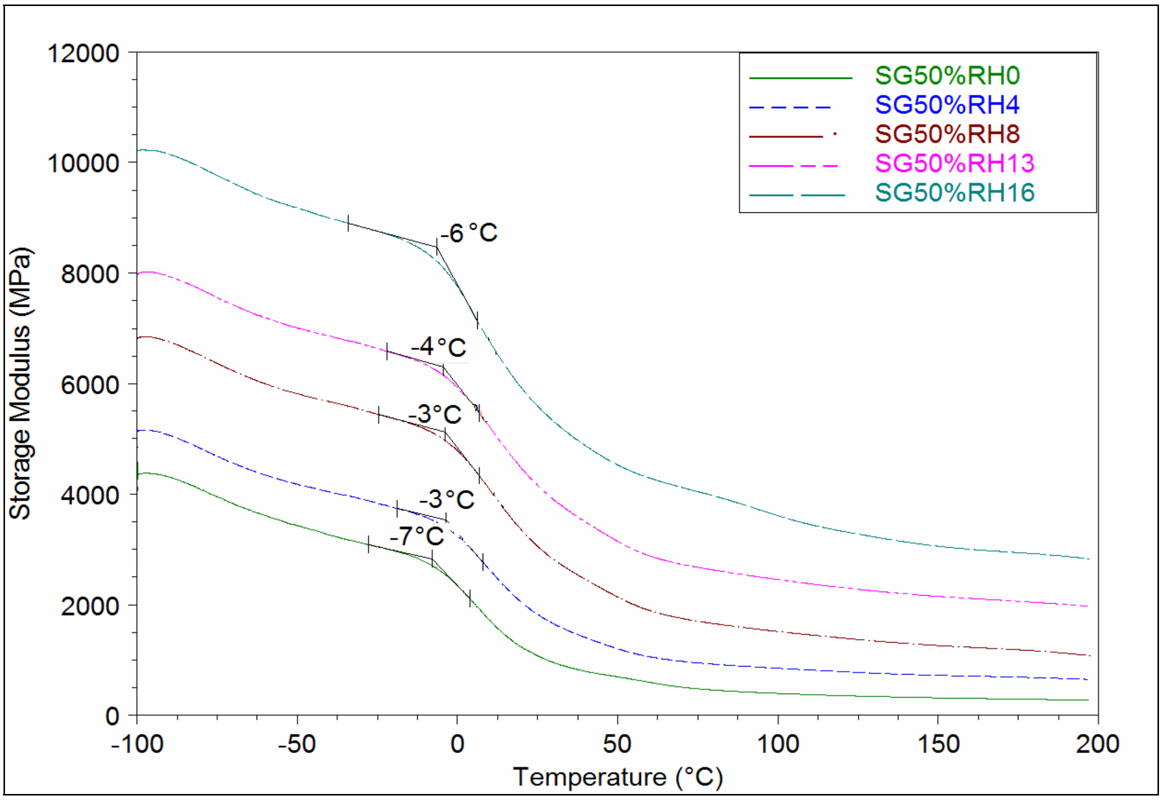

Figure 4.23: The storage modulus–temperature behaviour of injection- moulded short glass fibre composites at 50% RH condition

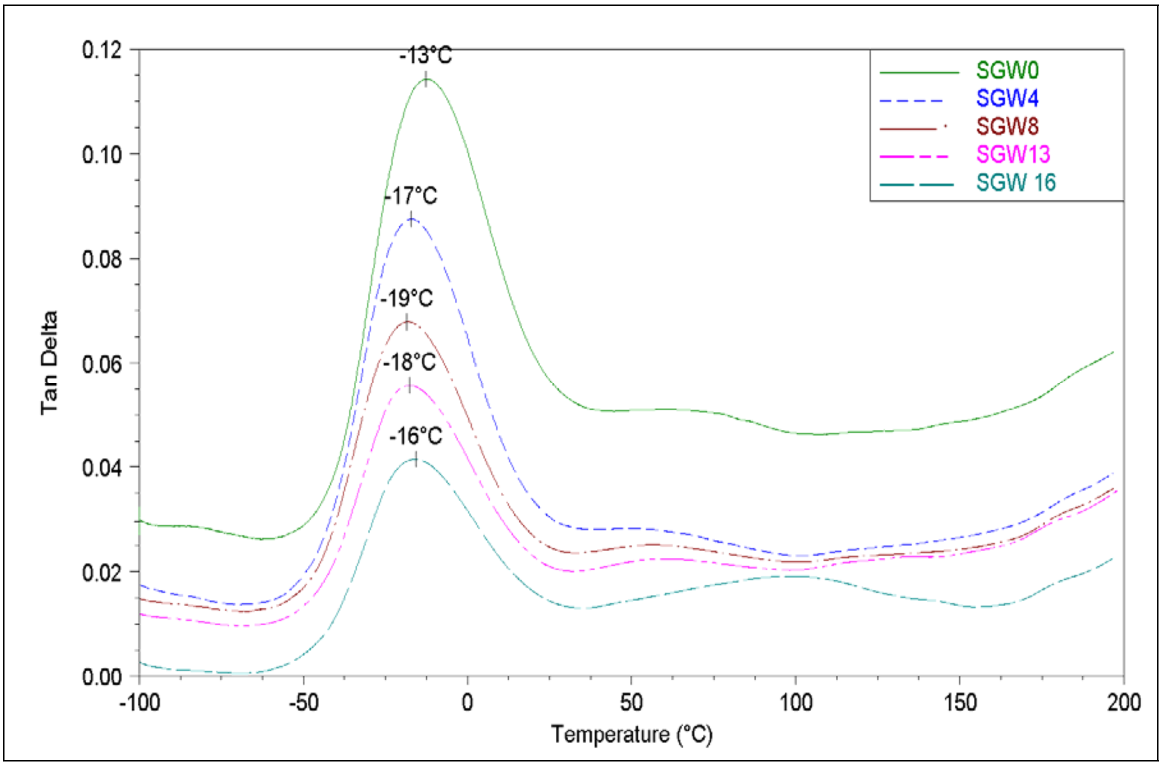

Figure 4.24: The tan delta–temperature behaviour of injection-moulded short glass fibre composites at wet condition

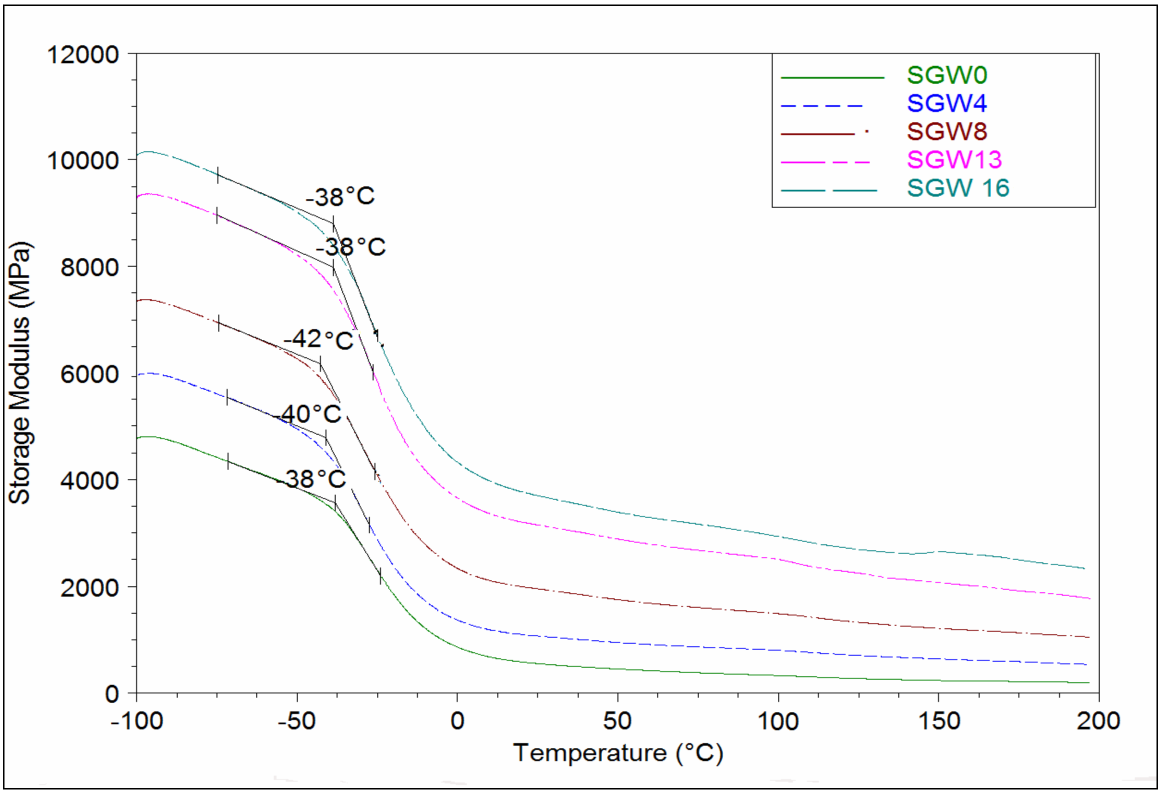

Figure 4.25: The storage modulus–temperature behaviour of injection- moulded short glass fibre composites at wet condition

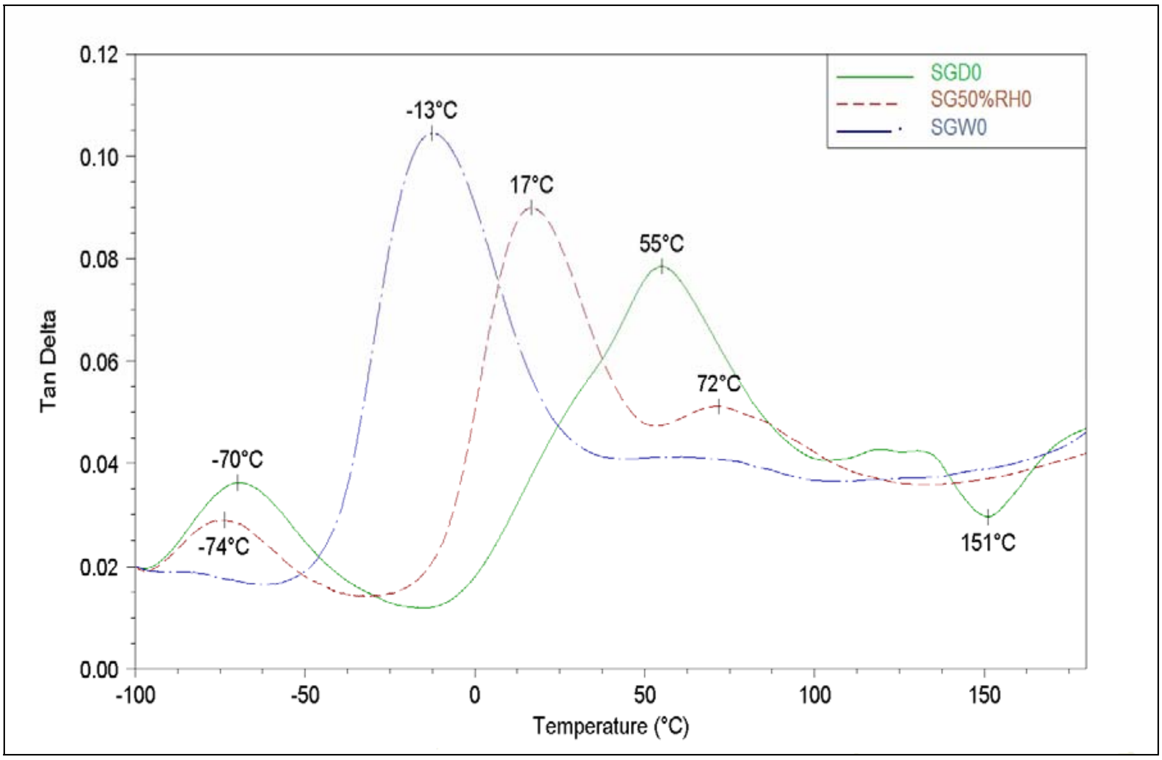

Figure 4.26: The tan delta–temperature behaviour of unreinforced polyamide 6,6 matrix at different conditions

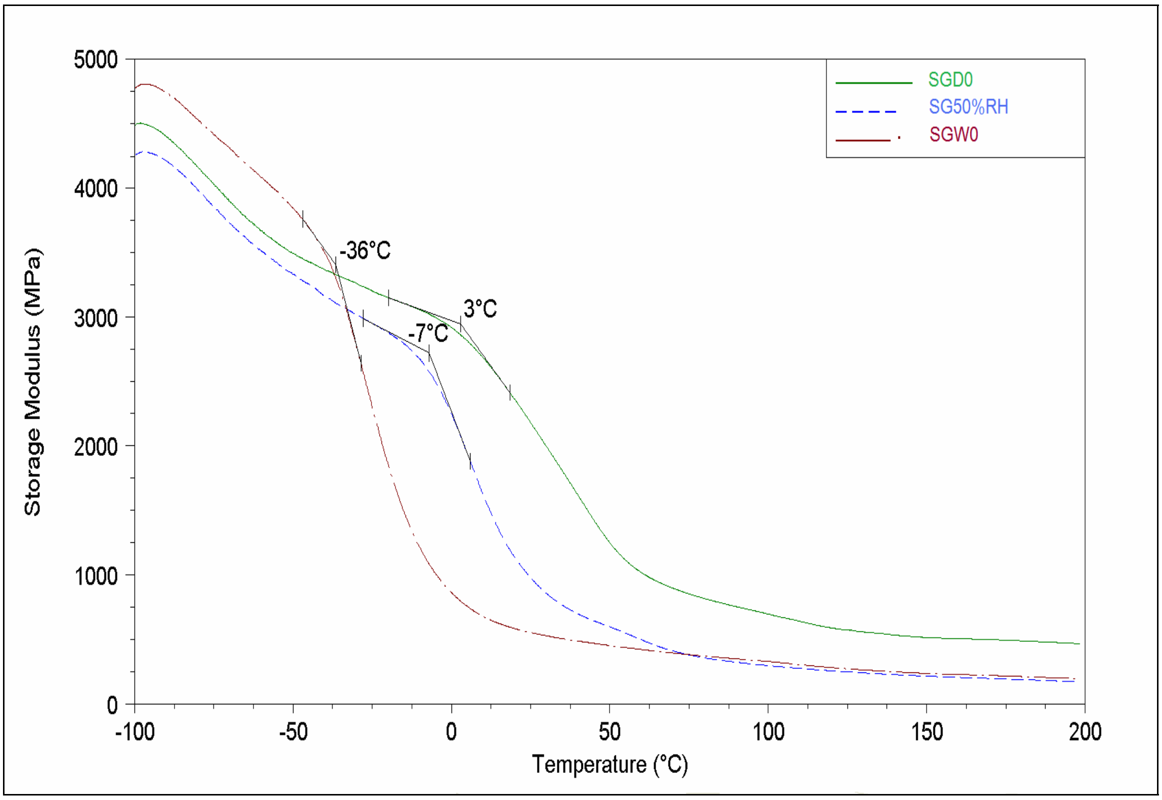

Figure 4.27: The storage modulus–temperature behaviour of unreinforced polyamide 6,6 matrix at different conditions

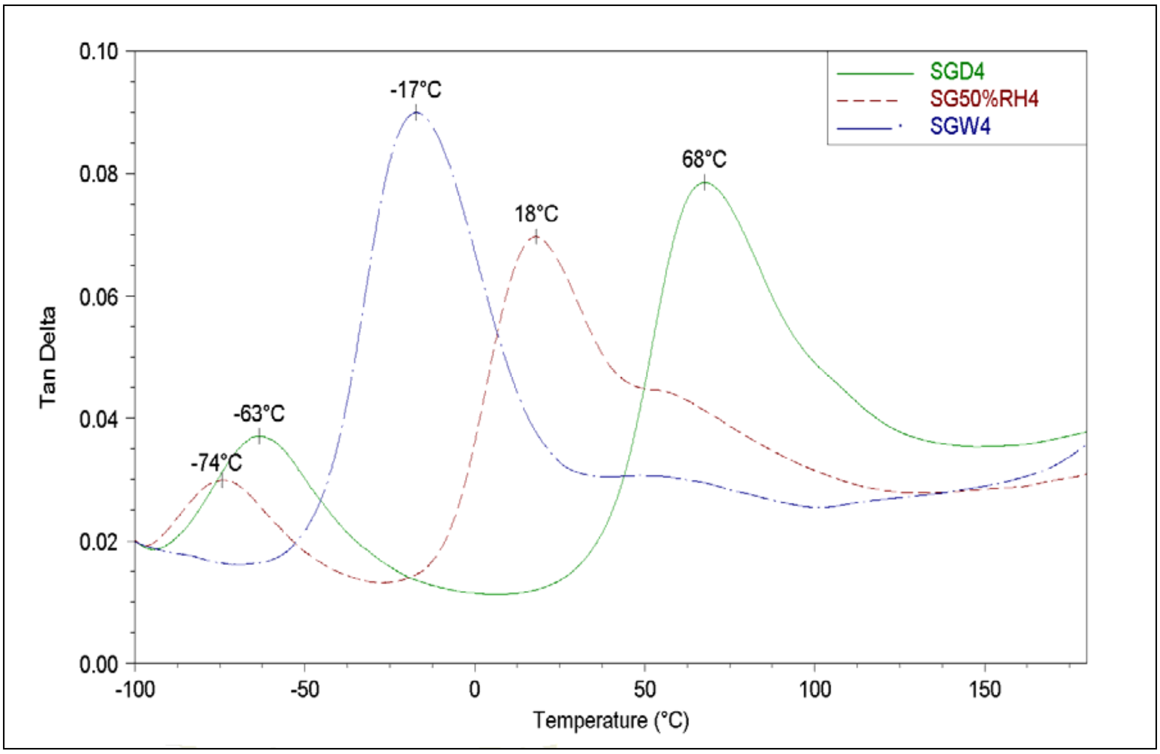

Figure 4.28: The tan delta–temperature behaviour of 4% V_f glass fibre composites at different conditions

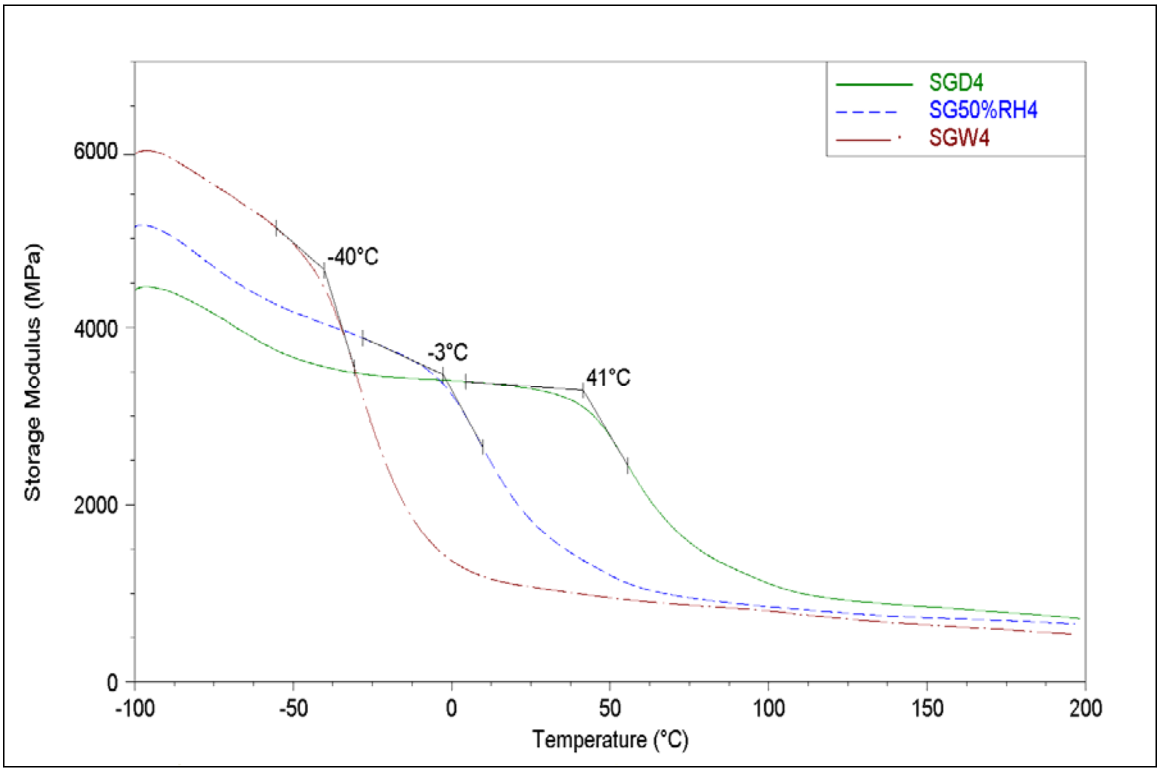

Figure 4.29: The storage modulus–temperature behaviour of 4% V_f glass fibre composites at different conditions

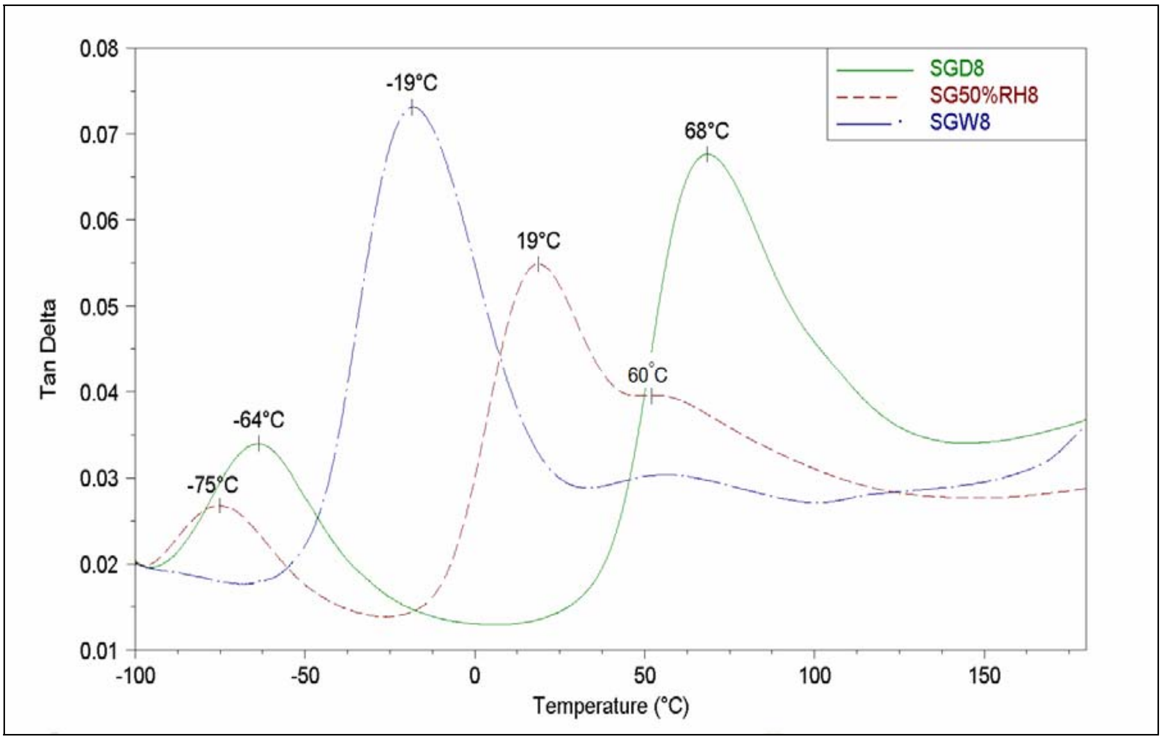

Figure 4.30: The tan delta–temperature behaviour of 8% V_f glass fibre composites at different conditions

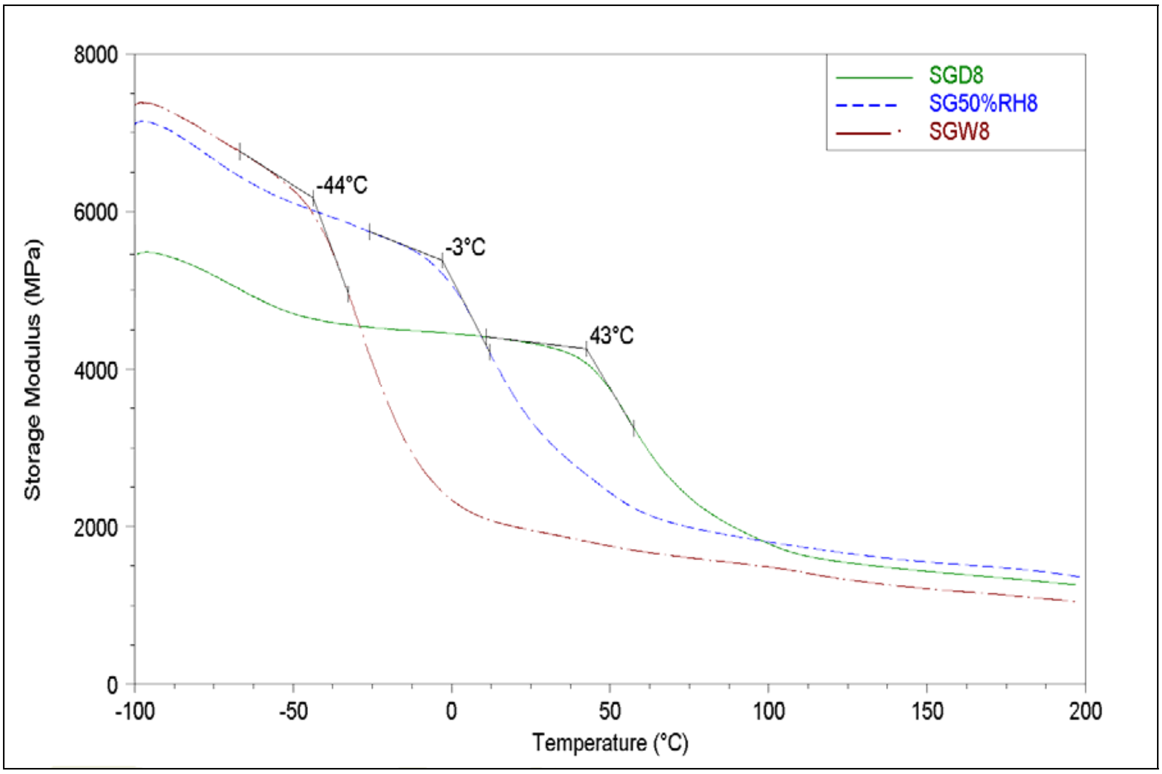

Figure 4.31: The storage modulus–temperature behaviour of 8% V_f glass fibre composites at different conditions

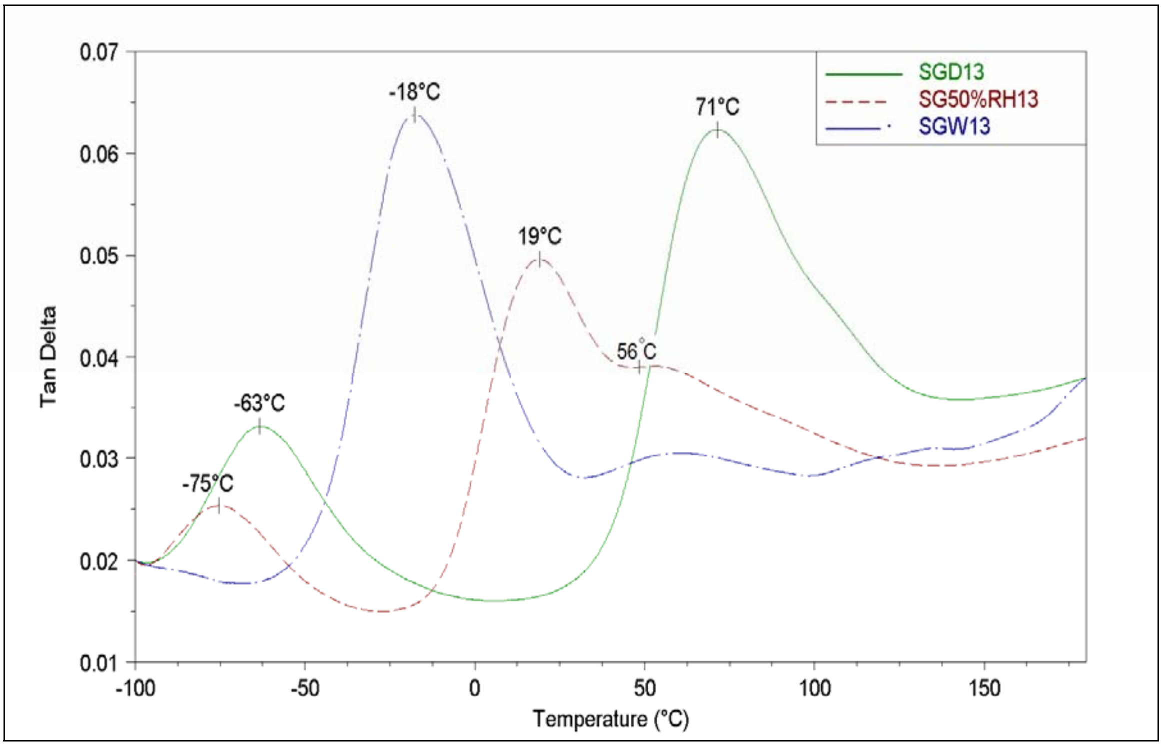

Figure 4.32: The tan delta–temperature behaviour of 13% V_f glass fibre composites at different conditions

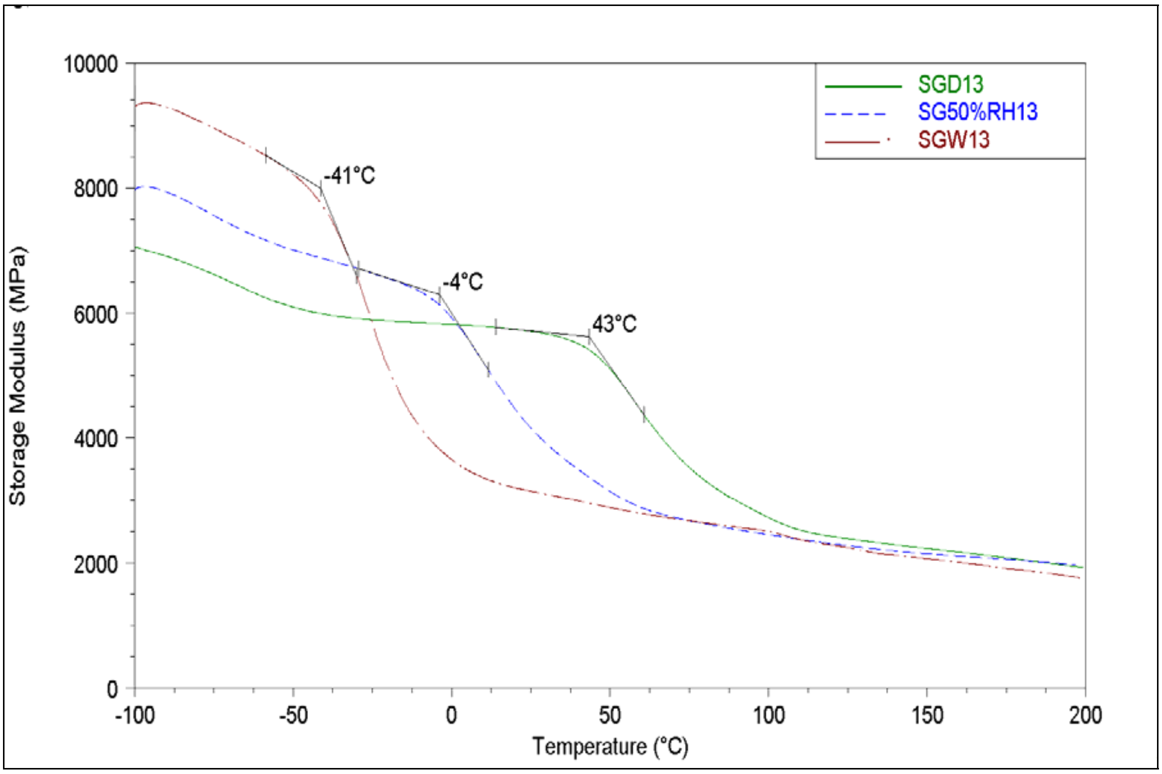

Figure 4.33: The storage modulus–temperature behaviour of 13% V_f glass fibre composites at different conditions

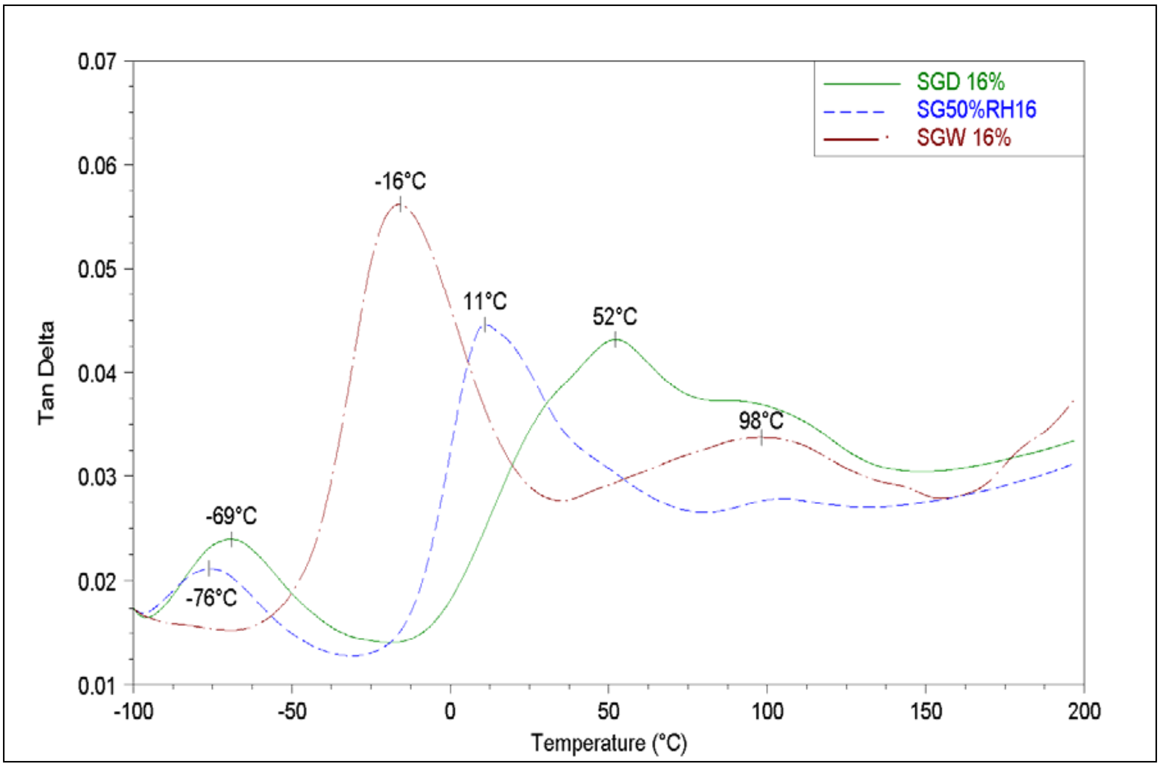

Figure 4.34: The tan delta–temperature behaviour of 16% V_f glass fibre composites at different conditions

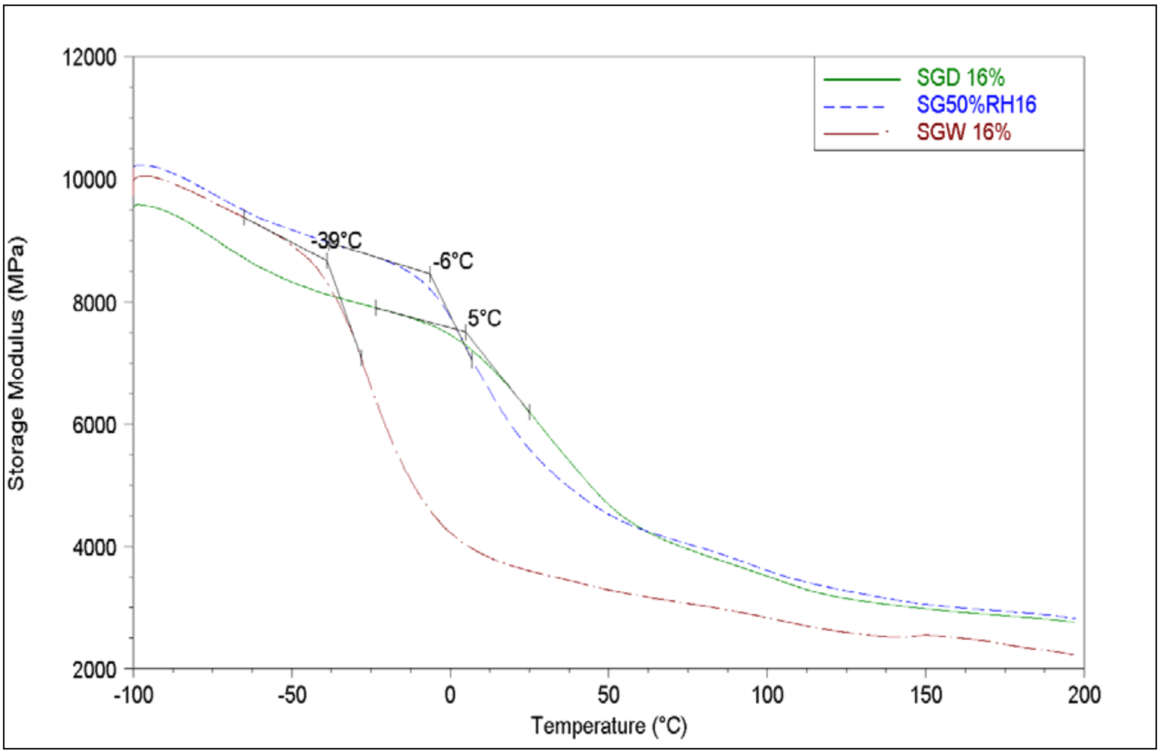

Figure 4.35: The storage modulus–temperature behaviour of 16% V_f glass fibre composites at different conditions

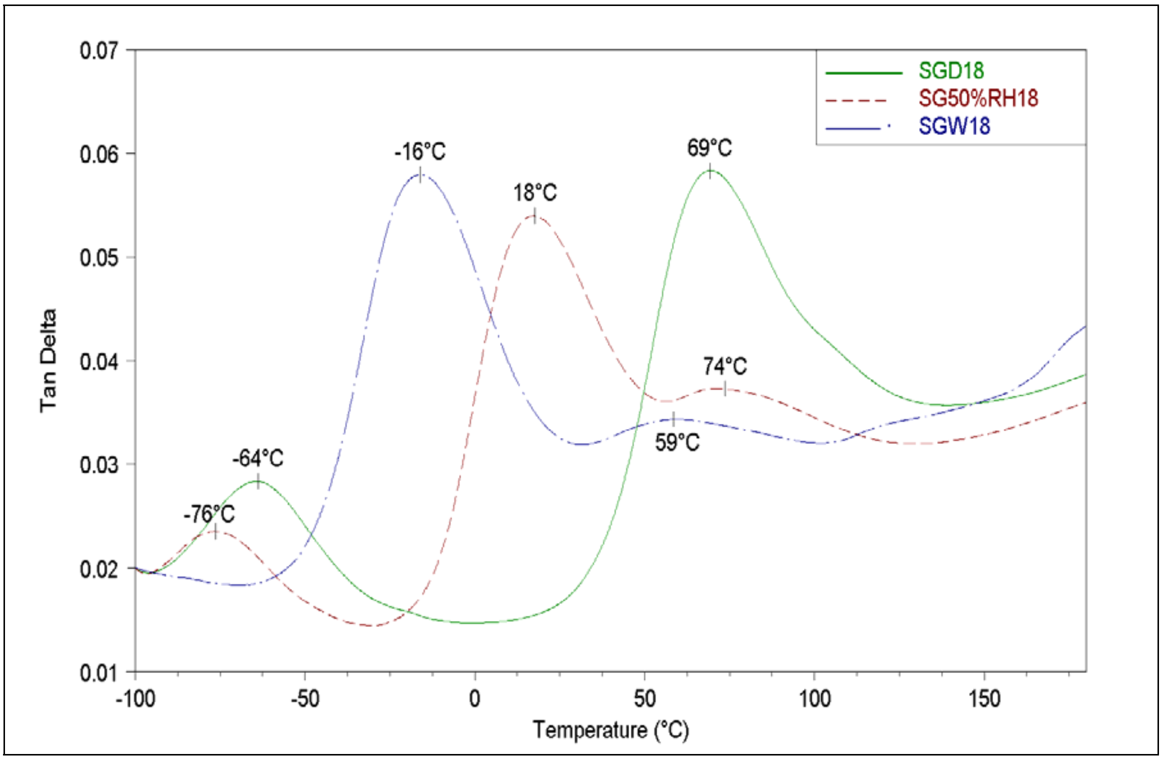

Figure 4.36: The tan delta–temperature behaviour of 18% V_f glass fibre composites at different conditions

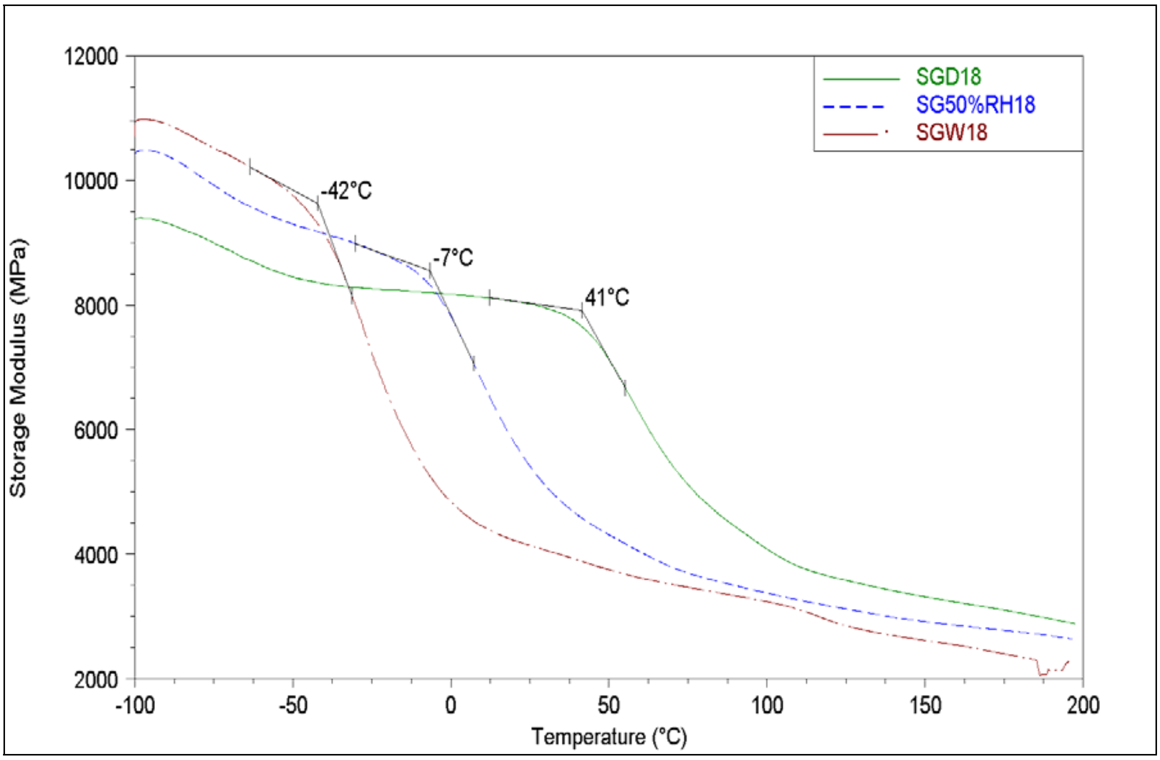

Figure 4.37: The storage modulus–temperature behaviour of 18% V_f glass fibre composites at different conditions

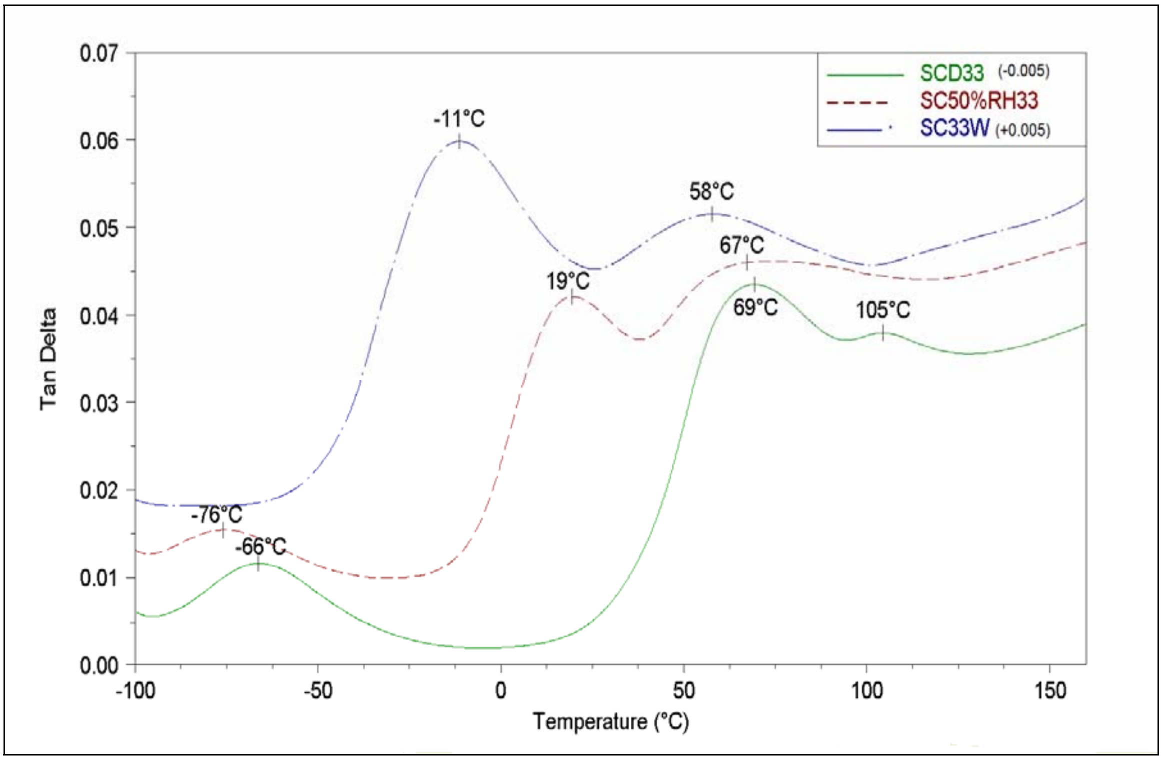

Figure 4.38: The tan delta–temperature behaviour of carbon fibre composites at different conditions

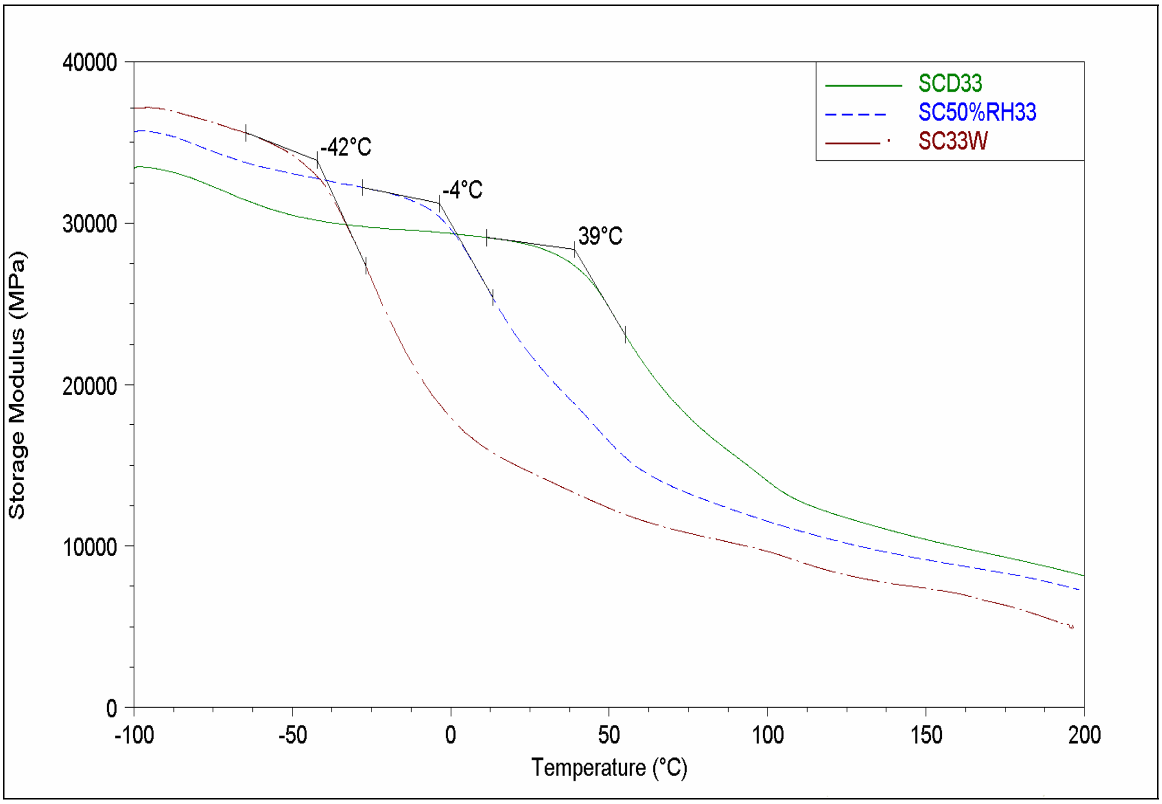

Figure 4.39: The storage modulus–temperature behaviour of carbon fibre composites at different conditions

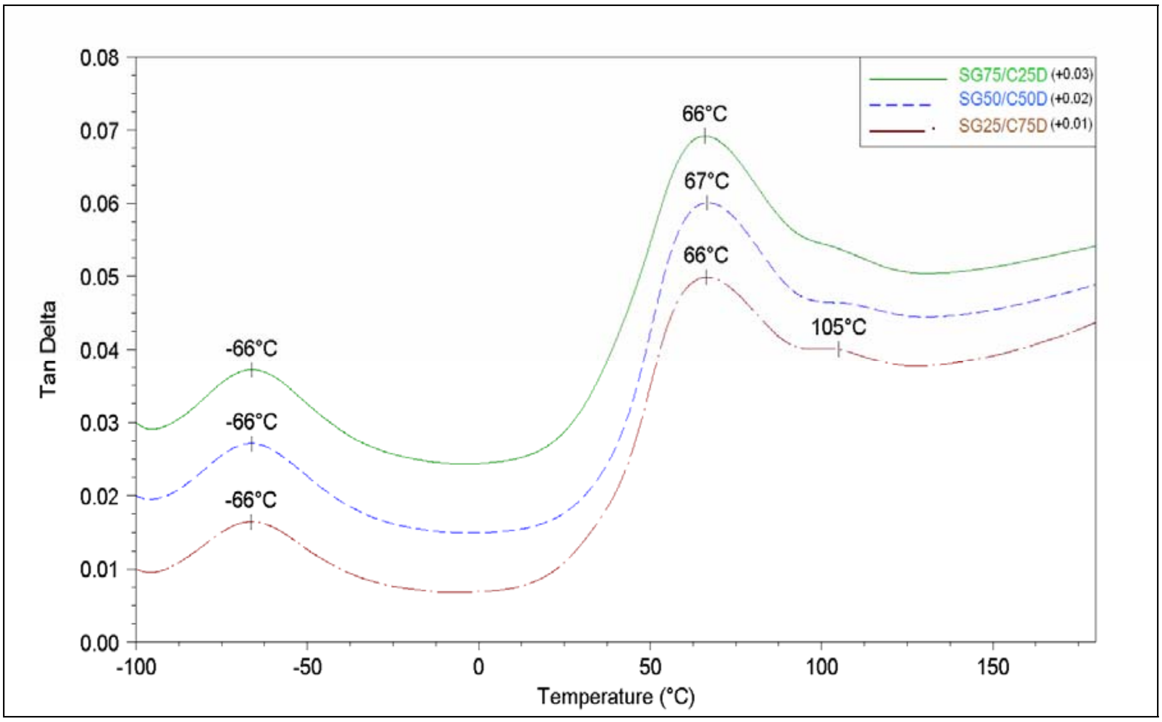

Figure 4.40: The tan delta–temperature behaviour of injection-moulded hybrid fibre composites at dry condition

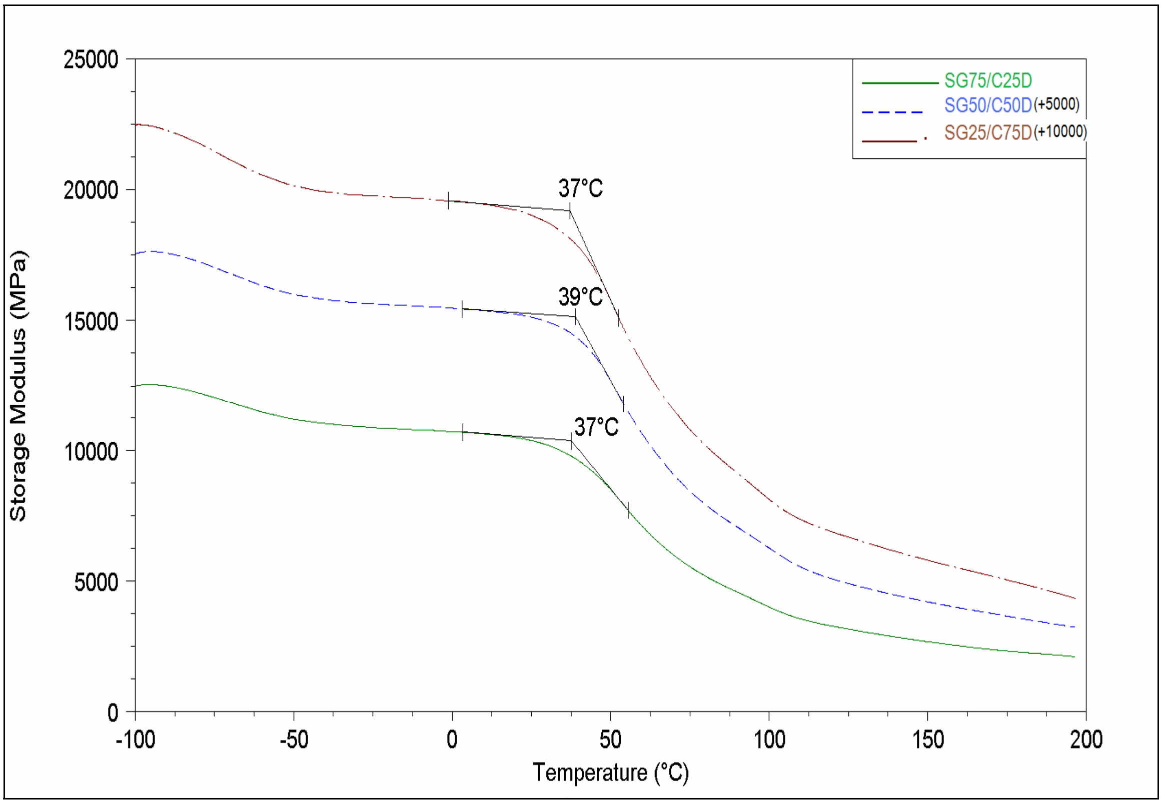

Figure 4.41: The storage modulus–temperature behaviour of injection-moulded hybrid fibre composites at dry condition

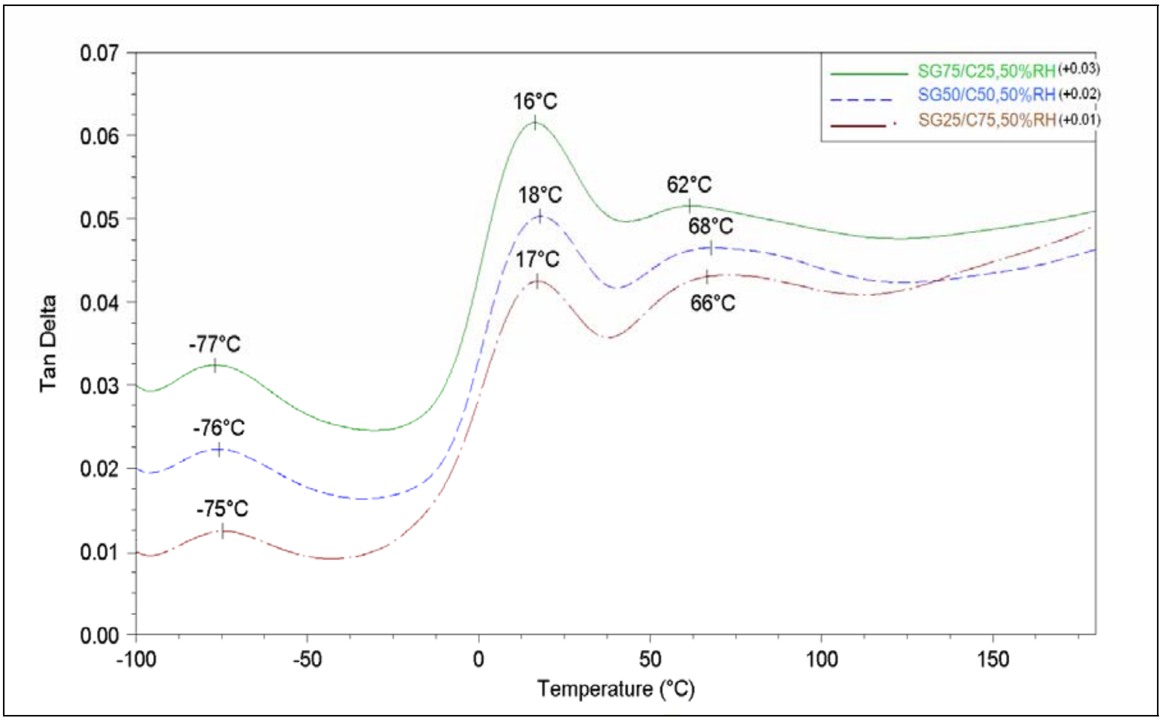

Figure 4.42: The tan delta–temperature behaviour of injection-moulded hybrid fibre composites at 50% RH condition

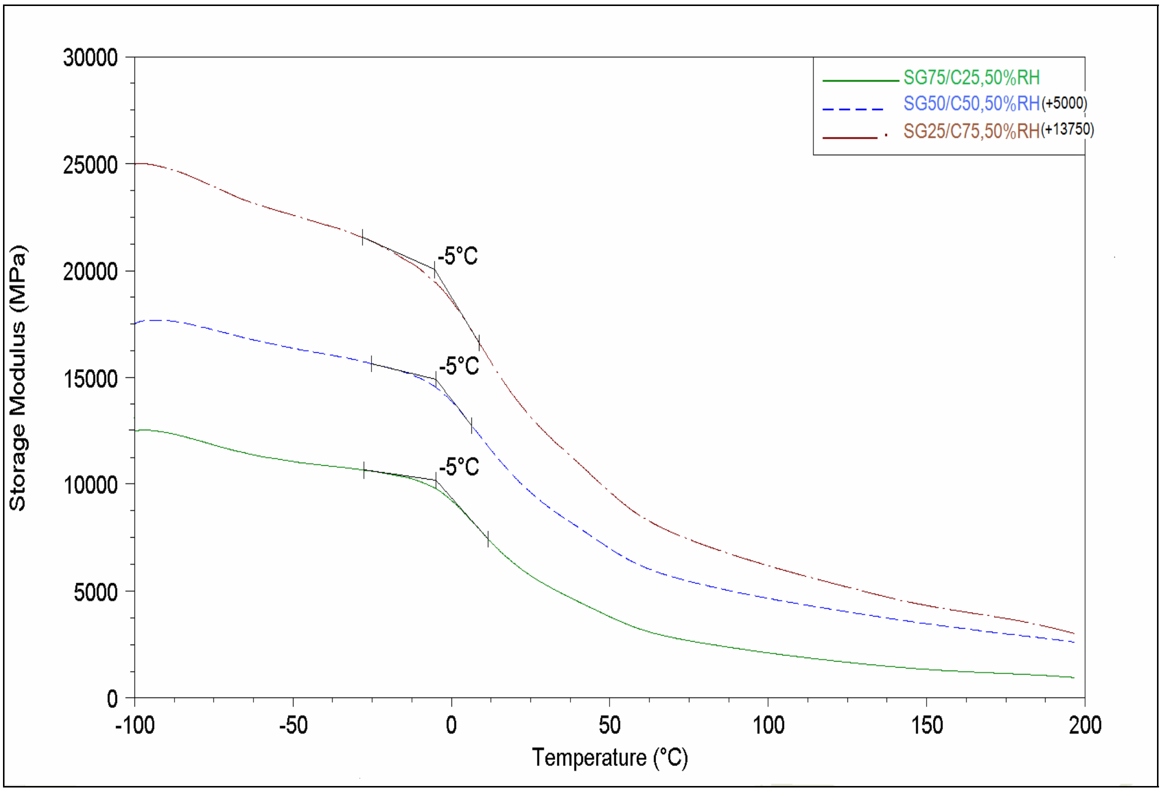

Figure 4.43: The storage modulus–temperature behaviour of injection-moulded hybrid fibre composites at 50% RH condition

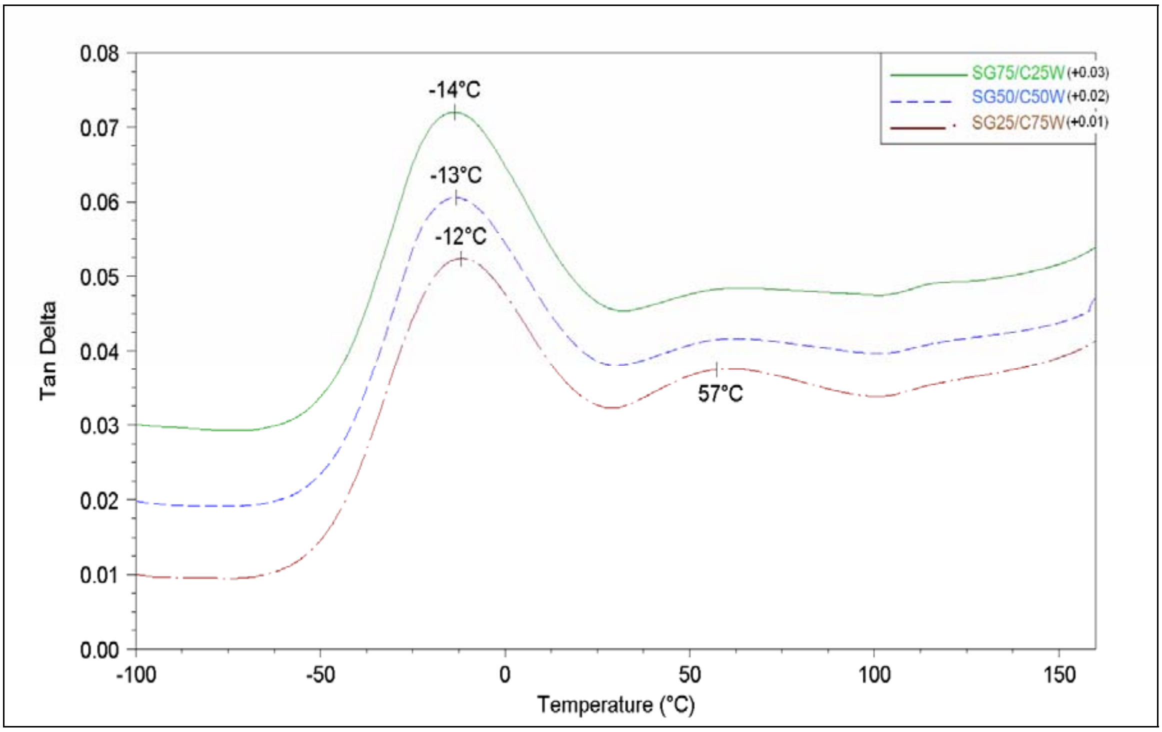

Figure 4.44: The tan delta–temperature behaviour of injection-moulded hybrid fibre composites at wet condition

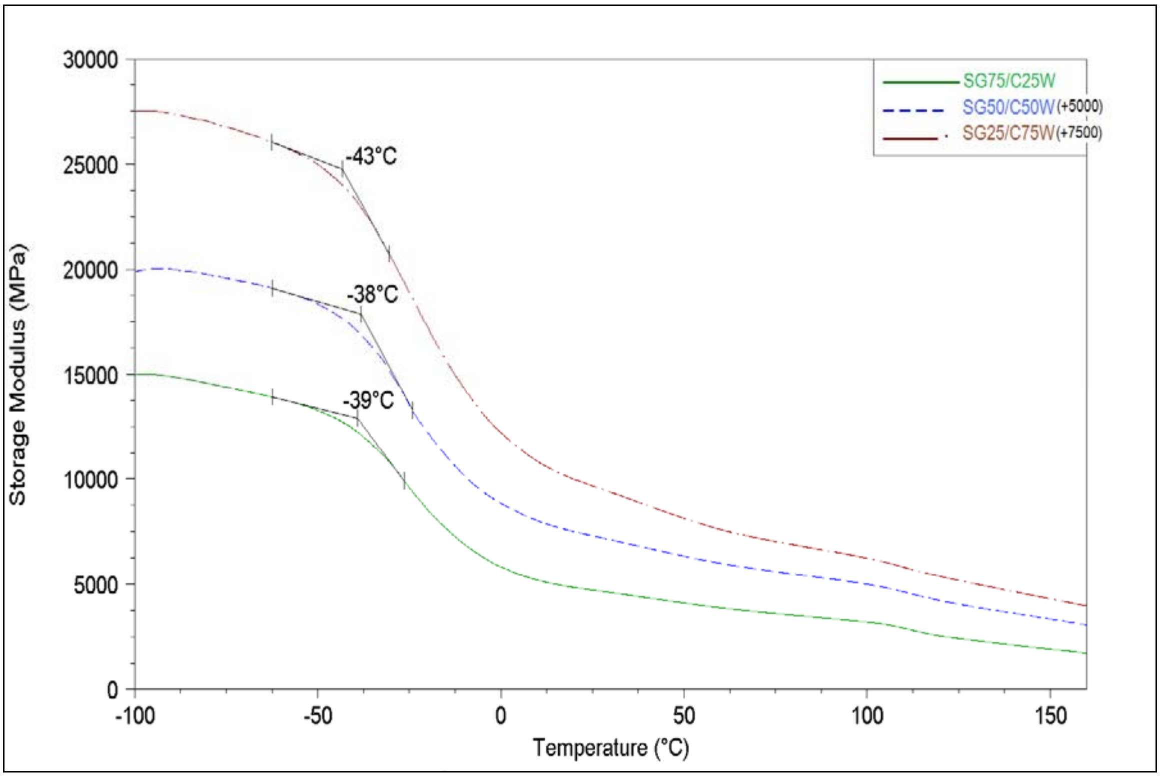

Figure 4.45: The storage modulus–temperature behaviour of injection-moulded hybrid fibre composites at wet condition

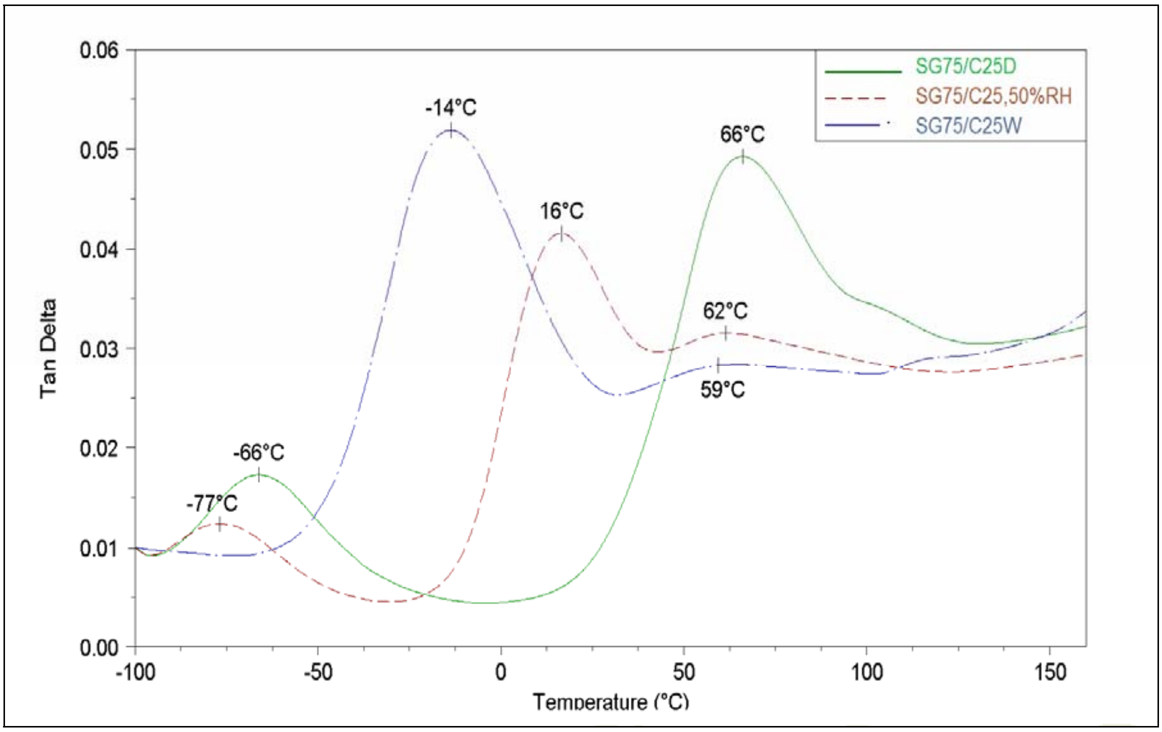

Figure 4.46: The tan delta–temperature behaviour of injection-moulded (SG75/C25) hybrid fibre composites at different conditions

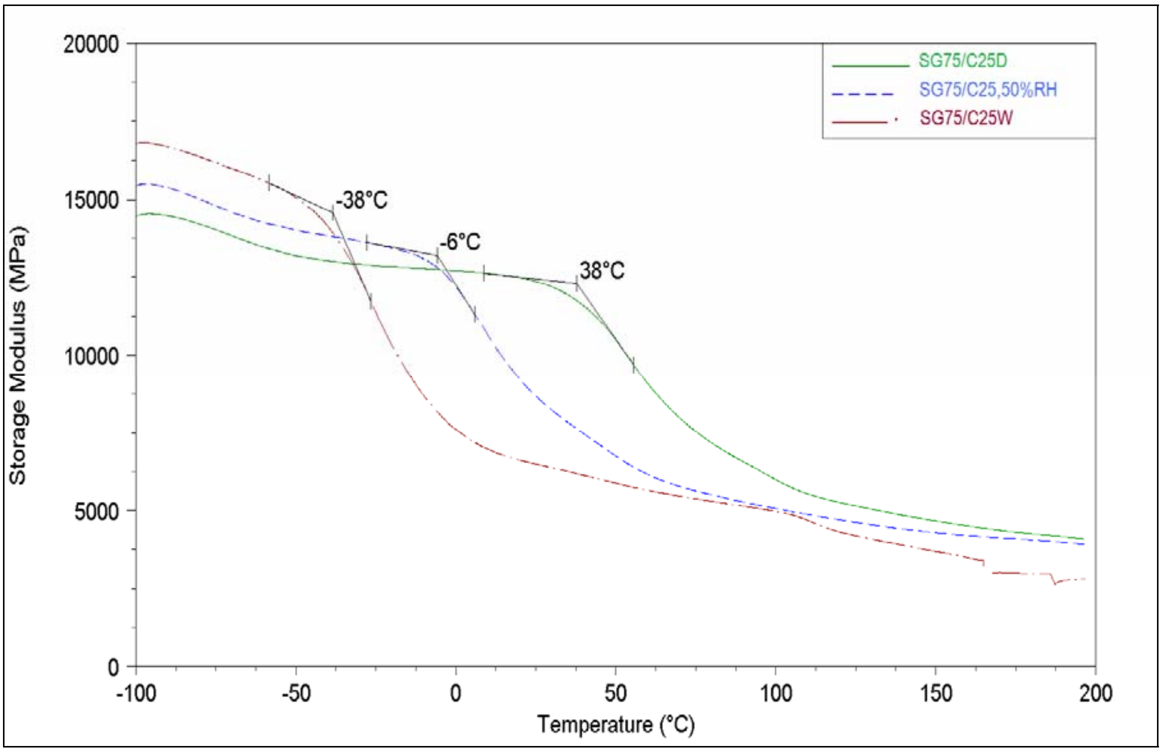

Figure 4.47: The storage modulus–temperature behaviour of injection-moulded (SG75/C25) hybrid fibre composites at different conditions

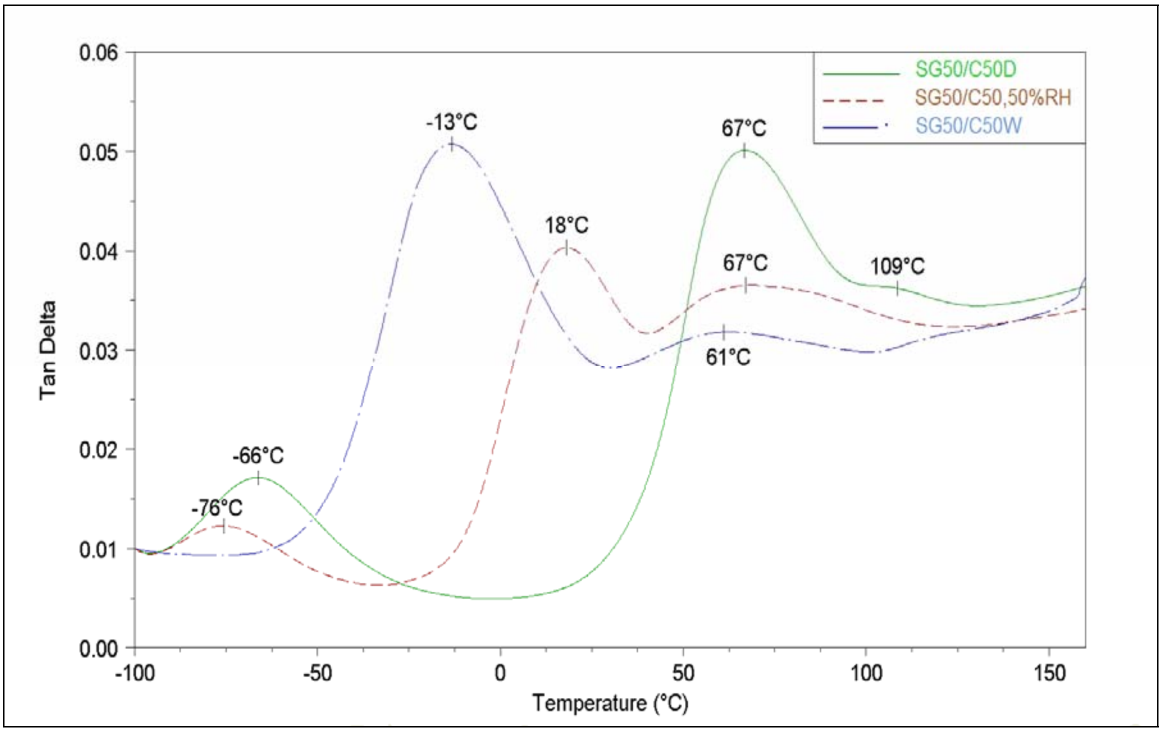

Figure 4.48: The tan delta–temperature behaviour of injection-moulded (SG50/C50) hybrid fibre composites at different conditions

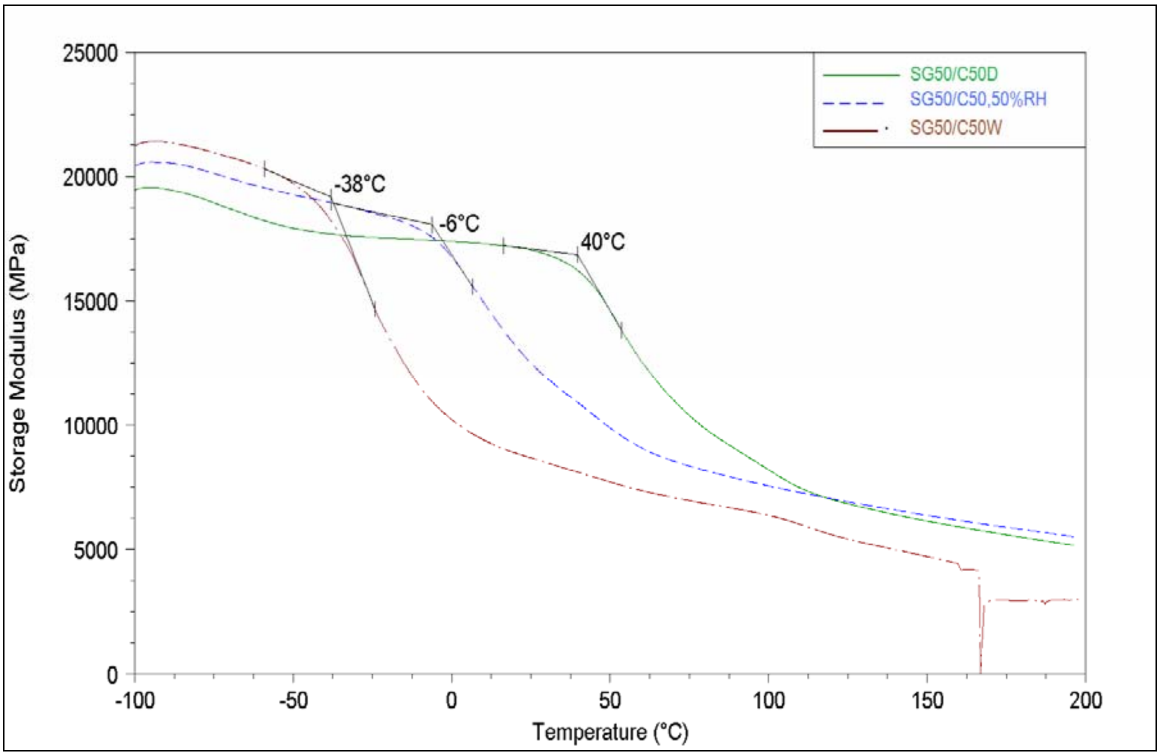

Figure 4.49: The storage modulus–temperature behaviour of injection-moulded (SG50/C50) hybrid fibre composites at different conditions

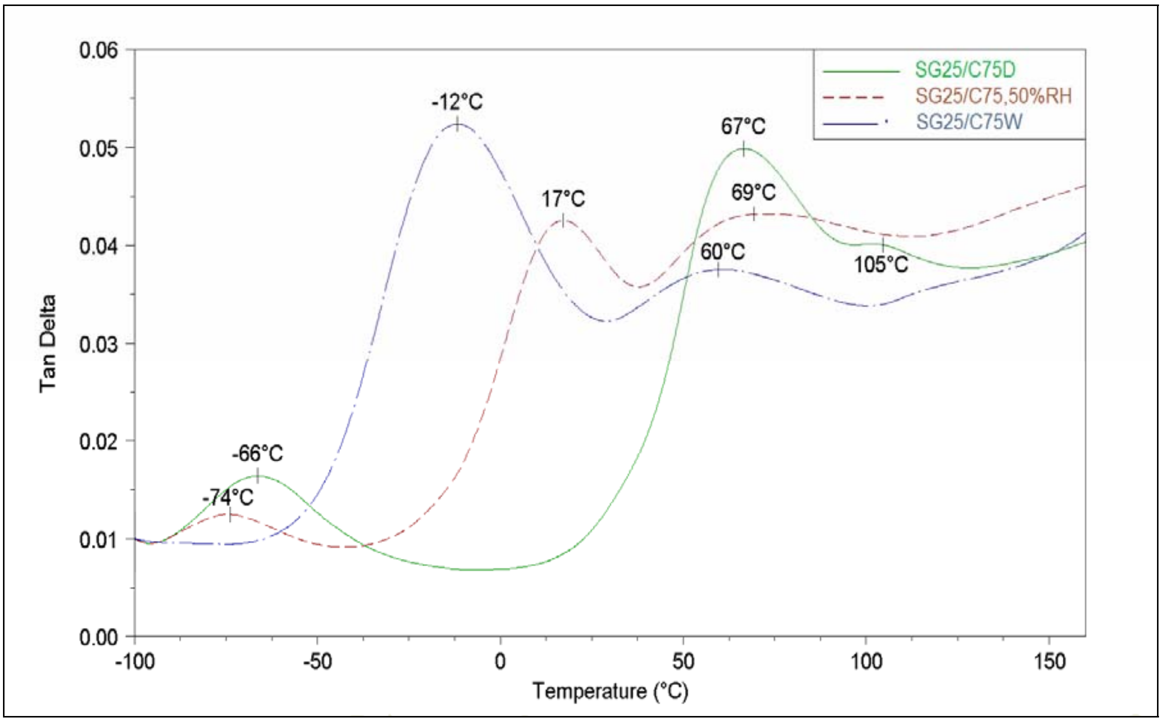

Figure 4.50: The tan delta–temperature behaviour of injection-moulded (SG25/C75) hybrid fibre composites at different conditions

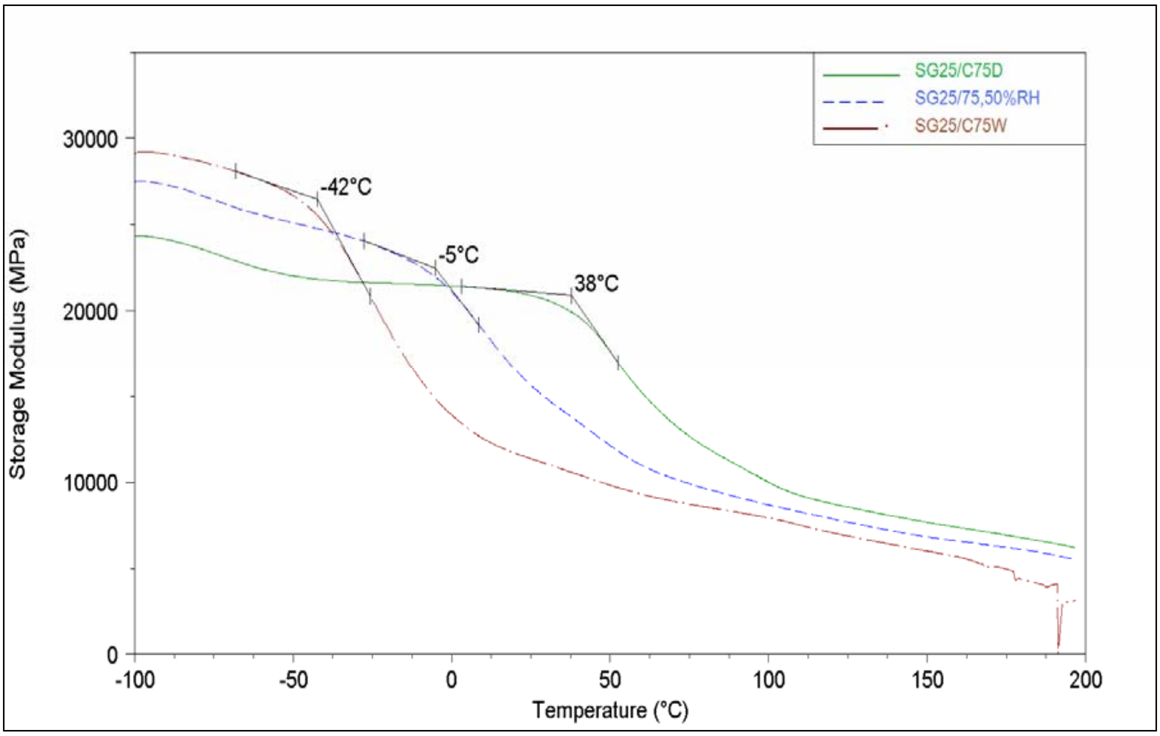

Figure 4.51: The storage modulus–temperature behaviour of injection-moulded (SG25/C75) hybrid fibre composites at different conditions

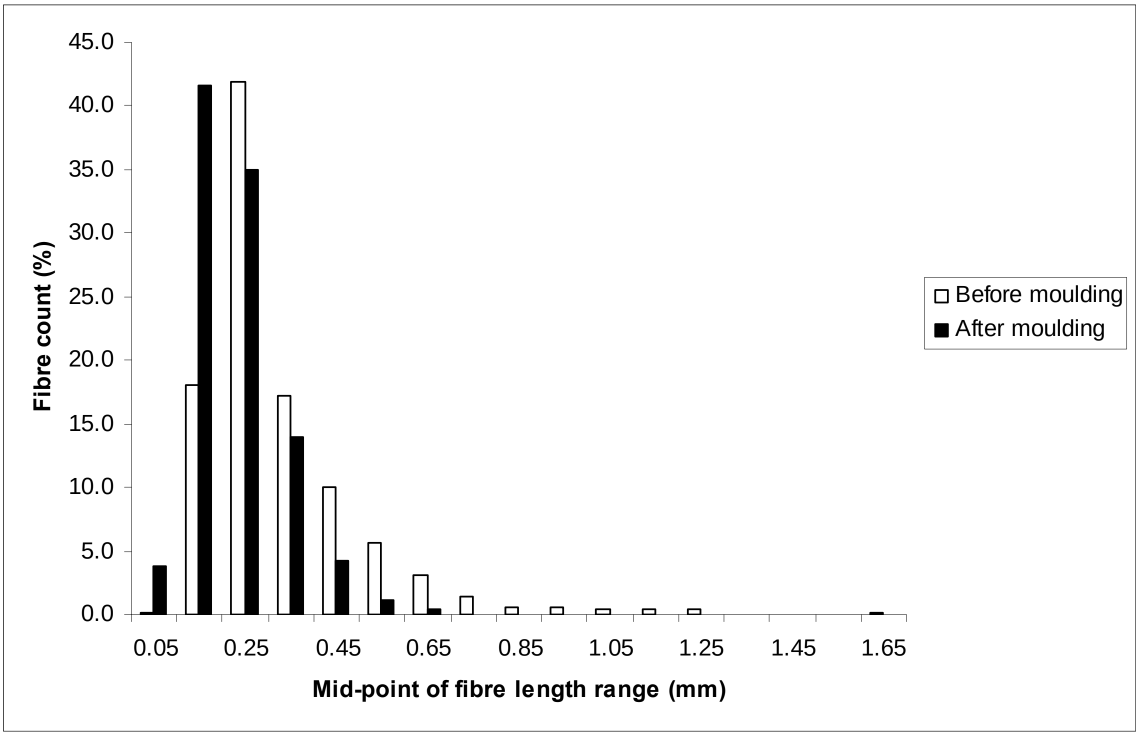

Figure 4.52: Fibre length distribution of short glass fibre composites for 18% V_f before and after moulding

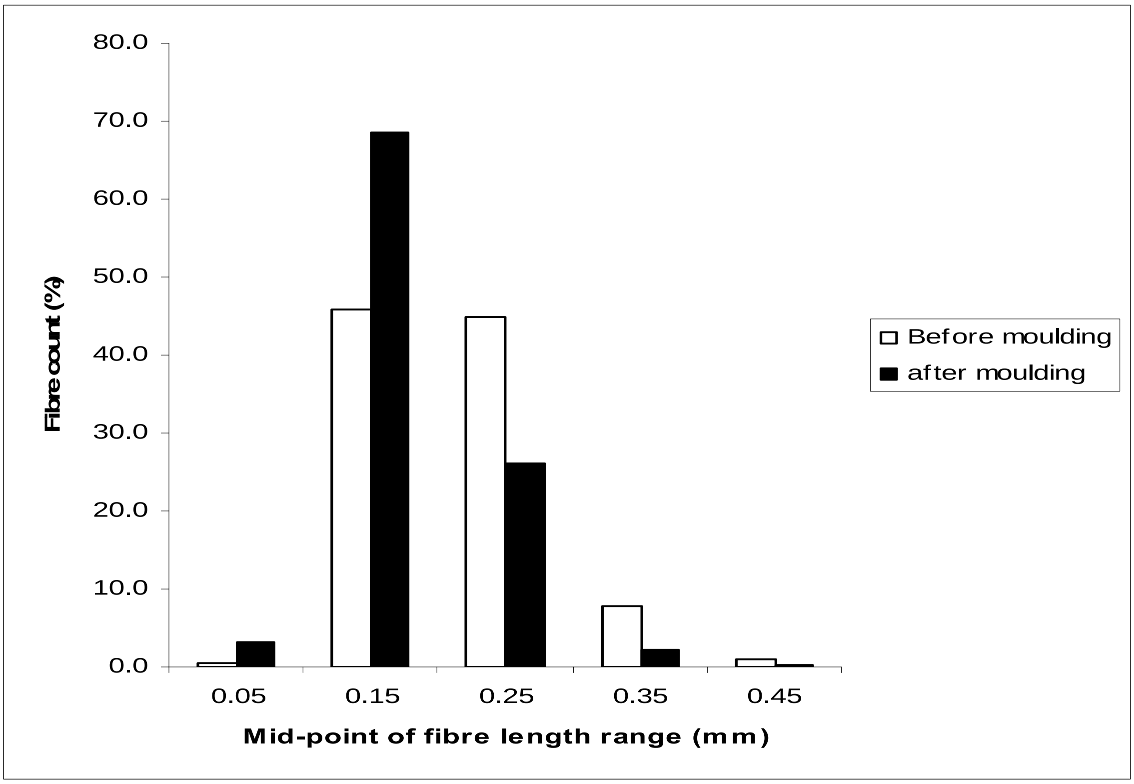

Figure 4.53: Fibre length distribution of short carbon fibre composites for 33% V_f before and after moulding

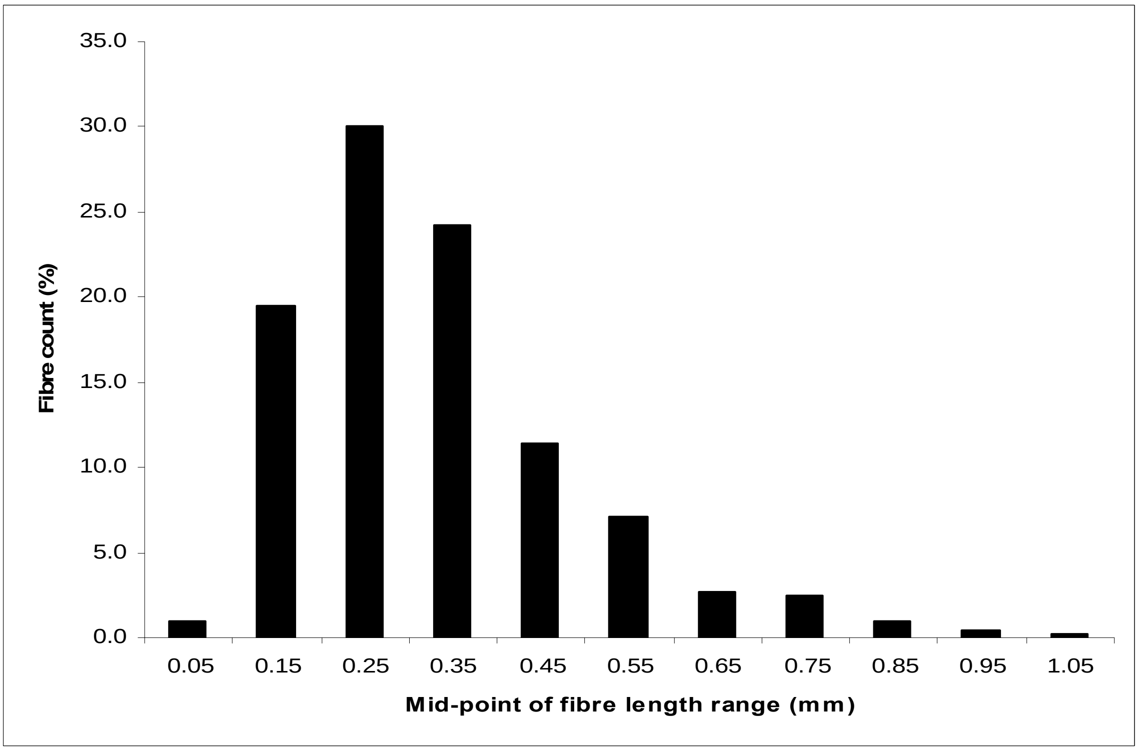

Figure 4.54: Fibre length distribution of short glass fibre composite (4% V_f)

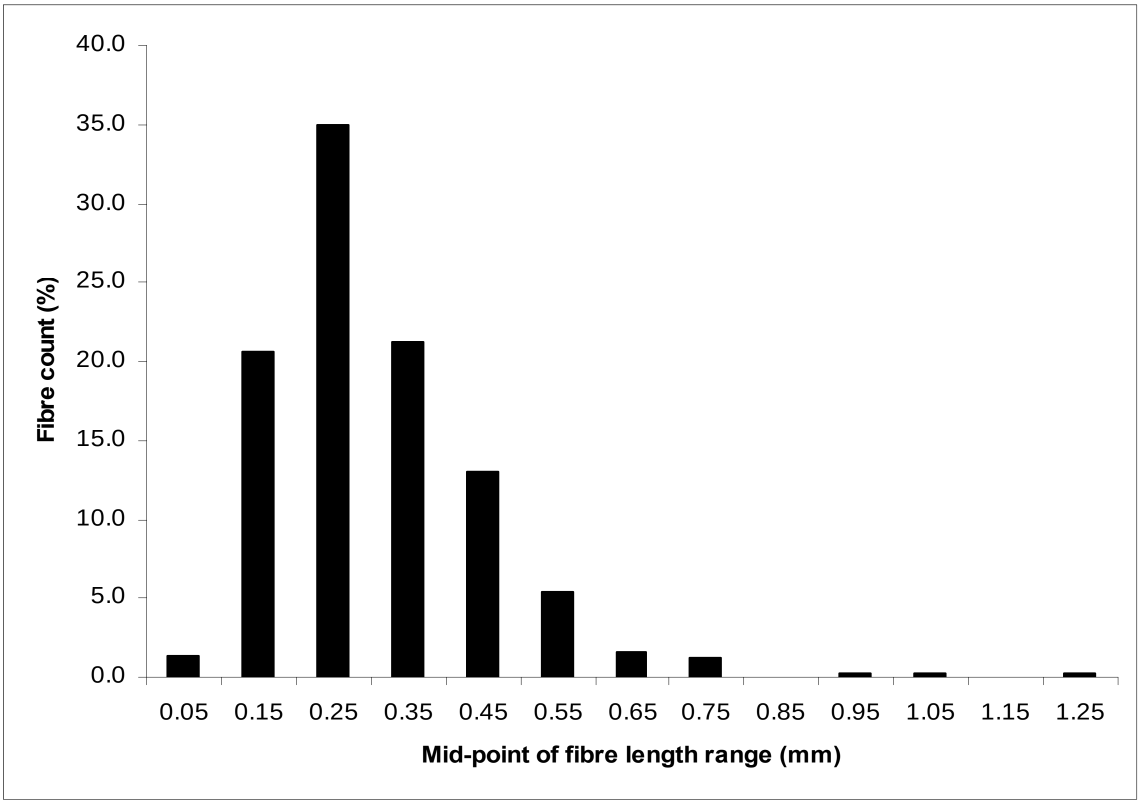

Figure 4.55: Fibre length distribution of short glass fibre composite (8% V_f)

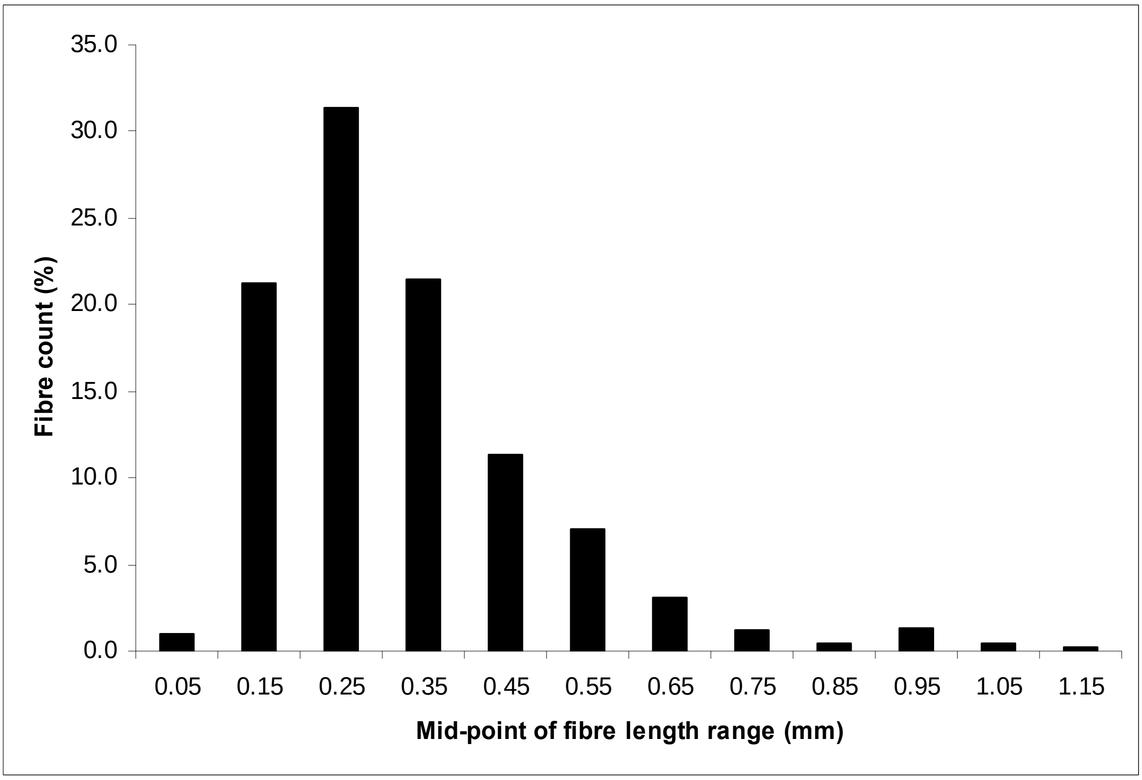

Figure 4.56: Fibre length distribution of short glass fibre composite (13% V_f)

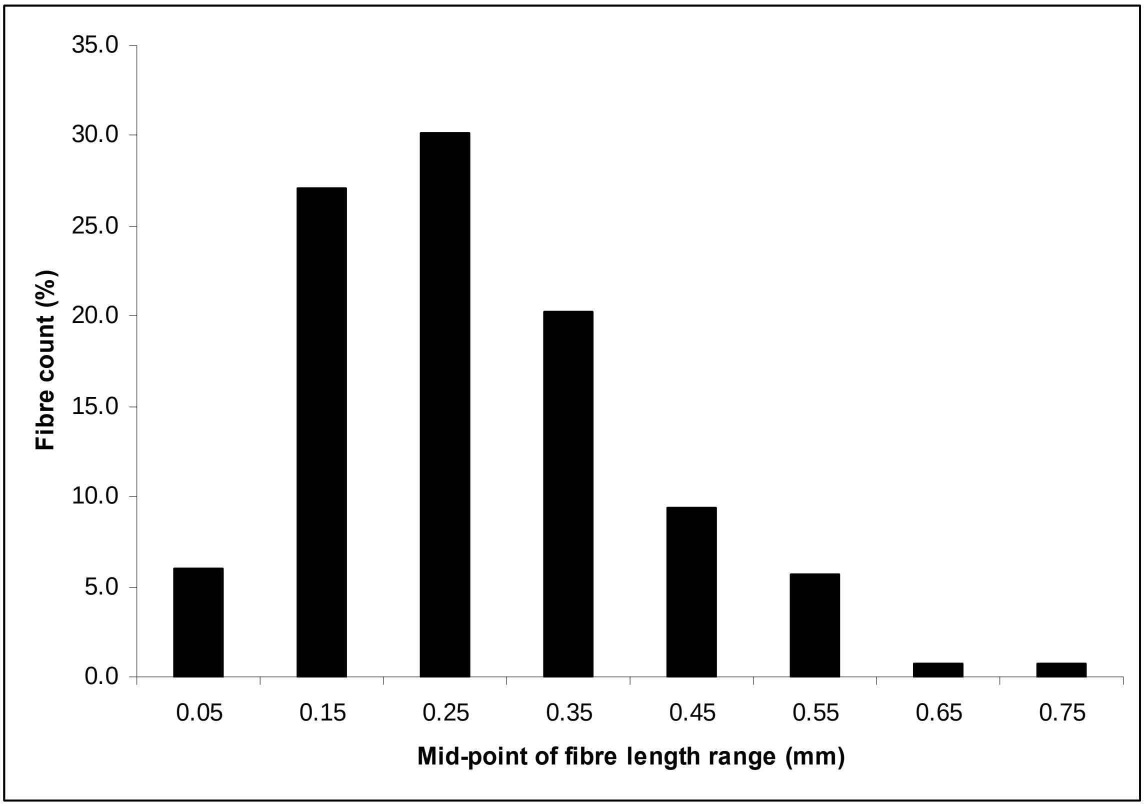

Figure 4.57: Fibre length distribution of short glass fibre composite (16% V_f)

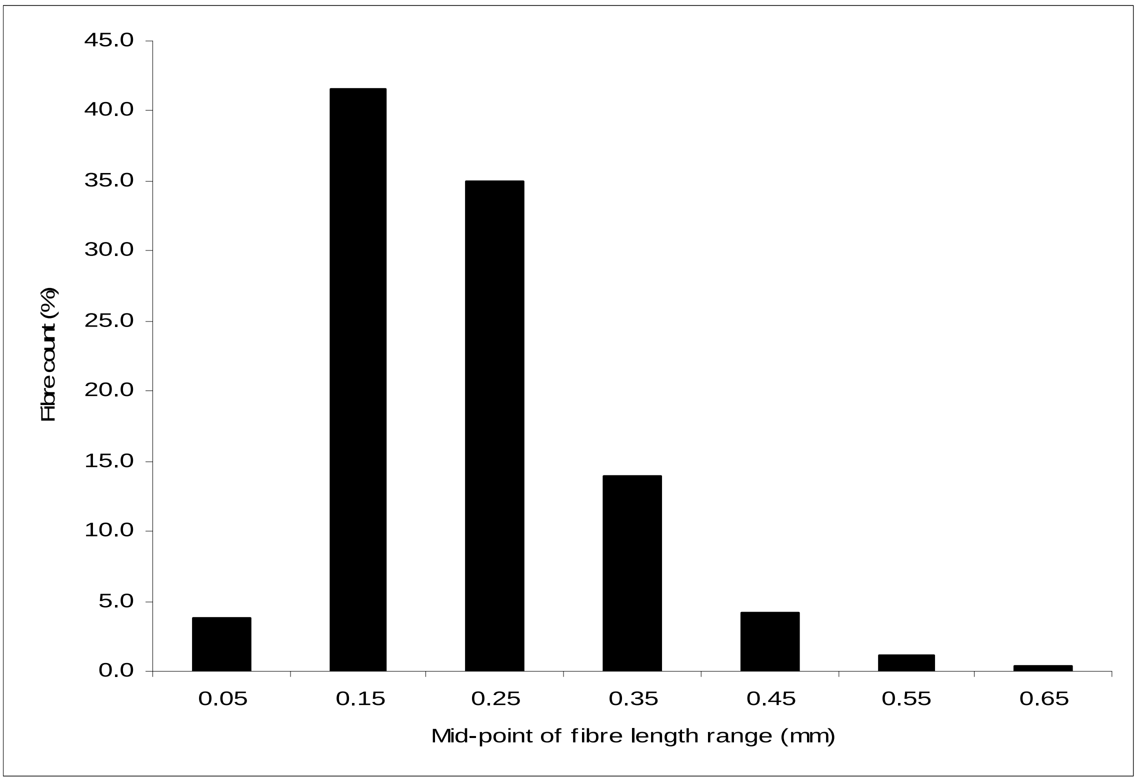

Figure 4.58: Fibre length distribution of short glass fibre composite (18% V_f)

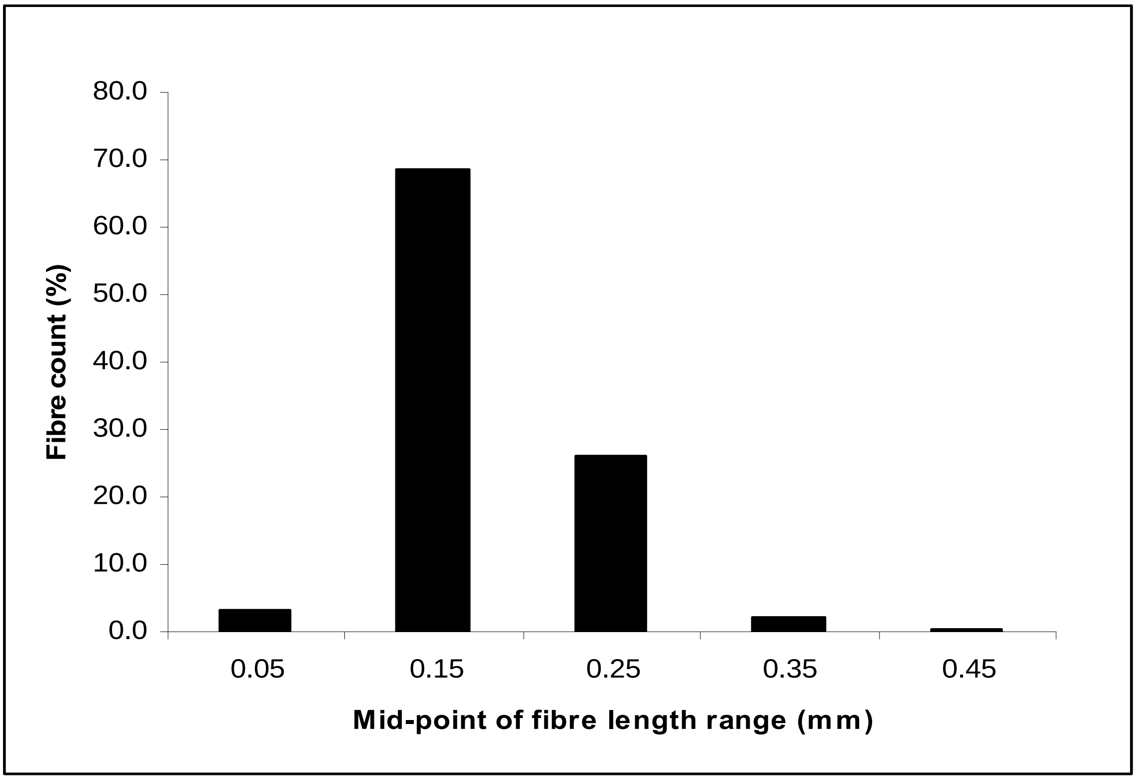

Figure 4.59: Fibre length distribution of short carbon fibre composite (33% V_f)

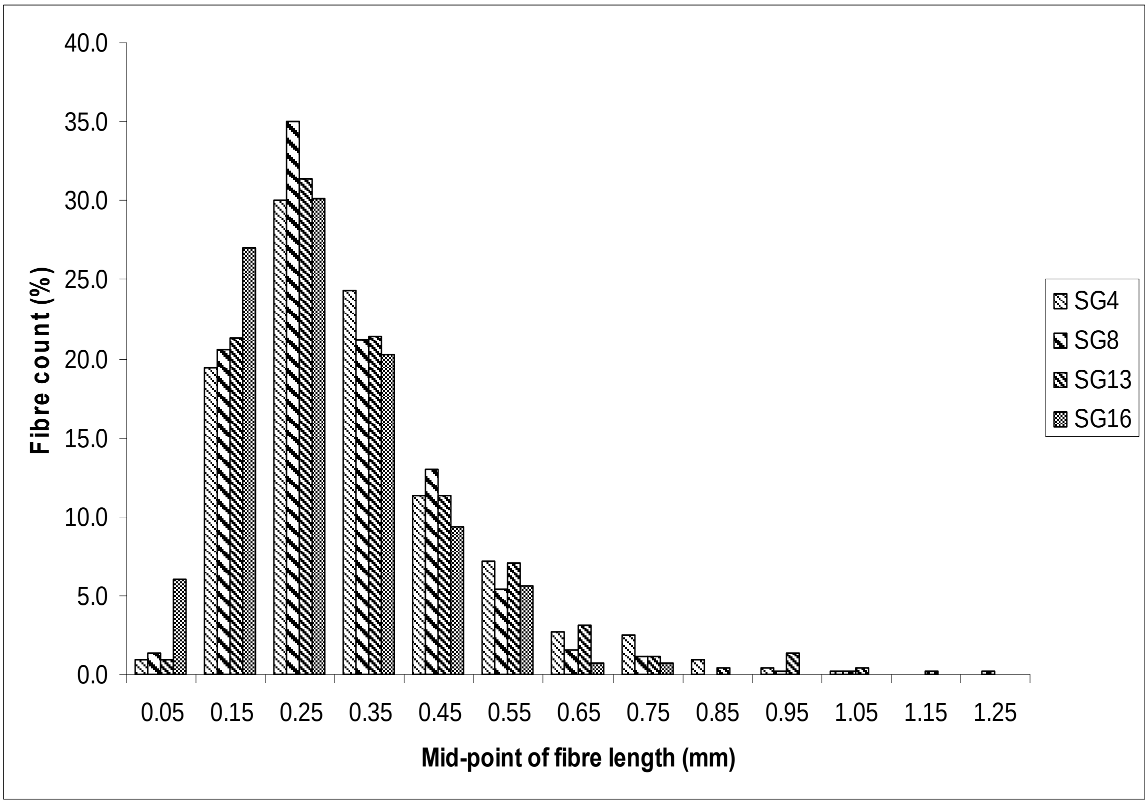

Figure 4.60: Fibre length distribution of short glass fibre composites

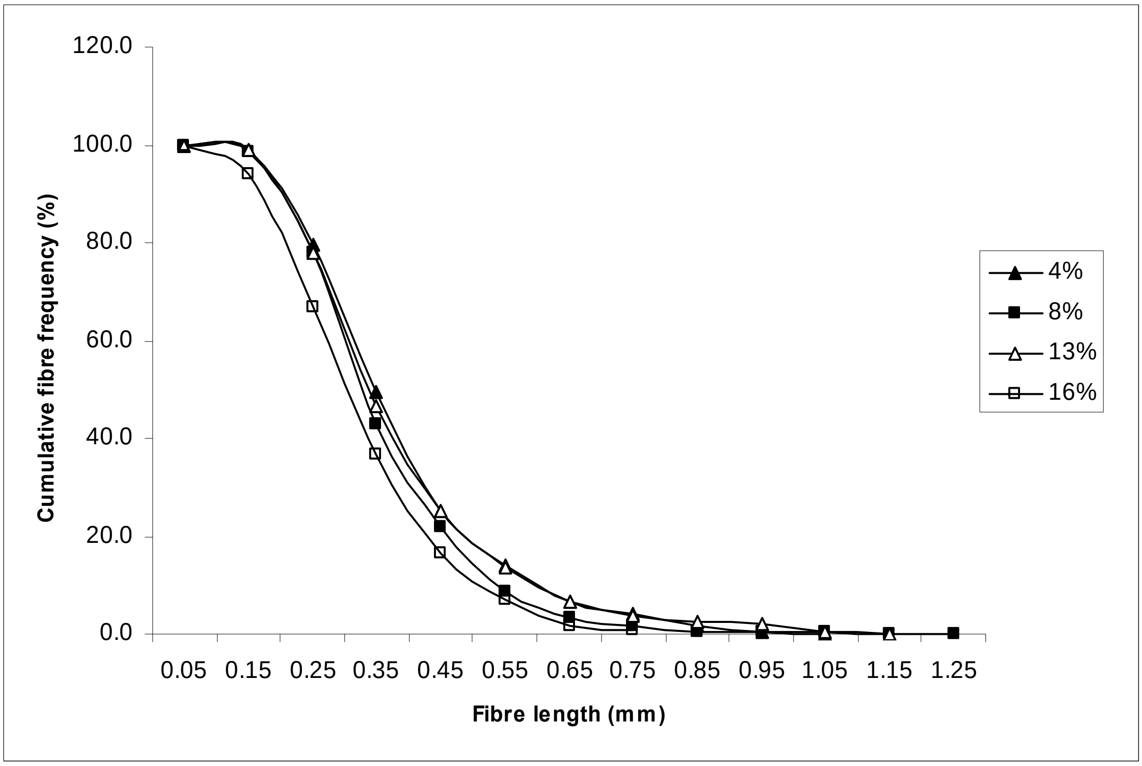

Figure 4.61: Cumulative fibre frequency of short glass fibre composites

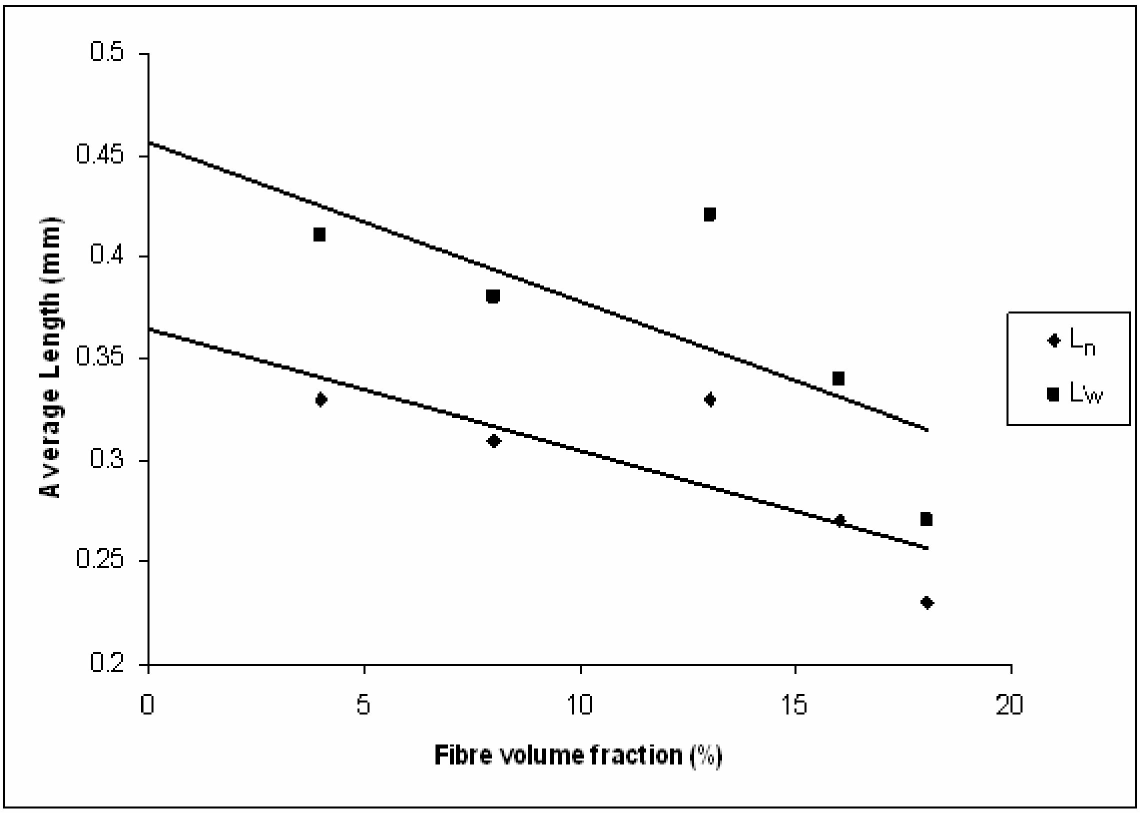

Figure 4.62: Average residual fibre length versus fibre volume fraction

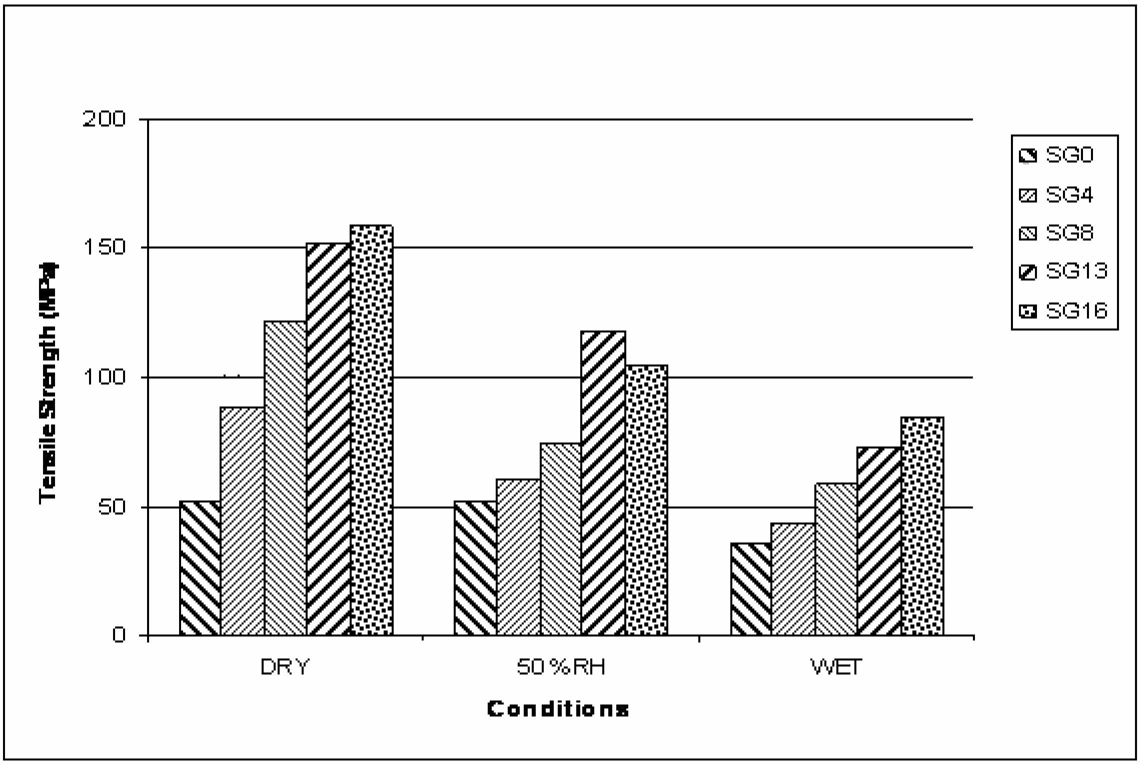

Figure 4.63: The tensile strength of injection-moulded short glass fibre composites for various fibre volume fractions at different conditions

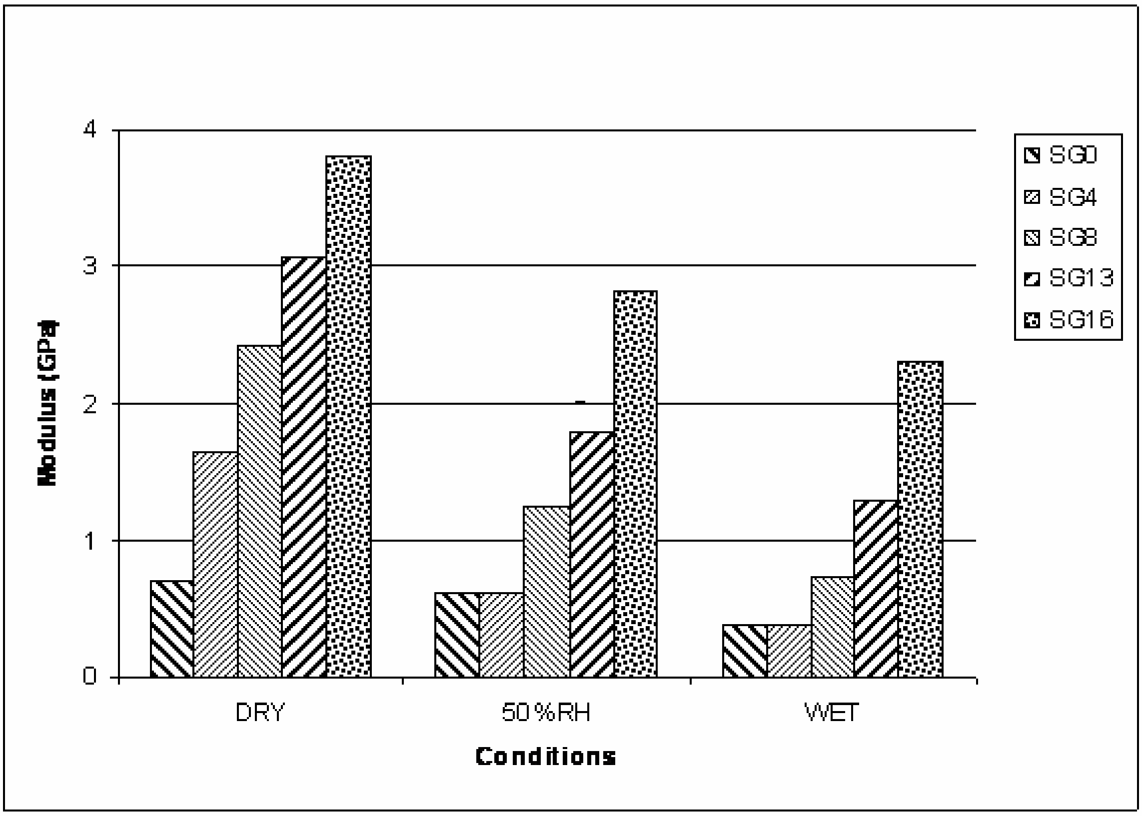

Figure 4.64: The tensile modulus of injection-moulded short glass fibre composites for various fibre volume fractions at different conditions

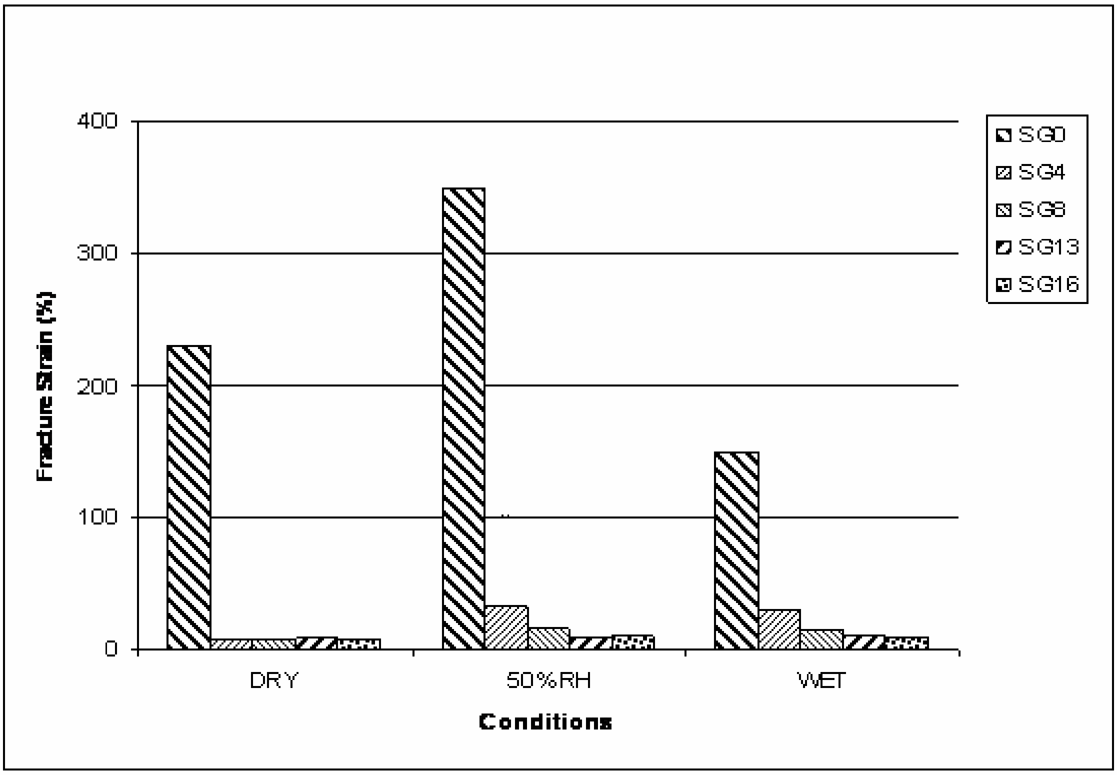

Figure 4.65: The fracture strain of injection-moulded short glass fibre composites for various fibre volume fractions at different conditions

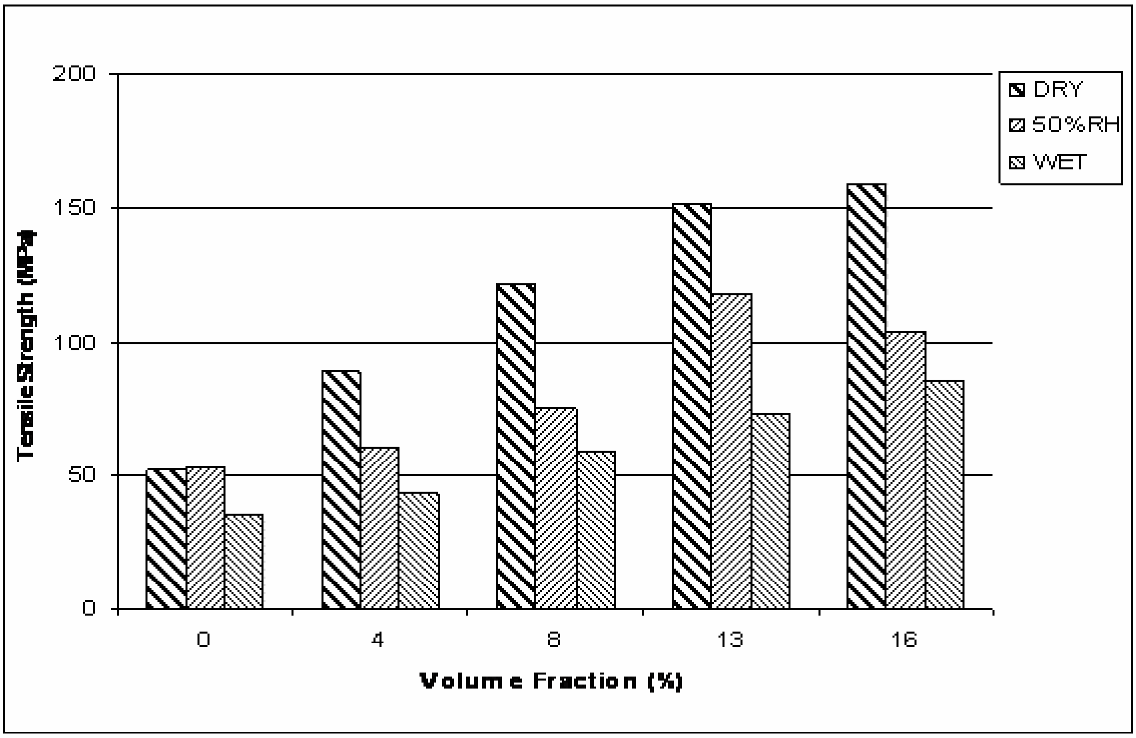

Figure 4.66: The tensile strength of injection-moulded short glass fibre composites at dry, 50% RH and wet condition for various fibre volume fractions

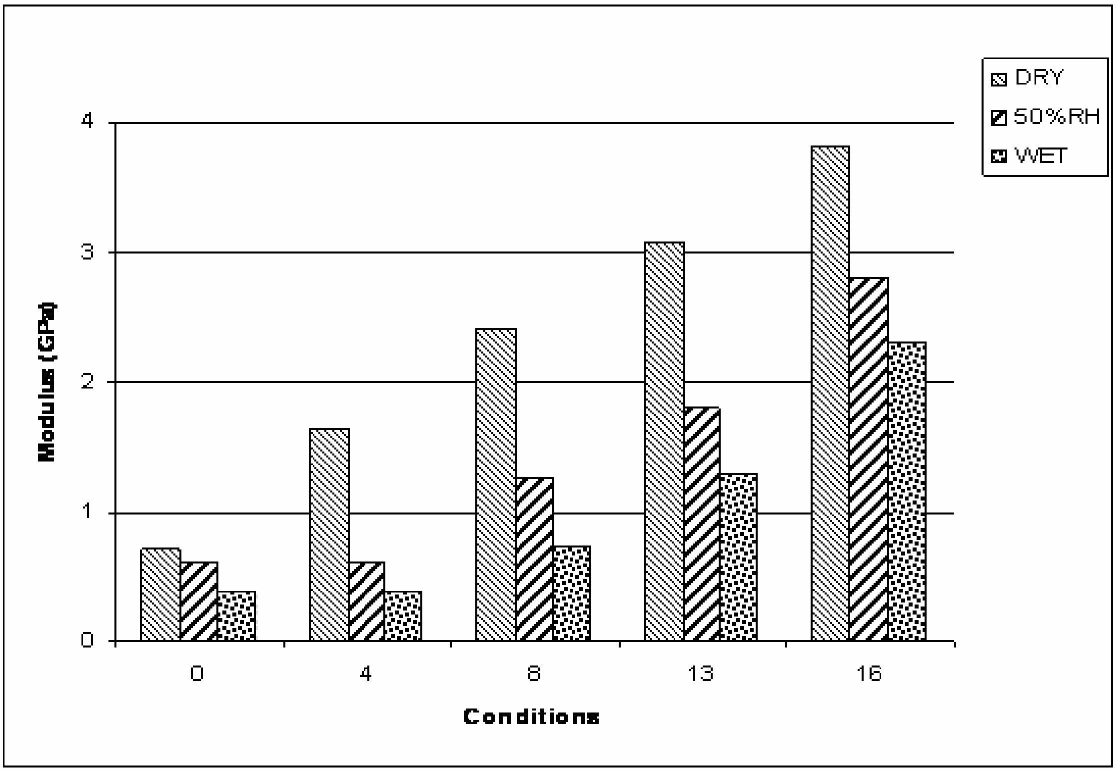

Figure 4.67: The tensile modulus of injection-moulded short glass fibre composite at dry, 50% RH and wet condition for various fibre volume fractions

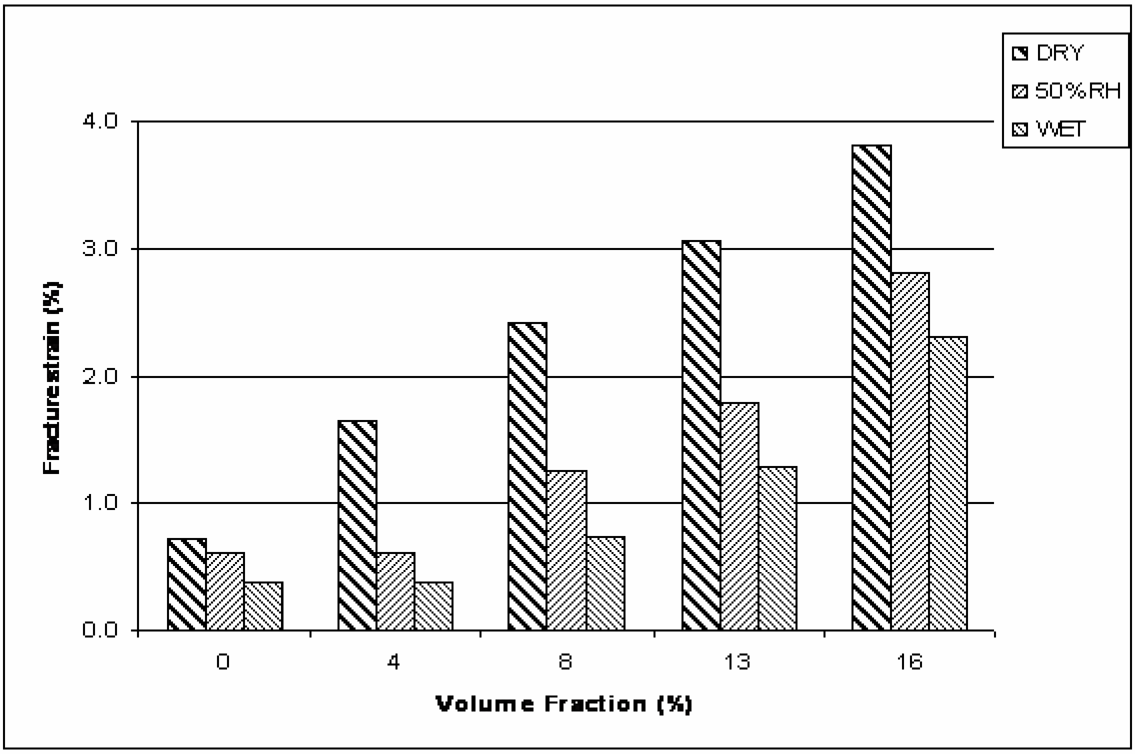

Figure 4.68: The fracture strain of injection-moulded short glass fibre composite at dry, 50% RH and wet condition for various fibre volume fractions

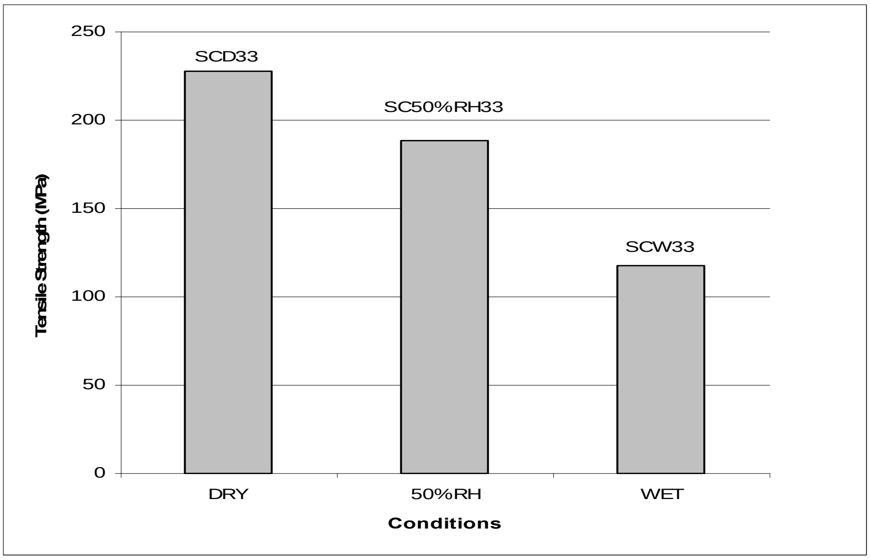

Figure 4.69: Tensile strength of carbon fibre composites at various conditions

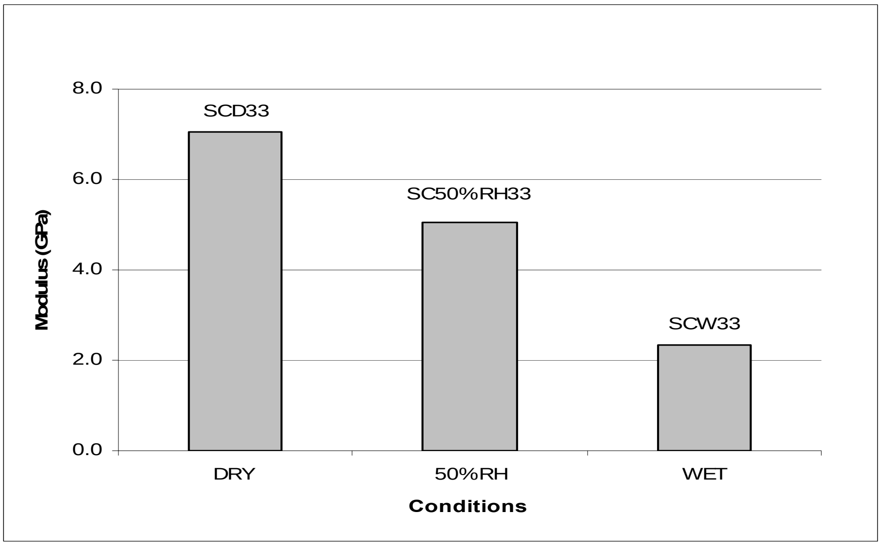

Figure 4.70: Tensile modulus of carbon fibre composites at various conditions

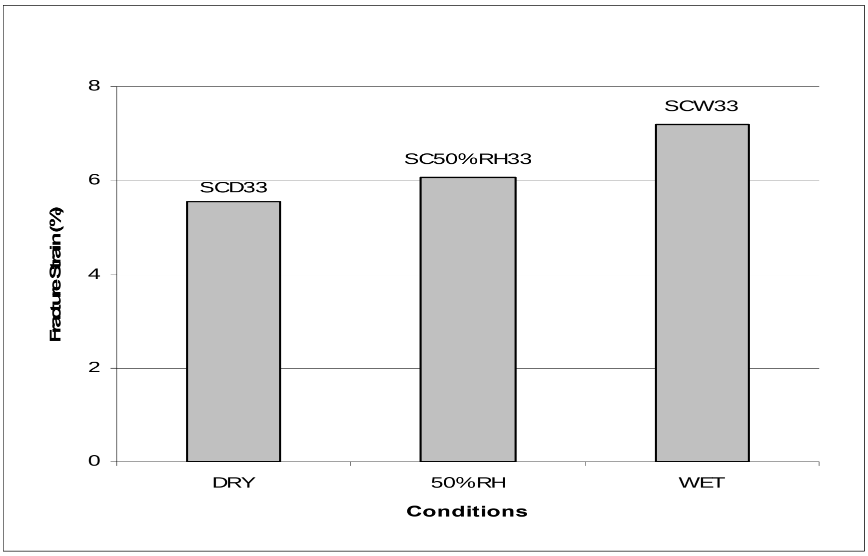

Figure 4.71: Fracture strain of carbon fibre composites at various conditions

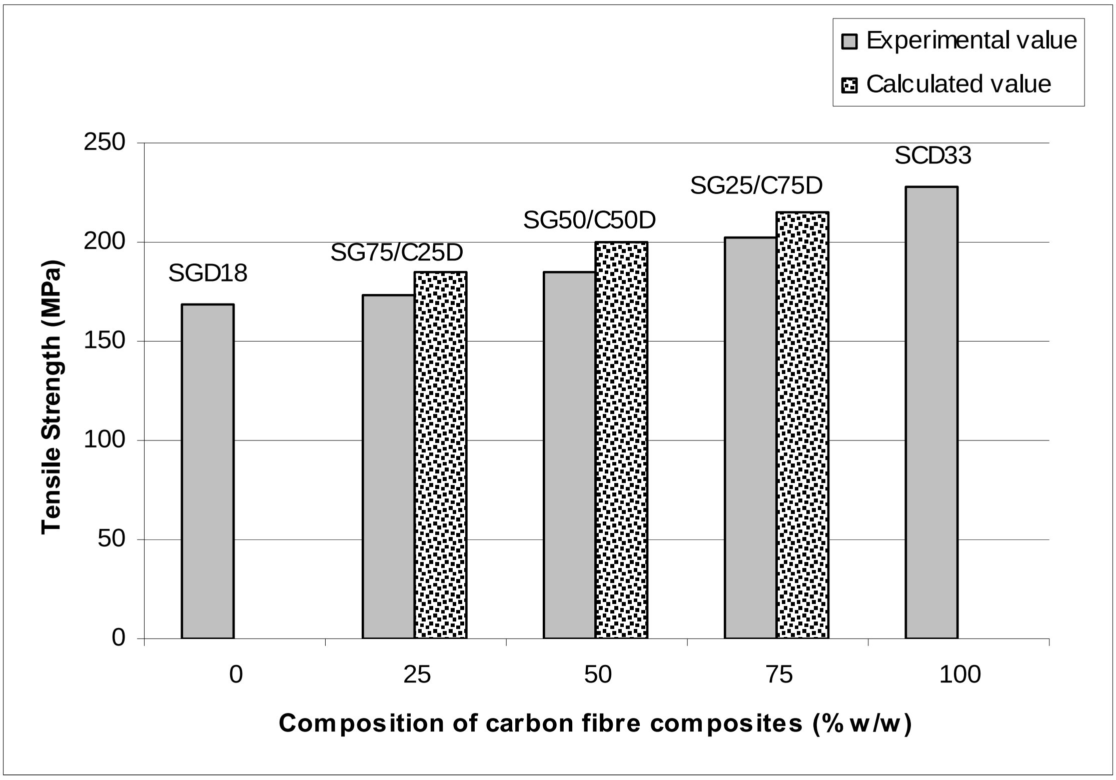

Figure 4.72: Tensile strength of hybrid fibre composites subjected to dry condition

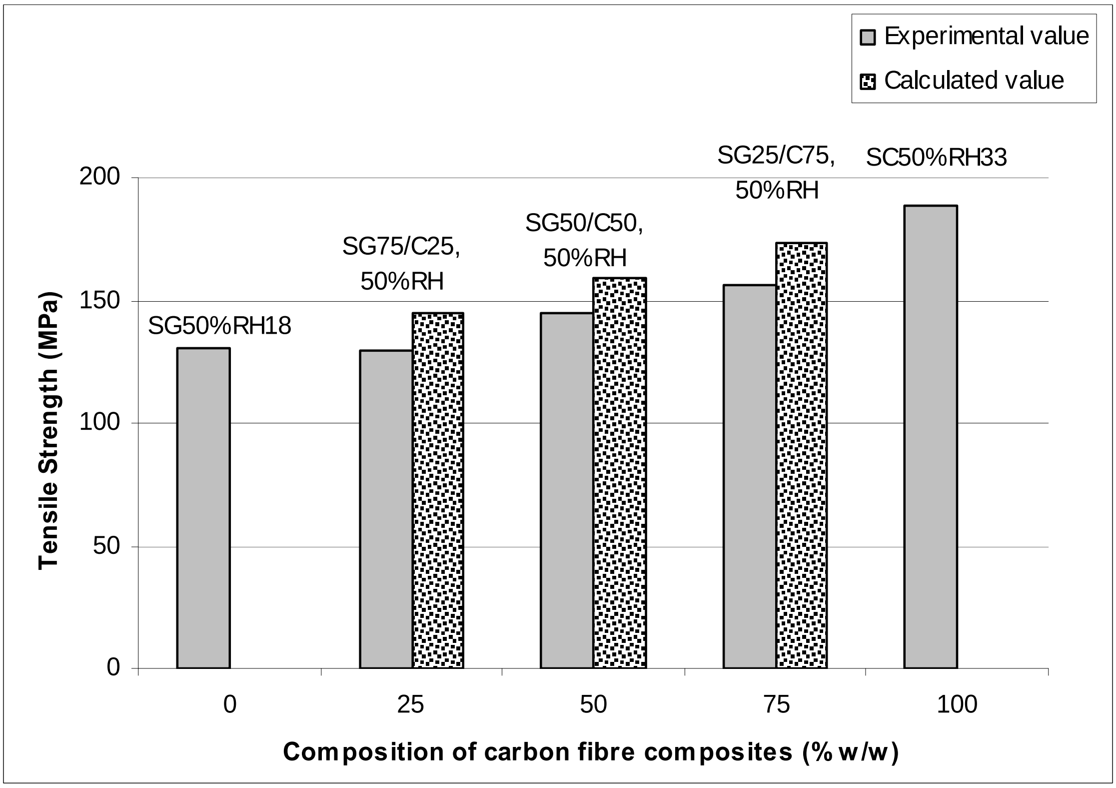

Figure 4.73: Tensile strength of hybrid fibre composites subjected to 50% RH condition

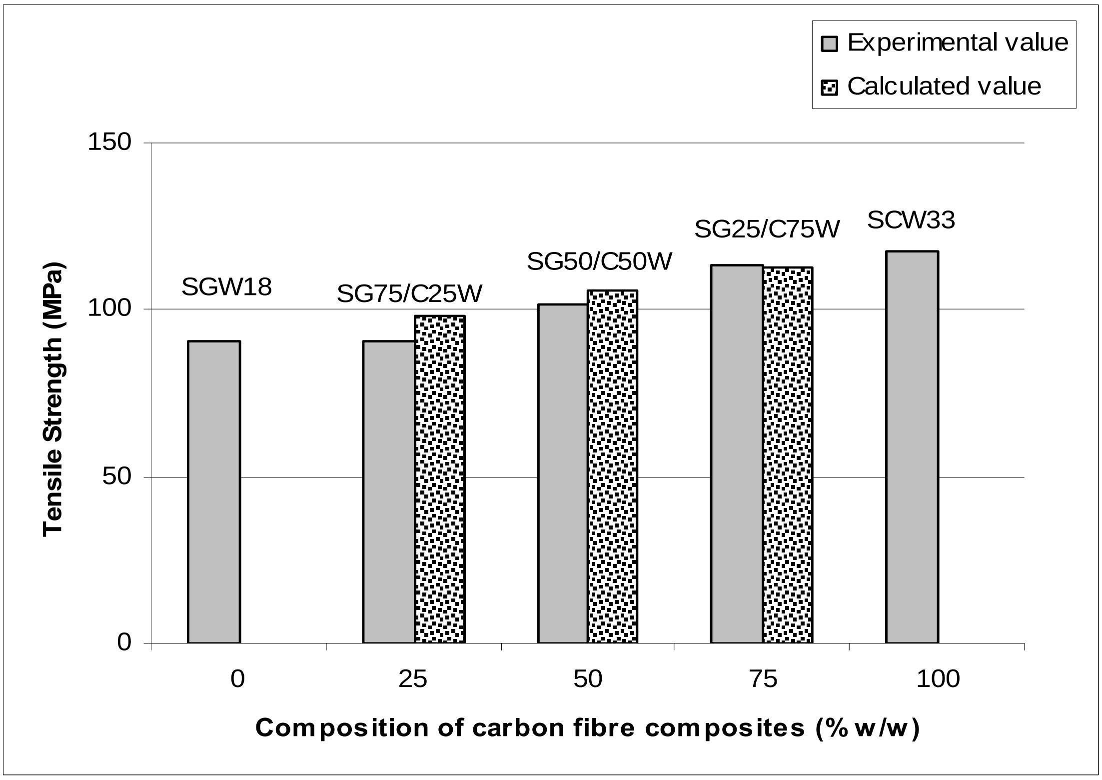

Figure 4.74: Tensile strength of hybrid fibre composites subjected to wet condition

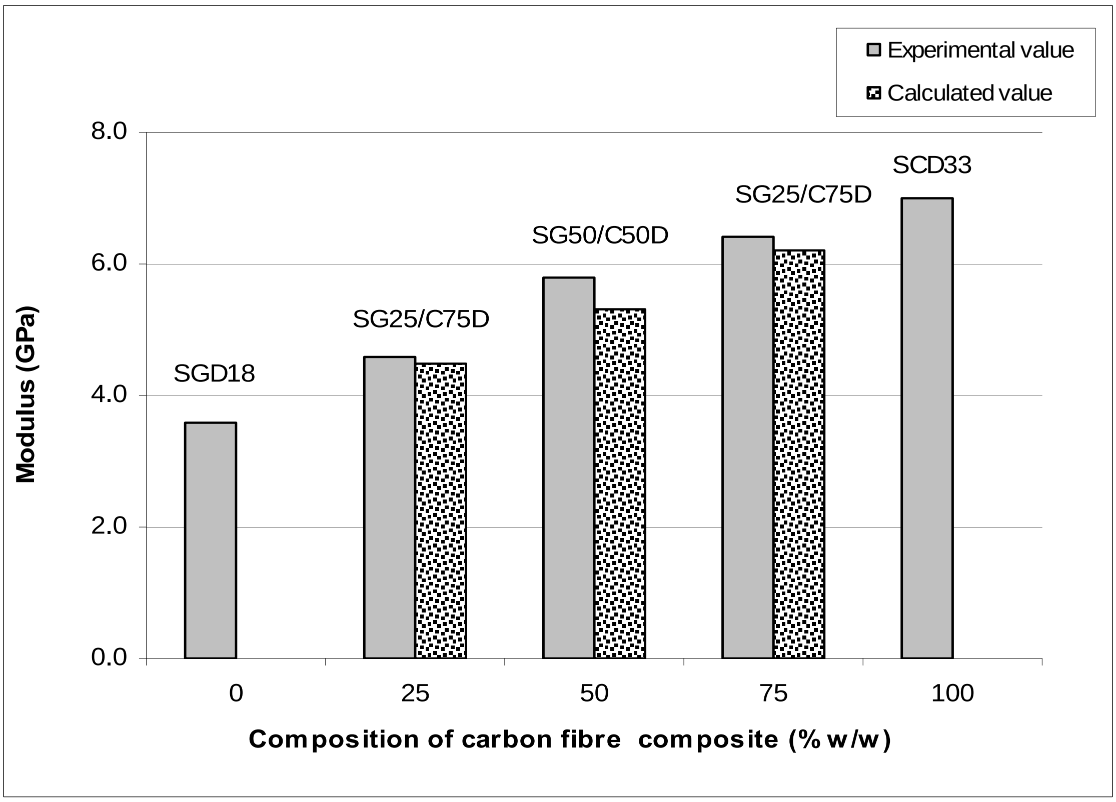

Figure 4.75: Tensile modulus of hybrid fibre composites subjected to dry condition

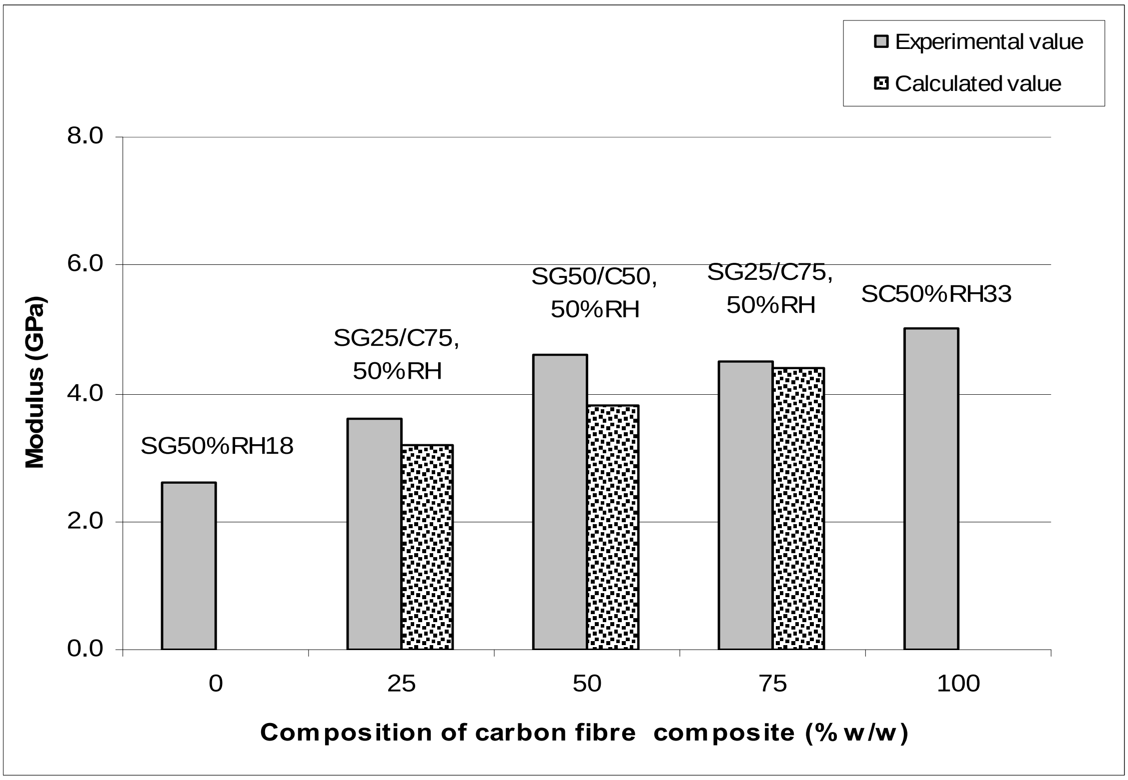

Figure 4.76: Tensile modulus of hybrid fibre composites subjected to 50% RH condition

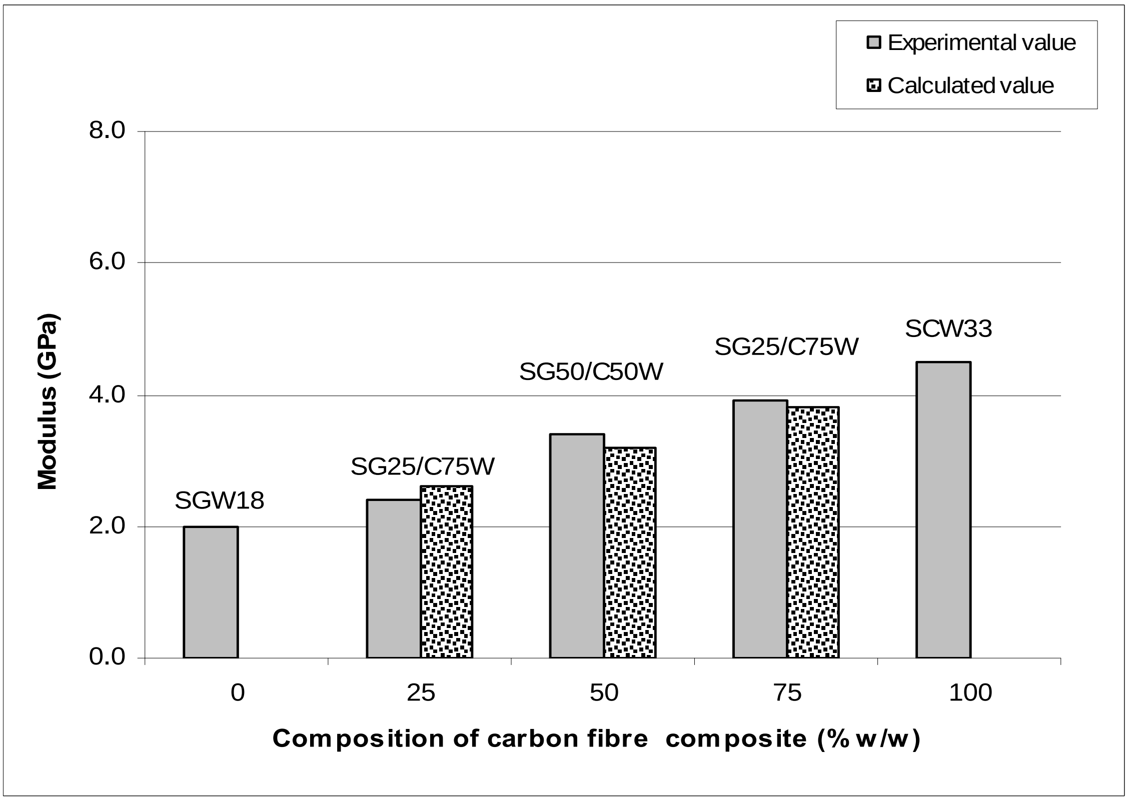

Figure 4.77: Tensile modulus of hybrid fibre composites subjected to wet condition

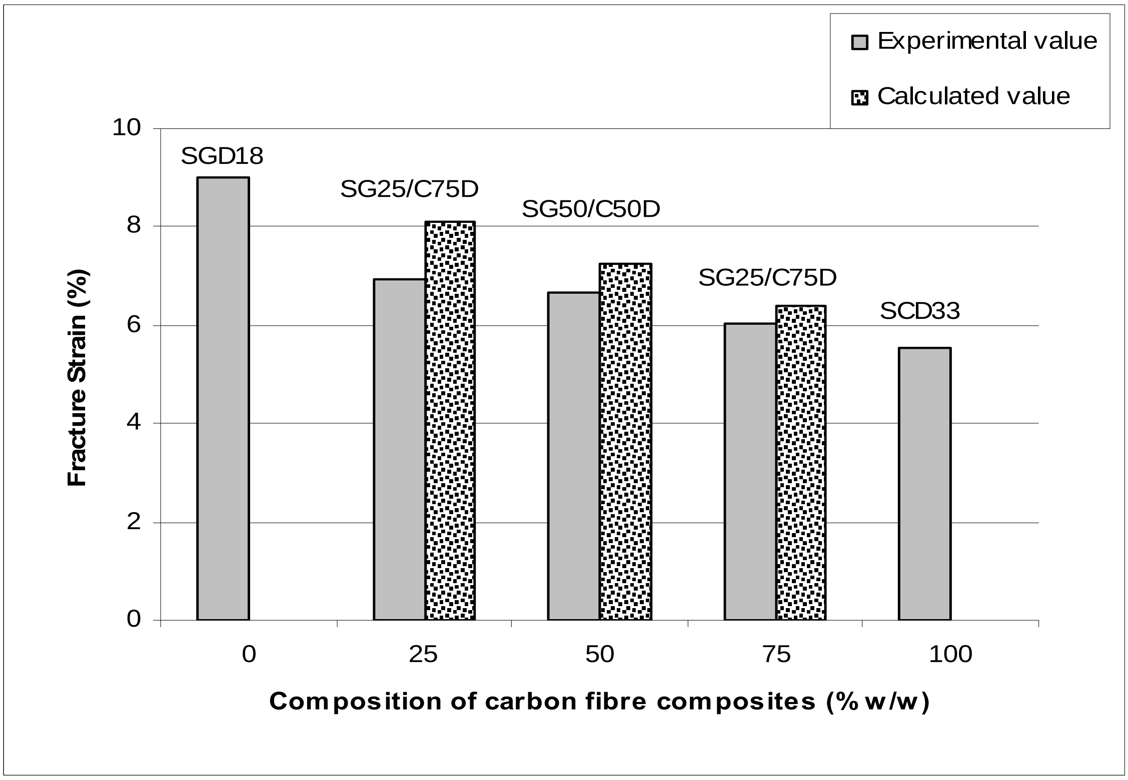

Figure 4.78: Fracture strain of hybrid fibre composites subjected to dry condition

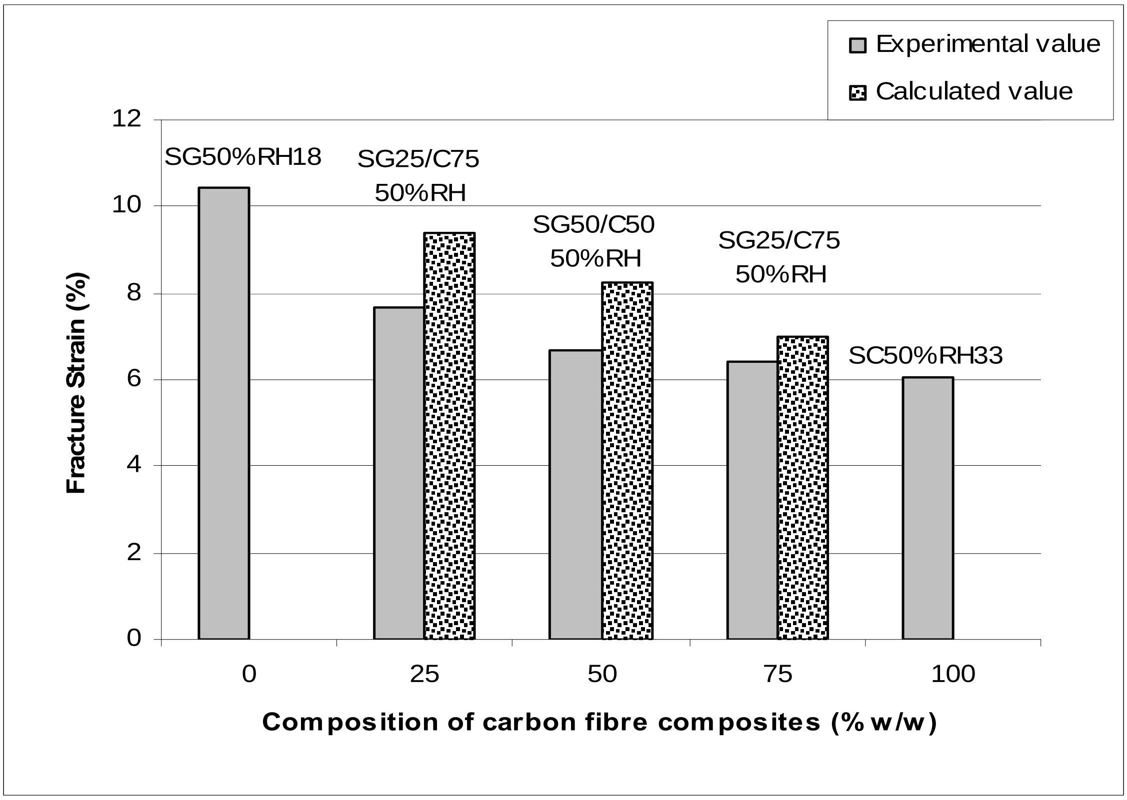

Figure 4.79: Fracture strain of hybrid fibre composites subjected to 50% RH condition

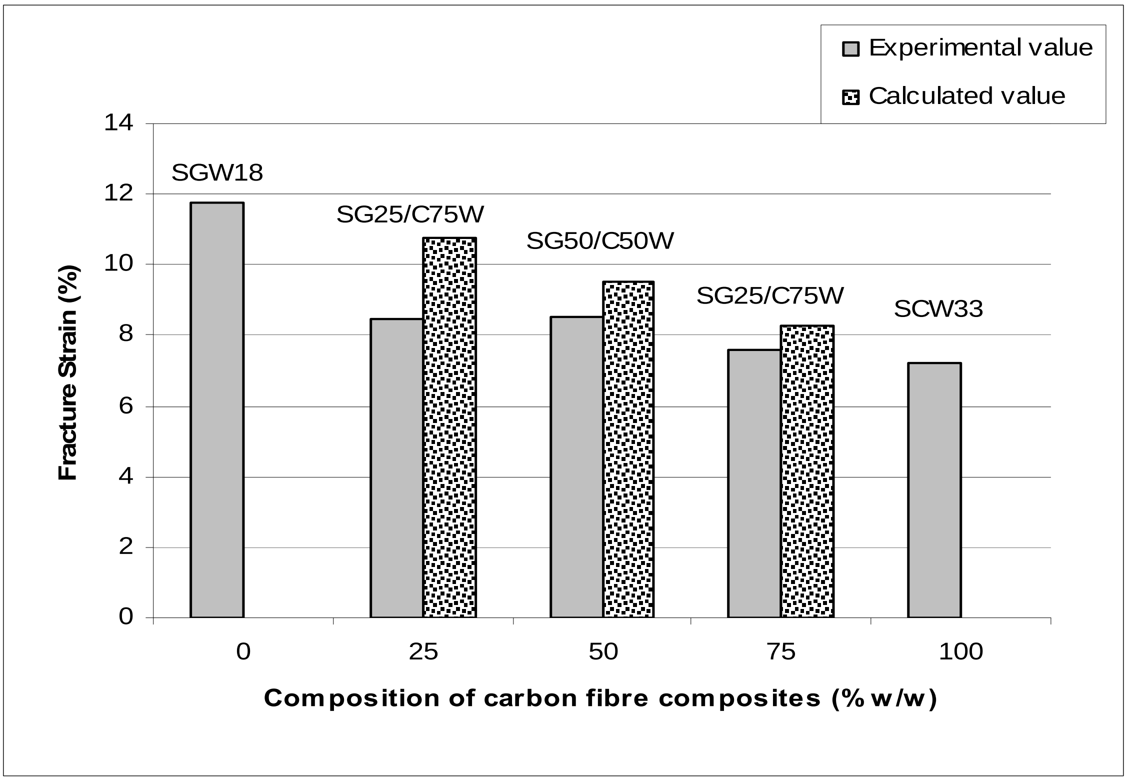

Figure 4.80: Fracture strain of hybrid fibre composites subjected to wet condition

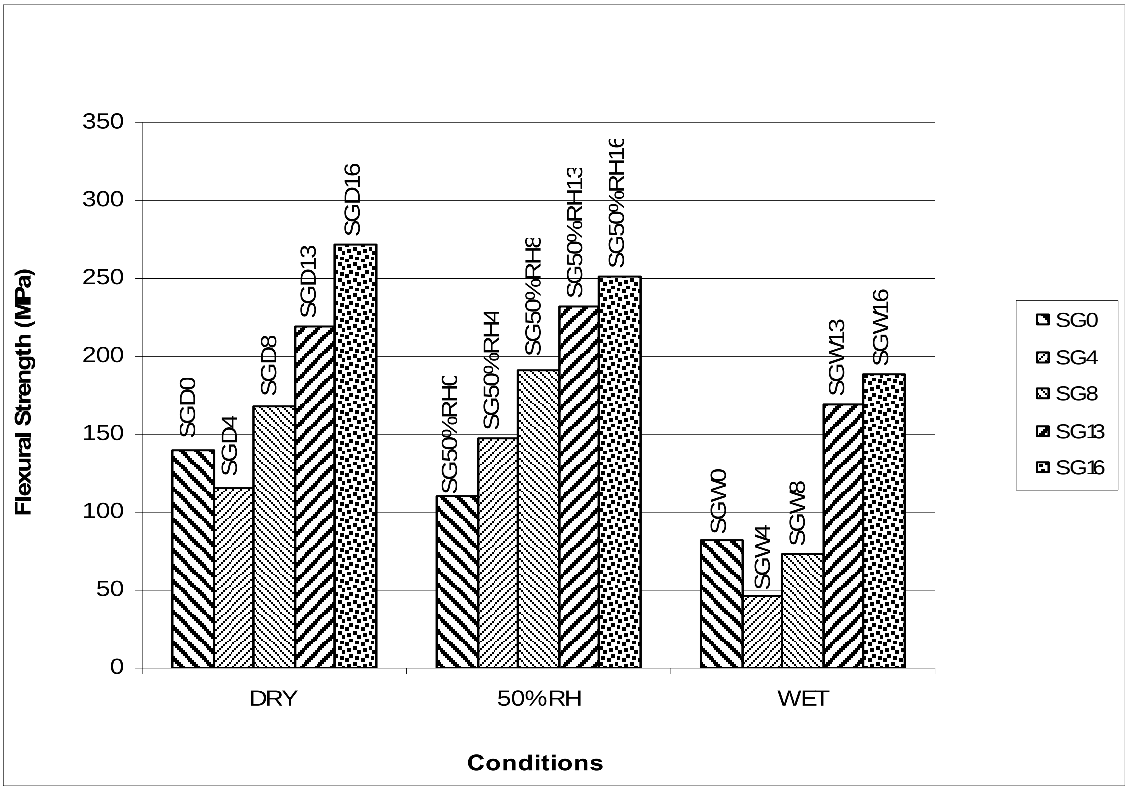

Figure 4.81: The flexural strength of injection-moulded short glass fibre composites for various fibre volume fractions at different conditions

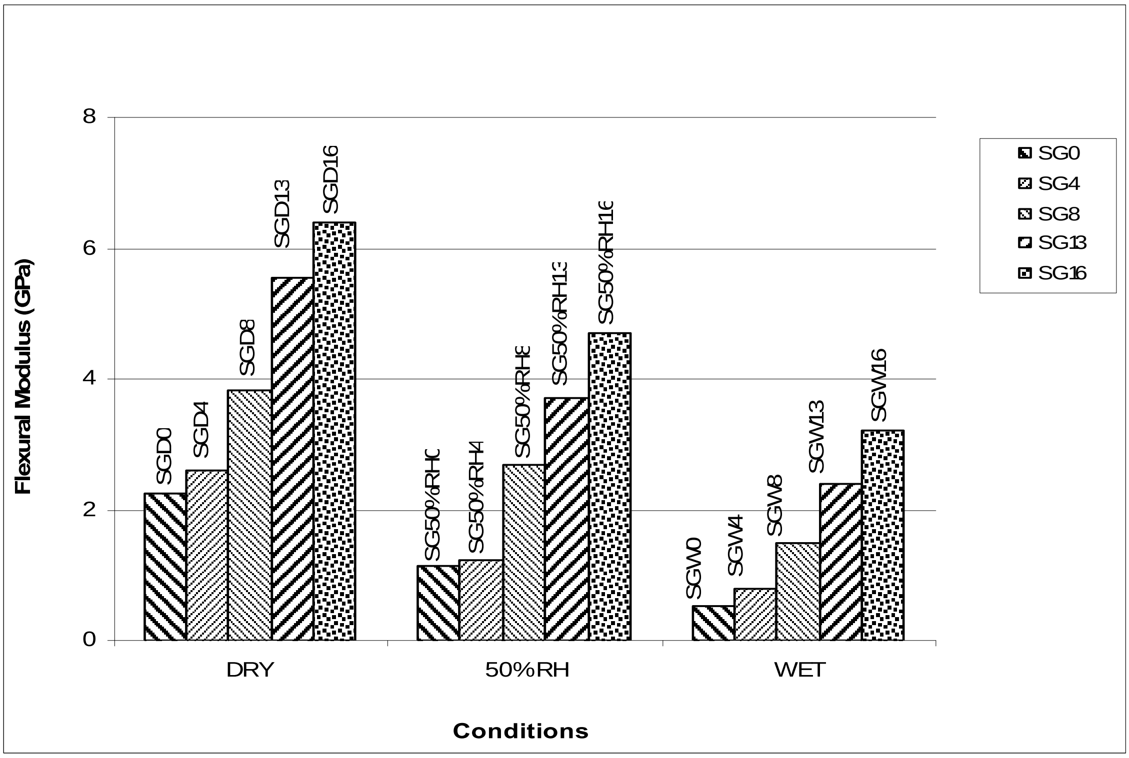

.

Figure 4.82: The flexural modulus of injection-moulded short glass fibre composites for various fibre volume fractions at different conditions

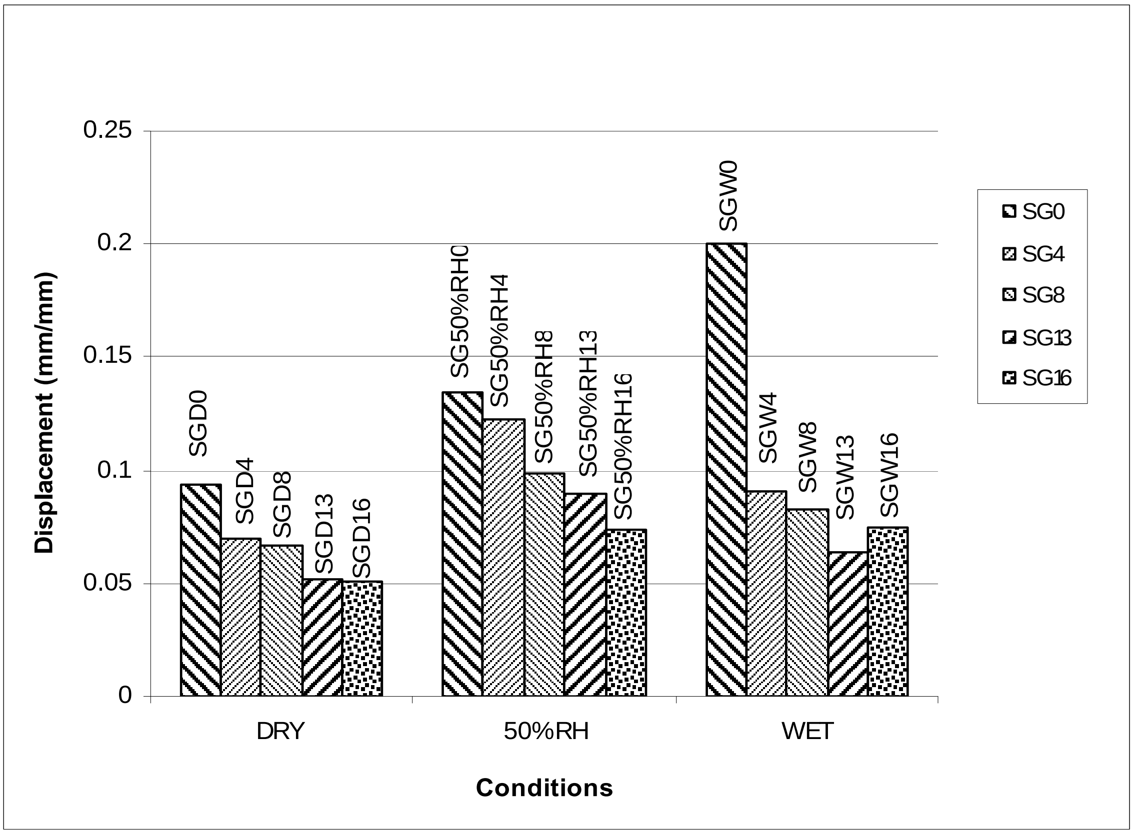

Figure 4.83: The flexural displacement of injection-moulded short glass fibre composites for various fibre volume fractions at different conditions

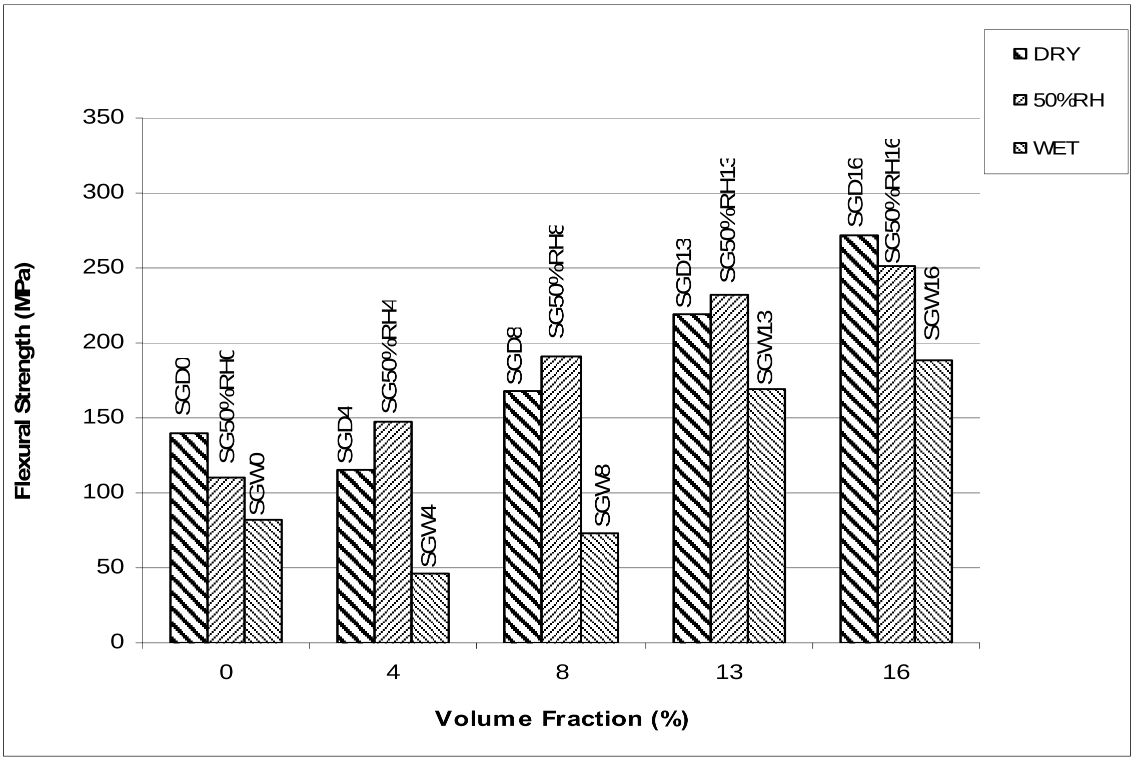

Figure 4.84: The flexural strength of injection-moulded short glass fibre composites at dry, 50% RH and wet condition for various fibre volume fractions

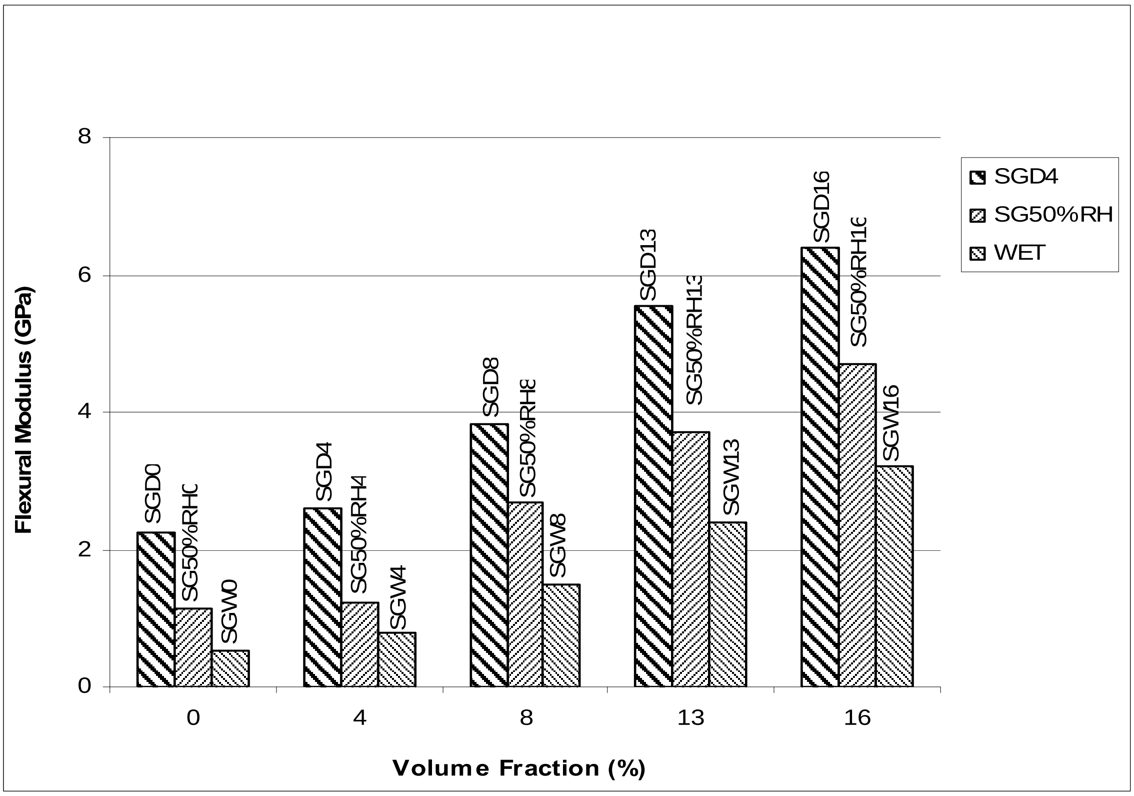

Figure 4.85: The flexural modulus of injection-moulded short glass fibre composites at dry, 50% RH and wet condition for various fibre volume fractions

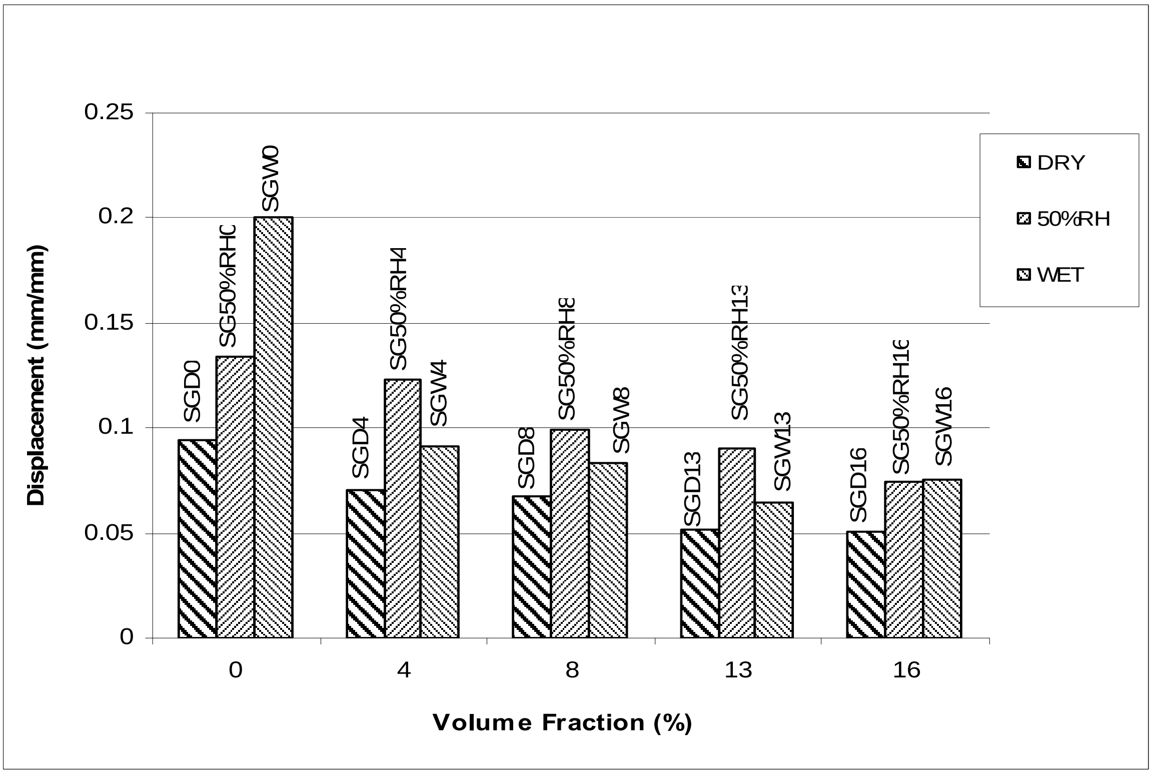

Figure 4.86: The flexural displacement of injection-moulded short glass fibre composites at dry, 50% RH and wet condition for various fibre volume fractions

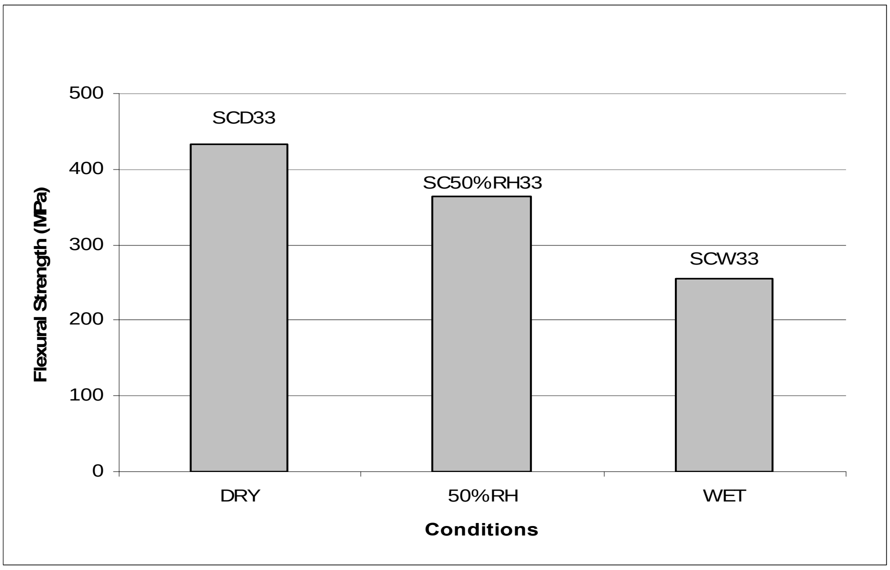

Figure 4.87: Flexural strength of carbon fibre composites at various conditions

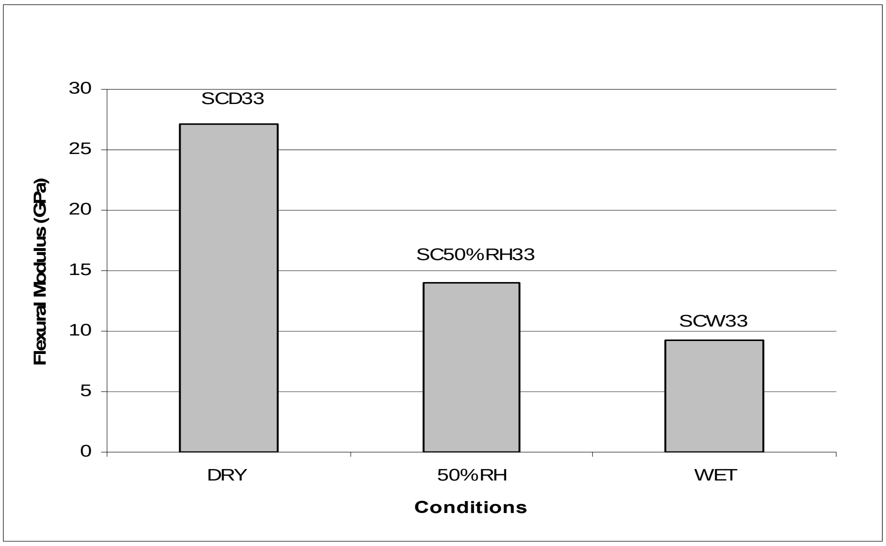

Figure 4.88: Flexural modulus of carbon fibre composites at various conditions

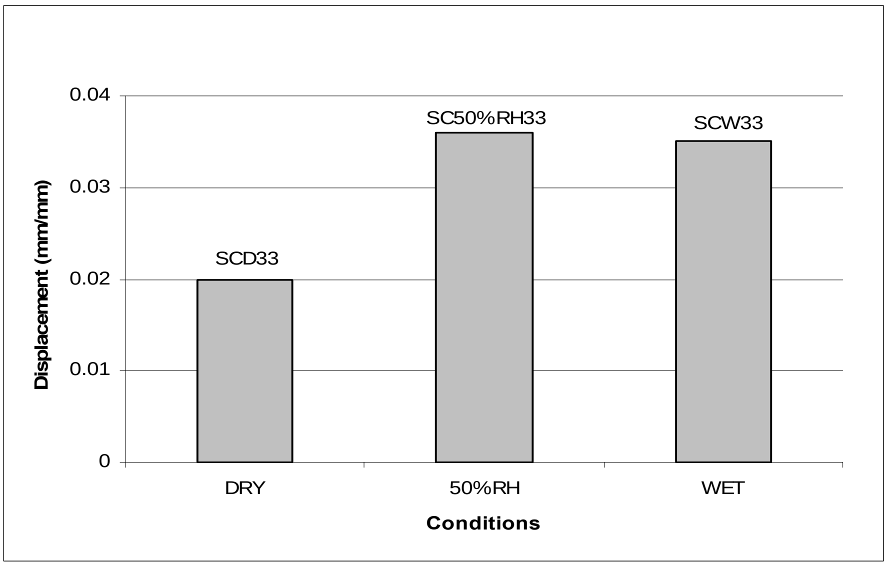

Figure 4.89: Flexural displacement of carbon fibre composites at various conditions

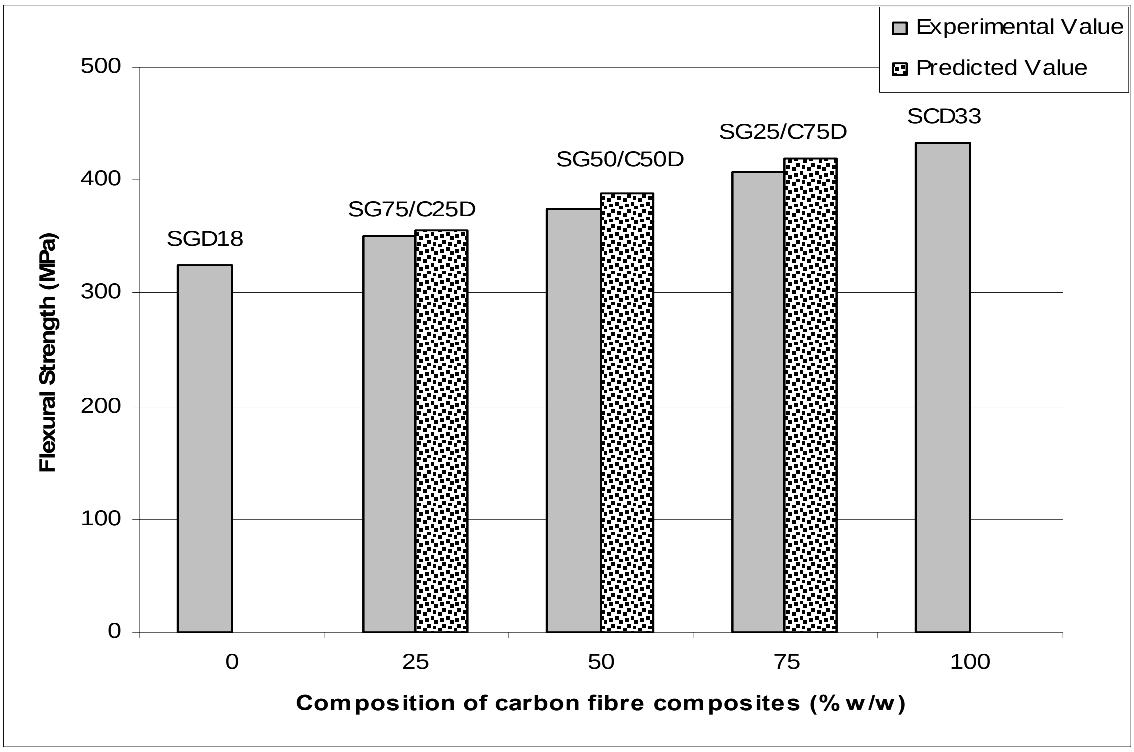

Figure 4.90: Flexural strength of composites subjected to dry condition

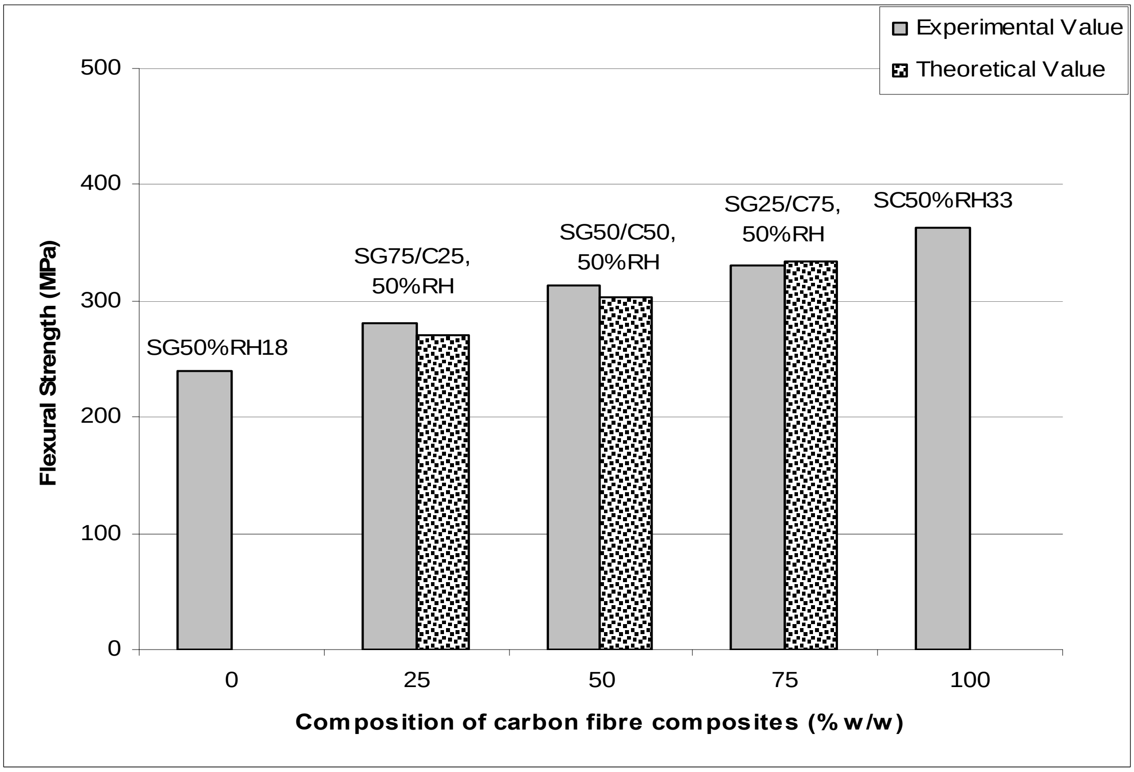

Figure 4.91: Flexural strength of composites subjected to 50% RH condition

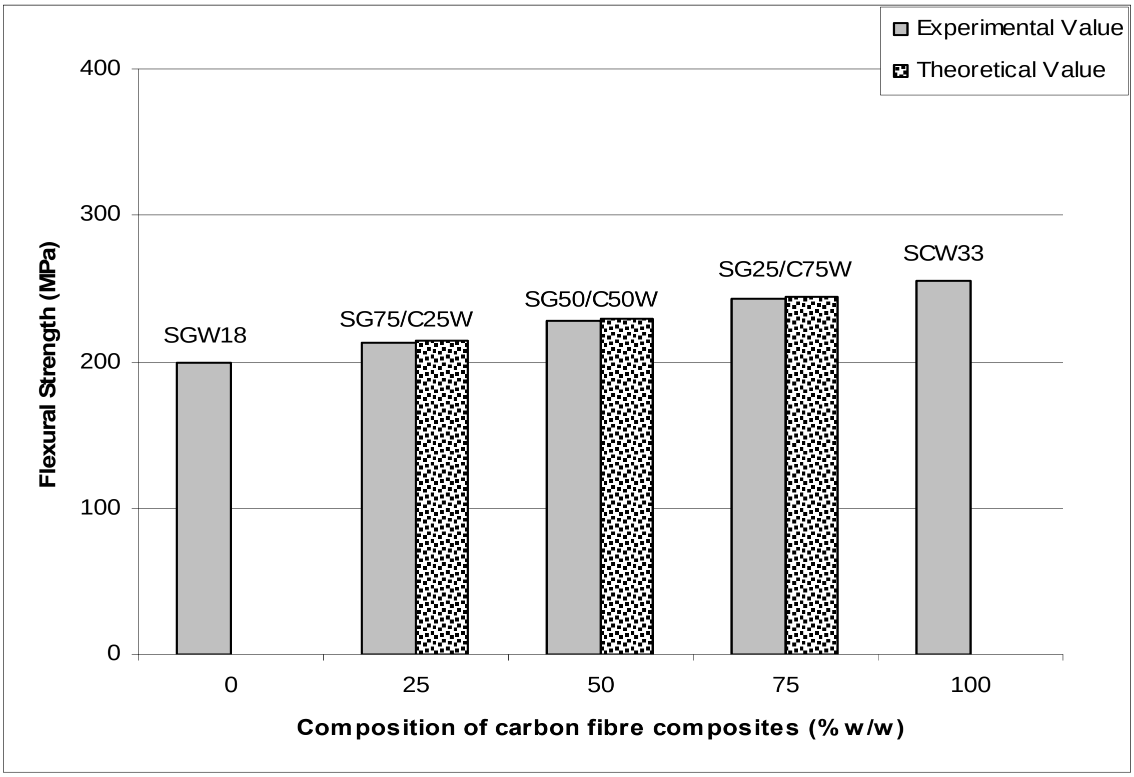

Figure 4.92: Flexural strength of composites subjected to wet condition

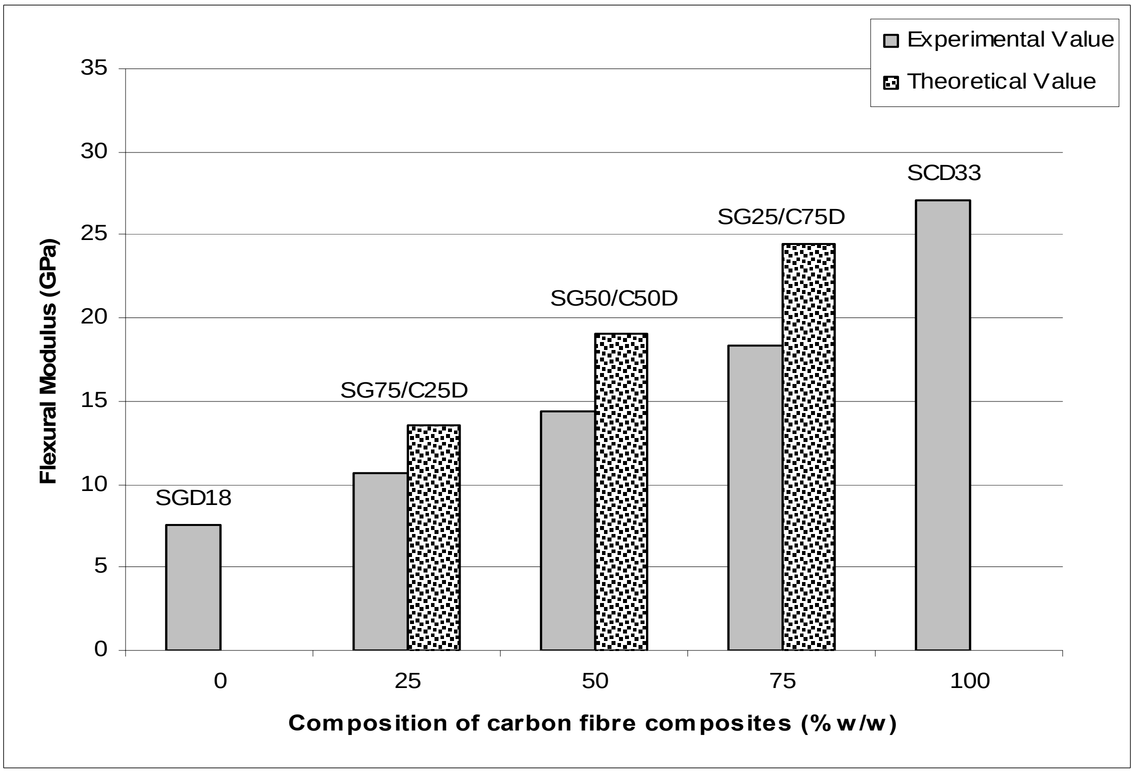

Figure 4.93: Flexural modulus of composites subjected to dry condition

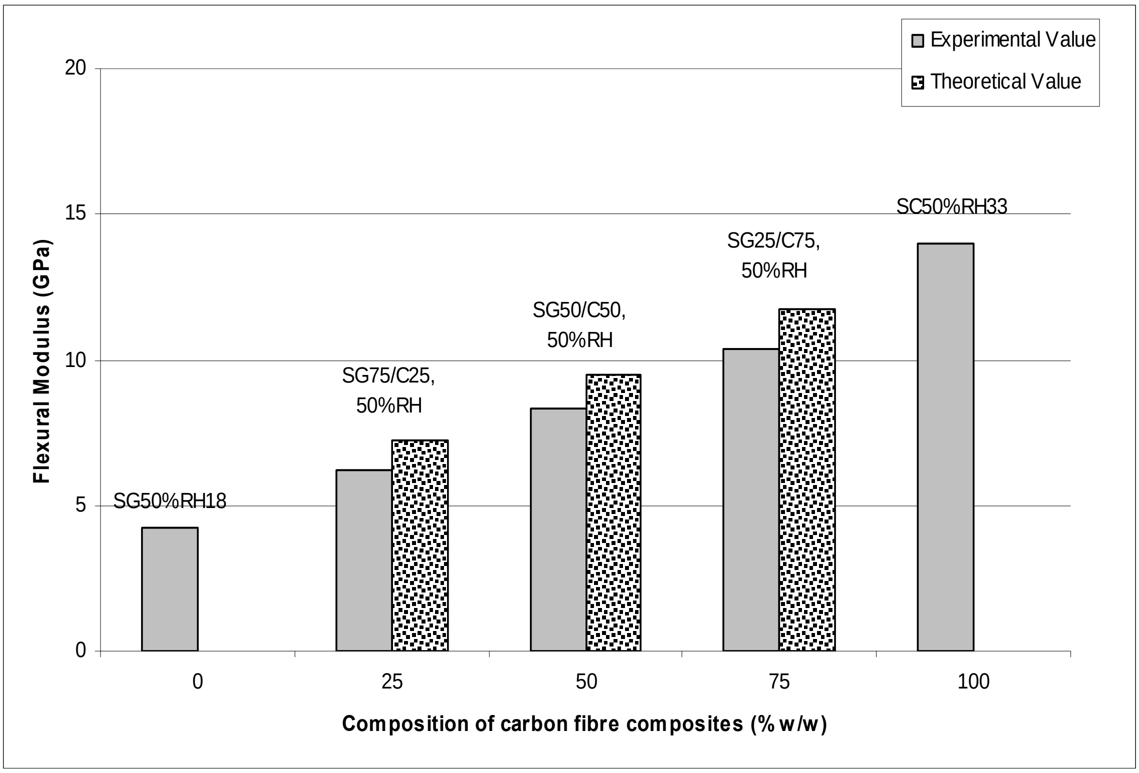

Figure 4.94: Flexural modulus of composites subjected to 50% RH condition

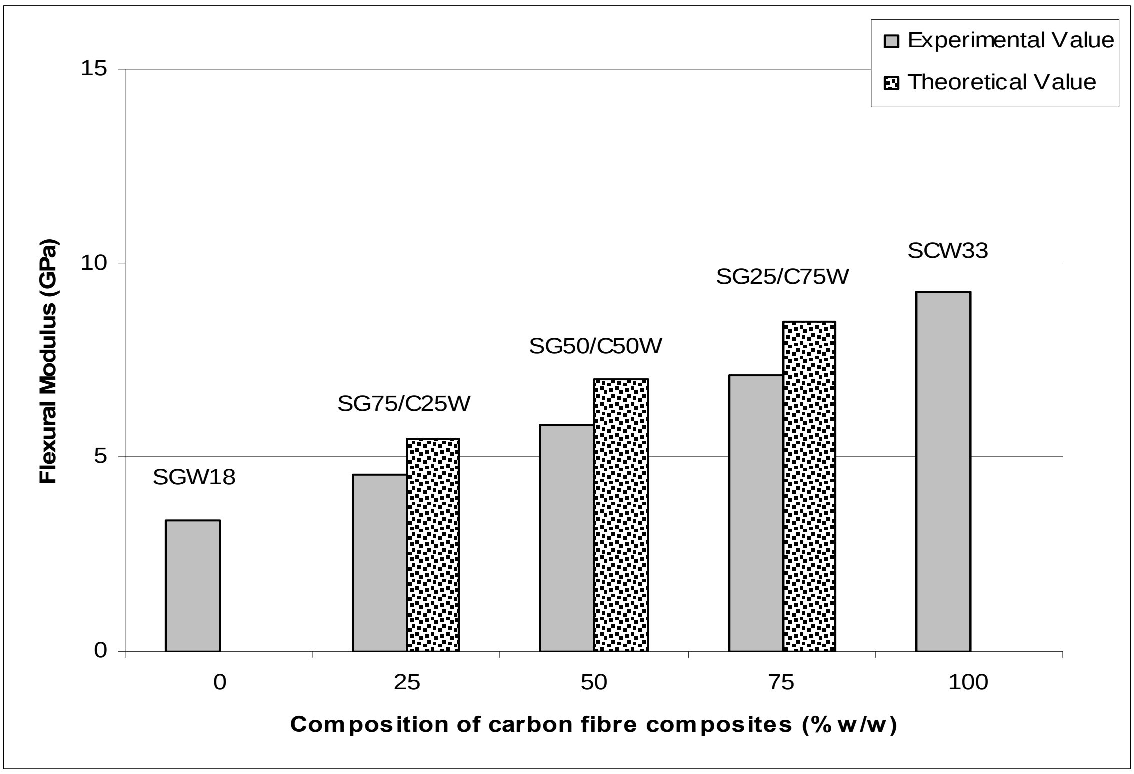

Figure 4.95: Flexural modulus of composites subjected to wet condition

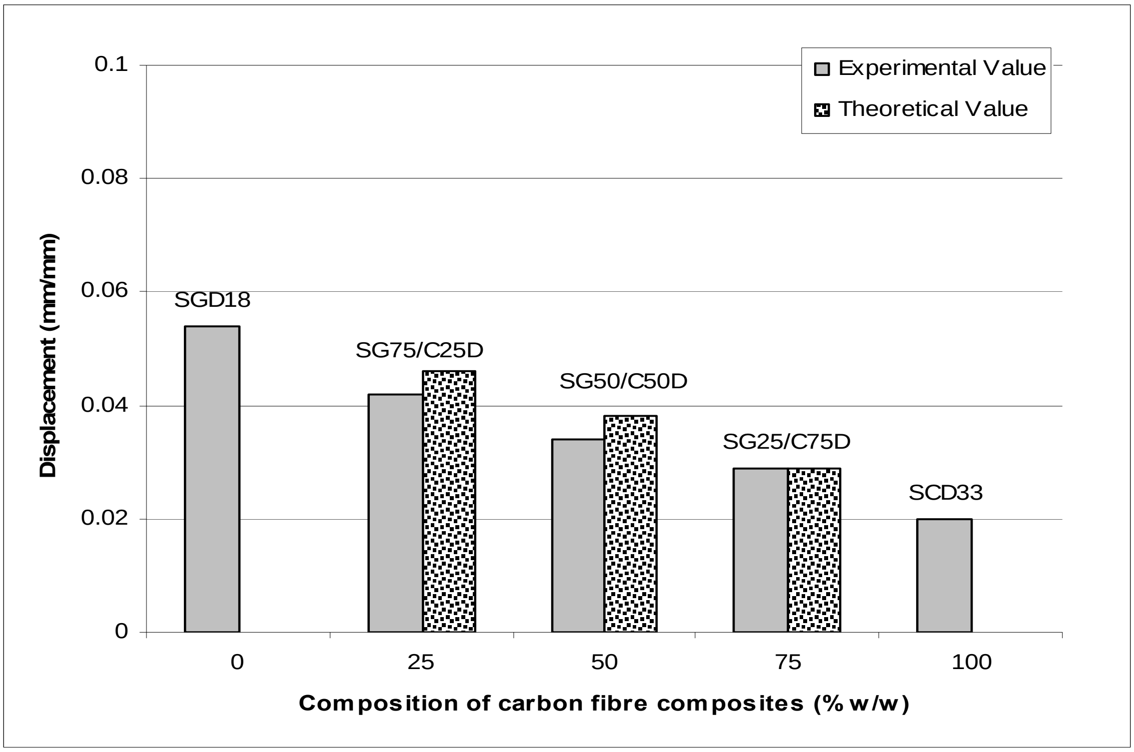

Figure 4.96: Flexural displacement of composites subjected to dry condition

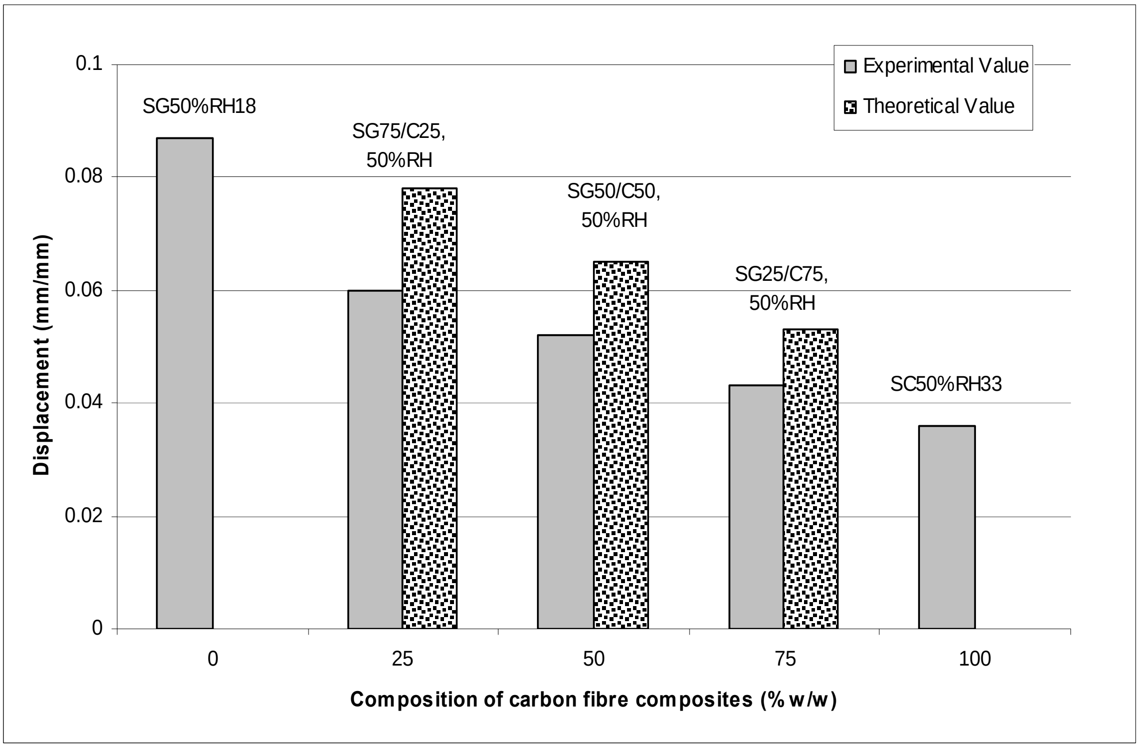

Figure 4.97: Flexural displacement of composites subjected to 50% RH condition

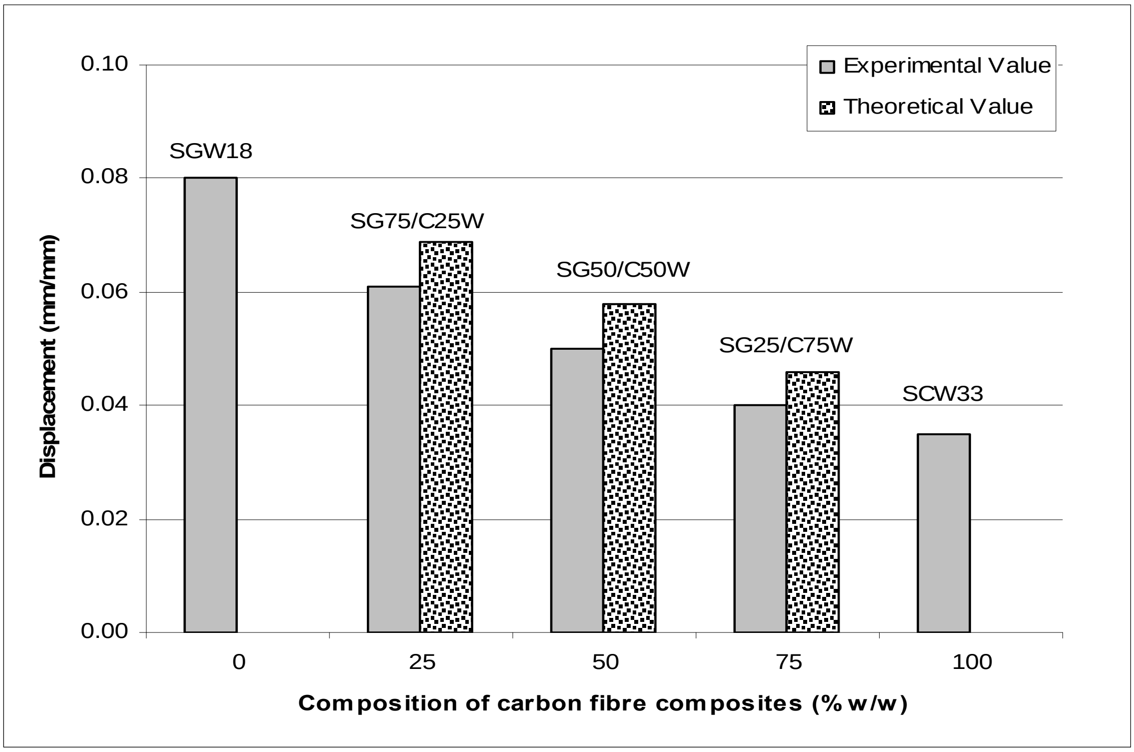

Figure 4.98: Flexural displacement of composites subjected to wet condition

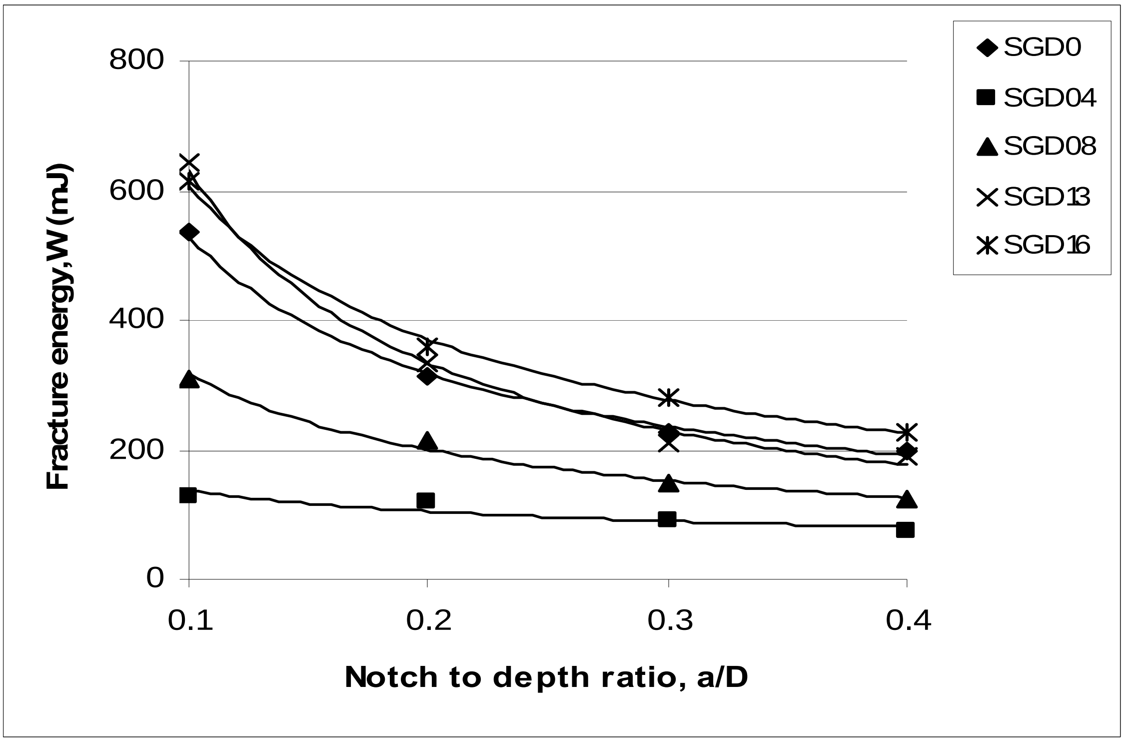

Figure 4.99: Variation of fracture energy with notch to depth ratio of composites subjected to dry condition

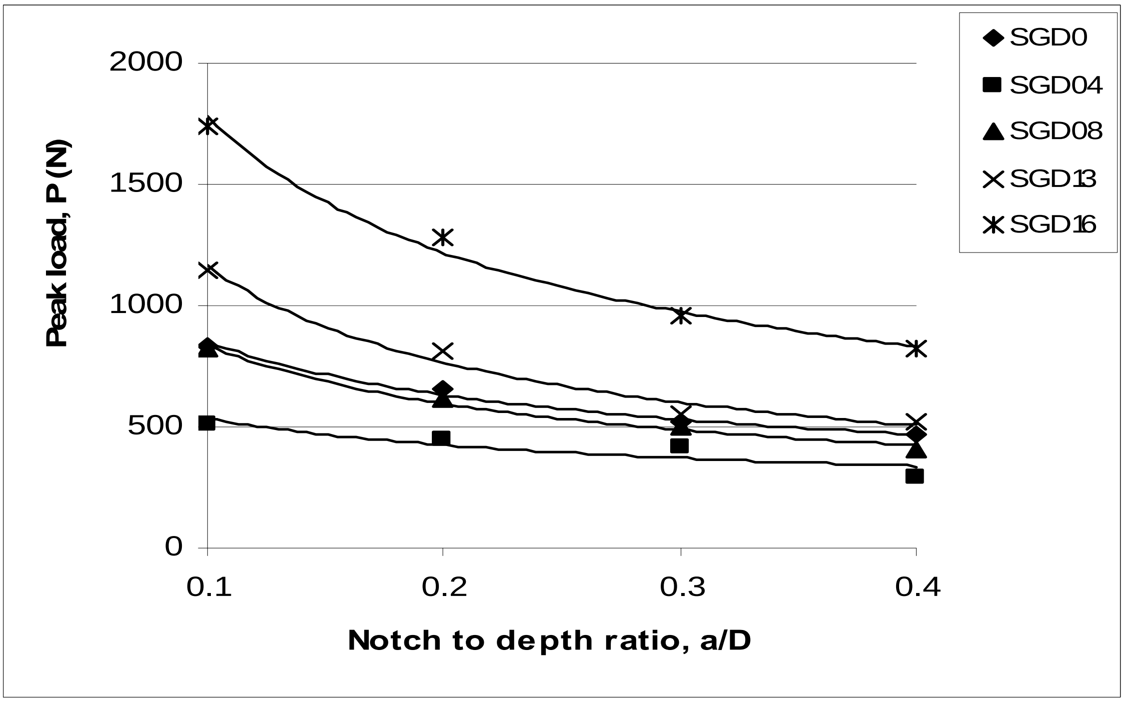

Figure 4.100: Variation of peak load with notch to depth ratio of composites subjected to dry condition

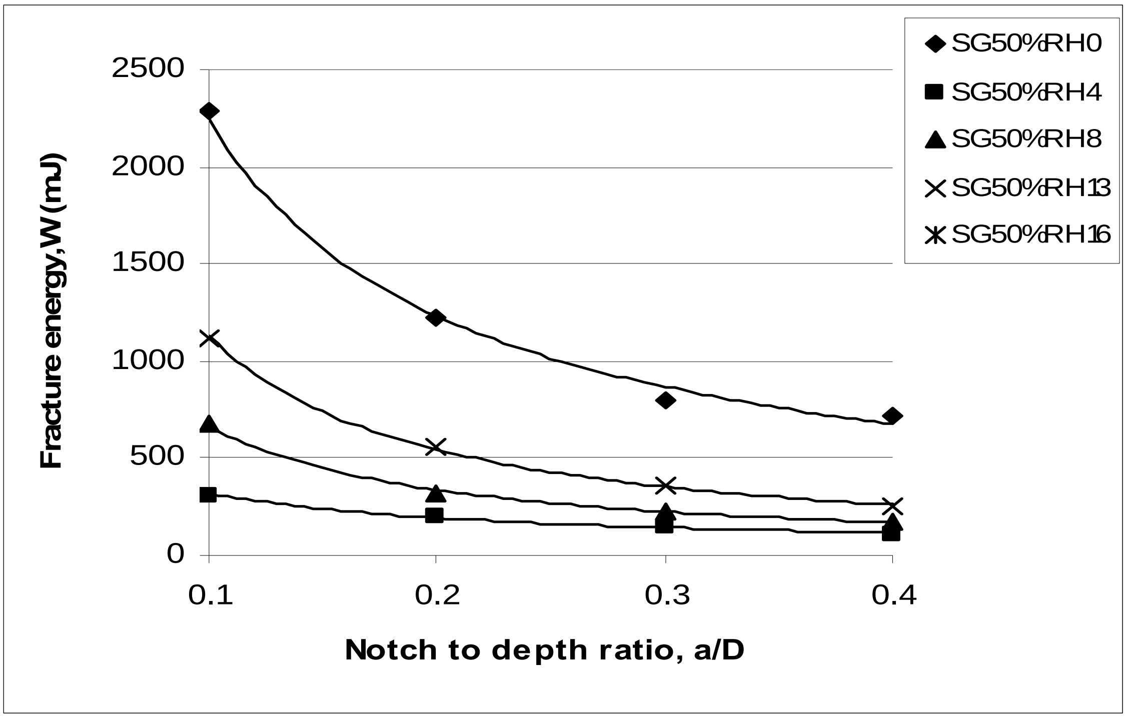

Figure 4.101: Variation of fracture energy with notch to depth ratio of composites subjected to 50% RH condition

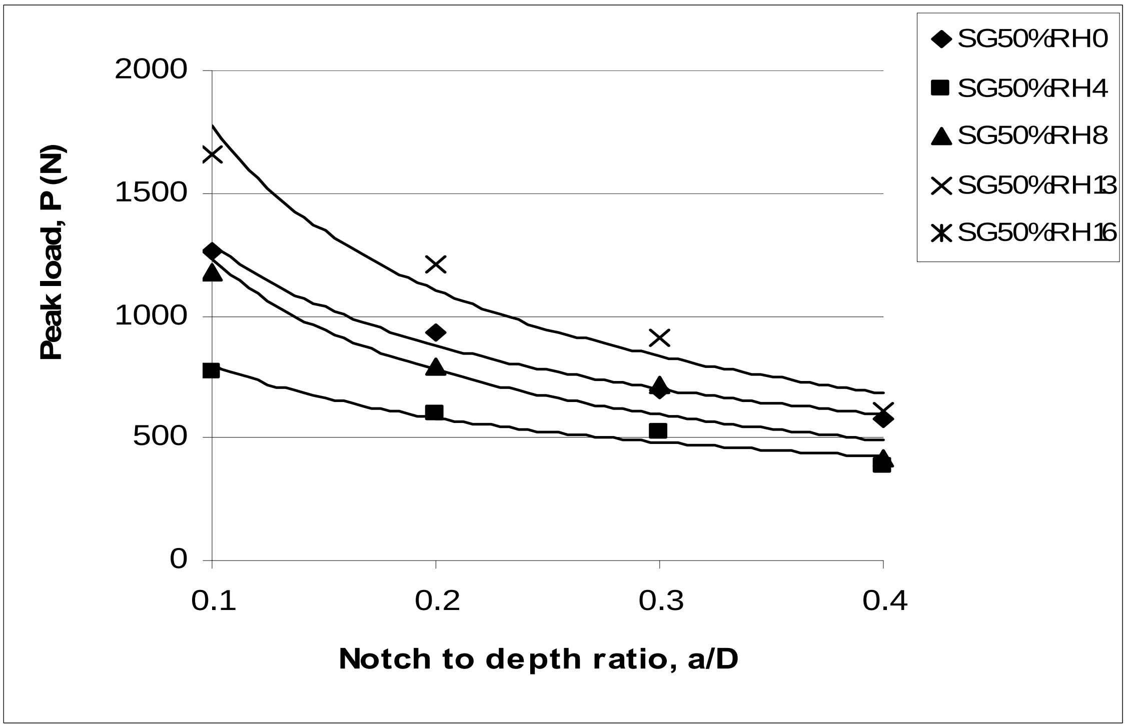

Figure 4.102: Variation of peak load with notch to depth ratio of composites subjected to 50% RH condition

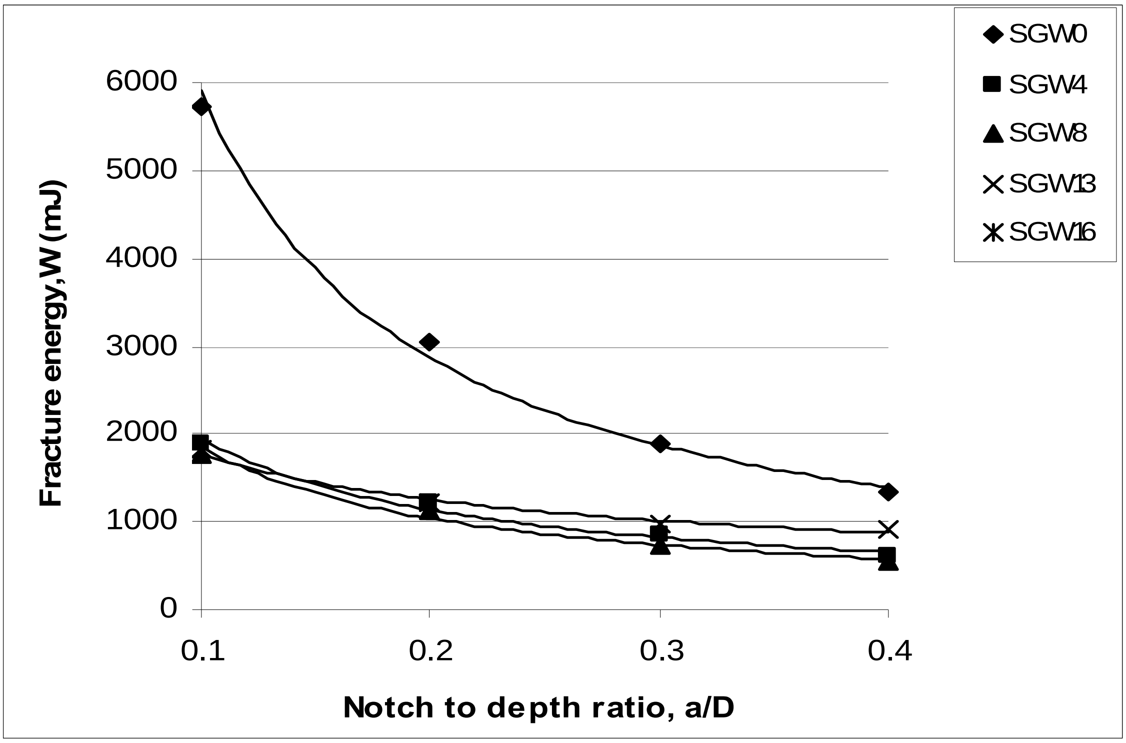

Figure 4.103: Variation of fracture energy with notch to depth ratio of composites subjected to wet condition

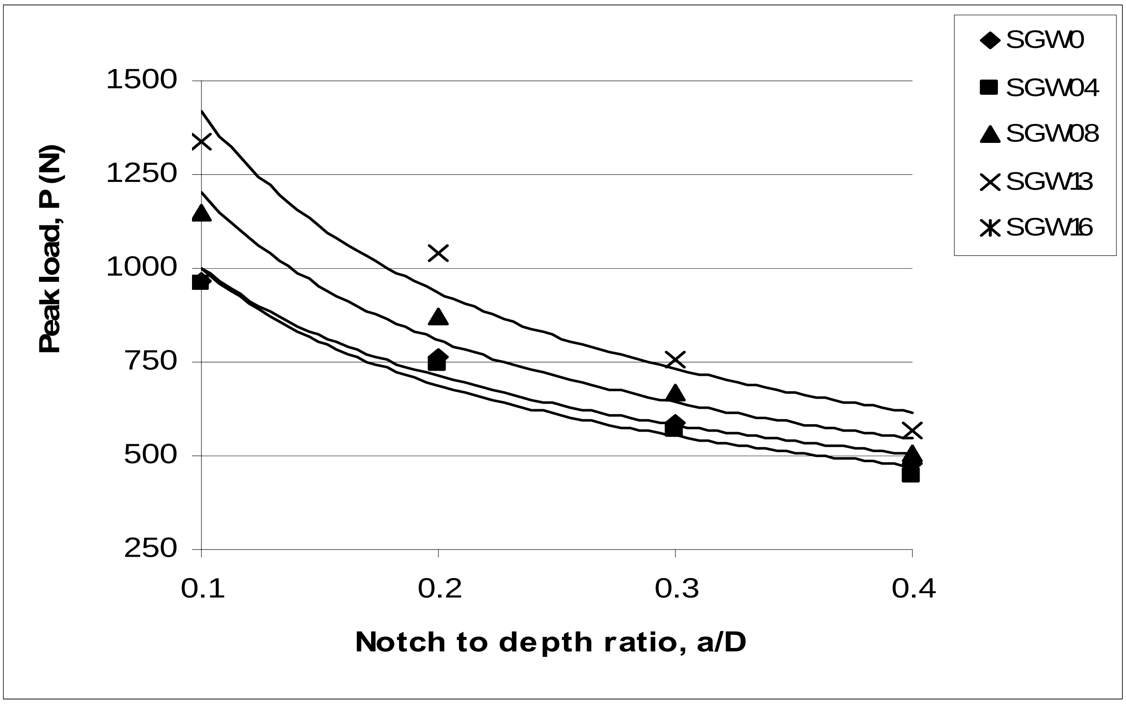

Figure 4.104: Variation of peak load with notch to depth ratio of composites subjected to wet condition

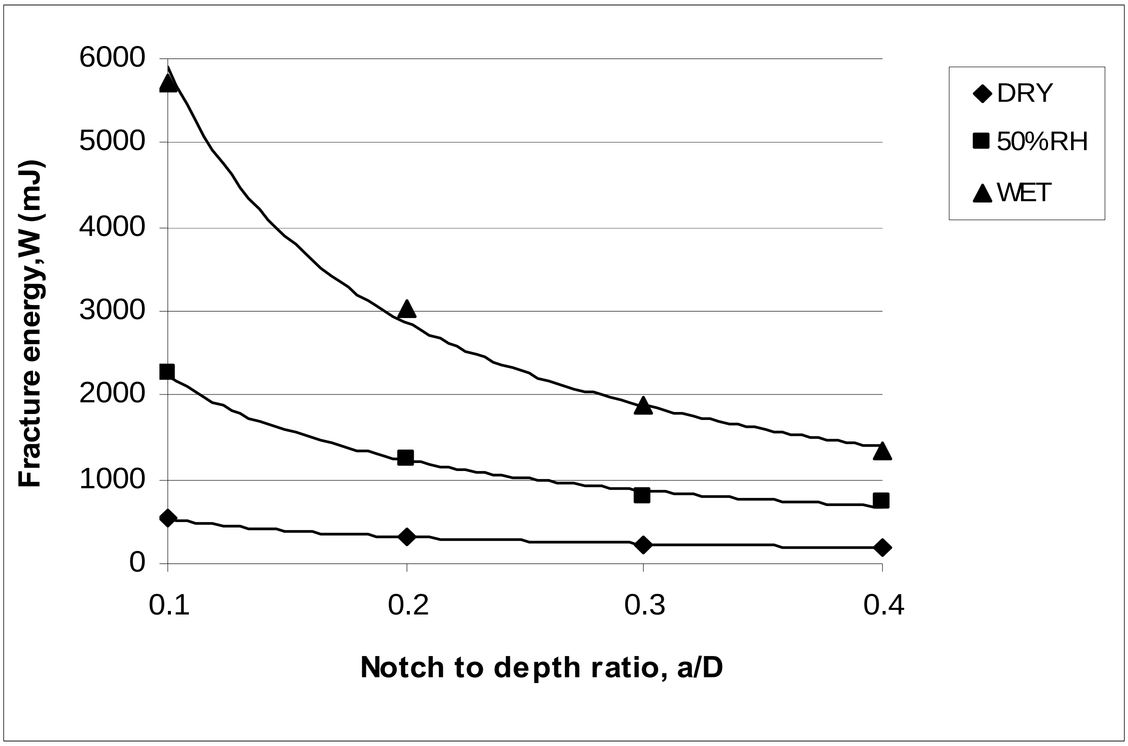

Figure 4.105: Variation of fracture energy with notch to depth ratio of unreinforced polyamide 6,6 matrix at different conditions

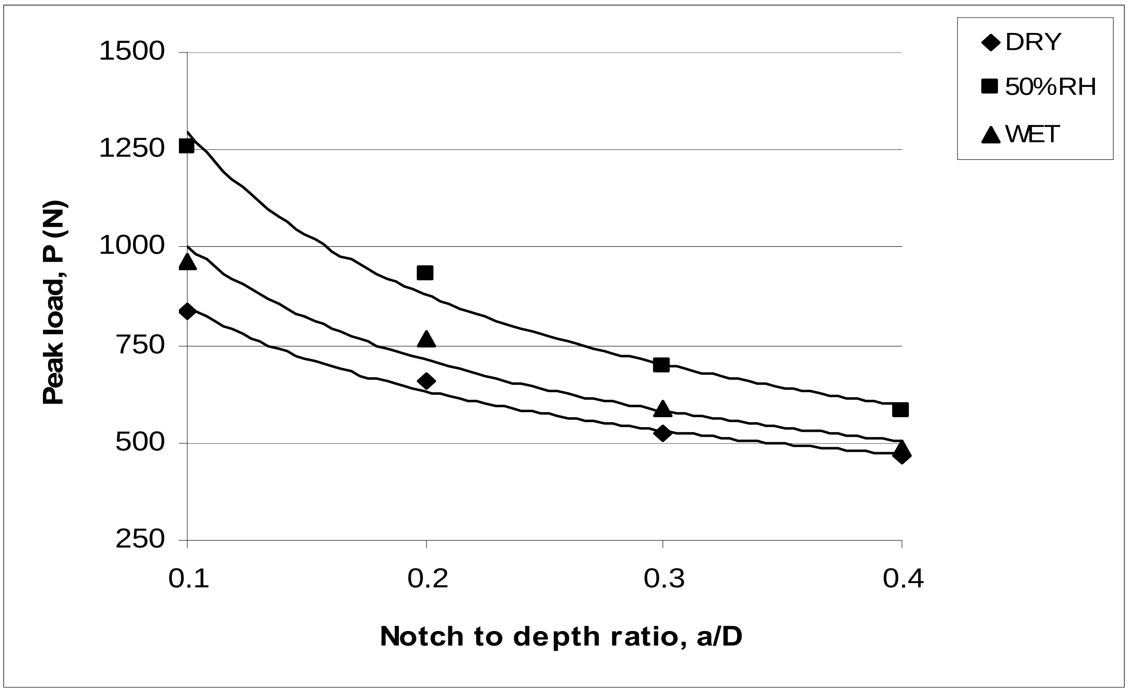

Figure 4.106: Variation of peak load with notch to depth ratio of unreinforced polyamide 6,6 matrix at different conditions

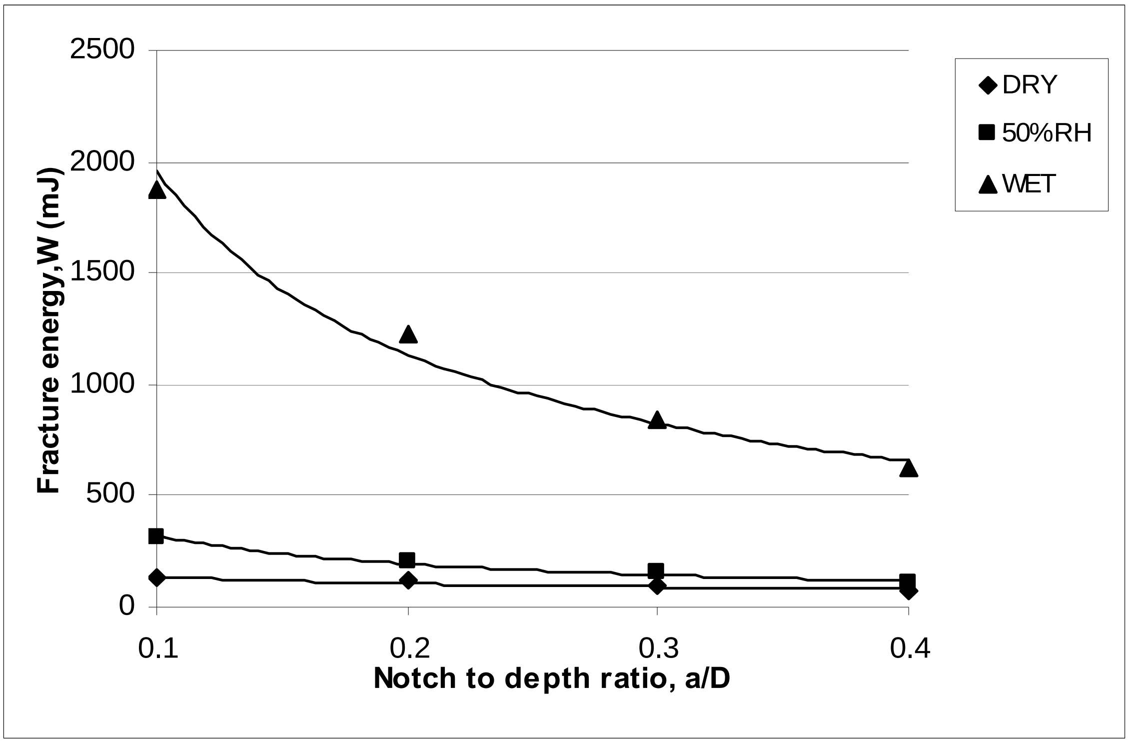

Figure 4.107: Variation of fracture energy with notch to depth ratio of glass fibre composites, V_f 4% at different conditions

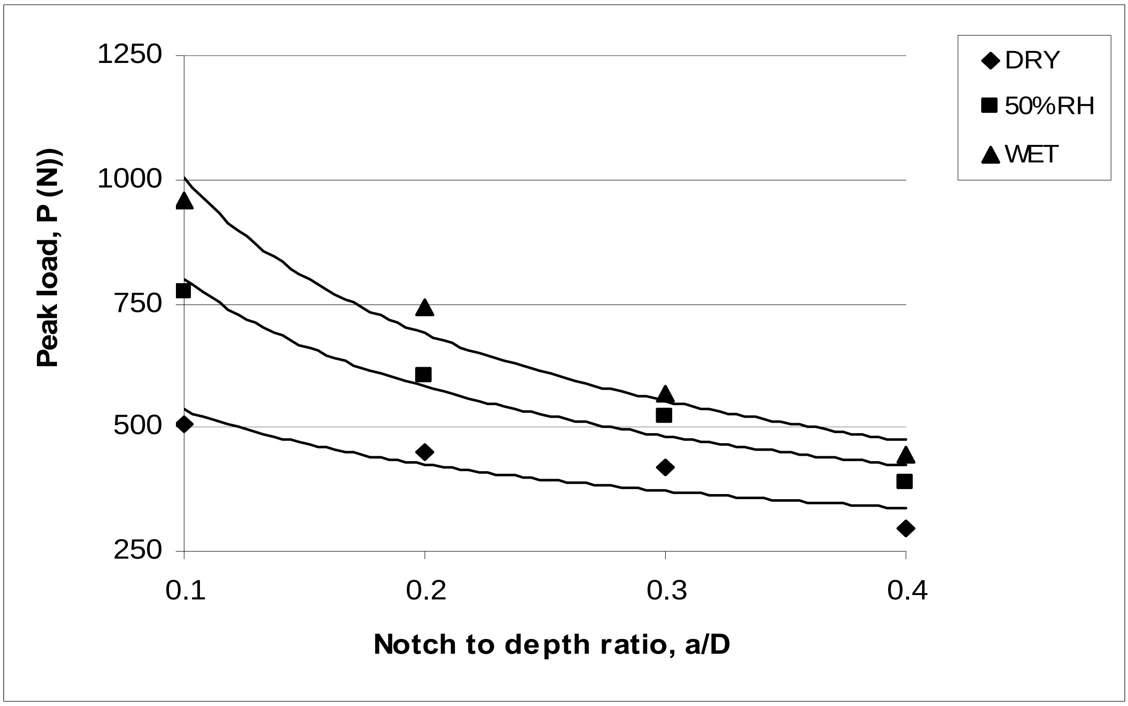

Figure 4.108: Variation of peak load with notch to depth ratio of glass fibre composites, V_f 4% at different conditions

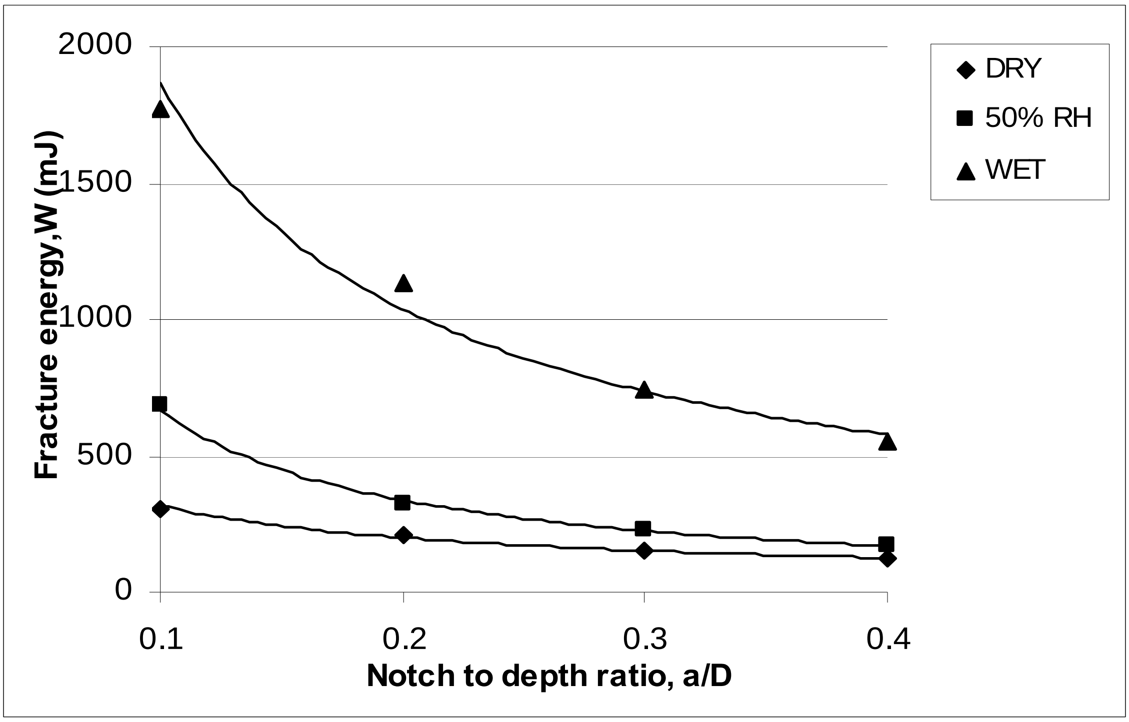

Figure 4.109: Variation of fracture energy with notch to depth ratio of glass fibre composites, V_f 8% at different conditions

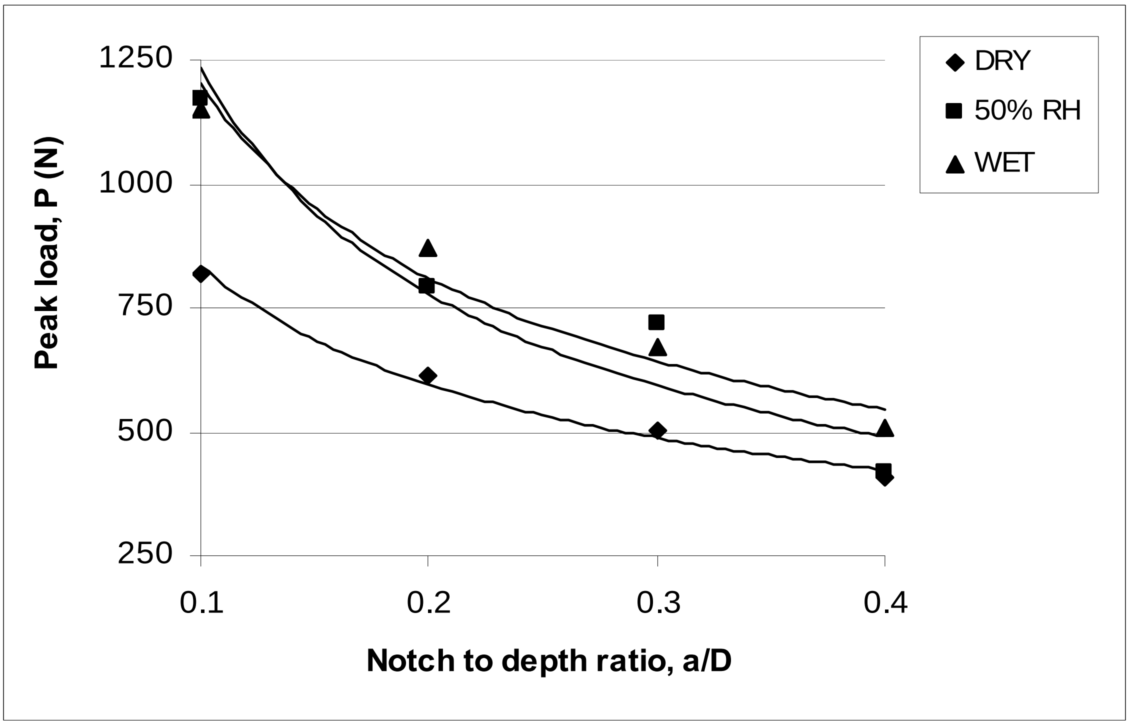

Figure 4.110: Variation of peak load with notch to depth ratio of glass fibre composites, V_f 8% at different conditions

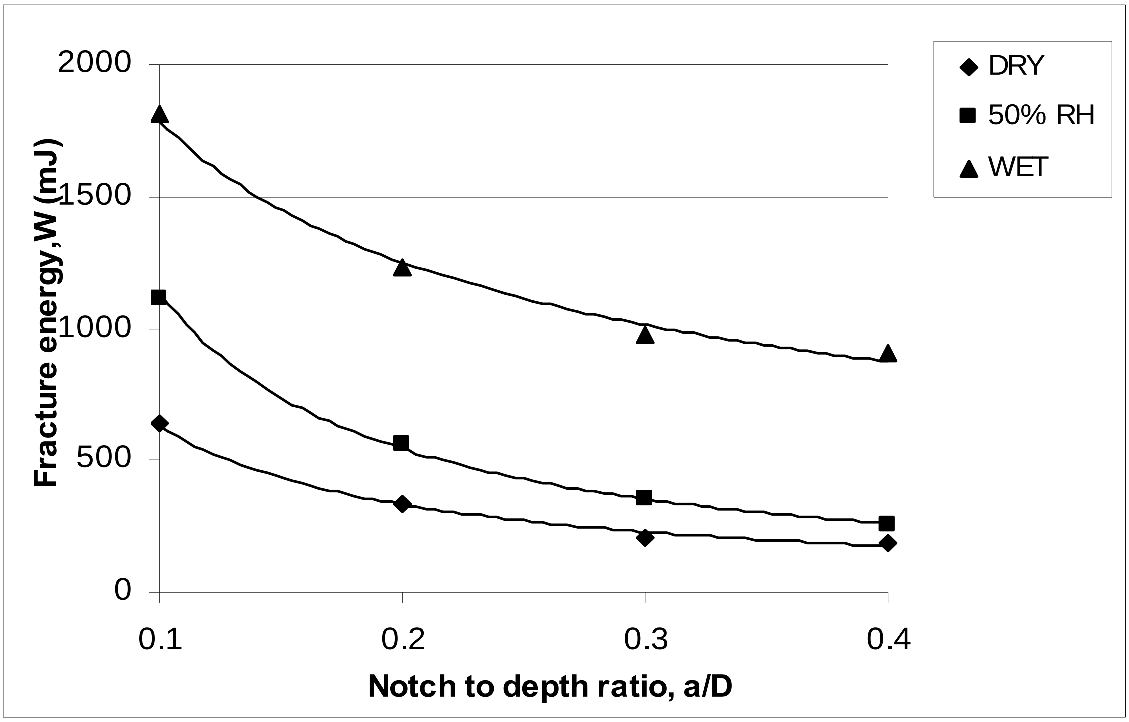

Figure 4.111: Variation of fracture energy with notch to depth ratio of glass fibre composites, V_f 13% at different conditions

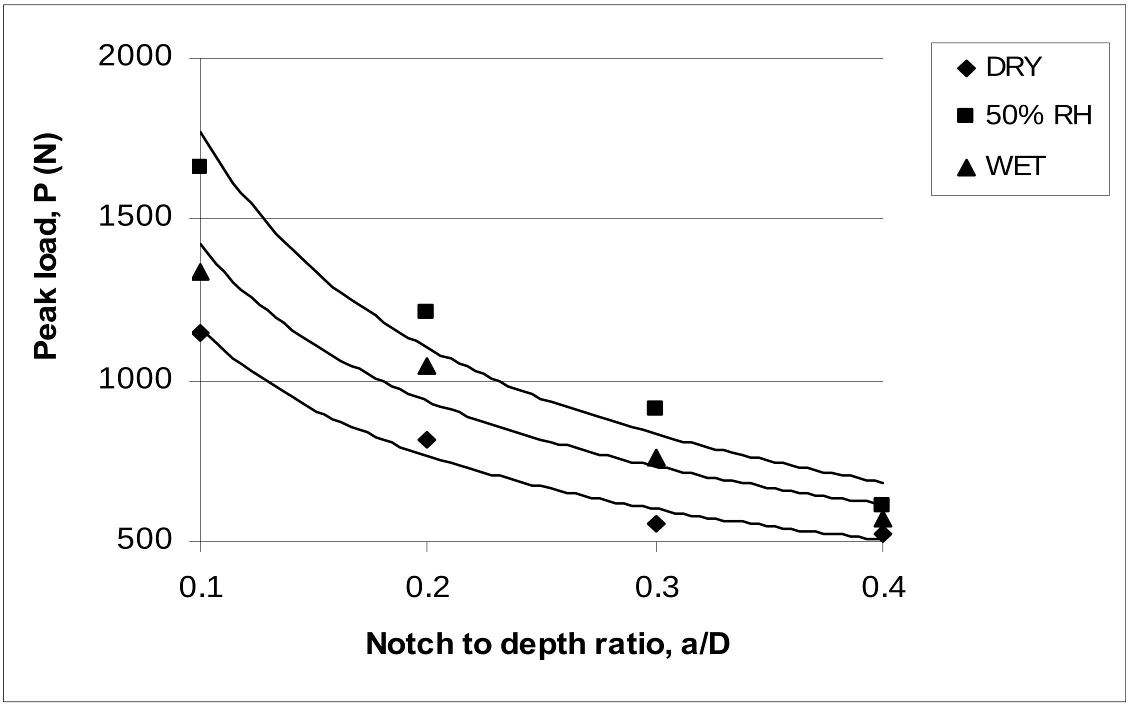

Figure 4.112: Variation of peak load with notch to depth ratio of glass fibre composites, V_f 13% at different conditions

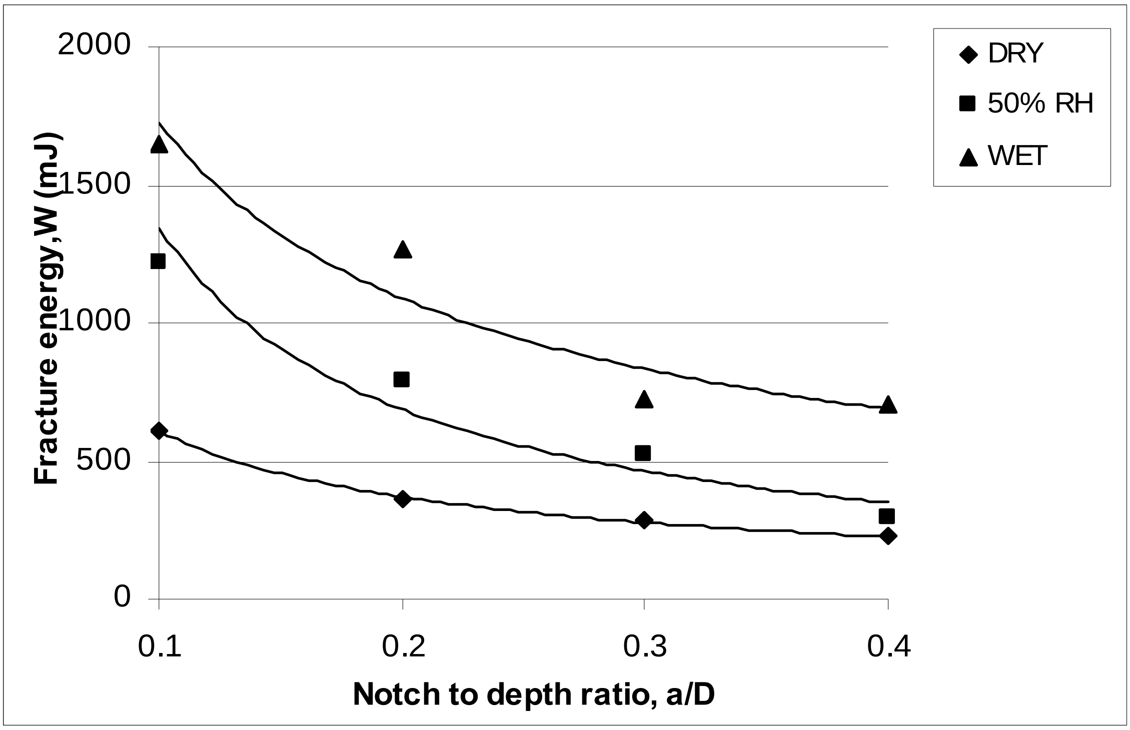

Figure 4.113: Variation of fracture energy with notch to depth ratio of glass fibre composites, V_f 16% at different conditions

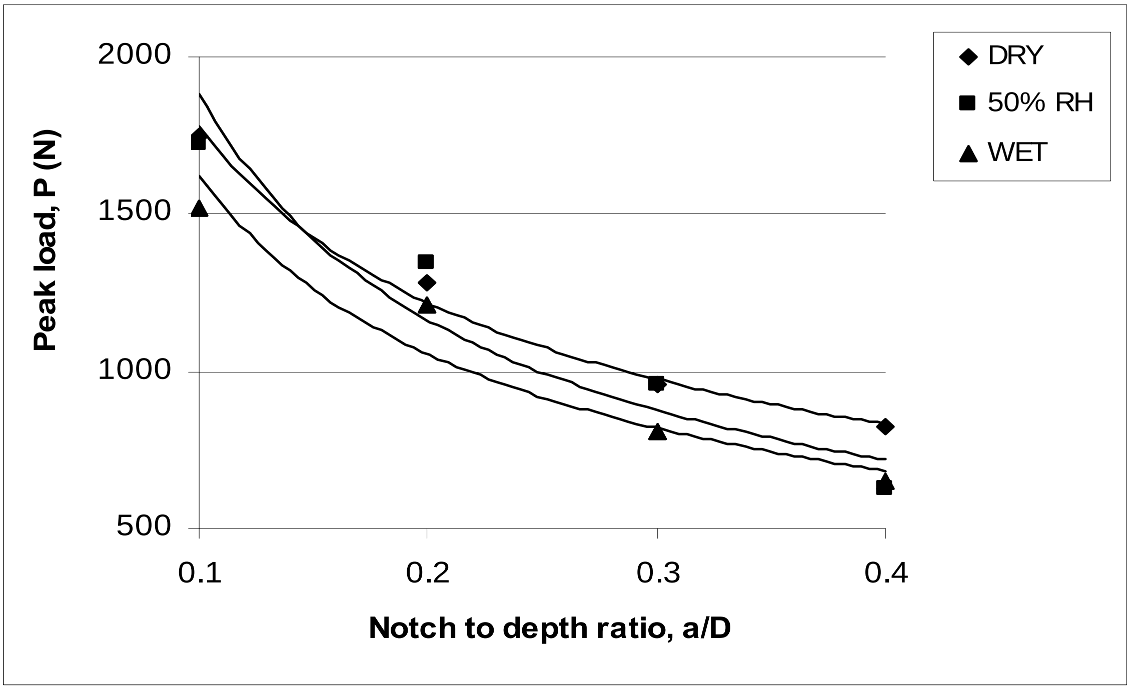

Figure 4.114: Variation of fracture energy with notch to depth ratio of glass fibre composites, V_f 16% at different conditions

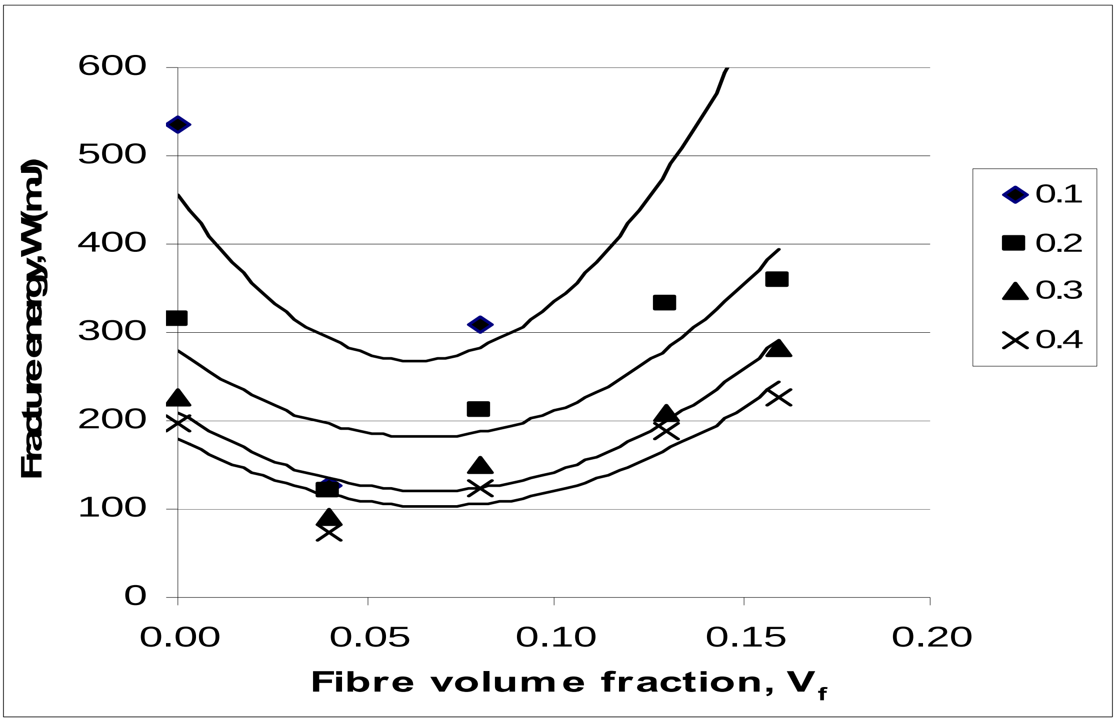

Figure 4.115: Variation of fracture energy of glass fibre composites with fibre volume fraction at various notches to depth ratio at dry condition

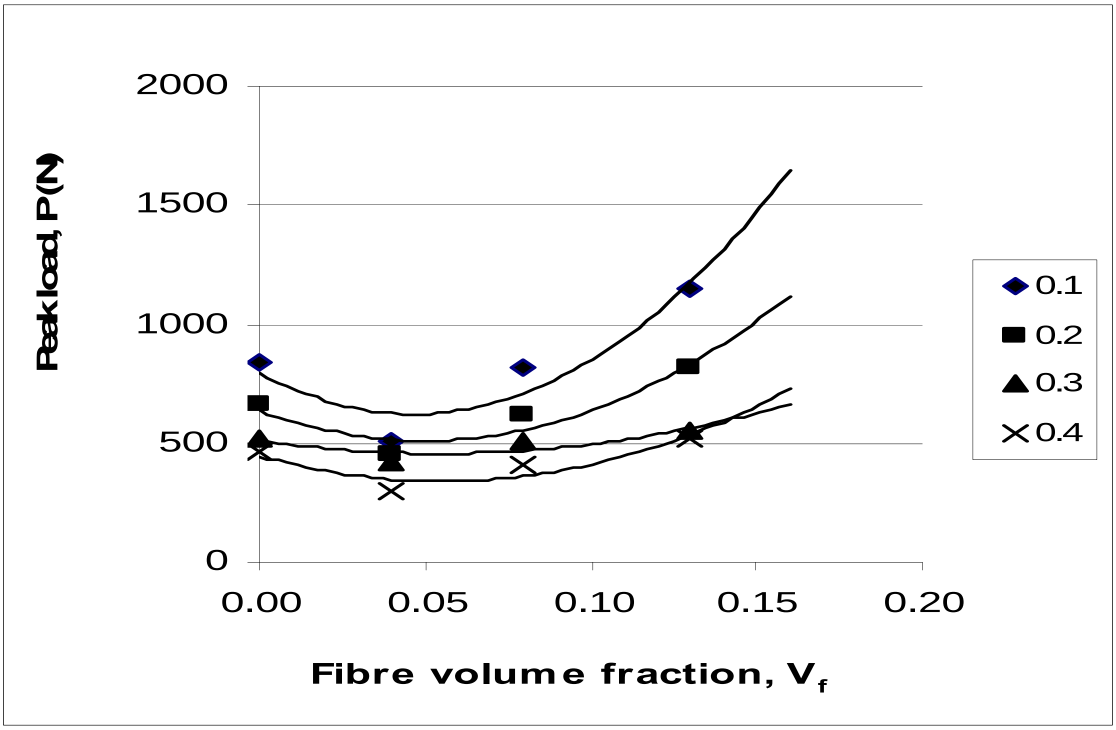

Figure 4.116: Variation of peak load of glass fibre composites with fibre volume fraction at various notches to depth ratio at dry condition

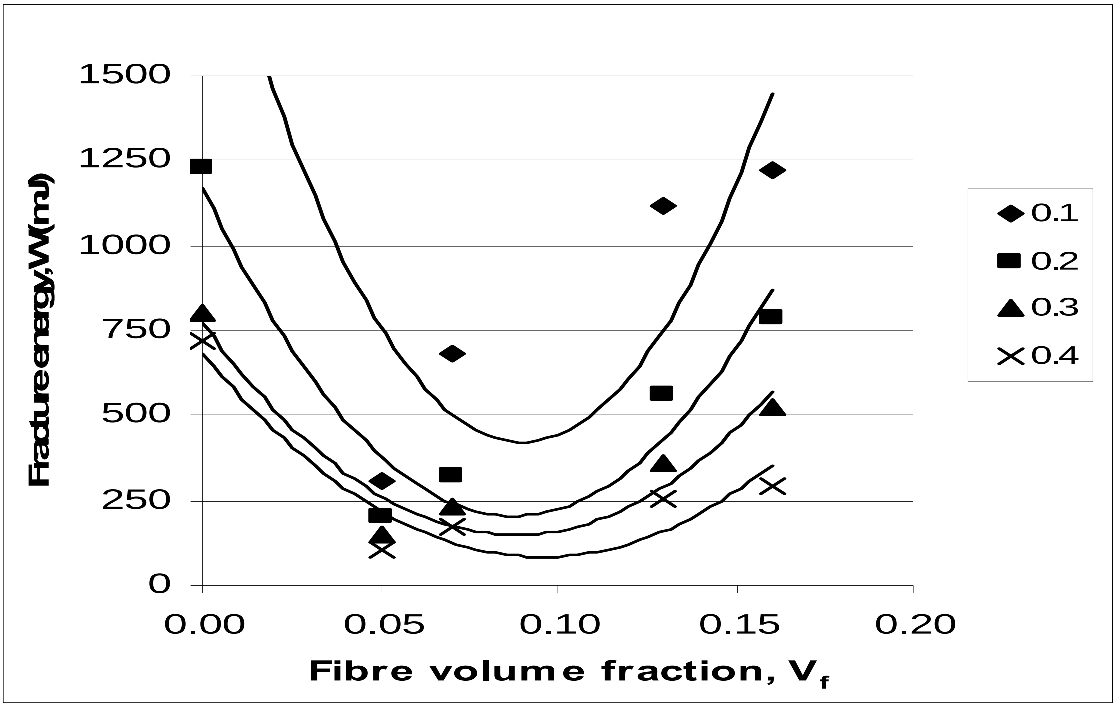

Figure 4.117: Variation of fracture energy of glass fibre composites with fibre volume fraction at various notches to depth ratio at 50% RH condition

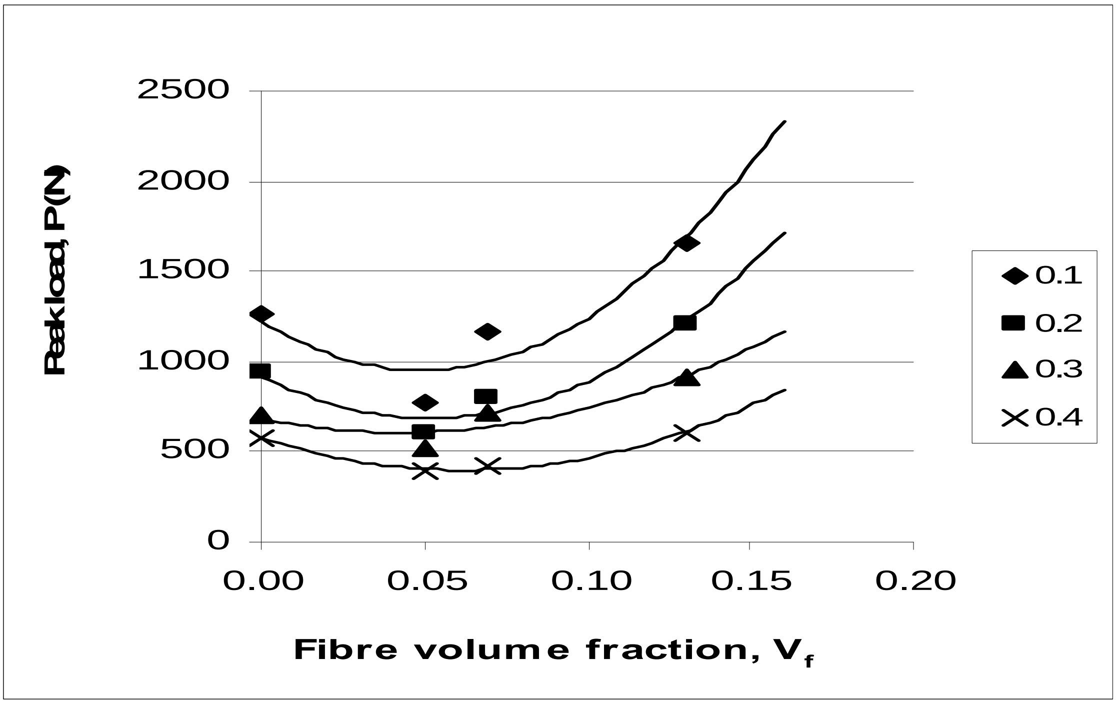

Figure 4.118: Variation of peak load of glass fibre composites with fibre volume fraction at various notches to depth ratio at 50% RH condition

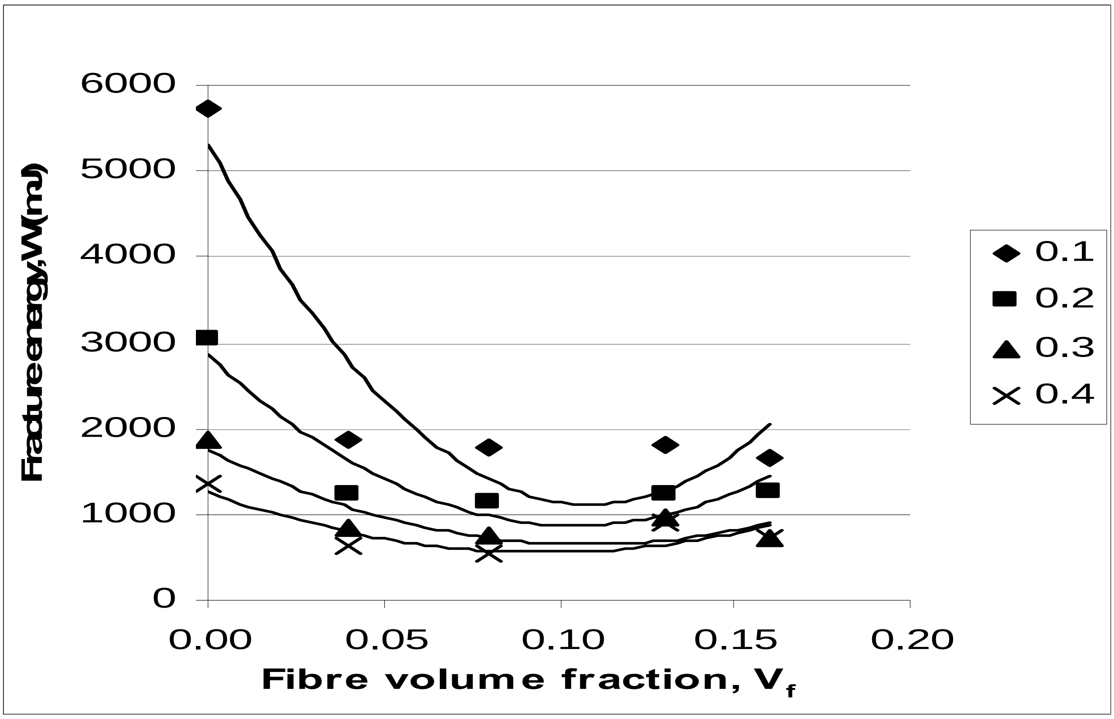

Figure 4.119: Variation of fracture energy of glass fibre composites with fibre volume fraction at various notches to depth ratio at wet condition

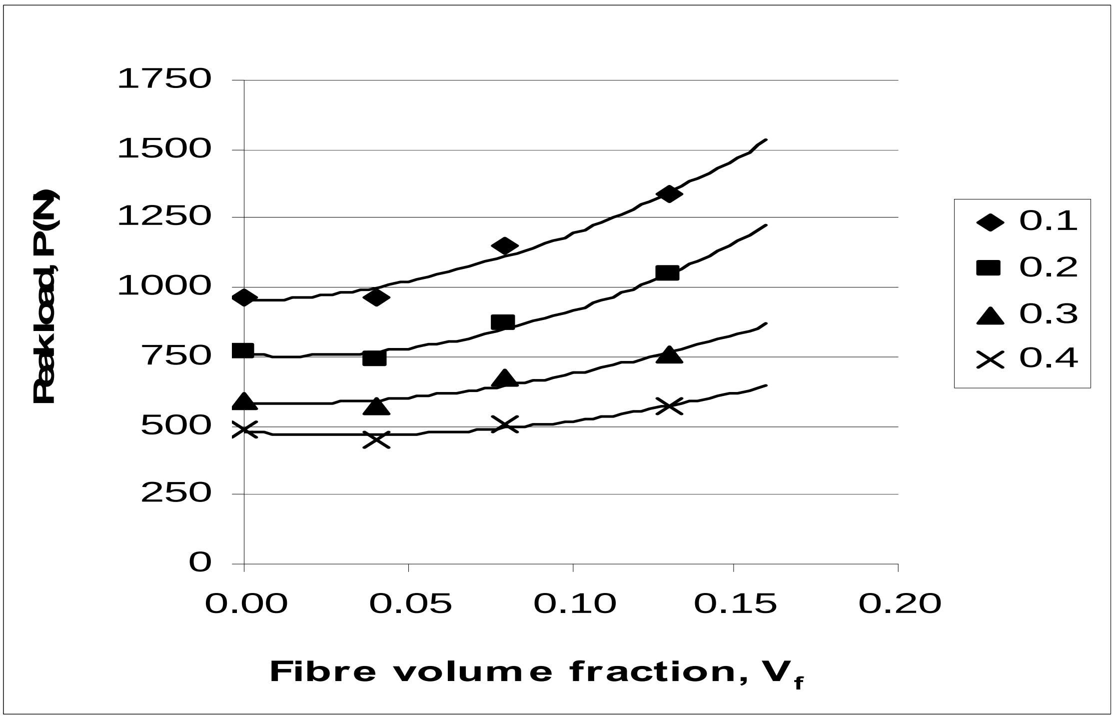

Figure 4.120: Variation of peak load of glass fibre composites with fibre volume fraction at various notches to depth ratio at wet condition

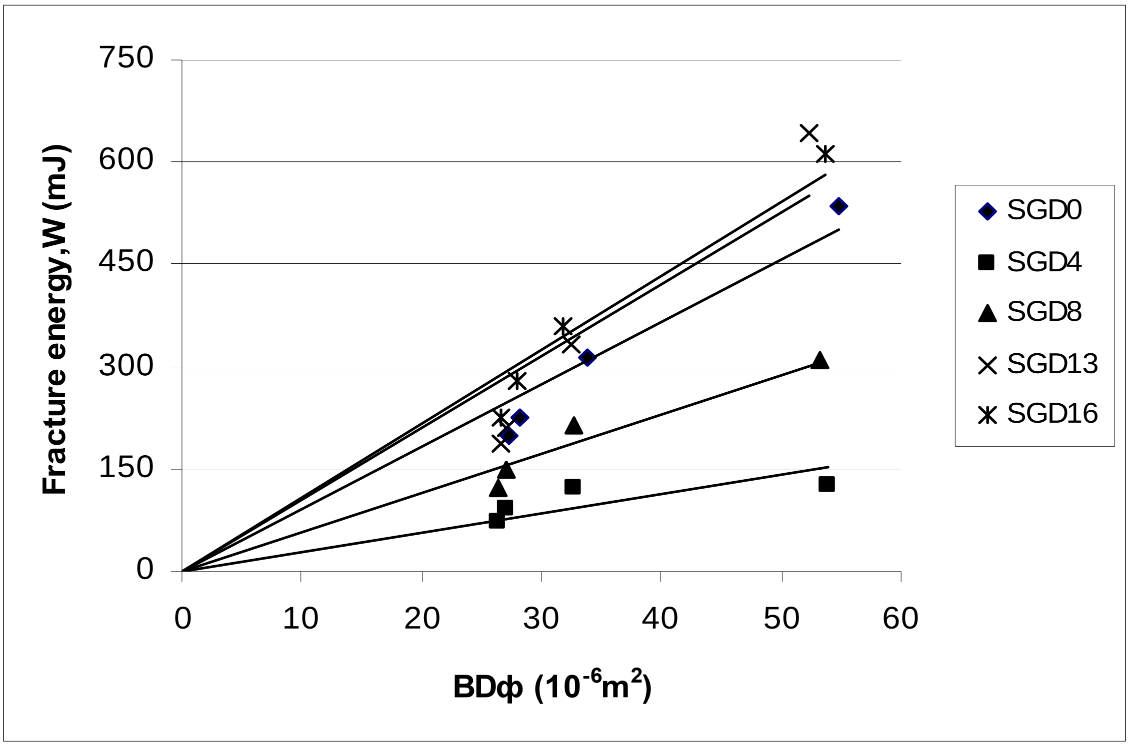

Figure 4.121: Variation of fracture energy with specimen geometry function of glass fibre composites at dry condition

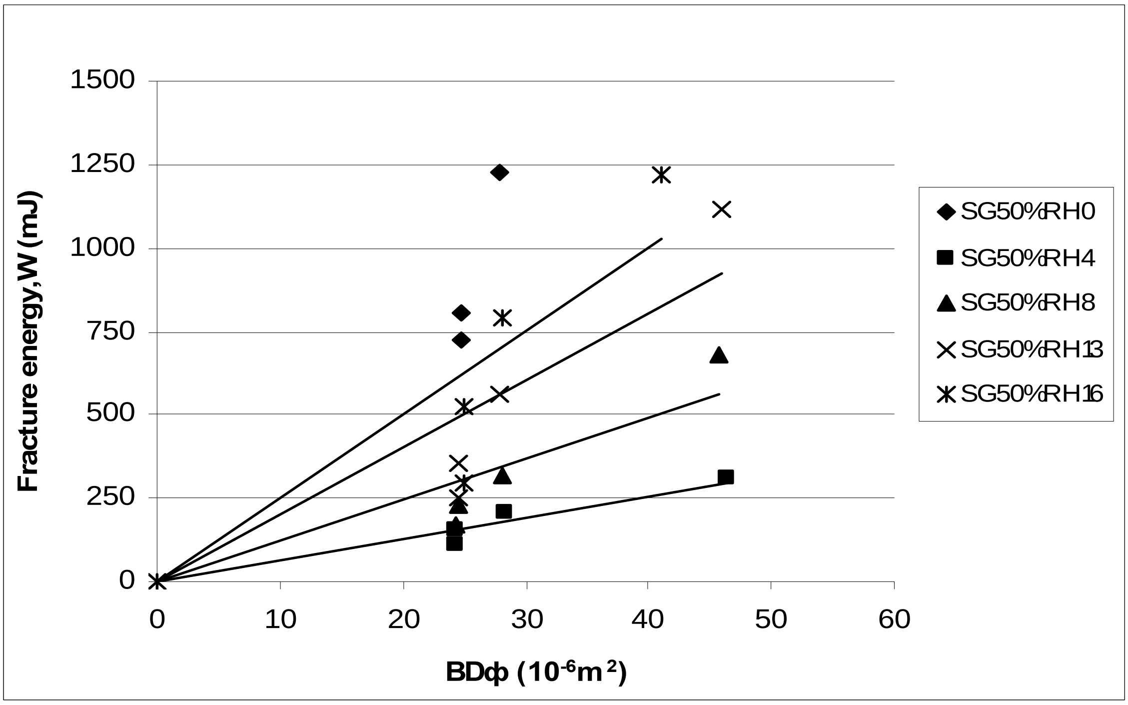

Figure 4.122: Variation of fracture energy with specimen geometry function of glass fibre composites at 50% RH condition

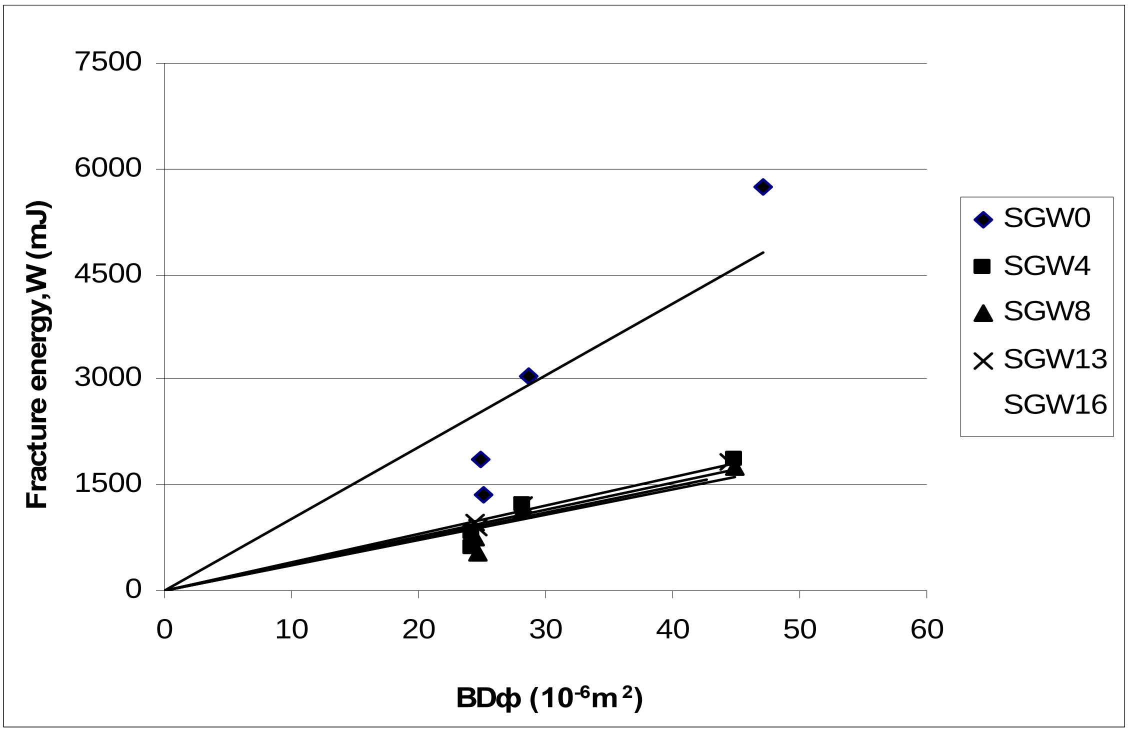

Figure 4.123: Variation of fracture energy with specimen geometry function of glass fibre composites at wet condition

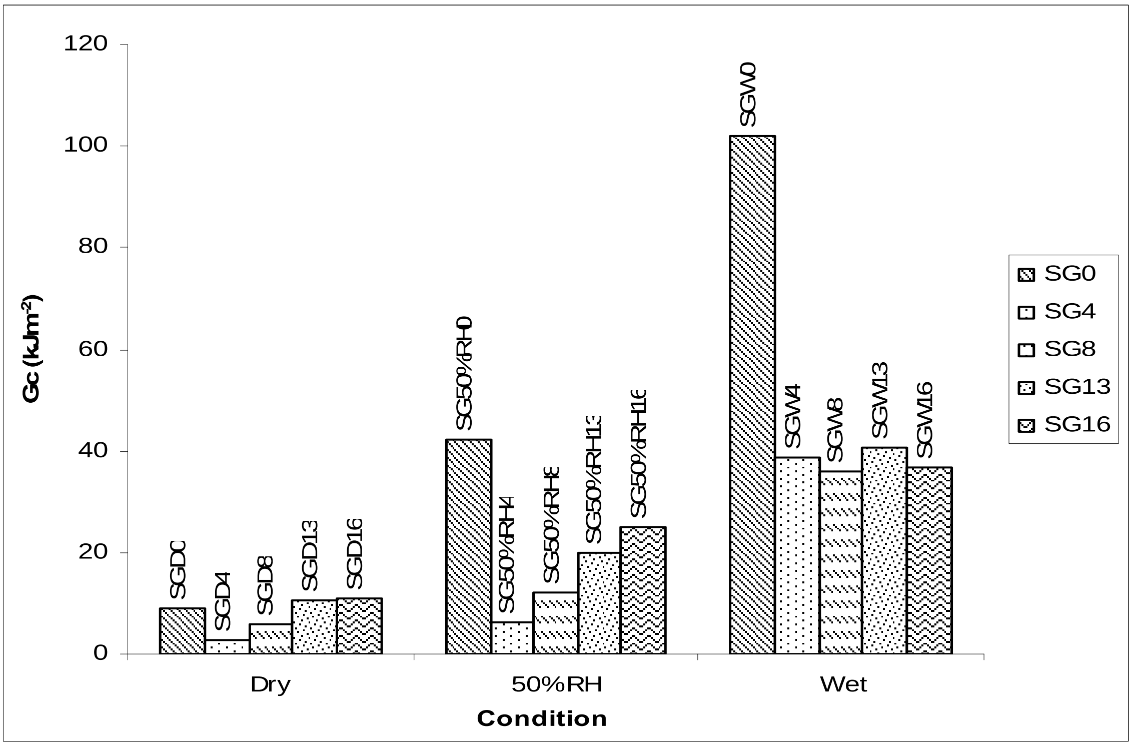

Figure 4.124: G_c values of glass fibre composites for various fibre volume fractions at different conditions

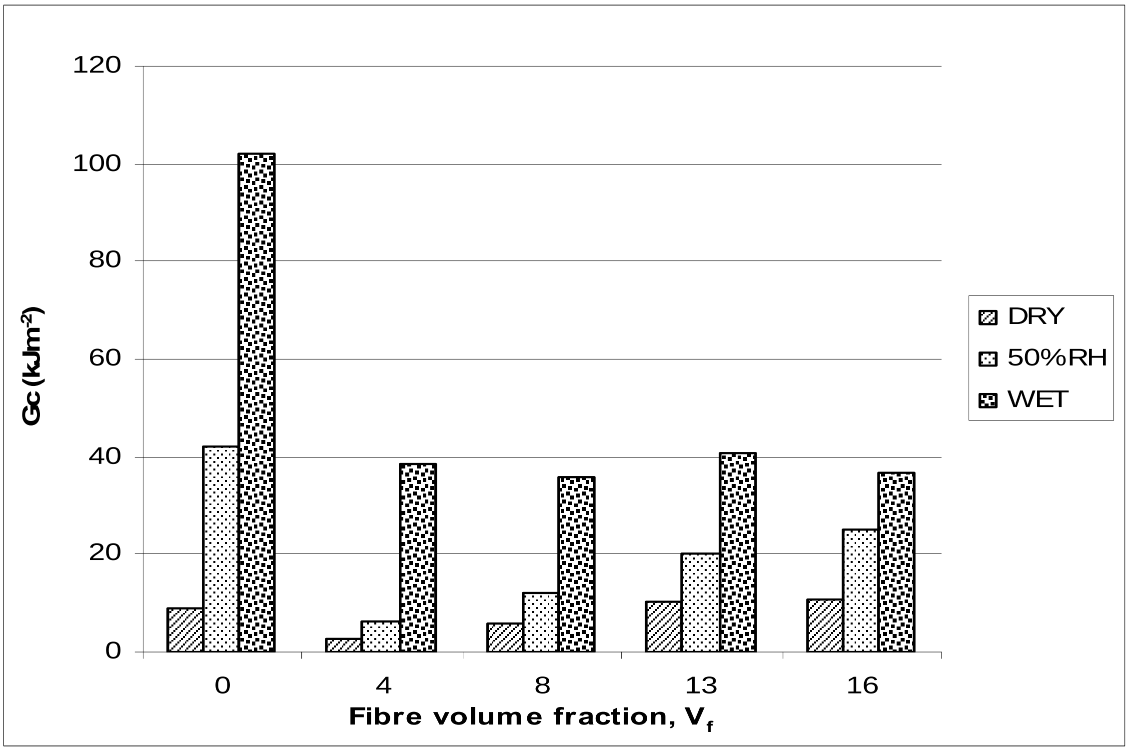

Figure 4.125: G_c values of glass fibre composites at dry, 50% RH and wet condition for various fibre volume fractions

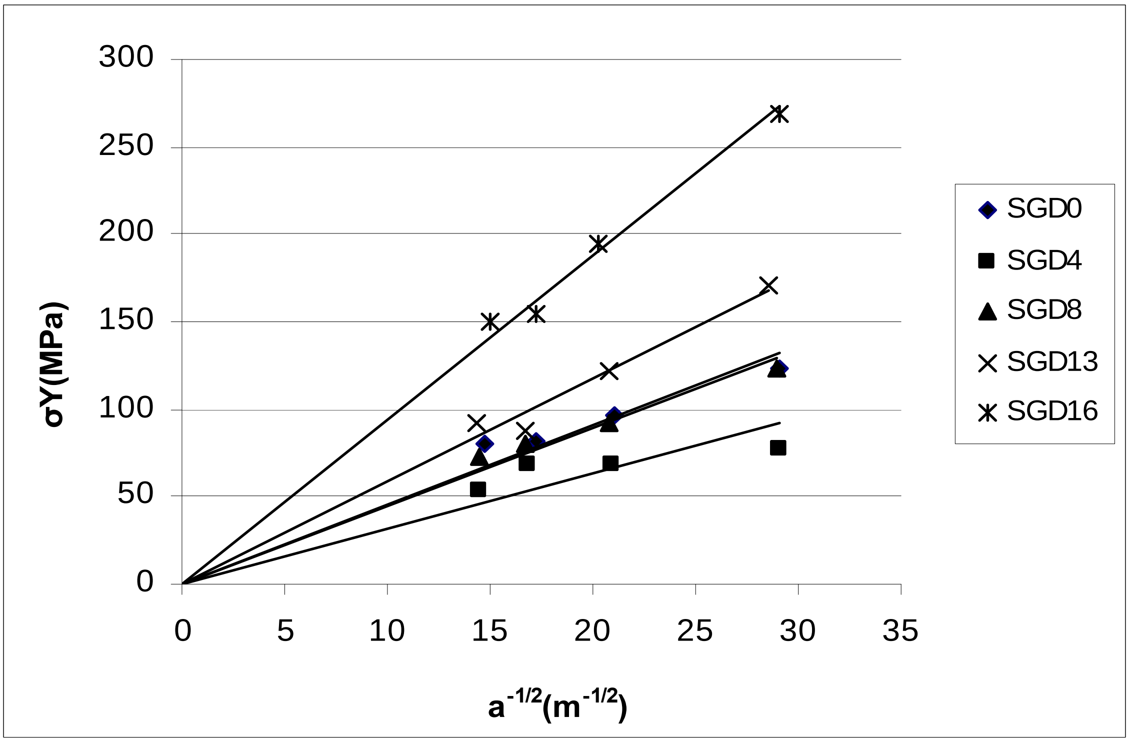

Figure 4.126: Variation of σY with $a^{-1/2}$ of glass fibre composites at dry condition

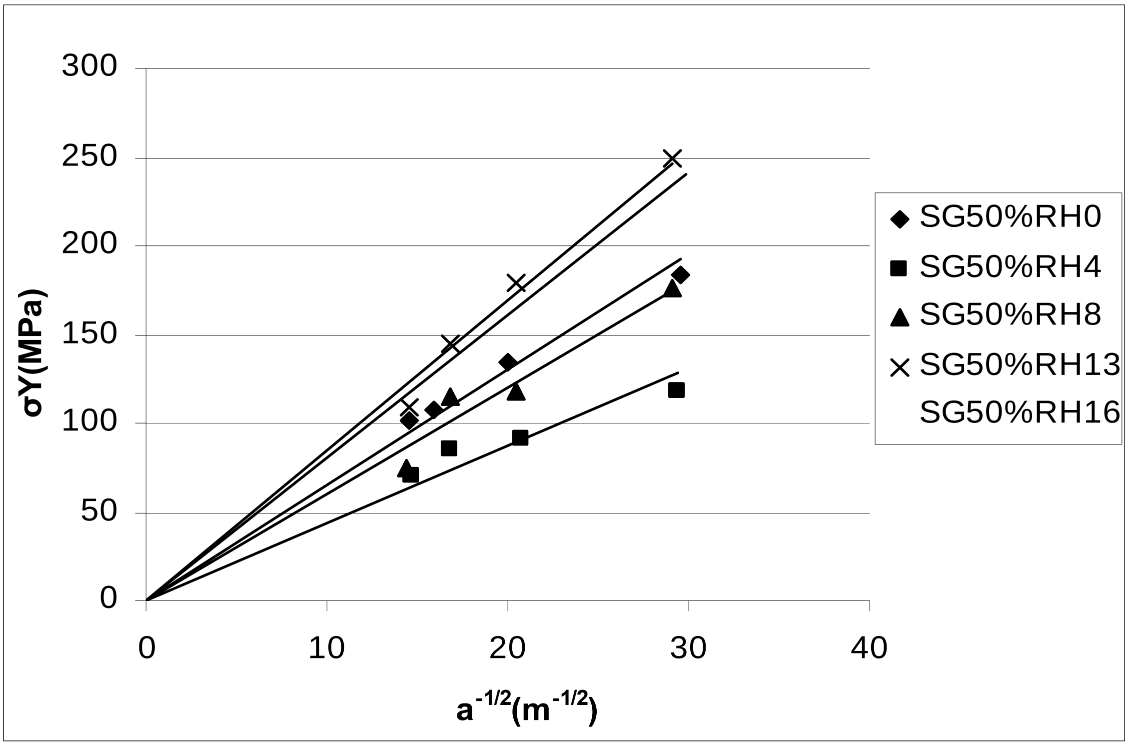

Figure 4.127: Variation of σY with $a^{-1/2}$ of glass fibre composites at 50% RH condition

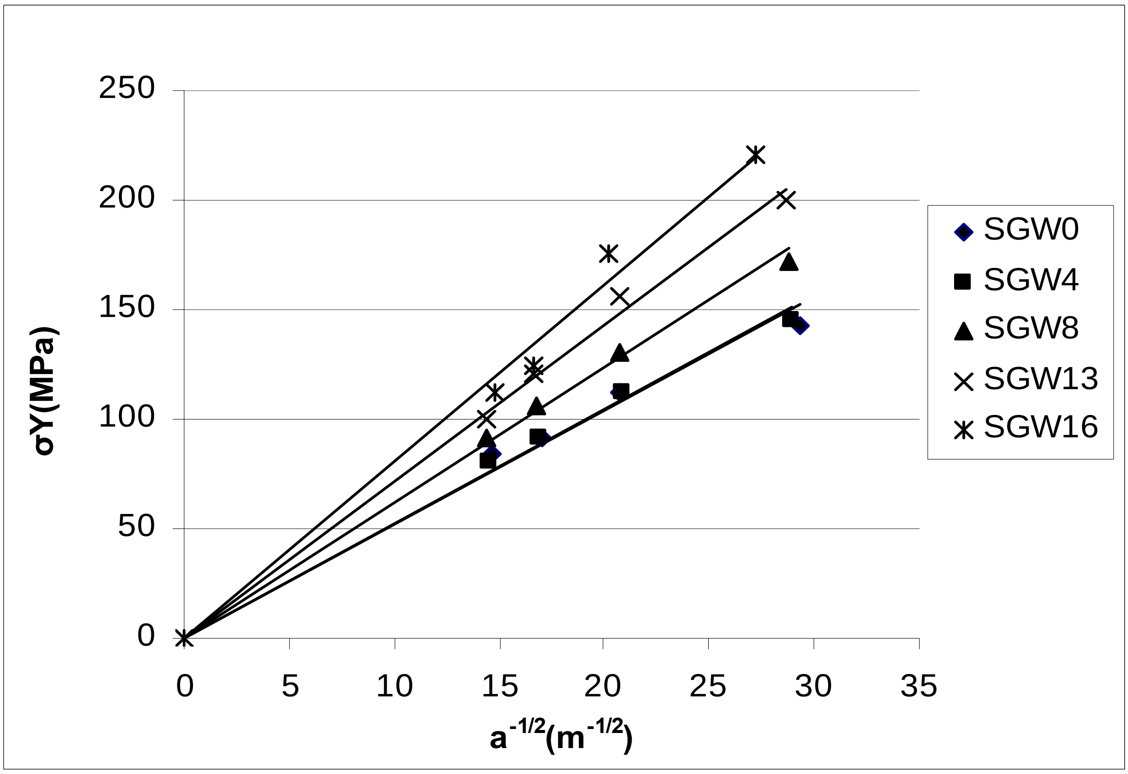

Figure 4.128: Variation of σY with $a^{-1/2}$ of glass fibre composites at wet condition

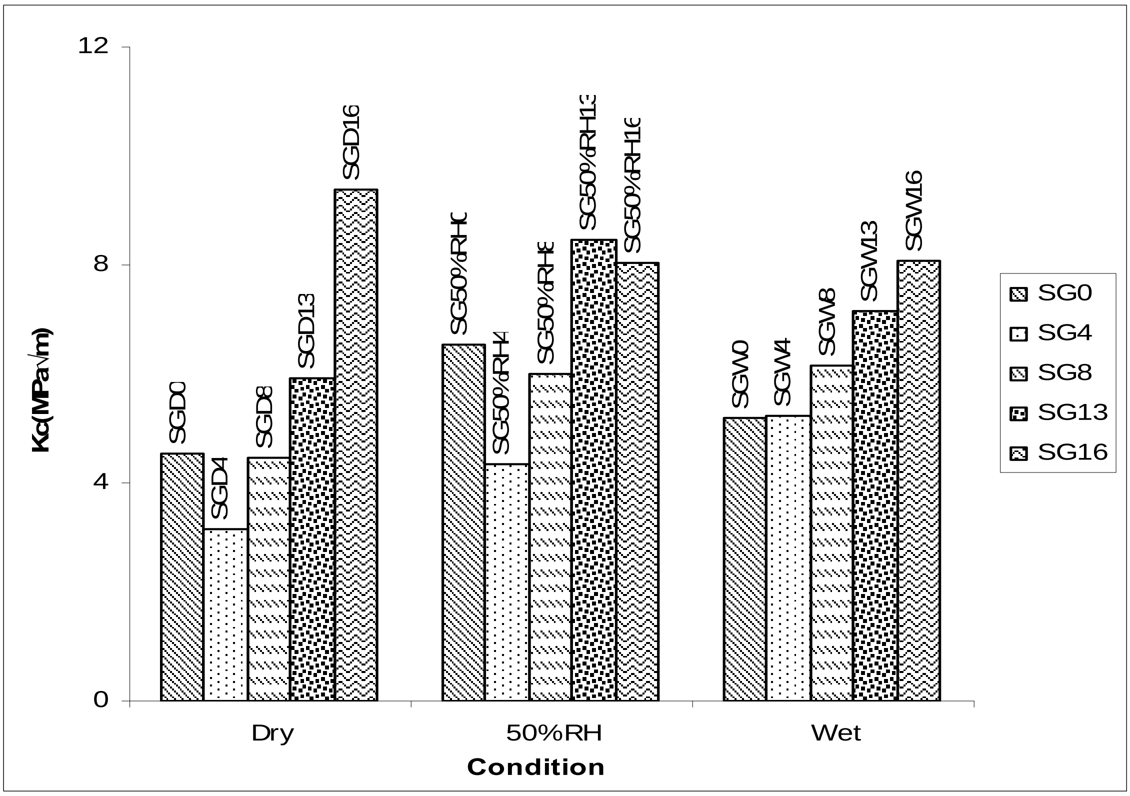

Figure 4.129: K_c values of glass fibre composites for various fibre volume fractions at different conditions

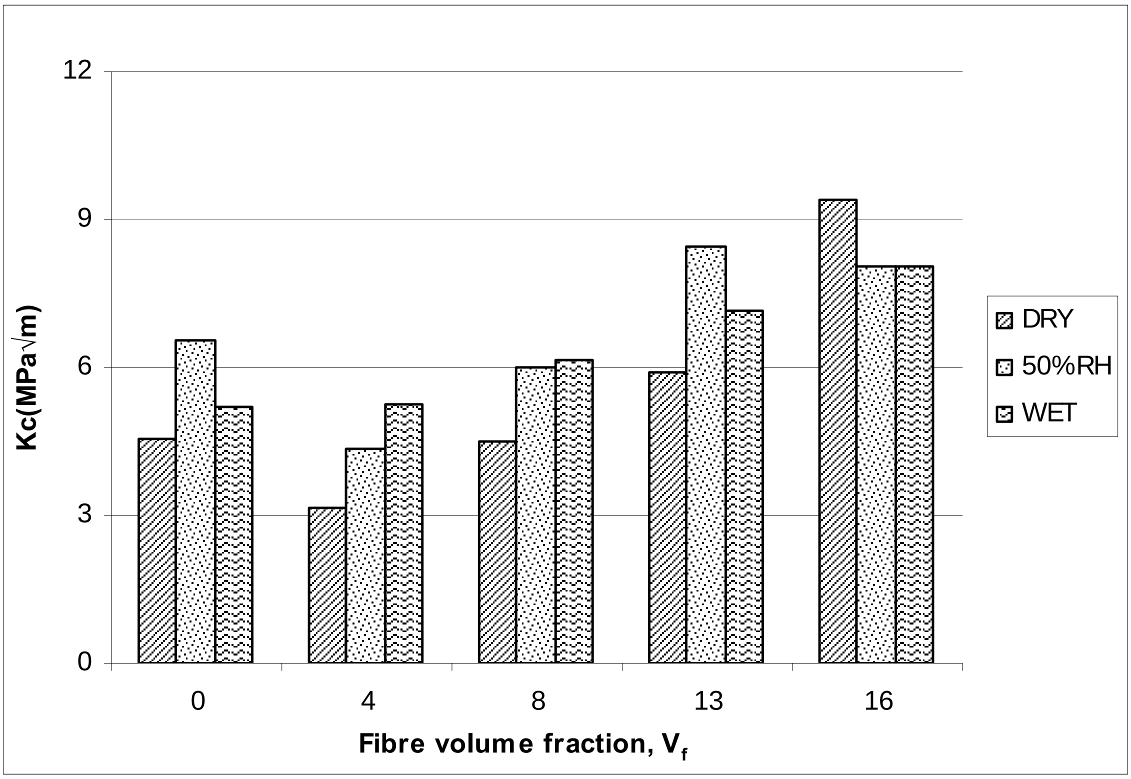

Figure 4.130: K_c values of glass fibre composites at dry, 50% RH and wet condition for various fibre volume fractions

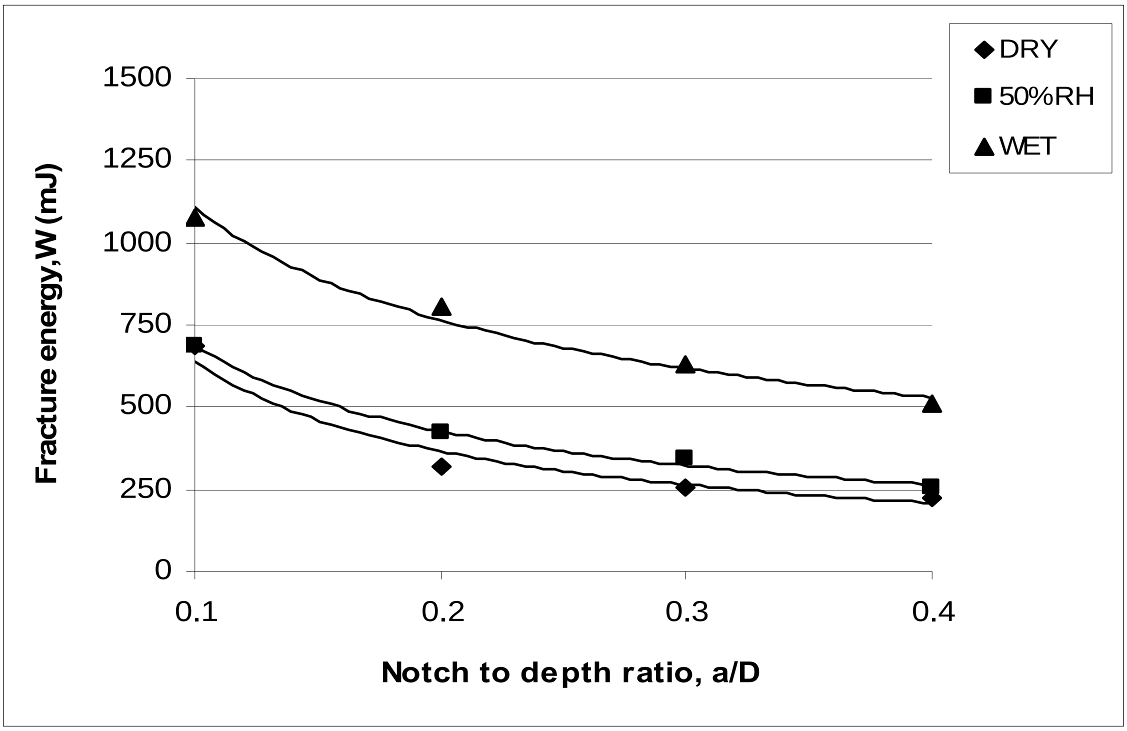

Figure 4.131: Variation of fracture energy with notch to depth ratio of carbon fibre composite at different conditions

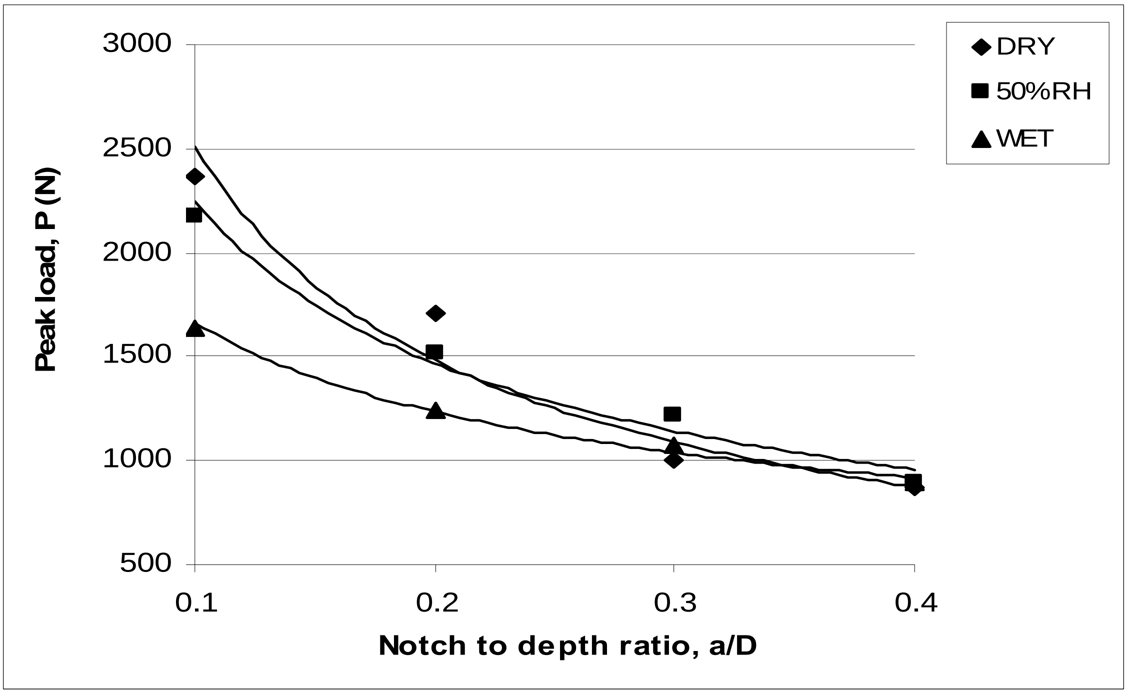

Figure 4.132: Variation of peak load with notch to depth ratio of carbon fibre composite at different conditions

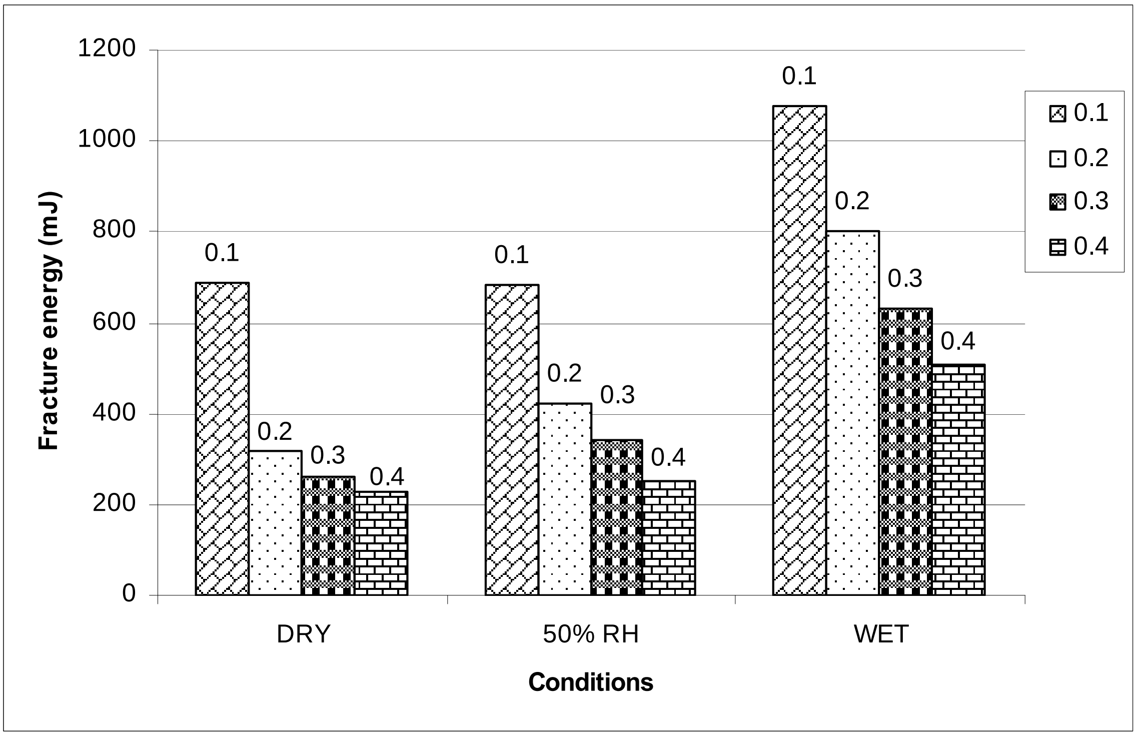

Figure 4.133: Variation of fracture energy with notch to depth ratio of carbon fibre composite at different conditions

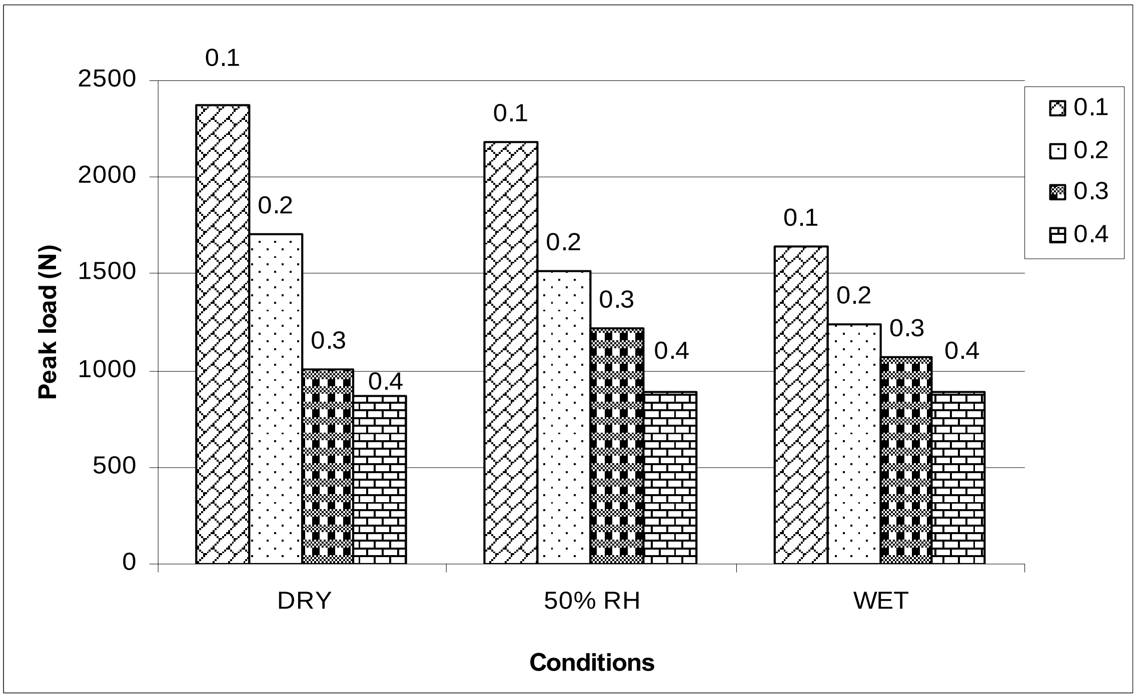

Figure 4.134: Variation of peak load with notch to depth ratio of carbon fibre composite at different conditions

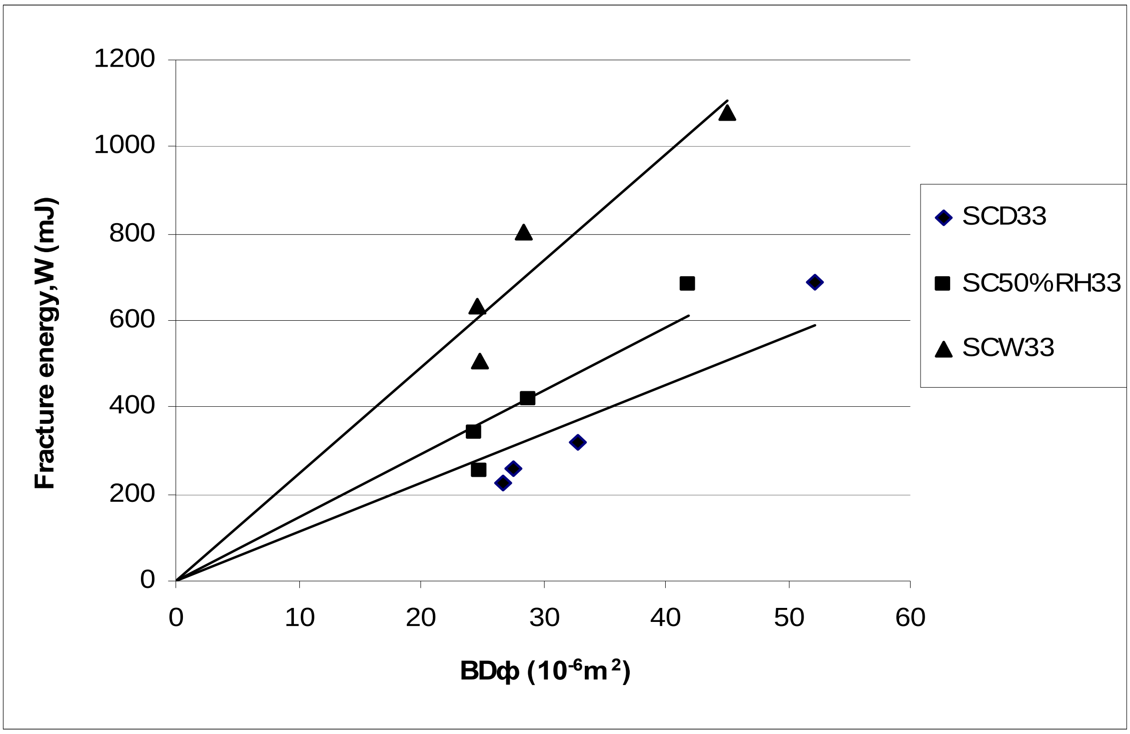

Figure 4.135: Variation of fracture energy with specimen geometry function of carbon fibre composites at dry condition

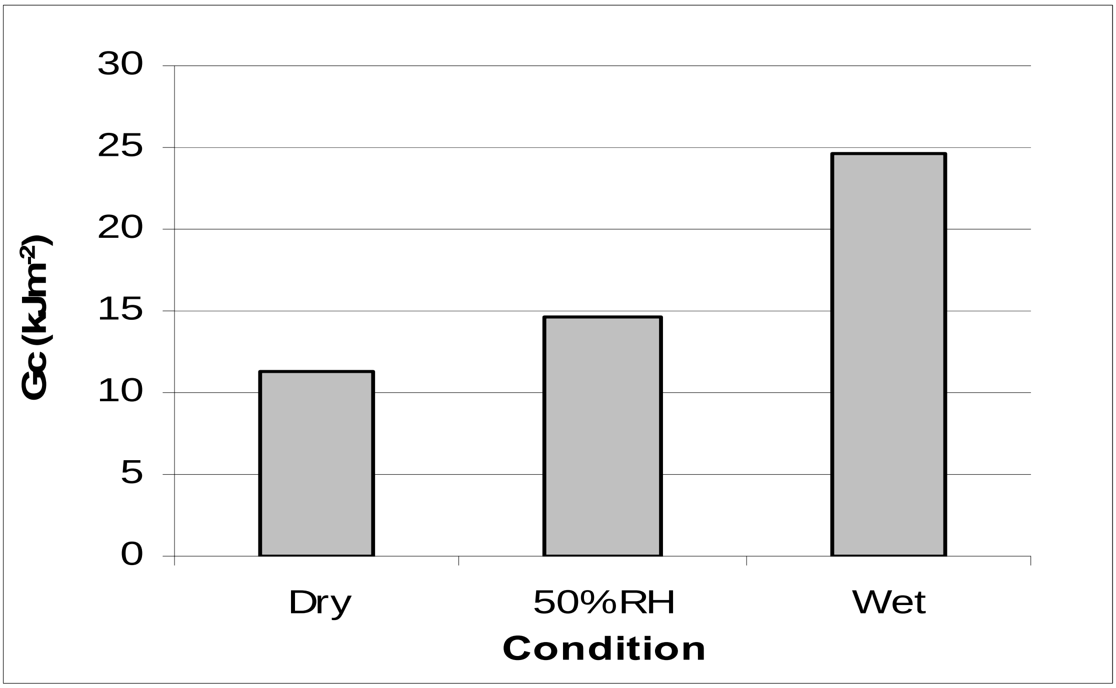

Figure 4.136: G_c values of carbon fibre composites at different conditions

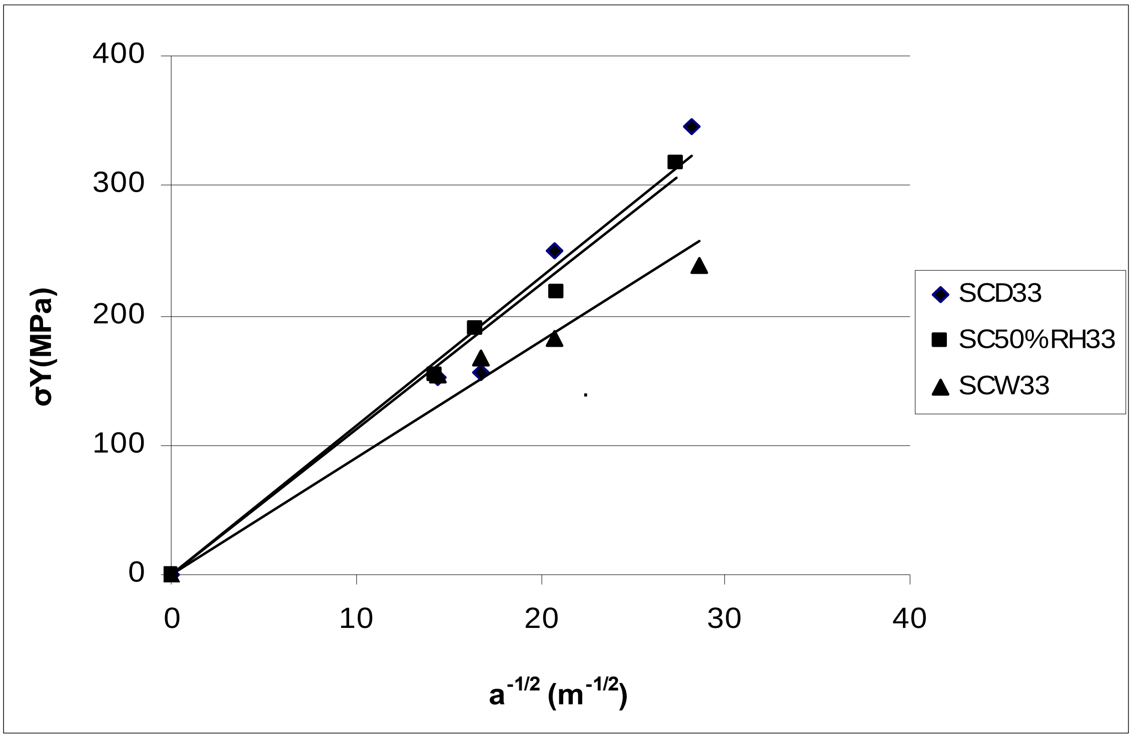

Figure 4.137: Variation of σY with $a^{-1/2}$ of carbon fibre composites at various conditions

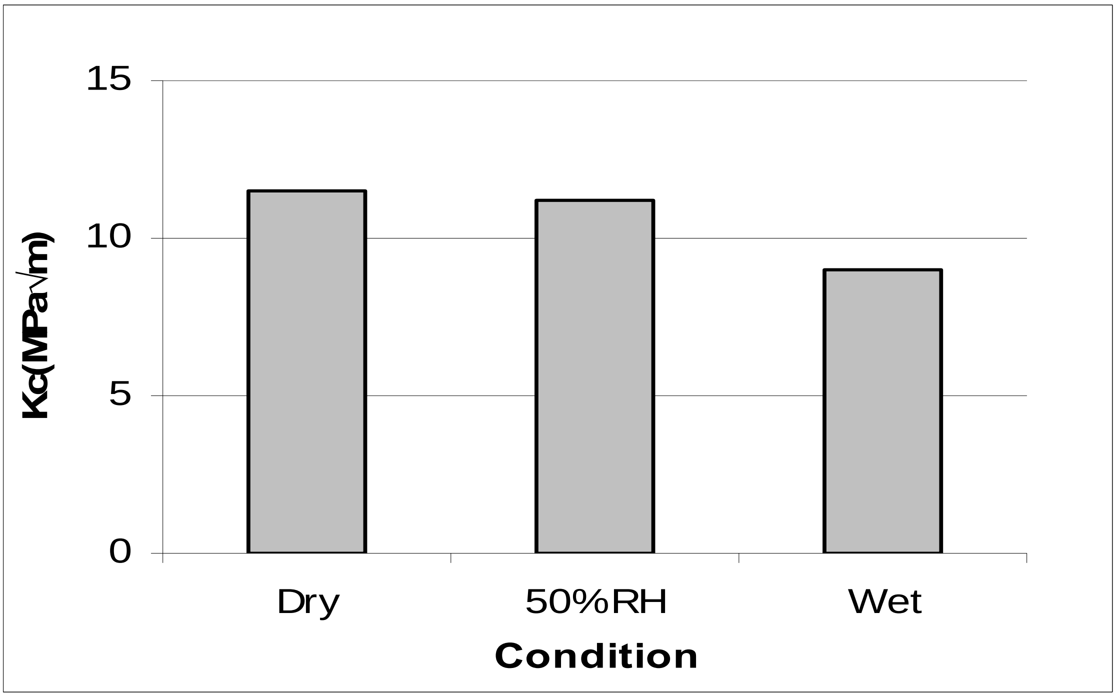

Figure 4.138: K_c values of carbon fibre composites at different conditions

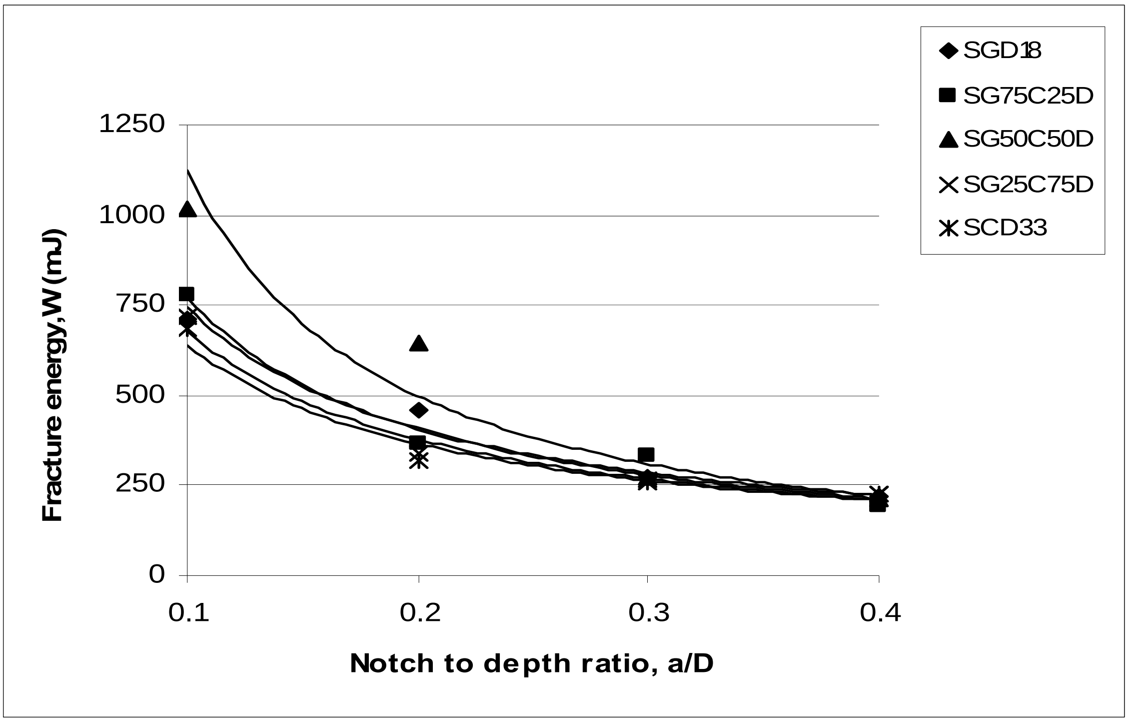

Figure 4.139: Variation of fracture energy with notch to depth ratio of hybrid fibre composite at dry condition

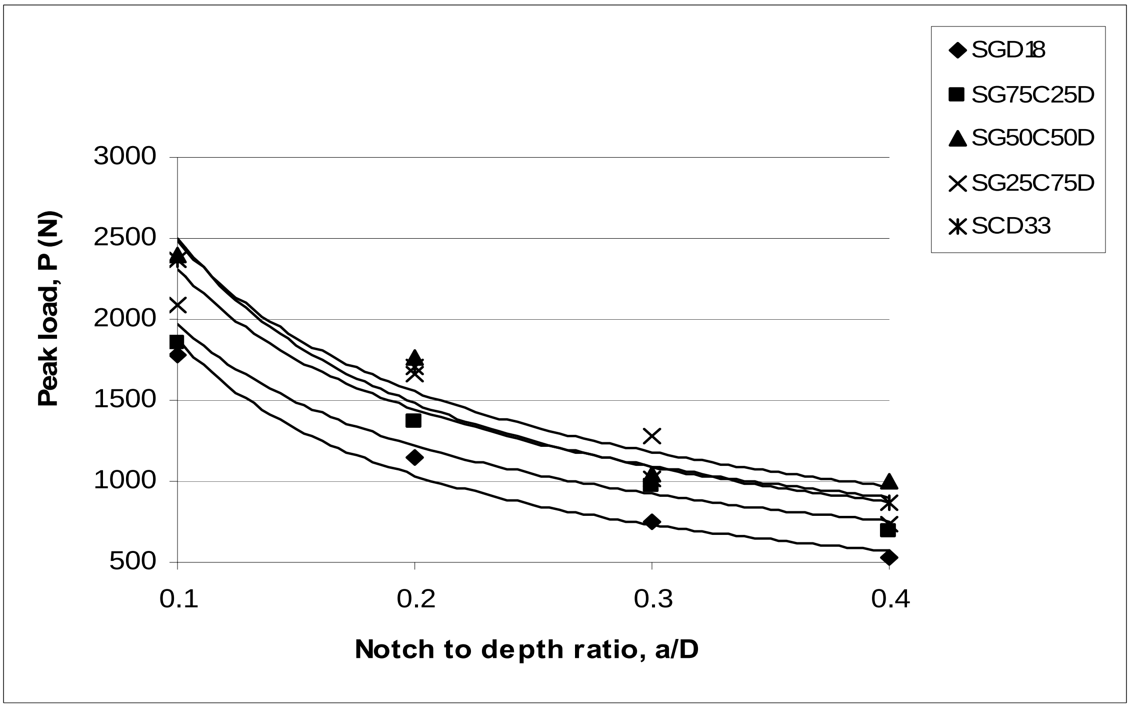

Figure 4.140: Variation of peak load with notch to depth ratio of hybrid fibre composite at dry condition

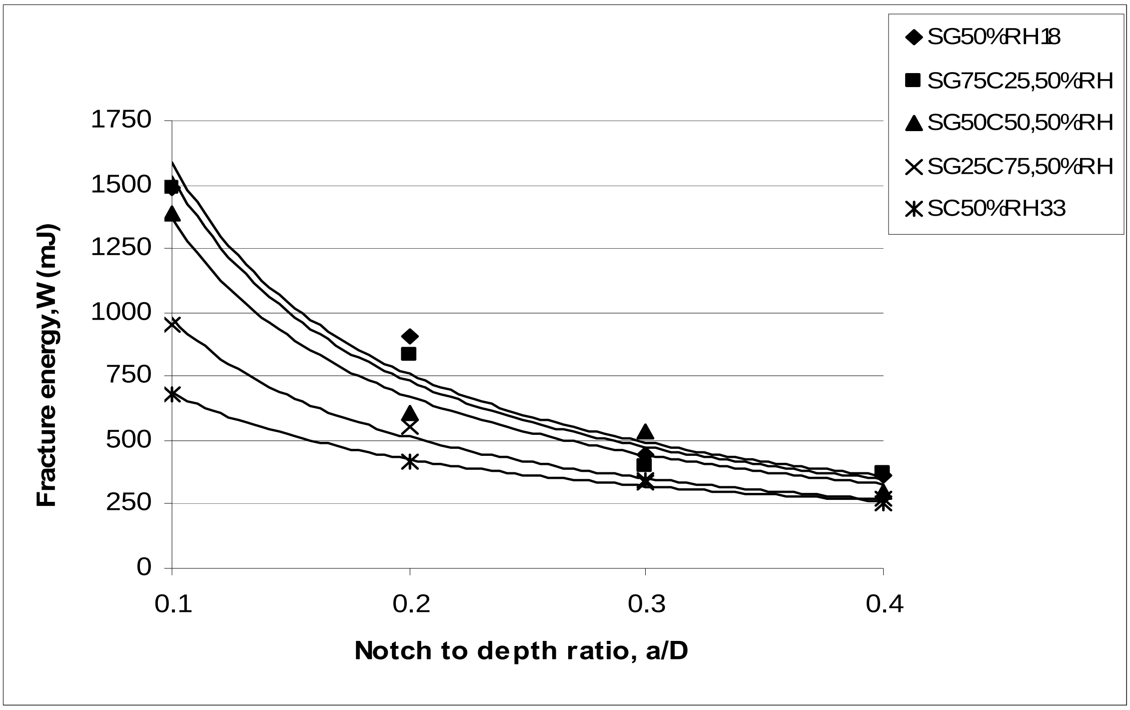

Figure 4.141: Variation of fracture energy with notch to depth ratio of hybrid fibre composite at 50% RH condition

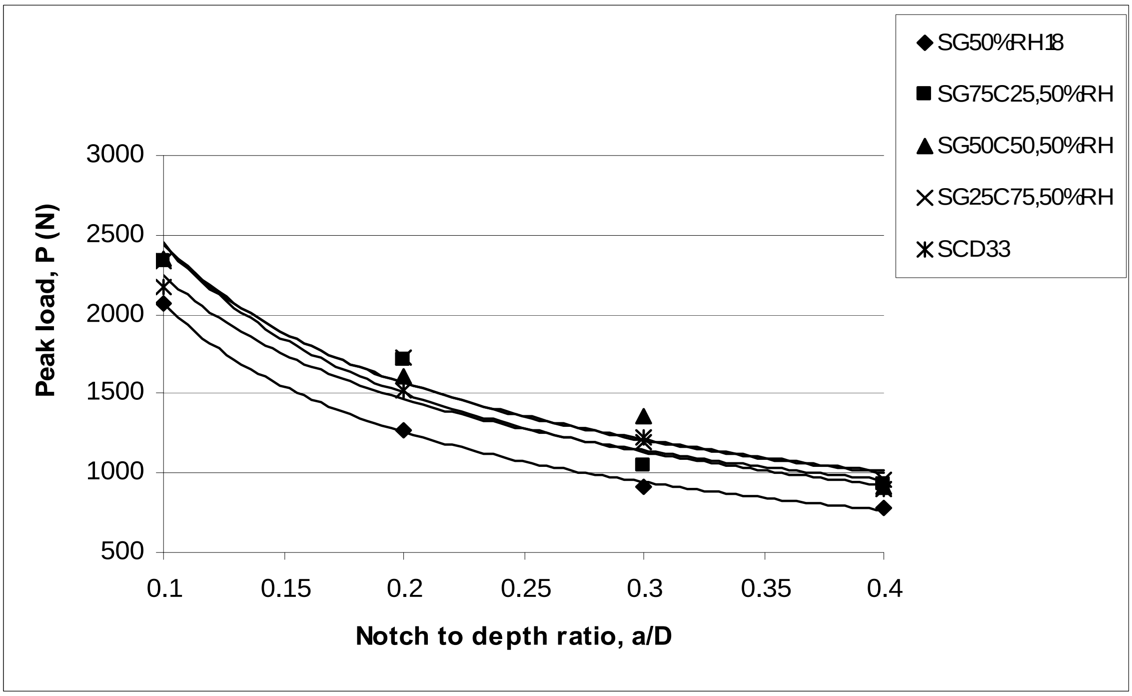

Figure 4.142: Variation of peak load with notch to depth ratio of hybrid fibre composite at 50% RH condition

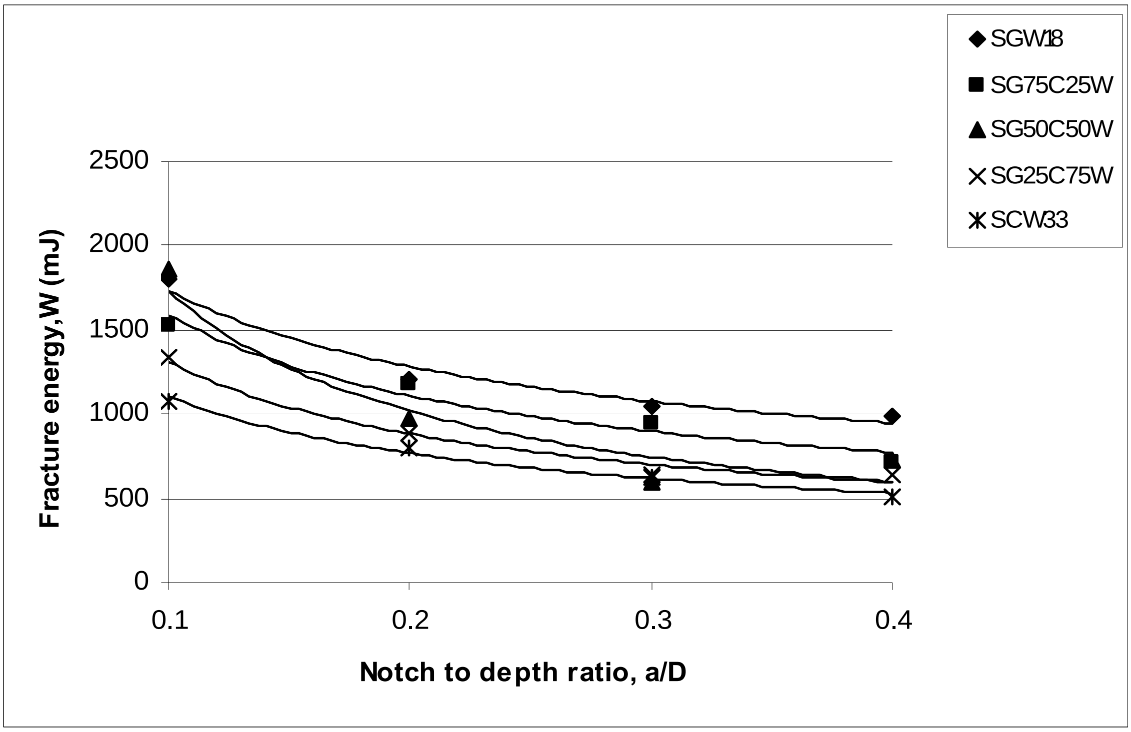

Figure 4.143: Variation of fracture energy with notch to depth ratio of hybrid fibre composite at wet condition

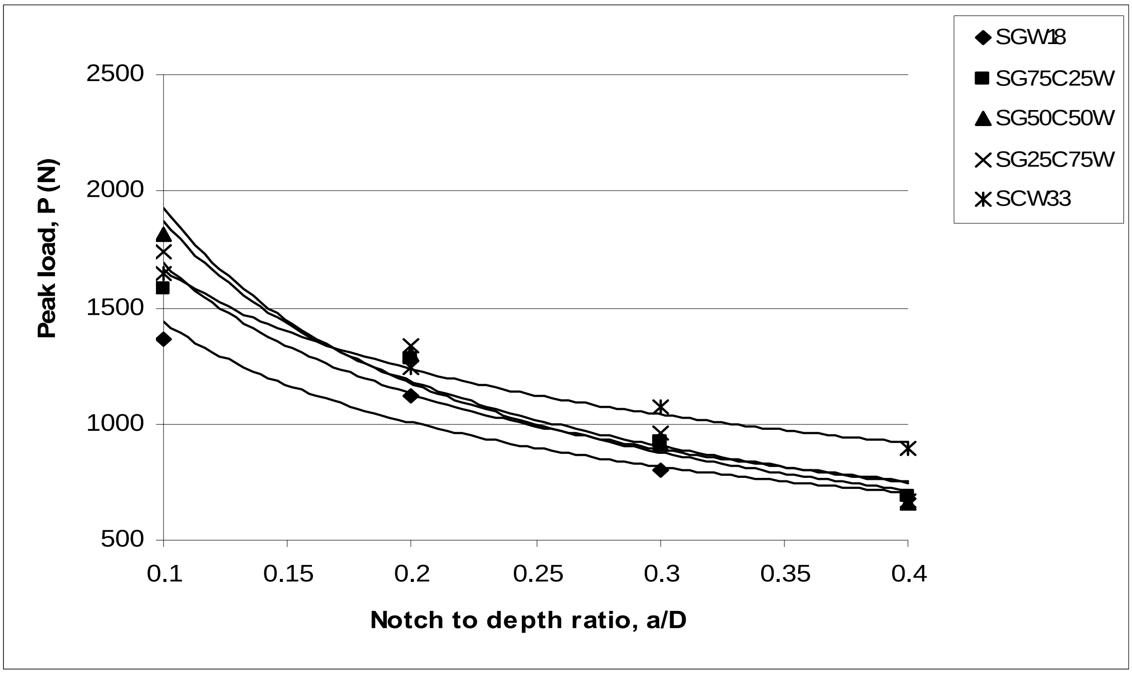

Figure 4.144: Variation of peak load with notch to depth ratio of hybrid fibre composite at wet condition

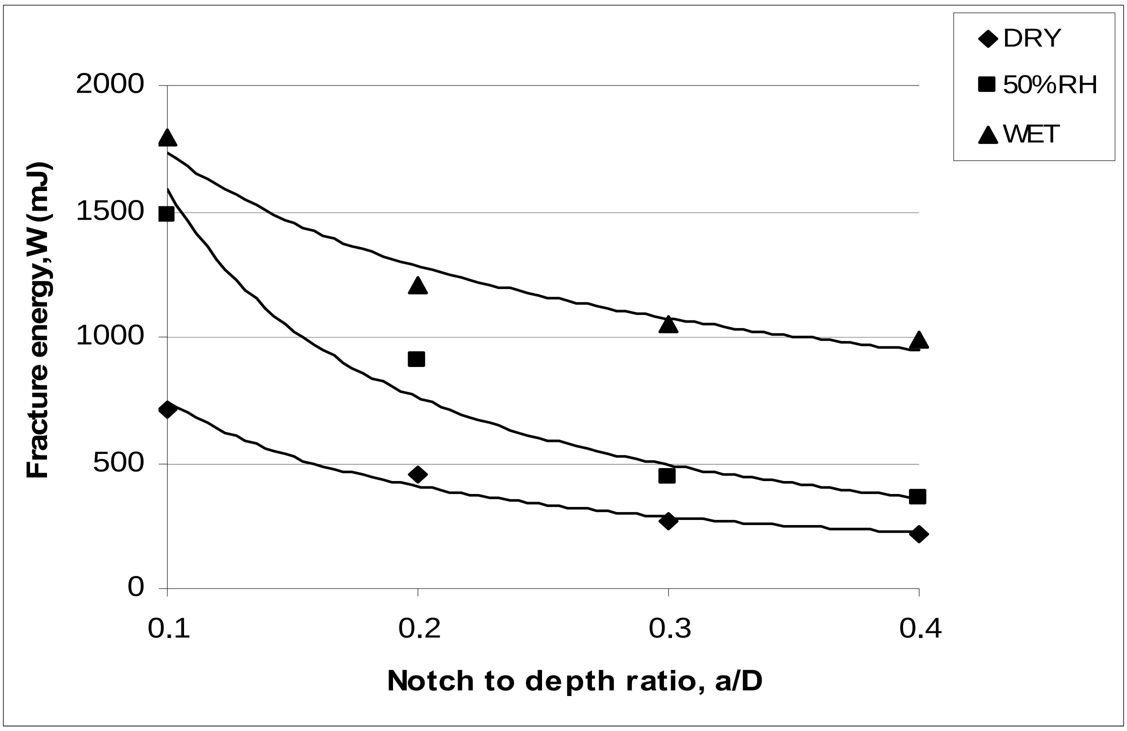

Figure 4.145: Variation of fracture energy with notch to depth ratio of 18% fibre volume fraction glass fibre composites at different conditions

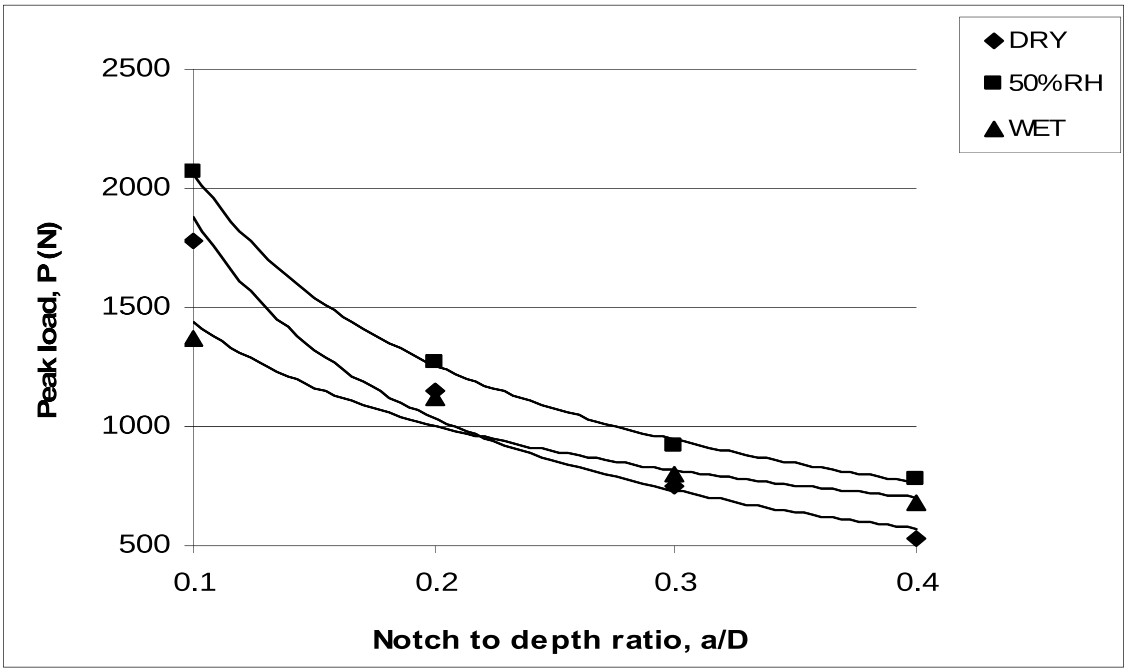

Figure 4.146: Variation of peak load with notch to depth ratio of 18% fibre volume fraction glass fibre composites at different conditions

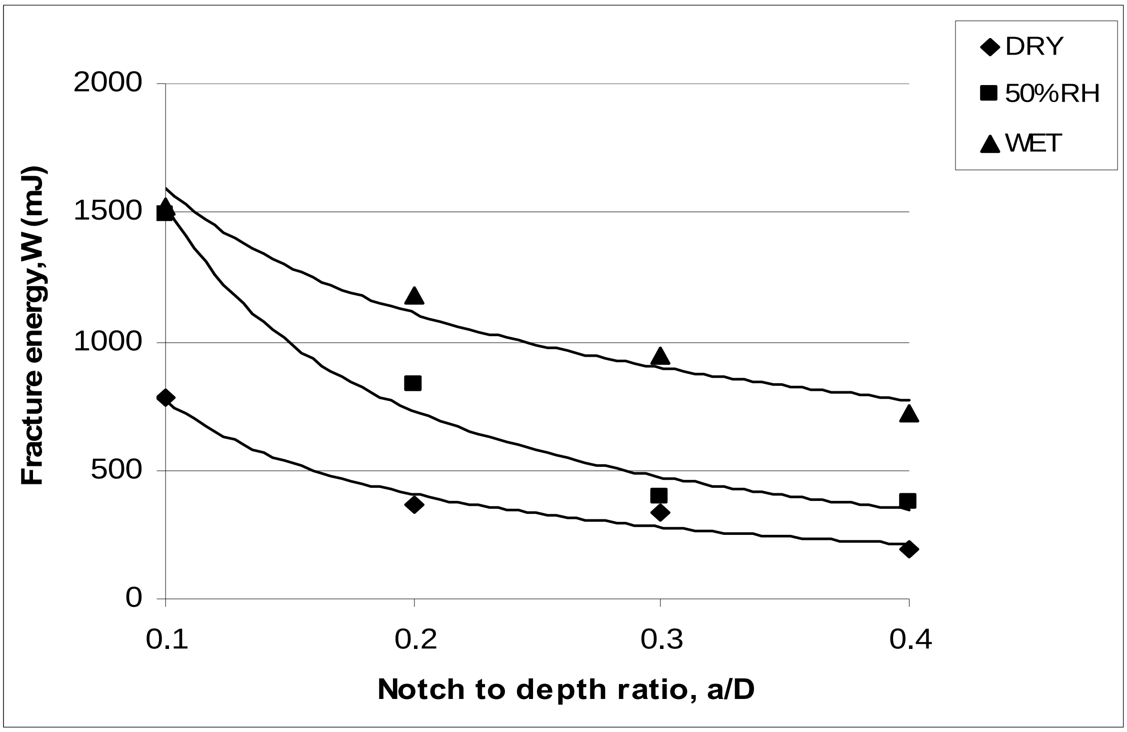

Figure 4.147: Variation of fracture energy with notch to depth ratio of SG75/C25 hybrid composites at different conditions

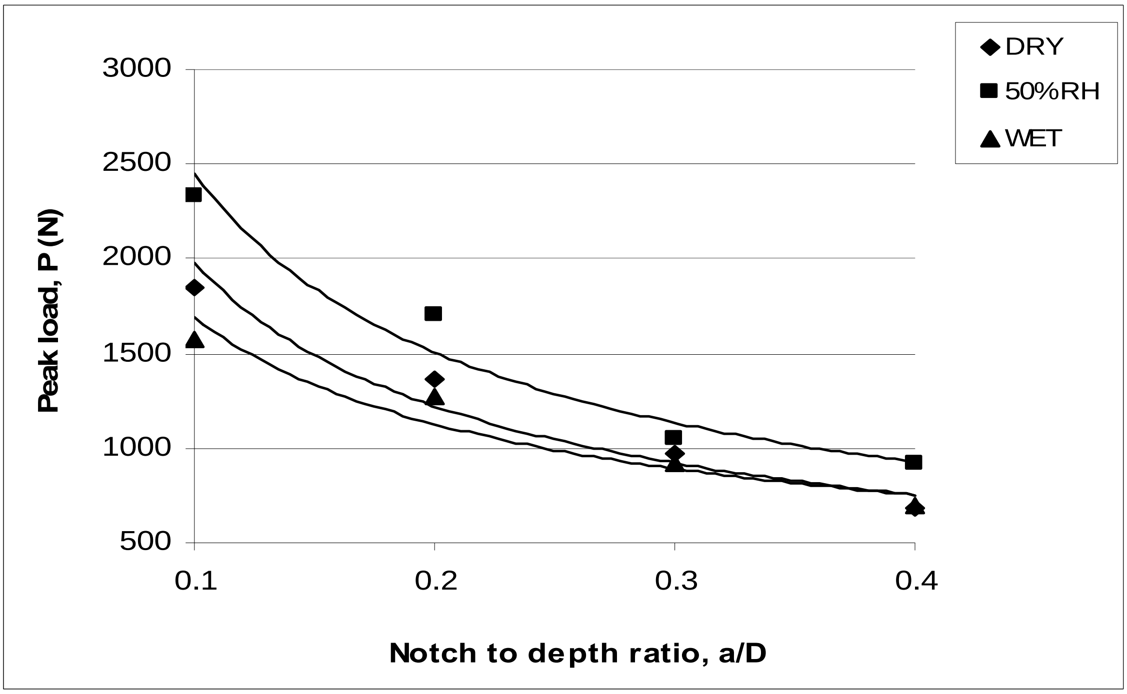

Figure 4.148: Variation of peak load with notch to depth ratio of SG75/C25 hybrid composites at different conditions

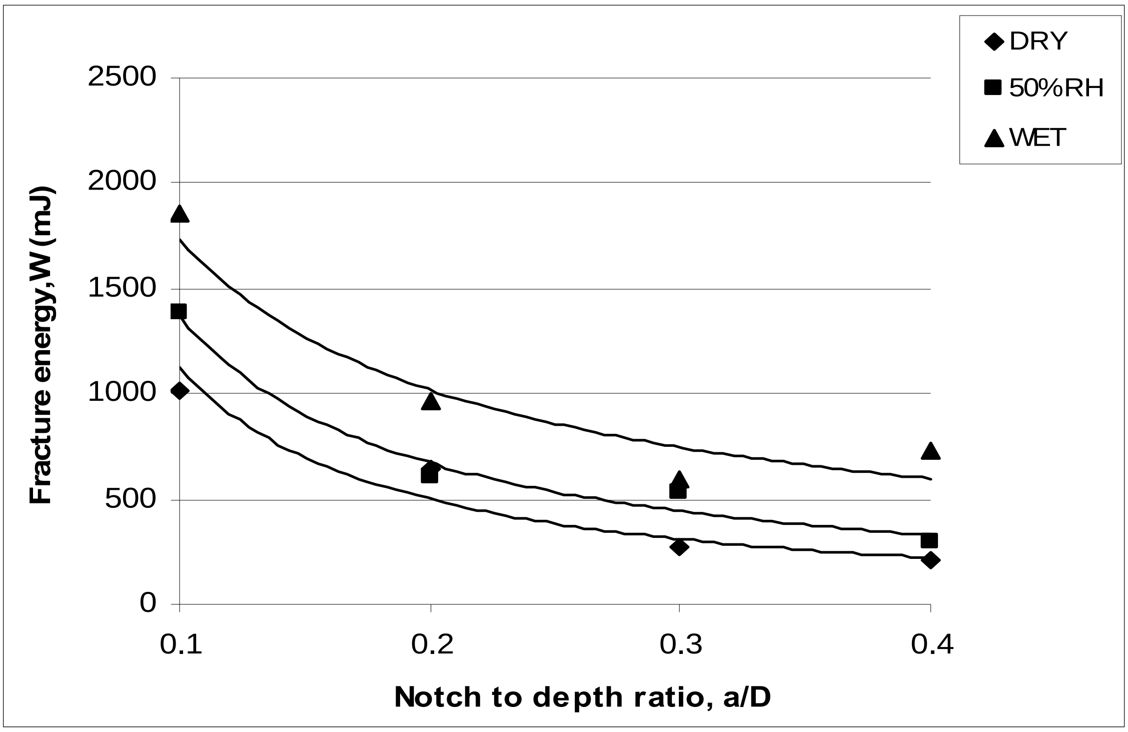

Figure 4.149: Variation of fracture energy with notch to depth ratio of SG50/C50 hybrid composites at different conditions

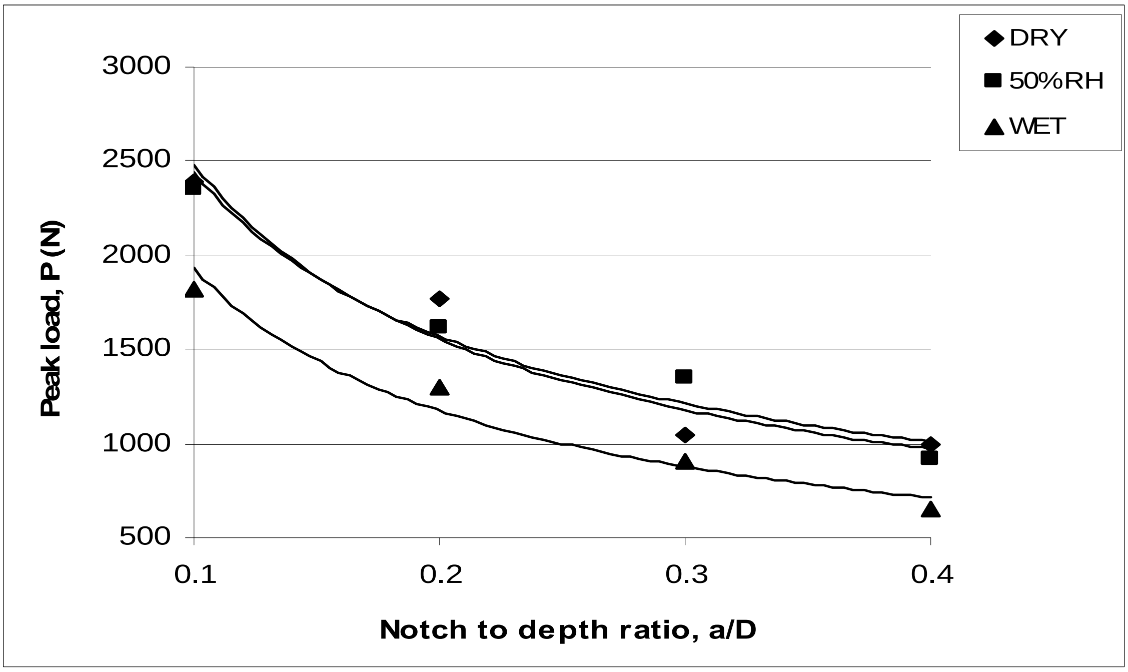

Figure 4.150: Variation of peak load with notch to depth ratio of SG50/C50 hybrid composites at different conditions

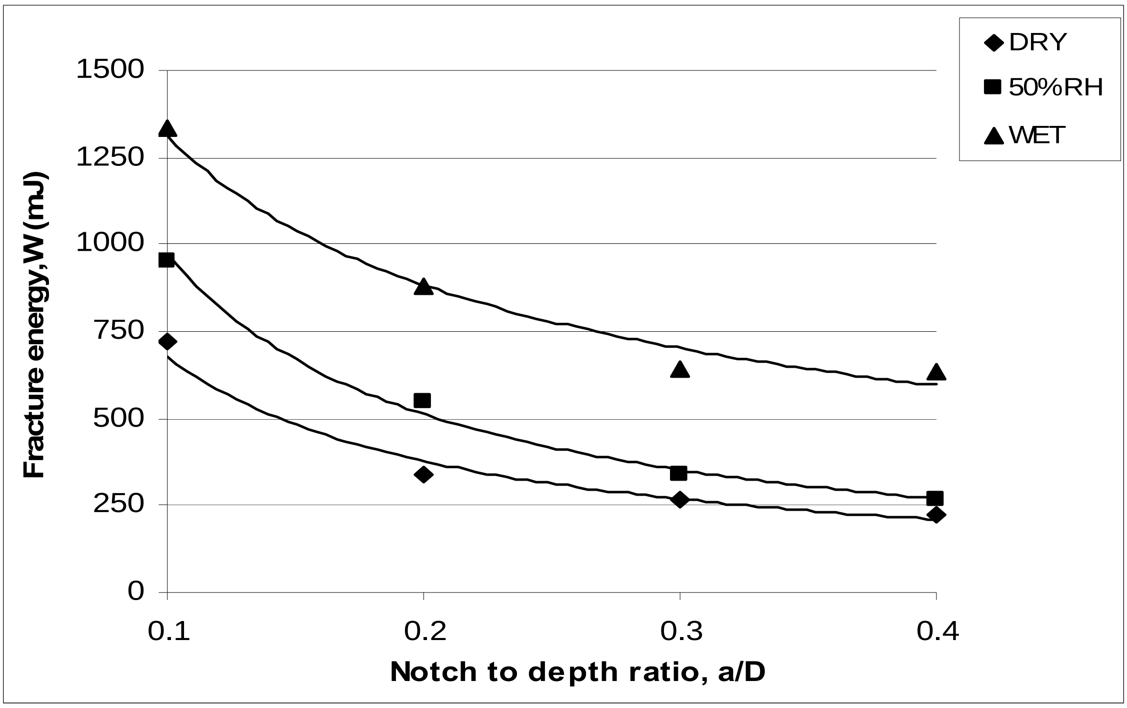

Figure 4.151: Variation of fracture energy with notch to depth ratio of SG25/C75 hybrid composites at different conditions

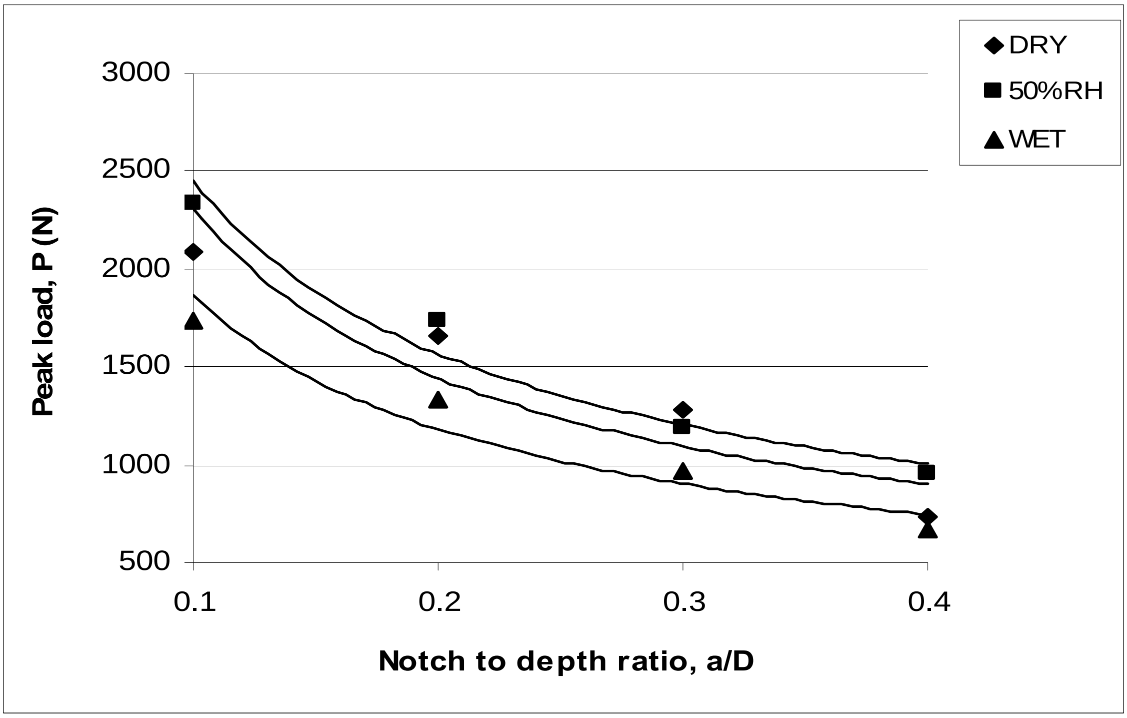

Figure 4.152: Variation of peak load with notch to depth ratio of SG25/C75 hybrid composites at different conditions

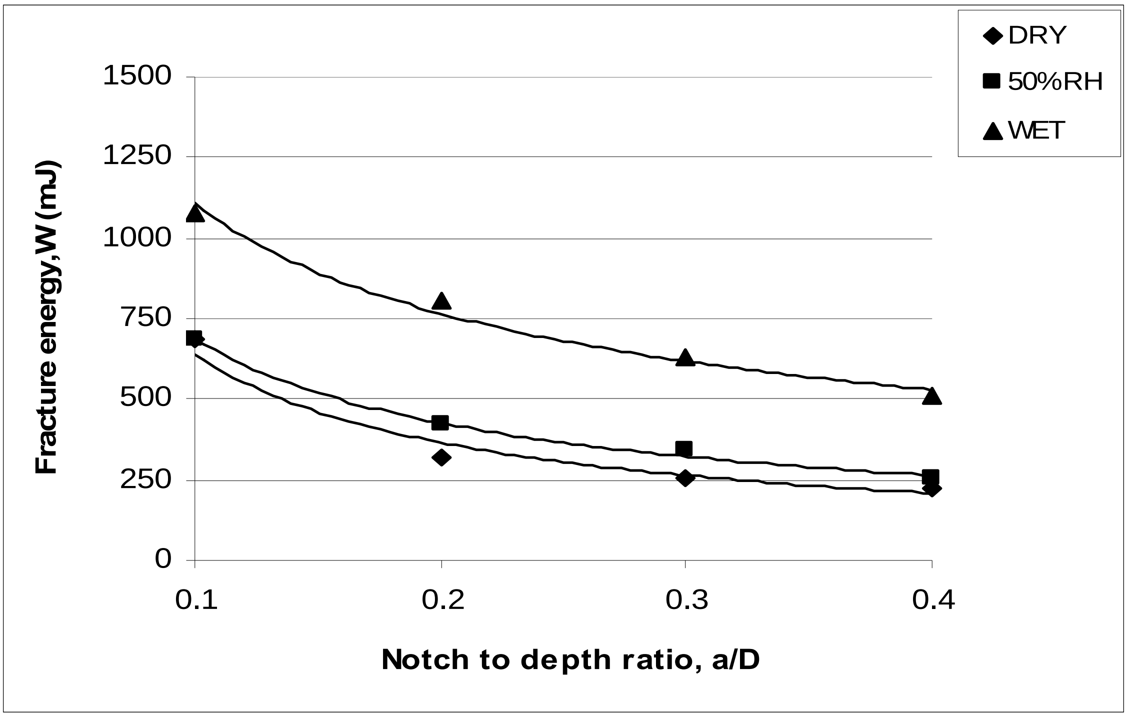

Figure 4.153: Variation of fracture energy with notch to depth ratio of carbon fibre composites at different conditions

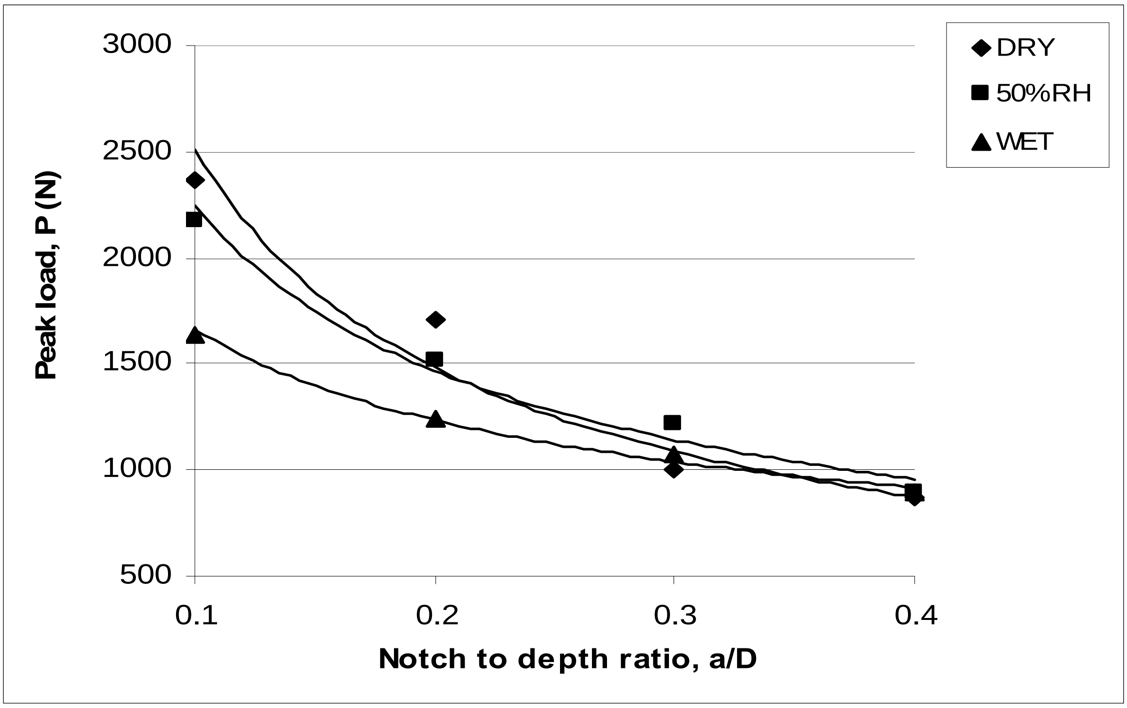

Figure 4.154: Variation of peak load with notch to depth ratio of carbon fibre composites at different conditions

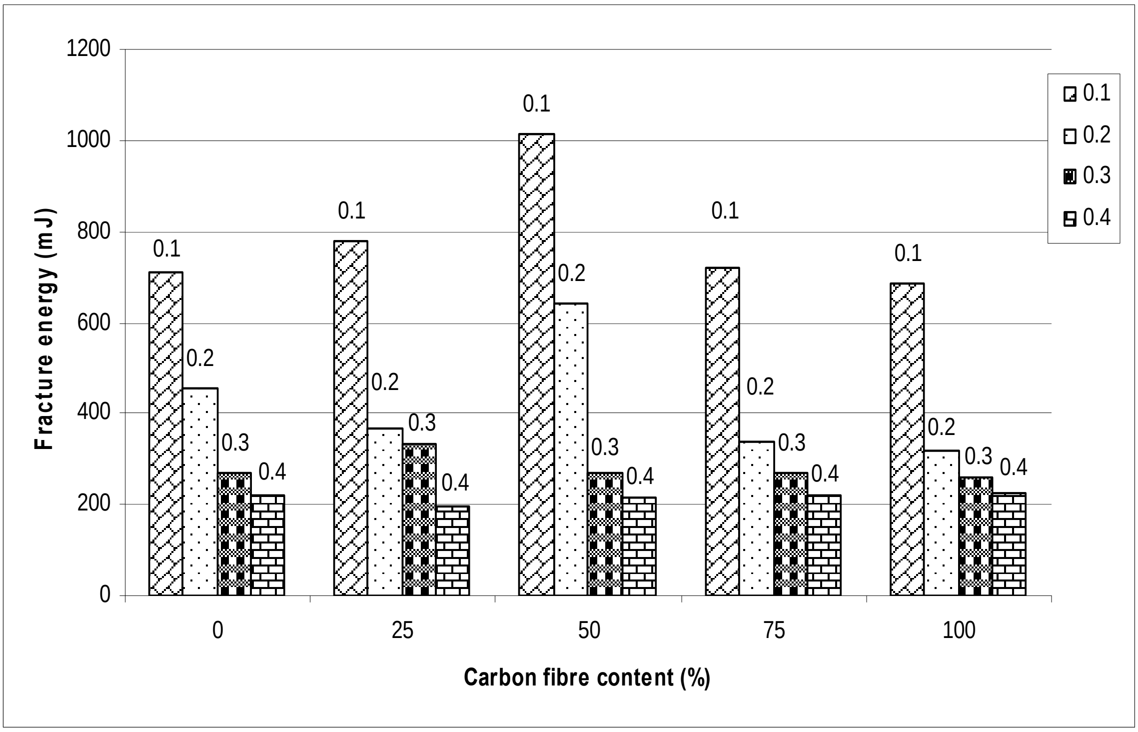

Figure 4.155: Variation of fracture energy of hybrid fibre composites with carbon fibre composite contents and a/D ratios at dry condition

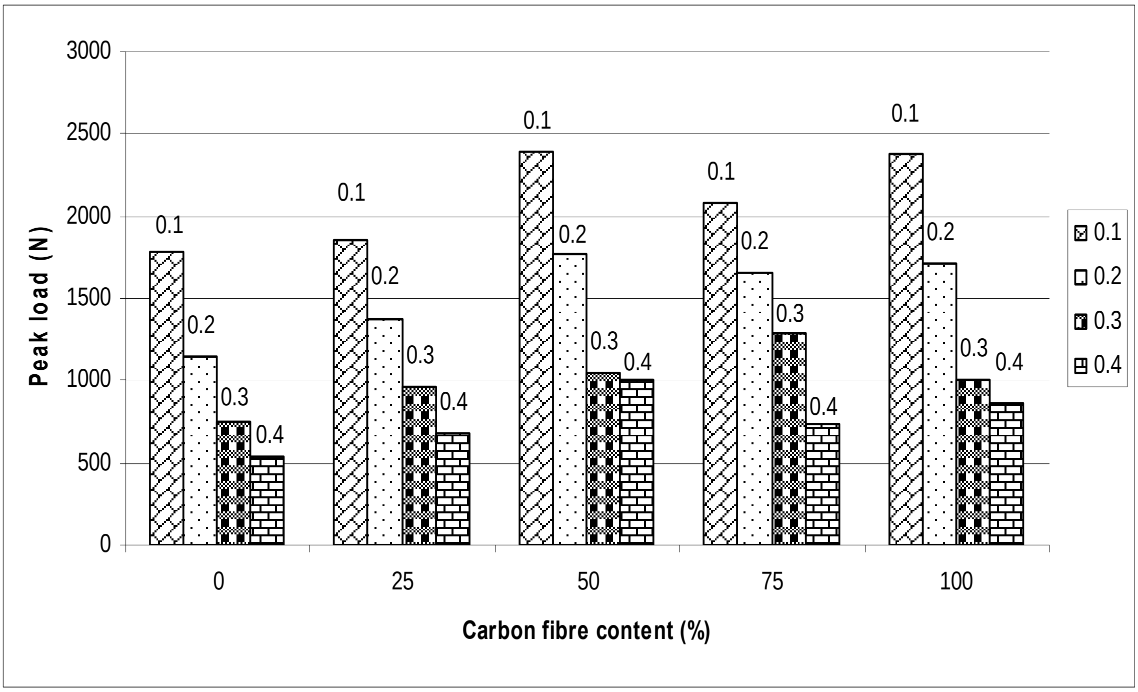

Figure 4.156: Variation of peak load of hybrid fibre composites with carbon fibre composite contents and a/D ratios at dry condition

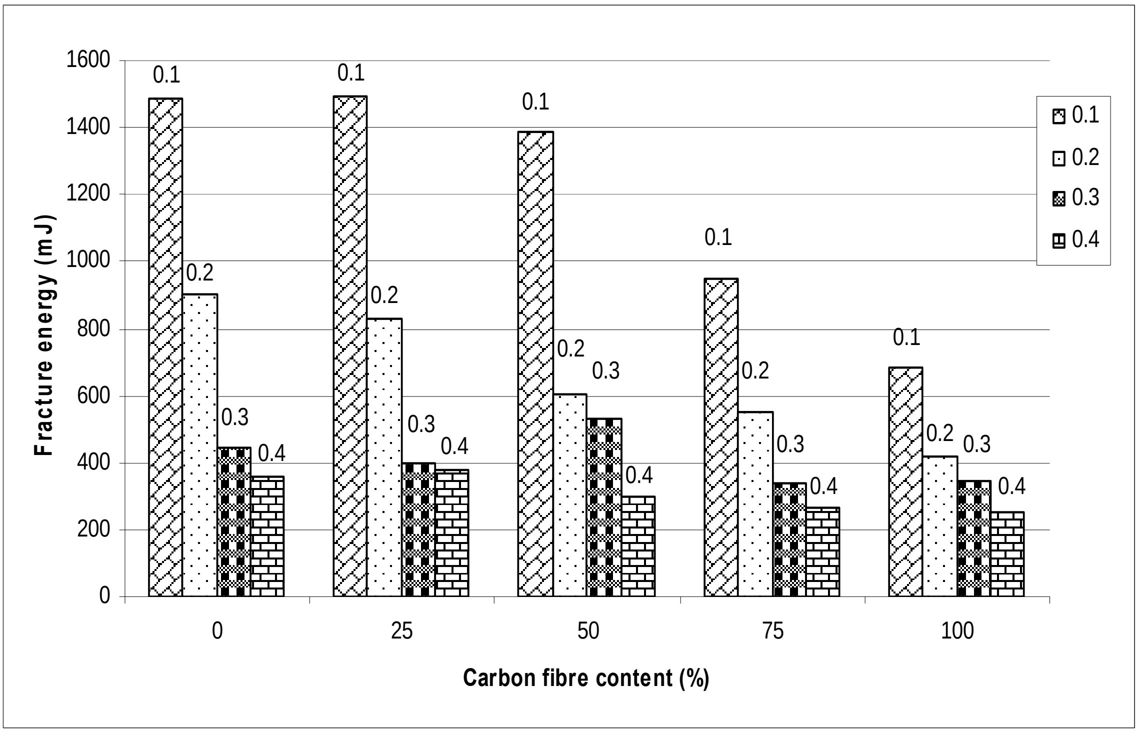

Figure 4.157: Variation of fracture energy of hybrid fibre composites with carbon fibre composite contents and a/D ratios at 50% RH condition

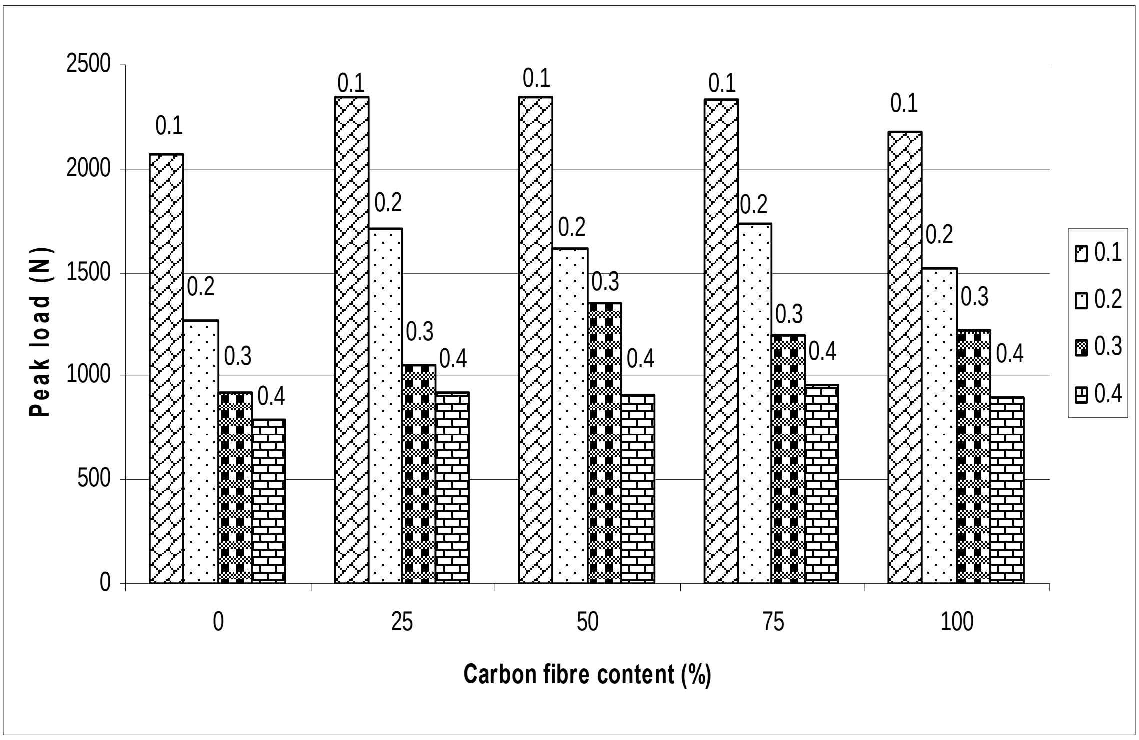

Figure 4.158: Variation of peak load of hybrid fibre composites with carbon fibre composite contents and a/D ratios at 50% RH condition

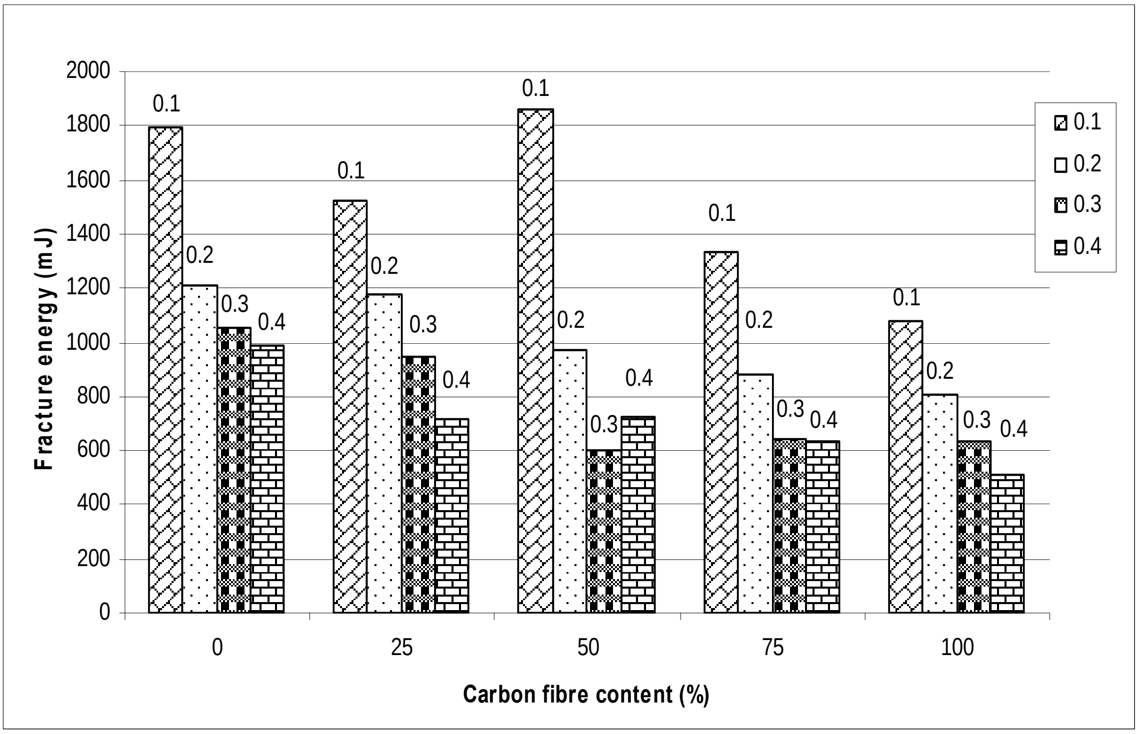

Figure 4.159: Variation of fracture energy of hybrid fibre composites with carbon fibre composite contents and a/D ratios at wet condition

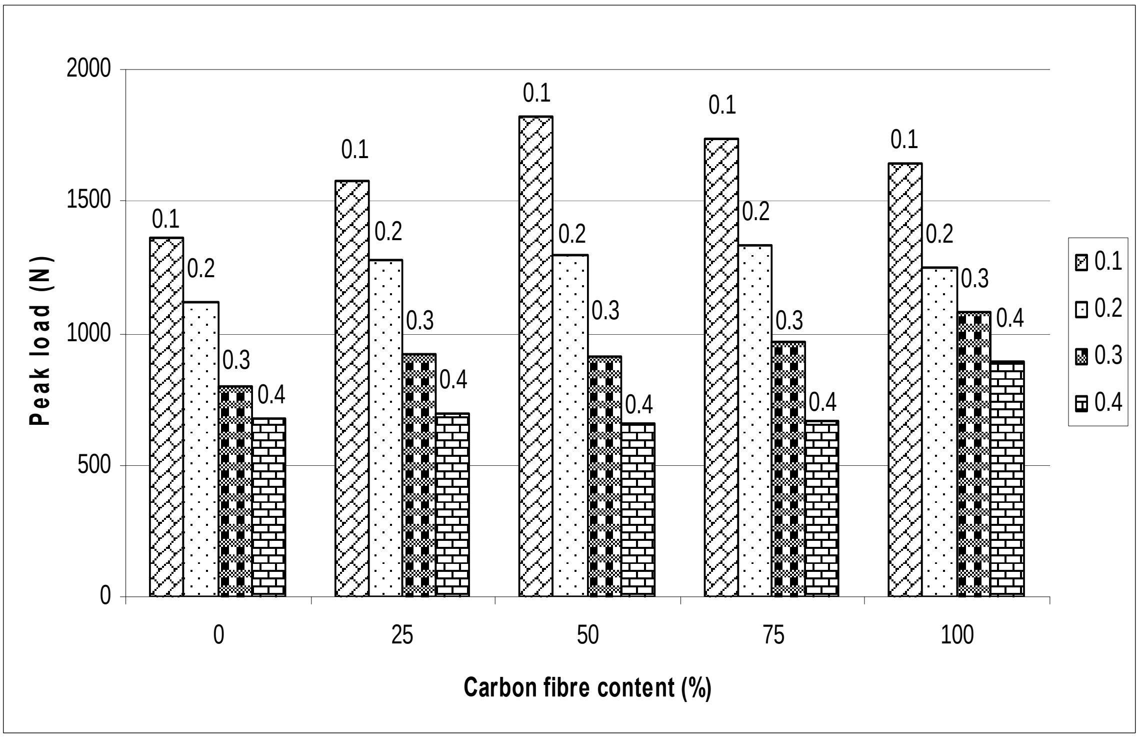

Figure 4.160: Variation of peak load of hybrid fibre composites with carbon fibre composite contents and a/D ratios at wet condition

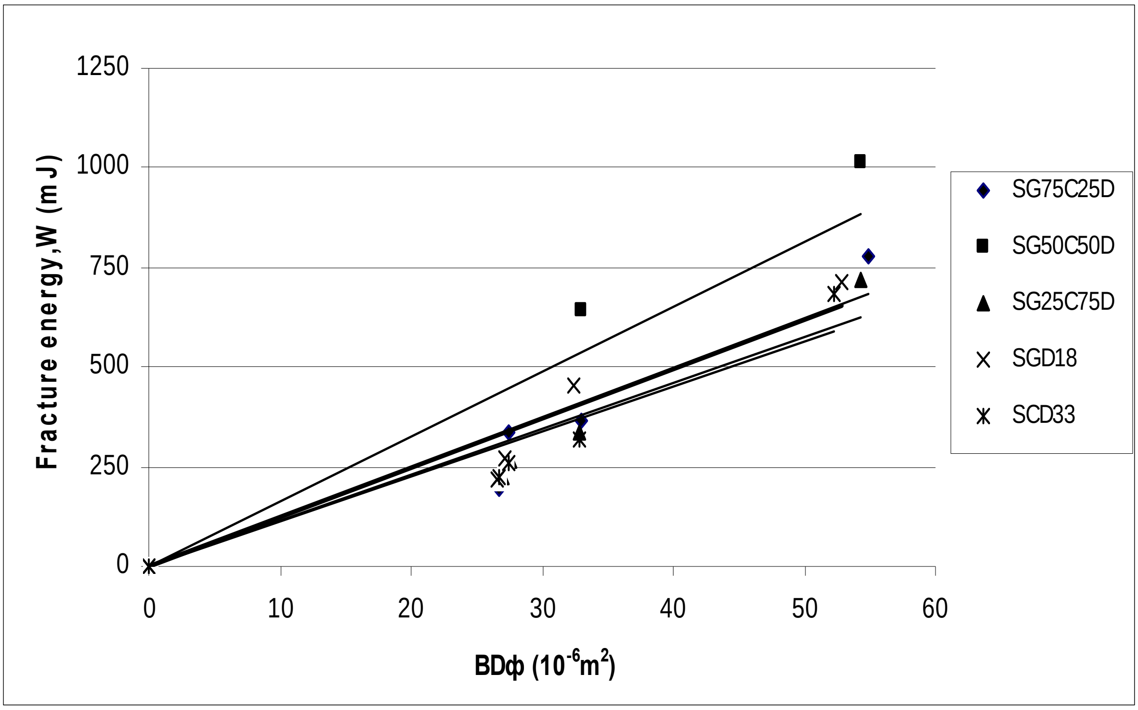

Figure 4.161: Variation of fracture energy with specimen geometry function of hybrid fibre composites at dry condition

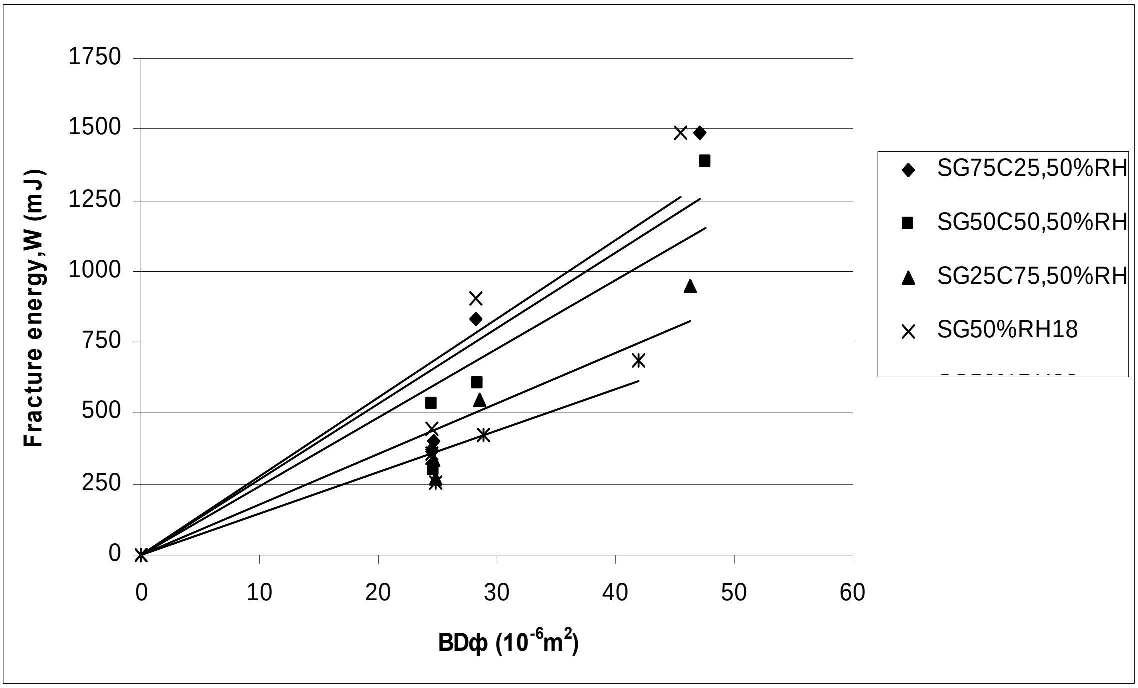

Figure 4.162: Variation of fracture energy with specimen geometry function of hybrid fibre composites at 50% RH condition

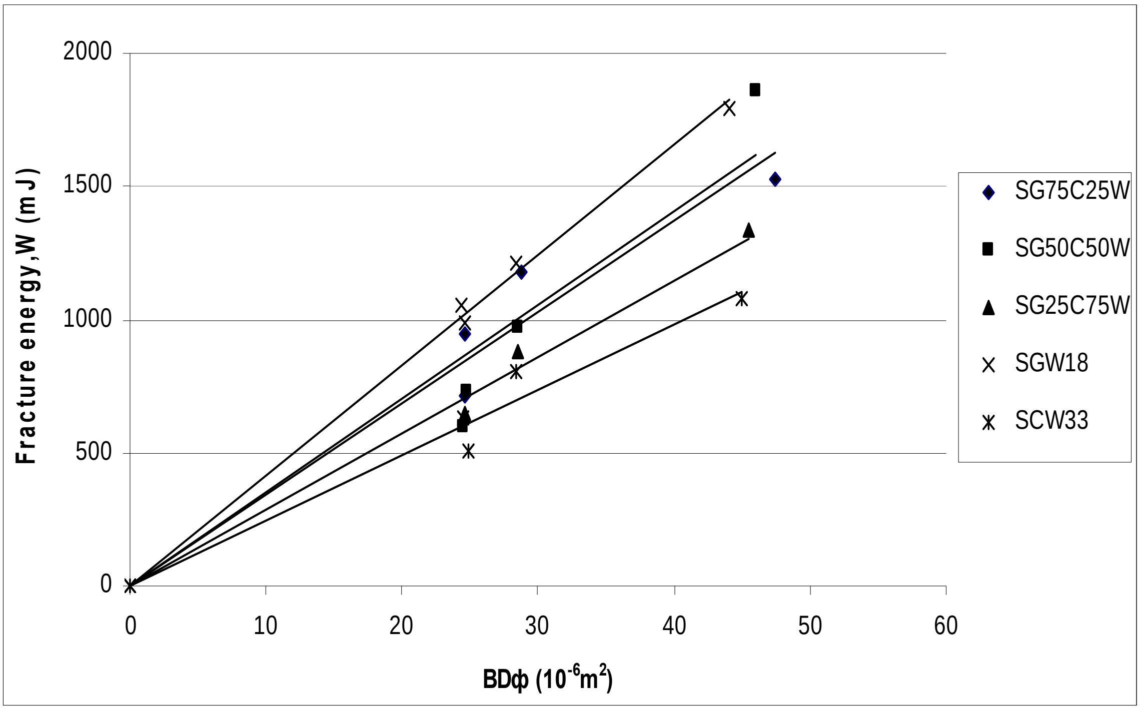

Figure 4.163: Variation of fracture energy with specimen geometry function of hybrid fibre composites at wet condition

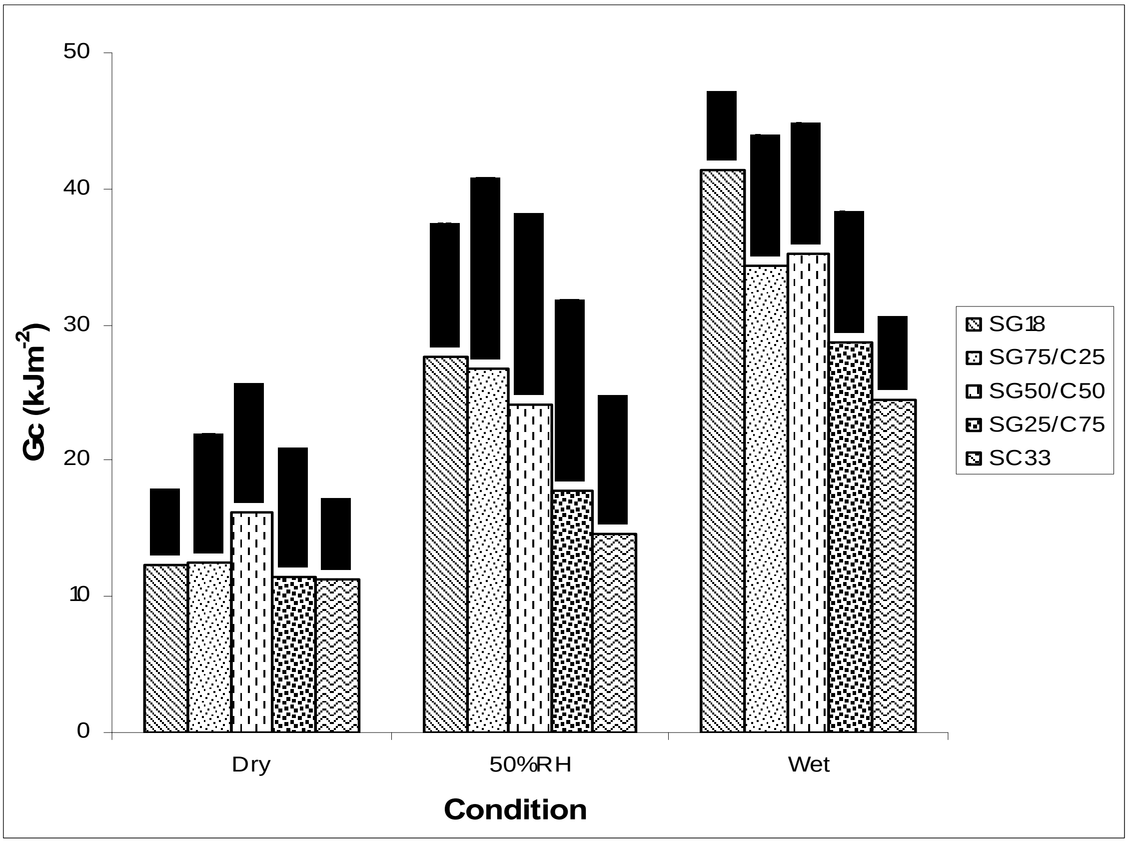

Figure 4.164: G_c values of hybrid fibre composites for various carbon fibre content at different conditions

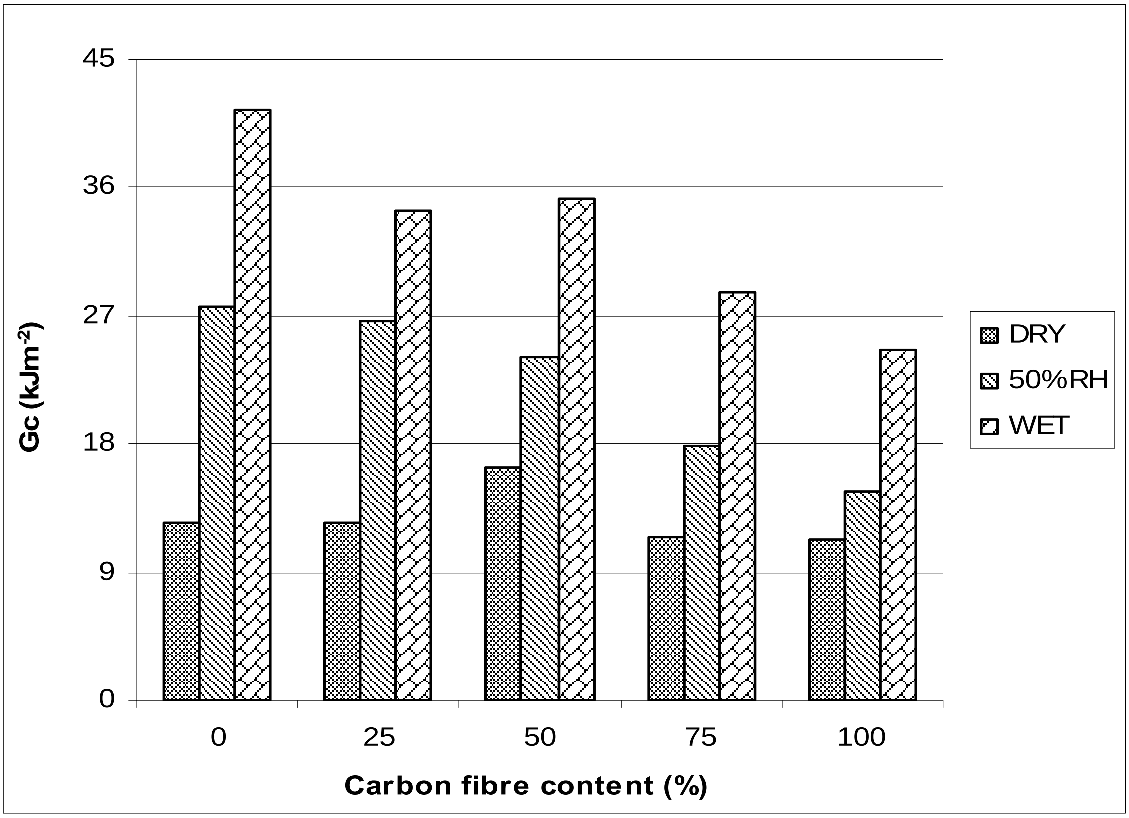

Figure 4.165: G_c values of hybrid fibre composites at dry, 50% RH and wet condition

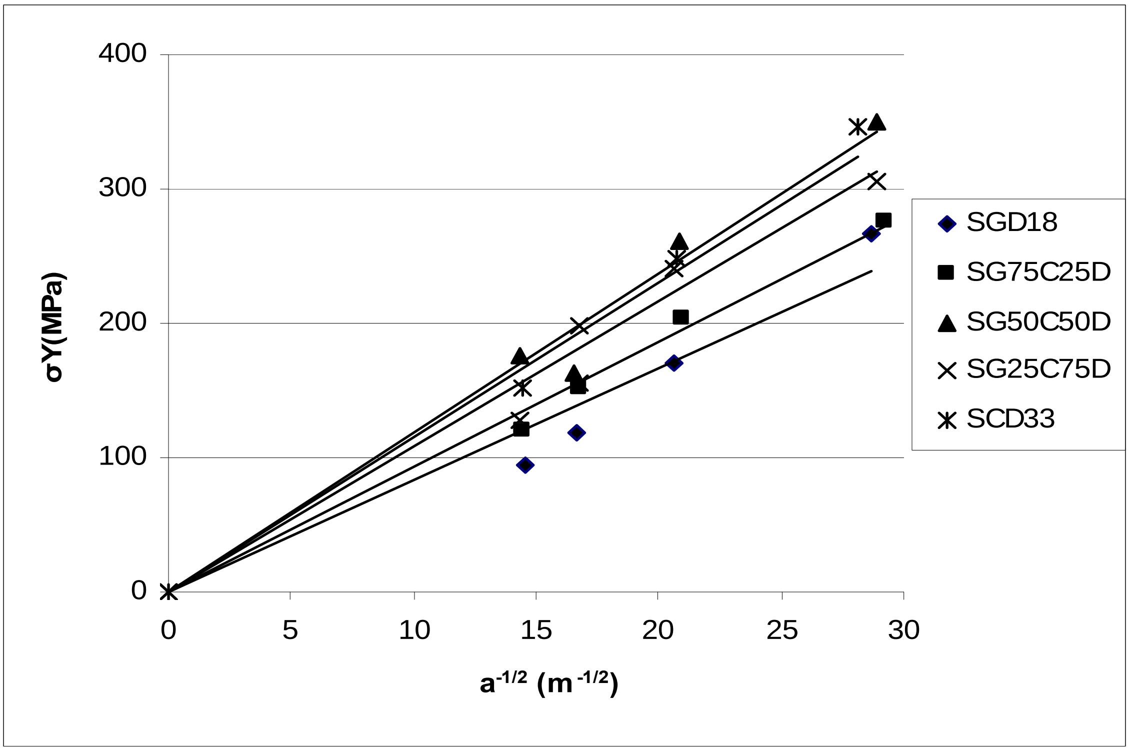

Figure 4.166: Variation of σY with $a^{-1/2}$ of hybrid fibre composites at dry condition

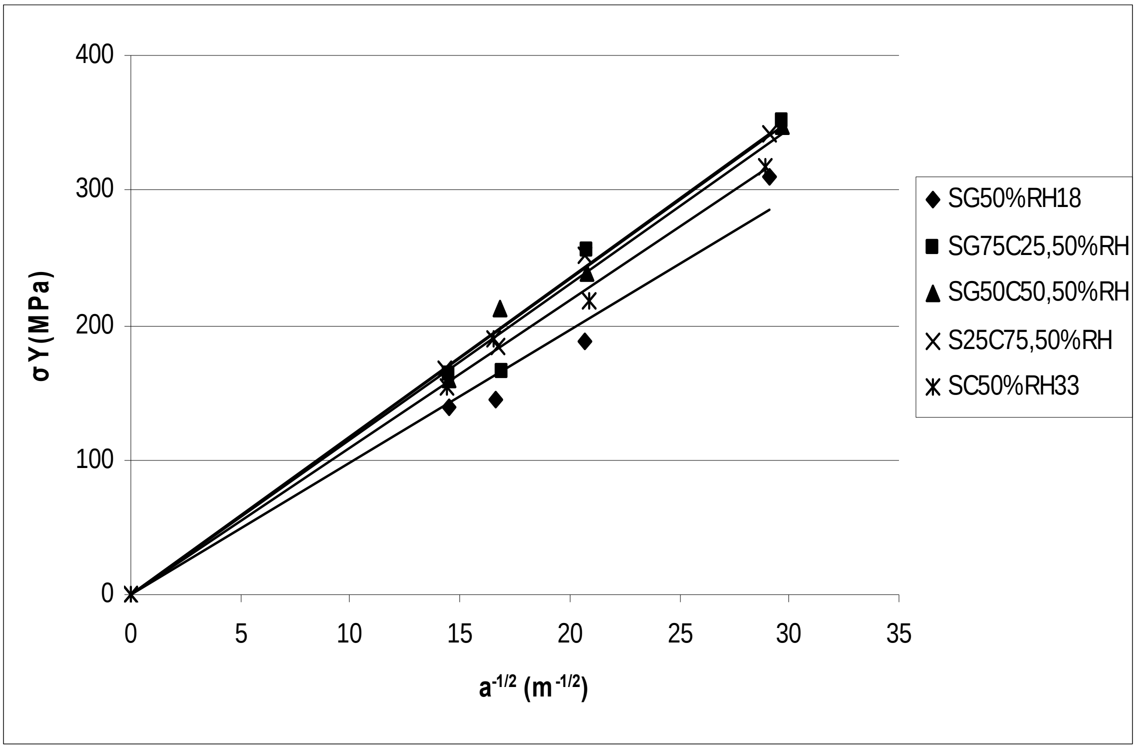

Figure 4.167: Variation of σY with $a^{-1/2}$ of hybrid fibre composites at 50% RH condition

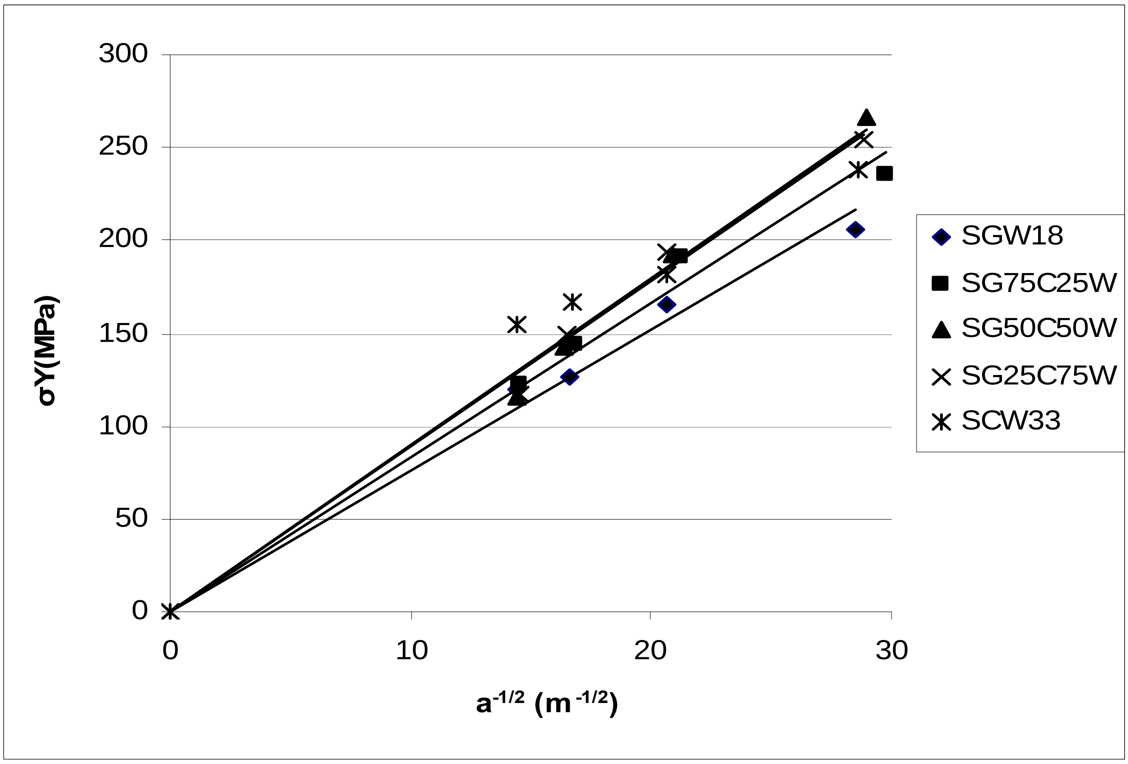

Figure 4.168: Variation of σY with $a^{-1/2}$ of hybrid fibre composites at wet condition

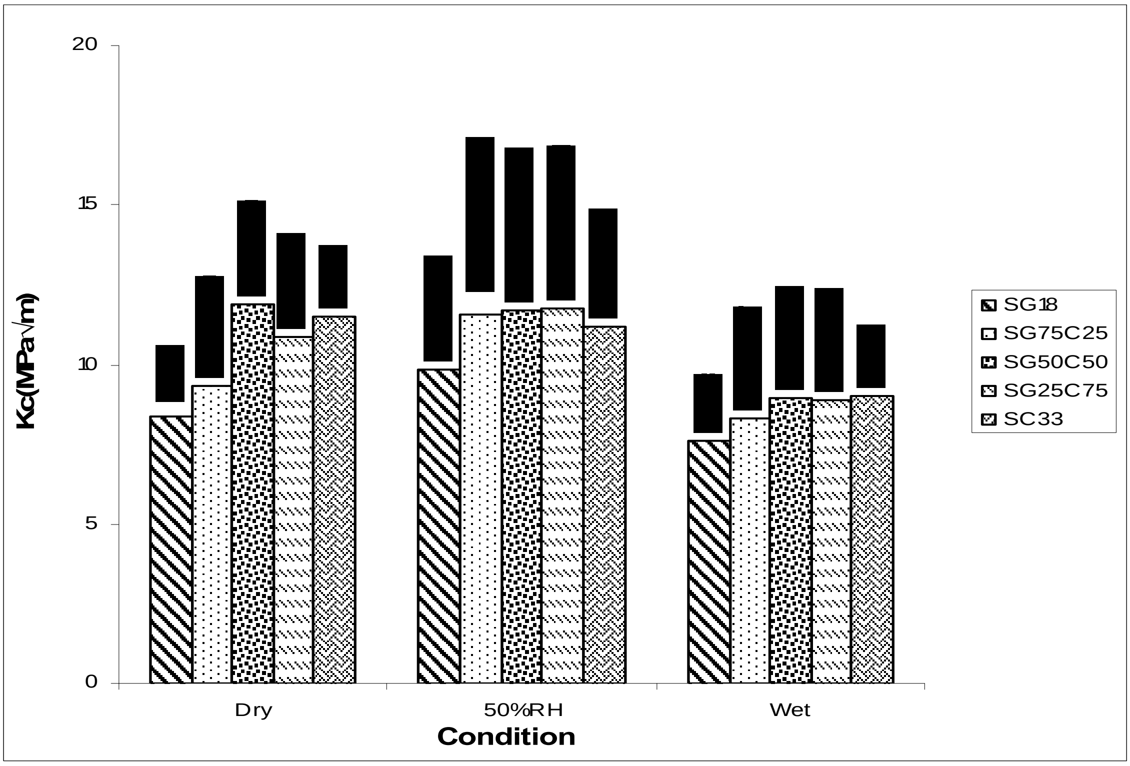

Figure 4.169: K_c values of hybrid composites for various carbon fibre content at different conditions

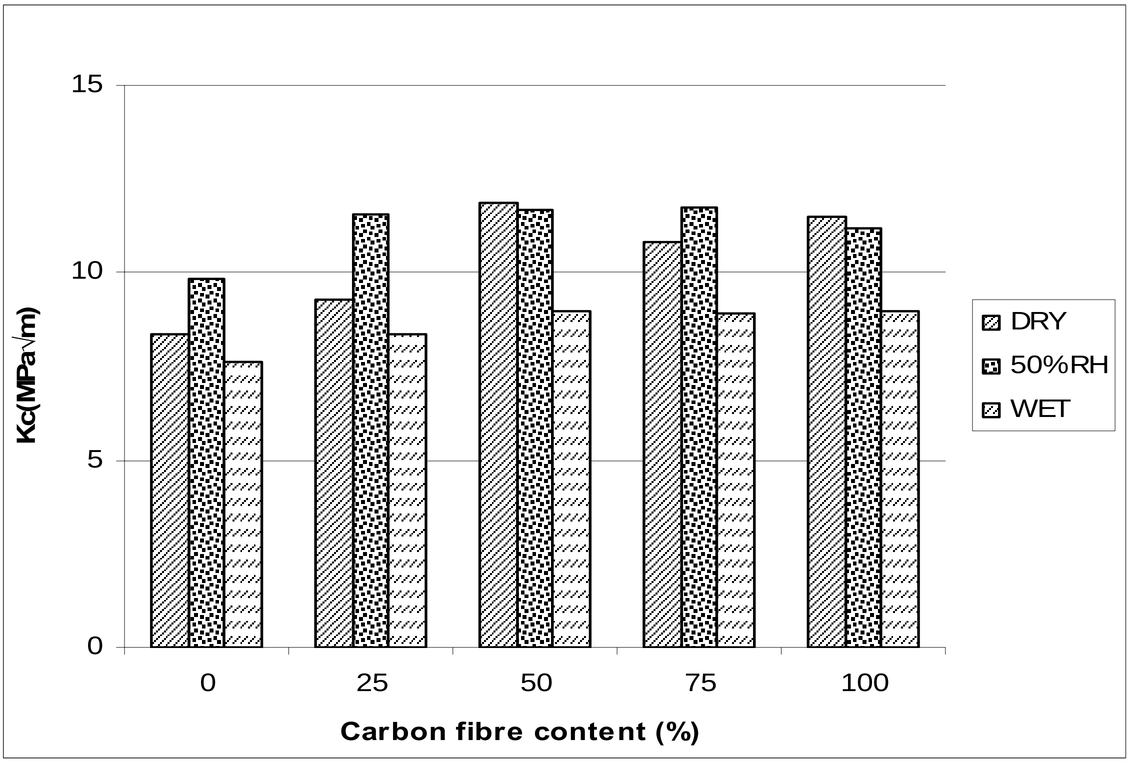

Figure 4.170: K_c values of hybrid composites at dry, 50% RH and wet condition

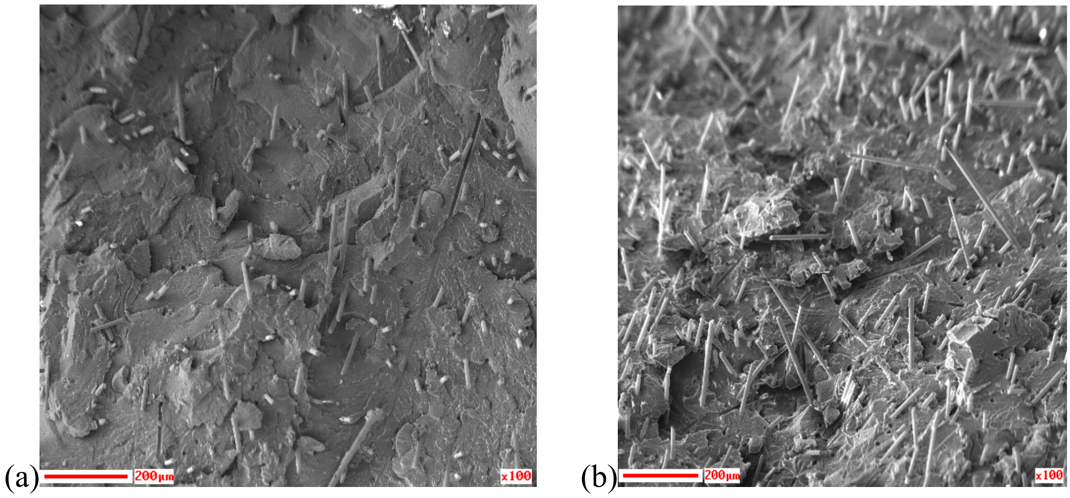

Figure 4.171: SEM micrographs of the fracture surfaces of the composites which shows fibre-matrix interfaces at (a) low fibre loading, V_f 4 % (b) high fibre loading, V_f 8 %

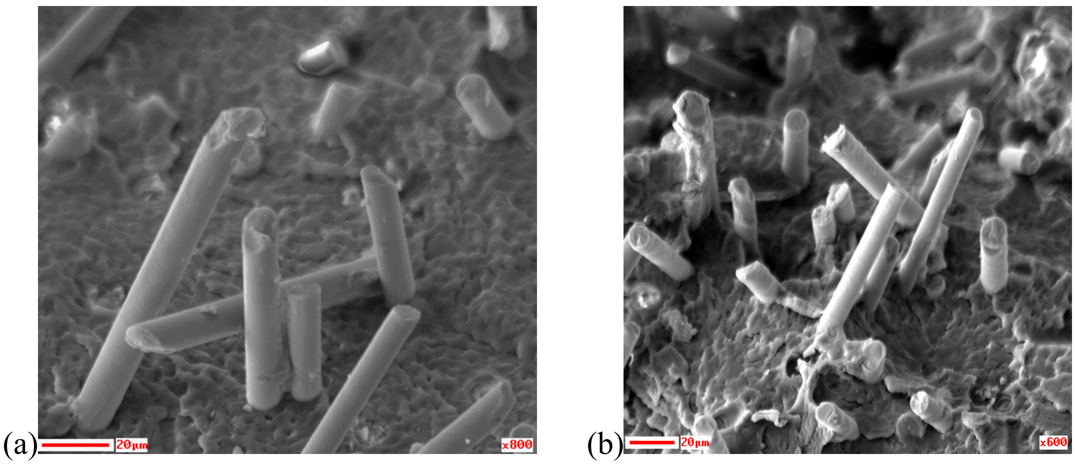

Figure 4.172: SEM micrographs of the fracture surfaces of the composites at various magnifications show the misalignment of the fibres

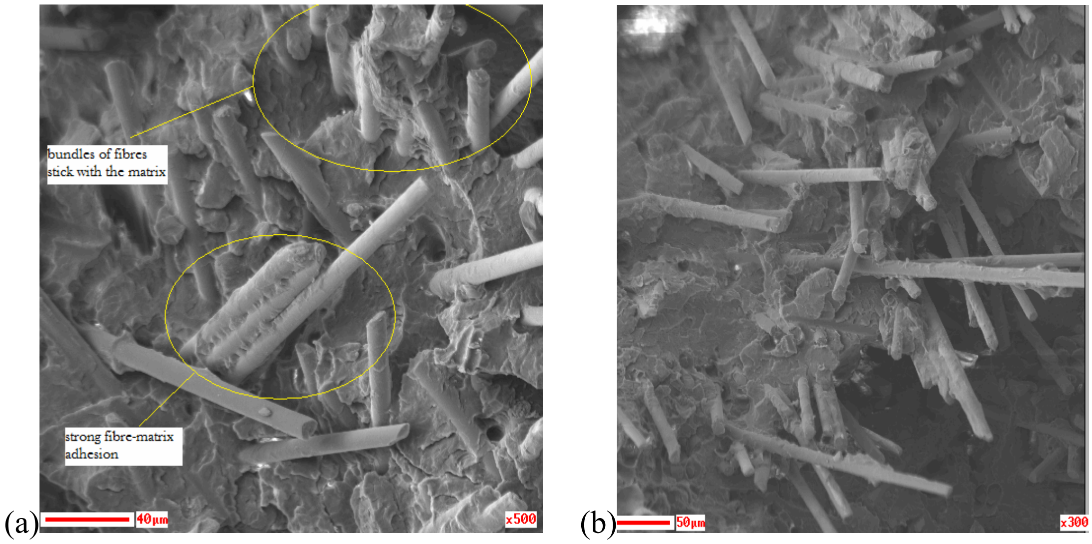

Figure 4.173: SEM micrographs taken from tensile fracture surface of glass fibre composite at dry as moulded condition

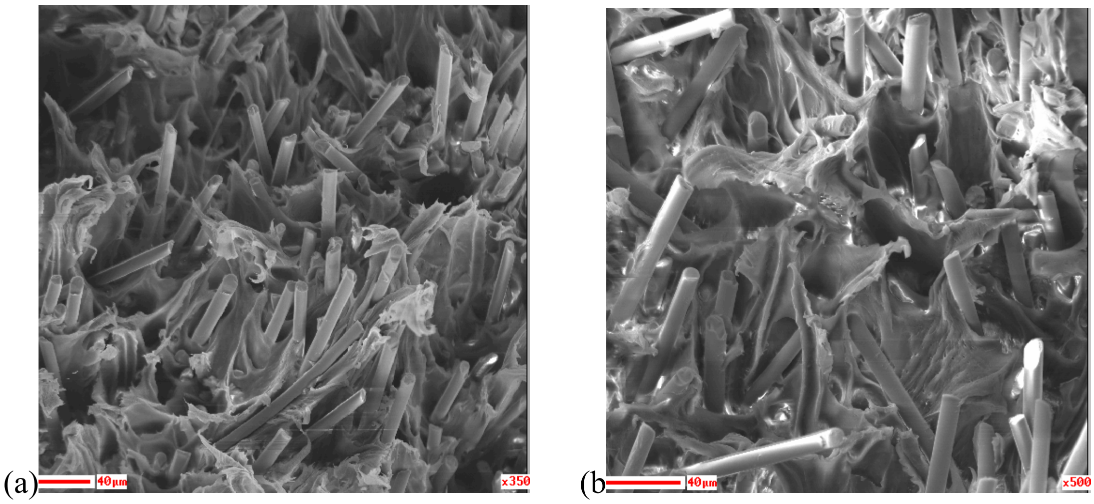

Figure 4.174: SEM micrographs taken from tensile fracture surface of glass fibre composite at wet condition

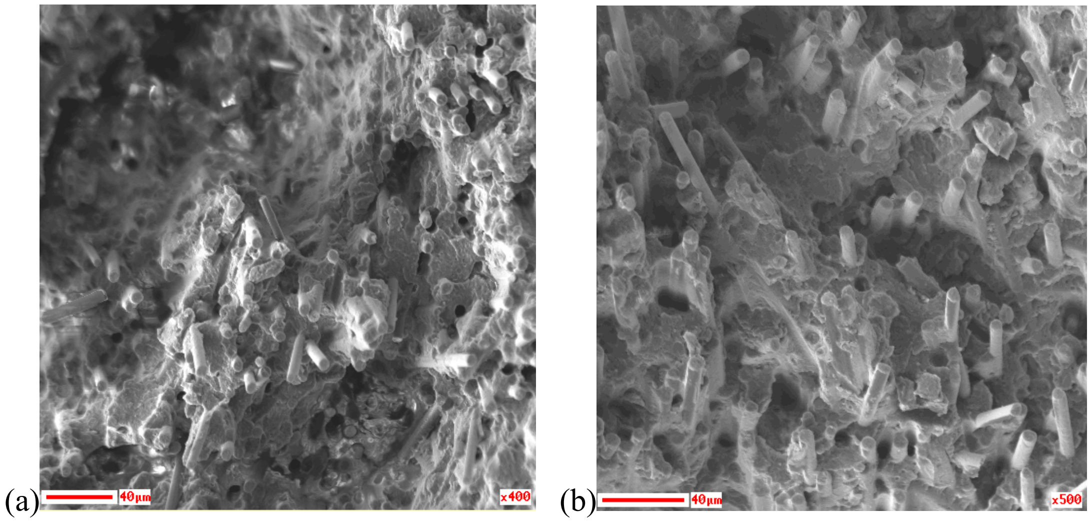

Figure 4.175: SEM micrographs taken from tensile fracture surface of carbon fibre composite at dry as moulded condition

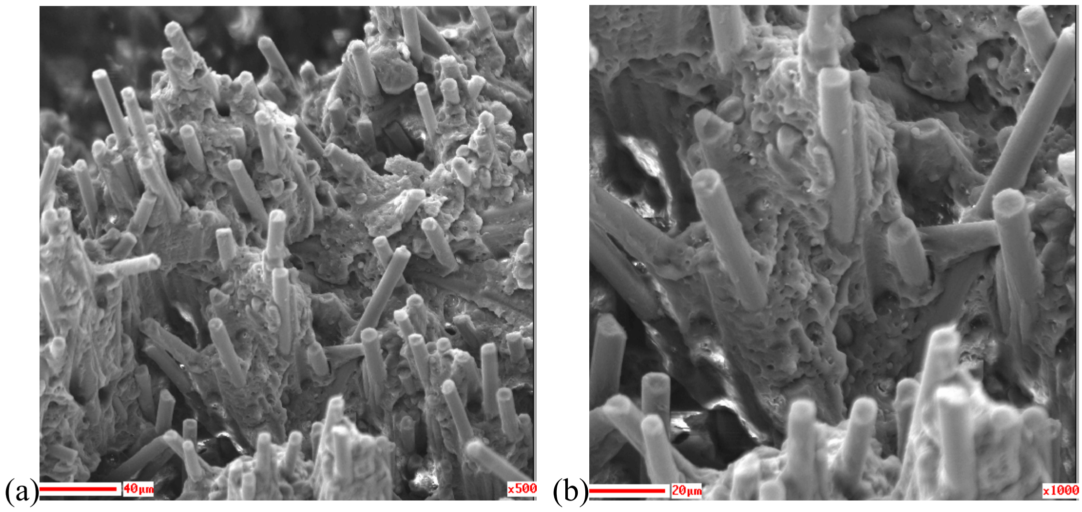

Figure 4.176: SEM micrographs taken from tensile fracture surface of carbon fibre composite at wet condition

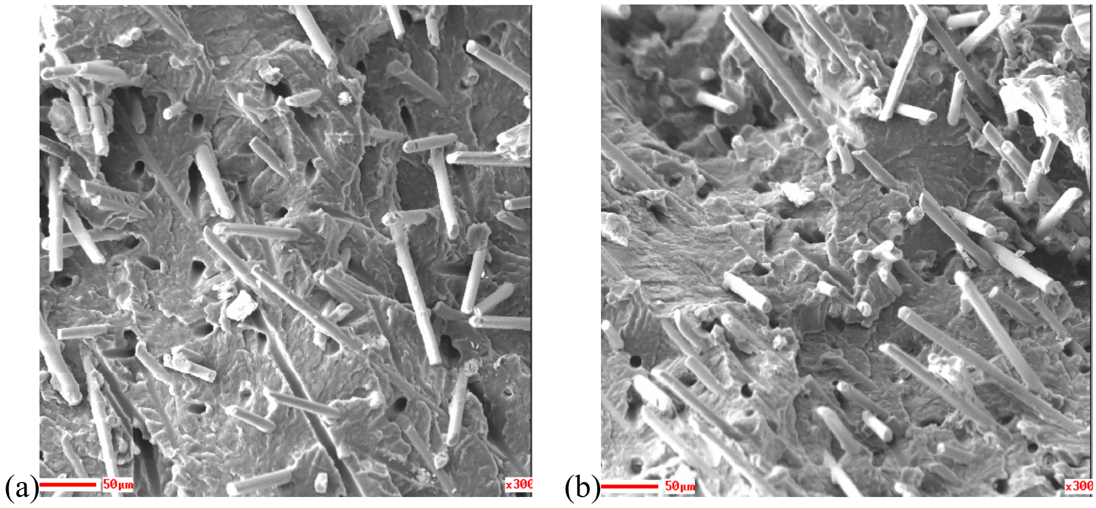

Figure 4.177: SEM micrographs taken from impact fracture surface of glass fibre composite at dry as moulded condition

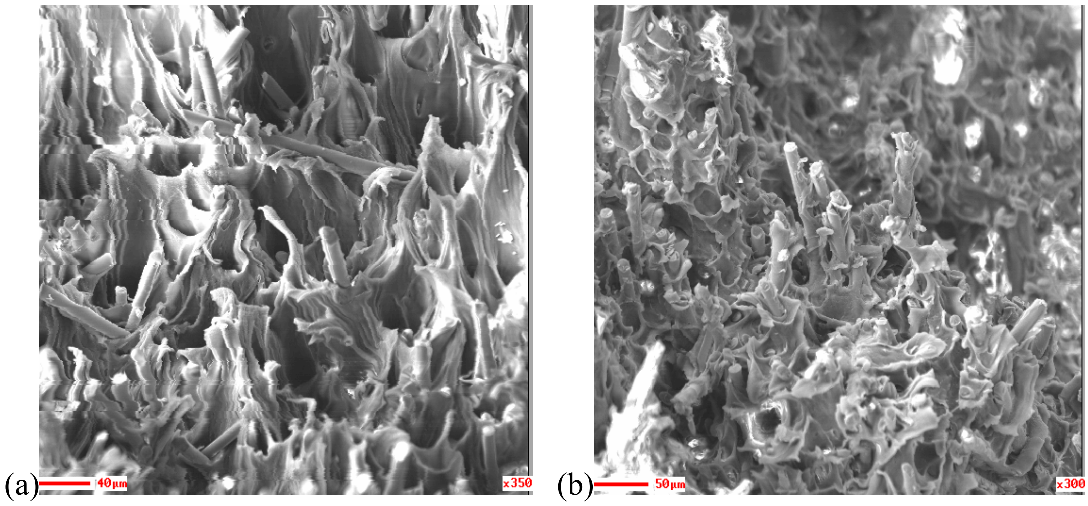

Figure 4.178: SEM micrographs taken from impact fracture surface of glass fibre composite after water immersion

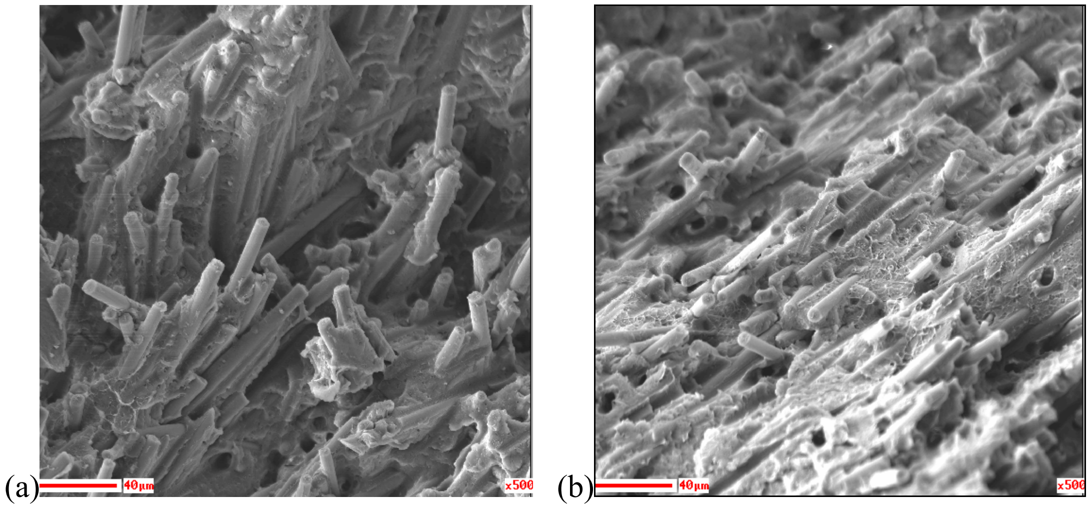

Figure 4.179: SEM micrographs taken from impact fracture surface of carbon fibre composite at dry as moulded condition

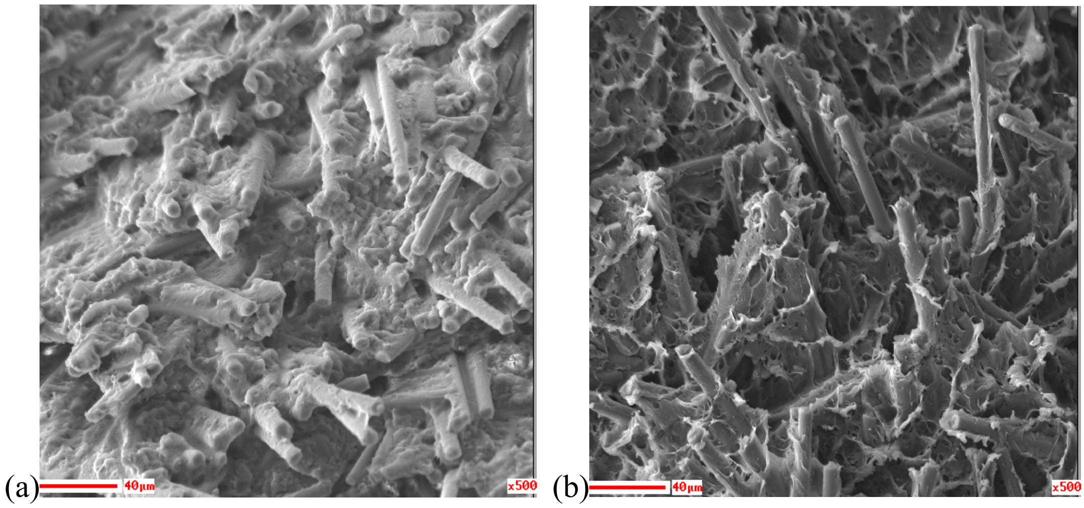

Figure 4.180: SEM micrographs taken from impact fracture surface of carbon fibre composite after immersed in water